Universidad de Oviedo

Departamento de Química Física y Analítica

Programa de Doctorado en Análisis Químico, Bioquímico y Estructural y Modelización Computacional

DISPOSITIVOS (BIO)ELECTROANALÍTICOS BASADOS EN TRANSDUCTORES DE CARBONO: ELECTRODOS SERIGRAFIADOS Y ALFILERES

Tesis Doctoral

Estefanía Costa Rama

Oviedo, Junio 2016

Tesis Doctoral: DISPOSITIVOS (BIO)ELECTROANALÍTICOS BASADOS EN TRANSDUCTORES DE CARBONO: ELECTRODOS SERIGRAFIADOS Y ALFILERES.

Directores: AGUSTÍN COSTA GARCÍA Y Mª TERESA FERNÁNDEZ ABEDUL.

Lugar y fecha de lectura: OVIEDO, 17 DE JUNIO DE 2016.

RESUMEN DEL CONTENIDO DE TESIS DOCTORAL

1.- Título de la Tesis	
Español/Otro Idioma: Dispositivos (bio)electroanalíticos basados en transductores de carbono: electrodos serigrafiados y alfileres	Inglés: (Bio)electroanalytical devices based on carbon transducers: screen-printed electrodes and pins

2.- Autor	
Nombre: Estefanía Costa Rama	DNI/Pasaporte/NIE: -G
Programa de Doctorado: Análisis Químico, Bioquímico y Estructural y Modelización Computacional	
Órgano responsable: Centro Internacional de Postgrado	

RESUMEN (en español)

Dentro de las tendencias actuales de la Química Analítica: automatización, simplificación, miniaturización y disminución de costes, son las dos últimas las más acusadas en los últimos años. Dentro de este contexto, los electrodos serigrafiados han sufrido un gran auge en aplicaciones electroanalíticas gracias a sus ventajosas características como su bajo coste, su carácter desechable y el pequeño volumen de muestra que requieren. Dando un paso más en estas dos tendencias, en los últimos años se han comenzado a desarrollar electrodos basados en materiales de bajo coste, de uso común y de gran disponibilidad como papel, hilos o transparencias.

Por otro lado, los biosensores electroquímicos, ejemplo claro de simplificación, son un área muy importante dentro de la Química Analítica ya que permiten obtener una respuesta rápida, barata y fiable a muchos de los retos que plantea el análisis (bio)químico en diversos campos como el análisis clínico, el medio ambiente o la industria (alimentaria, farmacéutica, …). Dentro de ellos, siguen siendo de gran importancia los ensayos enzimáticos y los inmunoensayos.

Por todo ello, el fundamento de esta tesis doctoral es el desarrollo de diferentes dispositivos (bio)electroanalíticos basados en transductores de carbono miniaturizados y de bajo coste para la determinación de diversos analitos de interés clínico y/o alimentario. Basándose en los diferentes dispositivos desarrollados, esta tesis se divide en tres partes que se detallarán a continuación.

En el primer capítulo se construyen y ponen a punto tres sensores enzimáticos para la determinación de glucosa, fructosa y etanol, utilizando como transductores electrodos serigrafiados de carbono comerciales. Los electrodos utilizados en este capítulo consisten en una celda electroquímica con tres electrodos (electrodo de trabajo, de referencia y auxiliar) serigrafiados sobre un soporte de cerámica. La tinta de carbono del electrodo de trabajo está modificada con un mediador redox. Utilizando estos electrodos y una metodología de inmovilización de las enzimas muy sencilla se obtienen sensores que permiten la determinación de los analitos en muestras reales (alimentos, bebidas y sangre).

El segundo capítulo trata del desarrollo de inmunosensores basados en electrodos serigrafiados de carbono. Además de una revisión bibliográfica, en este capítulo se encuentra la fabricación de un immunosensor para la detección de un biomarcador de la enfermedad de Alzheimer y de un bi-immunosensor para dos biomarcadores del cáncer de mama. Para ello se utilizan dos electrodos serigrafiados con diseños diferentes: uno con un solo electrodo de trabajo y el otro con dos electrodos de trabajo que permite la detección de los dos biomarcadores simultáneamente. Además, en este caso los electrodos se han nanoestructurado con nanopartículas de oro para la mejora de sus características.

La parte final de esta tesis está dedicada a la utilización de transductores basados en alfileres de acero inoxidable modificados con tinta de carbono para el desarrollo de dispositivos electroanalíticos. Primero, utilizando estos transductores se desarrolla un biosensor de glucosa empleando la metodología desarrollada en el capítulo 1. Por último, e incorporando la tendencia de la automatización, se desarrolla un sistema de análisis por inyección en flujo (FIA) con detección electroquímica utilizando una sencilla celda basada en alfileres.

RESUMEN (en Inglés)

Within the currently trends in Analytical Chemistry: automation, simplification, miniaturization and low-cost, the last two are the most pronounced in recent years. In this context, the screen-printed electrodes have experienced a boom in electroanalytical applications due to its advantages such as low cost, disposability and low sample volume required. Stepping forward in these trends, during the last years electrodes based on inexpensive, common and worldwide available materials such as paper, thread or transparency films have been developed.

Moreover, electrochemical biosensors, a clear example of simplification, are very important in Analytical Chemistry since they allow a quick, cheap and reliable response for many challenges of (bio)chemistry analysis in many areas such as clinical analysis, environment or industry (food, pharmaceutical,…). Within, enzymatic and immuno- assays remain highly important.

Taking into account this considerations, this Ph.D. Memory is about the development of different (bio)electrochemical devices based on miniaturized and low-cost carbon transducers for the determination of several analytes with clinical and/or food industry interest. According to the different devices developed, this Ph.D. Memory can be divided in three parts that are commented below.

In the first chapter, enzymatic sensors are developed for the determination of glucose, fructose and ethanol, using commercial screen-printed carbon electrodes as transducers. These electrodes consists of a three-electrodes electrochemical cell (working, reference and counter electrodes) screen-printed on a ceramic substrate. The carbon ink of the working electrode is modified with a redox mediator included in the carbon. Using these electrodes and an easy methodology for the enzymes immobilization, enzymatic sensors are develop for the determination of the analytes in real samples (food, drinks and blood).

The second chapter is about development of immunosensors based on screen-printed carbon electrodes. Besides a review, in this chapter the fabrication of an immunosensor for the detection of one Alzheimer disease biomarker and of a bi-immunosensor for two breast cancer biomarkers is described. The screen-printed carbon electrodes used show different designs: one of them only has a working electrode, and the other has two working electrodes allowing the simultaneous determination of two biomarkers. Both screen-printed electrodes are nanostructured with gold nanoparticles in order to improve their characteristics.

The final of the Ph.D. Memory is about the using of transducers based on stainless-steel pins modified with carbon ink for the development of electroanalytical devices. First, a glucose sensor based on these transducers is constructed using a similar methodology to the described in chapter 1. Finally, adding the trend of automation, a flow injection electroanalytical system is developed using a simple electrochemical cell based on pins.

SR. PRESIDENTE DE LA COMISIÓN ACADÉMICA DEL PROGRAMA DE DOCTORADO EN ANÁLISIS QUÍMICO, BIOQUÍMICO Y ESTRUCTURAL Y MODELIZACIÓN COMPUTACIONAL

Índice

Producción Científica

I. Artículos científicos

Relacionados con esta Tesis

1. Julien Biscay, Estefanía Costa Rama, María Begoña González García, José Manuel Pingarrón Carrazón, Agustín Costa-García, "*Enzymatic sensor using mediator-screen printed carbon electrodes*", *Electroanalysis* 2011, 23 (1), 209-214. DOI: 10.1002/elan.201000471.
2. Julien Biscay, Estefanía Costa Rama, María Begoña González García, A. Julio Reviejo, José Manuel Pingarrón Carrazón, Agustín Costa García, "*Amperometric fructose sensor based on ferrocyanide modified screen-printed carbon electrode*", *Talanta* 2012, 88, 432-438. DOI: 10.1016/j.talanta.2011.11.013.
3. Estefanía Costa Rama, Julien Biscay, María Begoña González García, A. Julio Reviejo, José Manuel Pingarrón Carrazón, Agustín Costa García, "*Comparative study of different alcohol sensors based on screen-printed carbon electrodes*", *Analytica Chimica Acta* 2012, 728, 69-76. DOI: 10.1016/j.aca.2012.03.039.
4. Estefanía Costa Rama, María Begoña González-García; Agustín Costa-García, "*Competitive electrochemical immunosensor for amyloid-beta 1-42 detection based on gold nanostructurated screen-printed carbon electrodes*", *Sensors and Actuators B: Chemical* 2014, 201, 567-571. DOI: 10.1016/j.snb.2014.05.044.
5. Estefanía Costa Rama, Agustín Costa García, "*Screen-printed electrochemical immunosensors for the detection of cancer and cardiovascular biomarkers*", *Electroanalysis* 2016 (aceptado).
6. Estefanía C. Rama, Agustín Costa-García, M. Teresa Fernández-Abedul, "*Pin-based electrochemical sensor with multiplexing possibilities*", Biosensors & Bioelectronics (en revisión).
7. Estefanía C. Rama, Agustín Costa-García, M. Teresa Fernández-Abedul, "*Pin-based flow injection electroanalysis*", *Analytical Chemistry* (en revisión).

Tabla A: Factor de impacto (*Impact Factor*, IF) de las revistas donde aparecen publicados los artículos recogidos en esta Tesis Doctoral.

Revista	Año	IF	IF medio últimos 5 años	Área	Ranking (cuartil)	Estado del artículo
Electroanalysis	2011	2.872	2.409	Química Analítica	23/73 (Q2)	Publicado
	2014	2.138			36/74 (Q2)	Aceptado
Talanta	2012	3.498	3.670	Química Analítica	12/75 (Q1)	Publicado
Analytica Chimica Acta	2012	4.387	4.667	Química Analítica	7/75 (Q1)	Publicado
Sensors and Actuators B: Chemical	2014	4.097	4.286	Química Analítica	8/74 (Q1)	Publicado
Biosensors & Bioelectronics	2014	6.409	6.045	Química Analítica	3/74 (Q1)	En revisión
Analytical Chemistry	2014	5.636	5.794	Química Analítica	4/74 (Q1)	En revisión

Otros artículos científicos no relacionados con esta Tesis

1. Daniel Martín-Yerga, Estefanía Costa Rama, Agustín Costa-García, "*Electrochemical characterization of ordered mesoporous carbon screen-printed electrodes*", *Journal of Electrochemical Society* 2016, 163 (5), B176-B179. DOI: 10.1149/2.0871605jes.
2. Daniel Martín-Yerga, Estefanía Costa Rama, Agustín Costa-García, "*Electrochemical study and applications of selective electrodeposition of silver on quantum dots*", *Analytical Chemistry* 2016, 88 (7), 3739-3746. DOI: 10.1021/acs.analchem.5b04568.
3. Daniel Martín-Yerga, Estefanía Costa Rama, Agustín Costa García, "*Electrochemical study and determination of electroactive species with screen-printed electrodes*", *Journal of Chemical Education* 2016. DOI: 10.1021/acs.jchemed.5b00755.
4. O. Amor-Gutiérrez, E.C. Rama, M.T. Fernández-Abedul, A. Costa-García, "*Bioelectroanalysis in a drop: construction of a glucose biosensor*", *Journal of Chemical Education* (en revisión).

5. O. Amor-Gutiérrez, E. Costa Rama, A. Costa-García, M.T. Fernández-Abedul, "Paper-based enzymatic sensor with stencil-free ink and wire electrodes", *Biosensors & Bioelectronics* (en preparación).
6. A. García-Miranda Ferrari, O. Amor-Gutiérrez, E. Costa Rama, M.T. Fernández-Abedul, "Pin-based batch injection analysis", *Analytical Chemistry* (en preparación).

II. Artículos de conferencias ("*Proceedings*")

1. Raquel Marques, Joao Pacheco, Estefanía Rama, Subramanian Viswanathan, Henri Nouws, Cristina Delerue-Matos. "*Electrochemical sensors in breast cancer diagnostics and follow-up*" *International Journal of Cancer Therapy and Oncology* 2015, 3 (4), 34012.
2. E. Costa Rama, A. Costa García, M.T. Fernández-Abedul. "*Pin-based enzymatic electrochemical sensing*" *Procedia Technology* (en preparación).

III. Contribuciones a congresos

1. Julien Biscay, Estefanía Costa Rama, María Begoña González-García, José Manuel Pingarrón Carrazón, Agustín Costa-García. "*Enzymatic sensor using mediator-screen printed carbon electrodes*" (comunicación póster). 13th International Conference on Electroanalysis (ESEAC 2010). Junio 2010, Gijón, España.
2. Estefanía Costa Rama, María Begoña González-García, Agustín Costa-García. "*Estudio comparativo de distintos transductores nanoestructurados sobre electrodos serigrafiados*" (comunicación flash+póster). V Workshop en Nanociencia y Nanotecnología Analíticas. Septiembre 2011, Toledo, España.
3. Estefanía Costa Rama, María Begoña González-García, Agustín Costa-García. "*Electrochemical immunosensor based on nanostructured screen-printed carbon electrodes for detection of biomarkers of Alzheimer's disease*" (comunicación póster). 3rd International Conference on Bio-Sensing Technology. Mayo 2013, Sitges, España.
4. Estefanía Costa Rama, María Begoña González-García, Agustín Costa-García. "*Electrochemical immunosensor for detection of biomarkers of Alzheimer's Disease*" (comunicación póster). VI Workshop en Nanociencia y Nanotecnología Analíticas. Julio 2013, Alcalá de Henares, España.

5. Raquel C.B. Marques, Estefanía Costa Rama, Subramanian Viswanathan, Henri P.A. Nouws, Cristina Delerue-Matos, María Begoña González-García. "*Multiplexed electrochemical immunosensor for detection of breast cancer markers*" (comunicación póster). 15th International Conference on Electroanalysis (ESEAC 2014), Junio 2014, Malmö, Suecia.

6. Raquel C.B. Marques, Estefanía Costa Rama, Subramanian Viswanathan, Henri P.A. Nouws, Cristina Delerue-Matos, María Begoña González-García. "*Breast cancer diagnostics using an electrochemical immunosensor*" (comunicación póster). 19th Meeting of the Portuguese Electrochemical Society; XVI Iberian Meeting of Electrochemistry. Junio-Julio 2014, Aveiro, Portugal.

7. Estefanía Costa Rama, María Begoña González-García, Agustín Costa-García. "*Competitive electrochemical immunosensor for amyloid-beta 1-42 detection based on nanostructurated screen-printed carbon electrodes*" (comunicación póster). XXXV Reunión del Grupo de Electroquímica de la Real Sociedad Española de la Electroquímica; 1st E3 Mediterranean Symposium: Electrochemistry for Environment and Energy. Julio 2014, Burgos, España.

8. Raquel C.B. Marques, Joao Pacheco, Estefanía C. Rama, Subramanian Viswanathan, Henri P.A. Nouws, Cristina Delerue-Matos, M. Begoña González-García. "*Electrochemical sensors in breast cancer*" (comunicación póster). 1st ASPIC international congress. Noviembre 2014, Lisboa, Portugal.

9. Raquel C.B. Marques, Joao Pacheco, Estefanía C. Rama, Subramanian Viswanathan, Henri P.A. Nouws, Cristina Delerue-Matos. "*Electrochemical sensors in breast cancer diagnostics and follow-up*" (comunicación oral). BIT's 8th Annual World Cancer Congress. Mayo 2015, Beijing, China.

10. E. Costa Rama, A. Costa García, M.T. Fernández-Abedul. "*Pin-based enzymatic electrochemical sensing*" (comunicación póster). Biosensors 2016. Mayo 2016, Gothenburg, Suecia.

11. O. Amor Gutiérrez, E. Costa Rama, A. Costa-García, M.T. Fernández-Abedul. "Paper-based *enzymatic sensor with stencil-free ink and wire electrodes"* (comunicación póster). Biosensors 2016. Mayo 2016, Gothenburg, Suecia.

Estructura de la memoria

La estructura de esta Memoria, que está realizada como compendio de publicaciones, consta de las siguientes partes: un breve **Resumen** (en español e inglés) sintetizando el trabajo aquí presentado, un listado de todas las **Abreviaturas** que aparecen lo largo de la Memoria, un listado de las **Tablas y Figuras** (presentes en la Introducción), una breve **Introducción** que contextualiza el trabajo desarrollado, el planteamiento de los **Objetivos**, el apartado de **Resultados y Discusión** en el que se presentan los artículos científicos agrupados en tres **Capítulos**, y finalmente las **Conclusiones** generales obtenidas a lo largo de la Tesis Doctoral junto con las **Perspectivas de Futuro** planteadas para seguir con la línea de trabajo establecida en esta Tesis Doctoral (las Conclusiones y las Perspectivas de Futuro, así como el Resumen, se presentan en español e inglés siguiendo la normativa que rige para la obtención de la Mención Internacional en el título de Doctor).

A lo largo de esta Tesis Doctoral se desarrollan diversos biosensores (tanto enzimáticos como inmunosensores) y un sistema de análisis por inyección en flujo utilizando transductores de carbono. Por tanto, el apartado Resultados y Discusión se divide en tres capítulos atendiendo a los tipos de biosensores desarrollados y a los tipos de transductores utilizados. Estos capítulos son los siguientes:

- Capítulo I: **Sensores enzimáticos basados en electrodos serigrafiados**. Dentro de este capítulo se encuentran los siguientes artículos ya publicados:
    1. *Enzymatic sensor using mediator-screen printed carbon electrodes*.
    2. *Amperometric fructose sensor based on ferrocyanide modified screen-printed carbon electrode*.
    3. *Comparative study of different alcohol sensors based on screen-printed carbon electrodes*.
- Capítulo II: **Immunosensores basados en electrodos serigrafiados**. Este Capítulo está formado por dos artículos ya publicados y uno sin publicar (el número 6):
    4. *Screen-printed electrochemical immunosensors for the detection of cancer and cardiovascular biomarkers*.
    5. *Competitive electrochemical immunosensor for amyloid-beta 1-42 detection based on gold nanostructurated screen-printed carbon electrodes*.
    6. *Multiplexed electrochemical immunosensor for detection of breast cancer biomarkers*.

- Capítulo III: **Sistemas electroanalíticos utilizando alfileres como electrodos**. Dentro de este capítulo se encuentran los siguientes artículos que ya han sido enviados para su publicación:
    7. *Pin-based electrochemical sensor with multiplexing*.
    8. *Pin-based flow injection electroanalysis*.

Todos los artículos que componen este trabajo se presentan en un formato unificado con el resto de la Memoria para una lectura más cómoda.

Resumen

Dentro de las tendencias actuales de la Química Analítica: automatización, simplificación, miniaturización y disminución de costes, son las dos últimas las más acusadas en los últimos años. En este contexto, los electrodos serigrafiados han sufrido un gran auge en aplicaciones electroanalíticas gracias a sus ventajosas características como bajo coste, carácter desechable y el pequeño volumen de muestra que requieren. Dando un paso más en estas dos tendencias, en los últimos años se han comenzado a desarrollar electrodos utilizando sustratos de bajo coste, de uso común y de gran disponibilidad como papel, hilos o transparencias.

Por otro lado, los biosensores electroquímicos, ejemplo claro de simplificación, son un área muy importante dentro de la Química Analítica ya que permiten obtener una respuesta rápida, barata y fiable a muchos de los retos que plantea el análisis (bio)químico en diversos campos como el análisis clínico, el medio ambiente o la industria (alimentaria, farmacéutica, …). Dentro de ellos, siguen siendo de gran importancia los biosensores enzimáticos y los inmunosensores.

Por todo ello, el fundamento de esta Tesis Doctoral es el desarrollo de diferentes dispositivos (bio)electroanalíticos basados en transductores de carbono miniaturizados y de bajo coste para la determinación de diversos analitos de interés clínico y/o alimentario. Basándose en los diferentes dispositivos desarrollados, esta Tesis se divide en tres partes que se detallarán a continuación.

En el **primer capítulo** trata la construcción y puesta a punto de tres sensores enzimáticos para la determinación de glucosa, fructosa y etanol, utilizando como transductores electrodos serigrafiados de carbono comerciales. Los electrodos utilizados en este capítulo consisten en una celda electroquímica de tres electrodos (electrodo de trabajo, de referencia y auxiliar) serigrafiados sobre un soporte de cerámica. La tinta de carbono del electrodo de trabajo está modificada con un mediador redox. Utilizando estos electrodos y una metodología de inmovilización de las enzimas muy sencilla se obtienen sensores que permiten la determinación de los analitos en muestras reales (alimentos, bebidas y sangre).

El **segundo capítulo** trata del desarrollo de inmunosensores basados en electrodos serigrafiados de carbono. Además de una revisión bibliográfica, en este capítulo se encuentra la fabricación de un immunosensor para la detección de un biomarcador de la enfermedad de Alzheimer y de un bi-immunosensor para dos biomarcadores del cáncer de mama. Para ello se utilizan dos electrodos serigrafiados con diseños diferentes: uno con un solo electrodo de

trabajo y otro con dos, lo que permite la detección de los dos biomarcadores simultáneamente. Además, en este caso los electrodos se han nanoestructurado con nanopartículas de oro para la mejora de sus características.

La **parte final** de esta Tesis está dedicada a la utilización de alfileres de acero inoxidable modificados con tinta de carbono como electrodos para el desarrollo de dispositivos electroanalíticos. En primer lugar, utilizando estos transductores se desarrolla un biosensor de glucosa empleando una metodología similar a la desarrollada en el Capítulo I. También se muestra la versatilidad que los alfileres permiten en cuanto al diseño de dispositivos construyendo un dispositivo con cuatro electrodos de trabajo para la determinación simultánea de diferentes analitos. Por último, se desarrolla un sistema de análisis por inyección en flujo con detección electroquímica utilizando una sencilla celda basada en alfileres.

Abstract

Within the current trends in Analytical Chemistry: automation, simplification, miniaturization and low-cost, the last two are the most pronounced in recent years. In this context, screen-printed electrodes have experienced a boom in electroanalytical applications due to their advantages such as low cost, disposability and low sample volume required. Advancing, in these trends, during the last years electrodes based on inexpensive, common and worldwide available materials such as paper, thread or transparency films have been developed.

On the other hand, electrochemical biosensors, a clear example of simplification, are very important in Analytical Chemistry since they allow a quick, cheap and reliable response for many challenges of (bio)chemical analysis in areas such as clinical analysis, environmental or industry (food, pharmaceutical,…). Among them, enzymatic and immunosensors remain highly important.

Taking into account these considerations, the reason of this Ph.D. Memory is the development of different (bio)electrochemical devices based on miniaturized and low-cost carbon transducers for the determination of several analytes with clinical and/or food industry interest. According to the different devices developed, this Ph.D. Memory can be divided in three parts that are commented below.

The **first chapter** deals with the development of enzymatic sensors for the determination of glucose, fructose and ethanol using commercial screen-printed carbon electrodes as transducers. These consist of a three-electrode electrochemical cell (working, reference and counter electrodes) screen-printed on a ceramic substrate. The carbon ink of the working electrode is modified with a redox mediator. Using these electrodes and an easy methodology for enzyme immobilization, enzymatic sensors for the determination of the analytes in real samples (food, drinks and blood) are developed.

The **second chapter** is about development of immunosensors based on screen-printed carbon electrodes. Besides a review, in this chapter the fabrication of an immunosensor for the detection of one Alzheimer's disease biomarker and of a bi-immunosensor for two breast cancer biomarkers is described. The screen-printed carbon electrodes used show different designs: one of them only has a working electrode, meanwhile the other one has two, allowing the simultaneous determination of two biomarkers. Both screen-printed electrodes are nanostructured with gold nanoparticles in order to improve their characteristics.

The **final part** of the Ph.D. Memory deals with the use of stainless-steel pins modified with carbon ink as electrodes for the development of electroanalytical devices. First, a glucose sensor based on these transducers is constructed using a similar methodology to the one described in Chapter 1. Moreover, the versatility pins offer to devices design is demonstrated by the construction of a device with four pins acting as working electrodes that allow multiplexed analysis. Finally, a flow injection electroanalytical system is developed using a simple electrochemical cell based on pins.

Lista de abreviaturas

3-IP	3-indoxil fosfato	*3-indoxyl phosphate*
µPAD	Dispositivo analítico microfluídico basado en papel	*Microfluidic paper-based analytical device*
Aβ	Beta-amiloide	*Beta-amyloid*
AA	Ácido ascórbico	*Ascorbic acid*
Ab	Anticuerpo	*Antibody*
ACS	Síndrome coronario agudo	*Acute coronary syndrome*
AD	Enfermedad de Alzheimer	*Alzheimer's disease*
ADP	Adenosín difosfato	*Adenosine diphosphate*
AFP	α-fetoproteína	*α-fetoprotein*
AgNP	Nanopartículas de plata	*Silver nanoparticles*
AHA	Asociación americana del corazón (EEUU)	*American Heart Association (USA)*
AOx	Alcohol oxidasa	*Alcohol oxidase*
AP	Fosfatasa alcalina	*Alkaline phosphatase*
APP	Proteína precursora de amiloide	*Amyloid precursor protein*
ASV	Voltamperometría de redisolución anódica	*Anodic stripping voltammetry*
AuNP	Nanopartícula de oro	*Gold nanoparticle*
BNP	Péptido natriurético tipo B	*B-type natriuretic peptide*
BSA	Albúmina de suero bovino	*Bovine serum albumin*
BTA	Antigen tumoral de vejiga	*Bladder tumour associated antigen*
CA	Antígeno carbohidratado	*Cancer antigen*
CDR	Regiones determinantes de complementariedad	*Complementarity determining regions*
CE	Electrodo auxiliar o contraelectrodo	*Counter electrode*

CEA	Antígeno carcinoembrionario	*Carcinoembryonic antigen*
CFA	Análisis en flujo continuo	*Continuous flow analysis*
CG	Cromatografía de gases	*Gas chromatographic*
CK-MB	Creatina quinasa MB	*Creatine kinase MB*
CNT	Nanotubo de carbono	*Carbon nanotube*
CRP	Proteína C reactiva	*C-reactive protein*
CSF	Líquido cerebroespinal	*Cerebrospinal fluid*
cTnT	Troponina cardiaca T	*Cardiac troponin T*
cTnI	Troponina cardiaca I	*Cardiac troponin I*
CV	Voltamperometría cíclica o Voltamperograma cíclico	*Cyclic voltammetry or Cyclic voltammogram*
CVD	Enfermedad cardiovascular	*Cardiovascular disease*
DNA / ADN	Ácido desoxiribonucleico	*Deoxyribonucleic acid*
DPV	Voltamperometría de pulso diferencial	*Differential pulse voltammetry*
DMF	N,N-dimetilformamida	*N,N-dimethylformamide*
EμPAD	Dispositivo electroanalítico microfluídico basado en papel	*Microfluidic paper-based electroanalytical device*
ECD	Dominio extracelular	*Extracellular domain*
ECG	Electrocardiograma	*Electrocardiogram*
EGFR	Receptor del factor de crecimiento epidérmico	*Epidermal growth factor receptor*
EI	Immunosensor electroquímico	*Electrochemical immunosensor*
EIS	Espectroscopía de impedancia electroquímica	*Electrochemical impedance spectroscopy*
ELISA	Ensayo por inmunoadsorción con enzimas ligados	*Enzyme linked immunosorbent assay*
ESC	Sociedad Europea de Cardiología	*European Society of Cardiology*
FAD	Dinucleótido de flavina adenina	*Flavin adenine dinucleotide*

$FcCO_2H$	Ácido ferroceno monocarboxílico	*Ferrocene monocarboxylic acid*
FDA	Agencia de alimentos y drogas (EEUU)	*Food and Drug Administration (USA)*
FDH	Fructosa deshidrogenasa	*Fructose dehydrogenase*
FDP	Proteína de degradación de la fibrina	*Fibrin degradation protein*
FET	Transistor de efecto de campo	*Field-effec transistor*
FIA	Análisis por inyección en flujo	*Flow injection analysis*
FID	Detector de ionización de llama	*Flame ionization detector*
FISH	Hibridación fluorescente *in situ*	*Fluorescent in situ hybridization*
FMN	mononucleótido deflavina	*Flavin mononucleotide*
fPSA*	PSA libre	*Free PSA*
G6PDH	Glucosa-6-fosfato deshidrogenasa	*Glucose-6-phosphate dehydrogenase*
GO	Óxido de grafeno	*Graphene oxide*
GOx	Glucosa oxidasa	*Glucose oxidase*
HA	Ácido hialurónico	*Hyaluronic acid*
HAase	Hialuronidasa	*Hyaluronidase*
hCG	Gonadotrofina coriónica humana	*Human chorionic gonadotropin*
HER	Reacción de evolución de hidrógeno	*Hydrogen evolution reaction*
HER	Receptor del factor de crecimiento epidérmico humano	*Human epidermal growth factor receptor*
HFABP	Proteína de unión de ácidos grasos específica del corazón	*Heart type fatty acid protein*
HPLC	Cromatografía líquida de alta eficacia	*High performance liquid chromatography*
HRP	Peroxidasa de rábano silvestre	*Horseradish peroxidase*
IFCC	Federación Internacional de Química clínica y Ciencias del Laboratorio Clínico	*International Federation of Clinical Chemistry and Laboratory Medicine*
Ig	Inmunoglobulina	*Immunoglobulin*

IHC	Inmunohistoquímica	*Immunohistochemistry*
IL-8	Interleucina 8	*Interleukin 8*
IUPAC	Unión Internacional de Química Pura y Aplicada	*International Union of Pure and Applied Chemistry*
LOD	Límite de detección	*Limit of detection*
LOQ	Límite de cuantificación	*Limit of quantification*
LSV	Voltamperometría lineal	*Linear sweep voltammetry*
MI	Infarto de miocardio	*Myocardial infarction*
MIP	Polímero molecularmente impreso	*Molecularly imprinted polymer*
MWCNT	Nanotubo de carbono de pared múltiple	*Multi-walled carbon nanotube*
NAD	Nicotinamida adenina dinucleótido	*Nicotinamide adenine dinucleotide*
$NADP^+$ ($NADPH^+$)	Nicotinamida adenina dinucleótido fosfato	*Nicotinamide adenine dinucleotide phosphate*
NIA	Instituto Nacional del Envejecimiento (EEUU)	*National Institute on Aging (USA)*
NMP22	Proteína matriz nuclear 22	*Nuclear matrix protein 22*
NSE	Enolasa neuroespecífica	*Neuron specific enolase*
NT-proBNP	Propéptido natriurético tipo B N-terminal	*N-terminal pro-B-type natriuretic peptide*
PAP	Fosfatasa ácida prostática	*Prostatic acid phosphatase*
PBS	Disolución reguladora de fosfato	*Phosphate buffer solution*
PGI	Fosfoglucosa isomerasa	*Phosphoglucose isomerase*
PLA	Ensayo de ligación por proximidad	*Proximity ligation assay*
POC	"Punto de cuidados"	*Point-of-care*
PQQ	Pirroloquinolina quinona	*Pyrroloquinoline quinone*
PSA*	Antígeno específico de prostata	*Prostate specific antigen*
PSA-ACT*	PSA complejada con α-1-antiquimotripsina	*PSA complexed with* α-1-antichymotrypsin

PVC	Policloruro de vinilo	*Poly(vinyl chloride)*
QD	"Puntos cuánticos"	*Quantum dots*
RE	Electrodo de referencia	*Reference electrode*
S-AP	Estreptavidina conjugada con fosfatasa alcalina	*Streptavidin conjugated to alkaline phosphatase*
SCC	Carcinoma de células escamosas	*Squamous cell carcinoma*
SFA	Análisis en flujo segmentado	*Segmented flow analysis*
SIA	Análisis por inyección secuencial	*Sequential injection analysis*
SAM	Monocapa autoensamblada	*Self-assembled monolayer*
SPCE	Electrodo serigrafiado de carbono	*Screen-printed carbon electrode*
AuNP-SPCE	Electrodo serigrafiado de carbon con nanopartículas de oro	*Gold nanoparticle screen-printed carbon electrode*
SPCPCE	Electrodo serigrafiado de carbon con ftalocianina de cobalto	*Screen-printed cobalto-phthalocyanine/carbon electrode*
SPE	Electrodo serigrafiado	*Screen-printed electrode*
SPFCE	Electrodo serigrafiado de carbon con ferrocianuro	*Screen-printed ferrocyanide/carbon electrode*
SPPBCE	Electrodo serigrafiado de carbon con Prussian Blue	*Screen-printed Prussian Blue/carbon electrode*
SWCNT	Nanotubo de carbon de pared simple	*Single-walled carbon nanotube*
SWV	Voltamperometría de onda cuadrada	*Square wave voltammetry*
Tris	Tris(hidroximetil)aminometano	*Tris(hydroxymethyl)aminomethane*
tPSA*	PSA total	*Total PSA*
UA	Ácido úrico	*Uric acid*
WE	Electrodo de trabajo	*Working electrode*
WHO / OMS	Organización Mundial de la Salud	*World Health Organization*

Índice de tablas y figuras

1. INTRODUCCIÓN GENERAL

1.1. Tendencias en Química Analítica

A lo largo de la historia las herramientas analíticas han ido experimentando grandes avances. En la época clásica, hasta aproximadamente los años 50, las medidas analíticas cuantitativas se llevaban a cabo utilizando balanzas y buretas. Entre los años 50 y 70 se desarrolló una amplia variedad de instrumentos (fotómetros, polarógrafos, cromatógrafos,…) lo que implicó un cambio radical en la forma de realizar las medidas analíticas. Entre los años 70 y 90 el empleo progresivo de la informática, tanto para el control de los sistemas analíticos como soporte para la quimiometría, supuso un gran avance en la evolución de la Química Analítica [1]. Actualmente el desarrollo de sistemas miniaturizados, portables, automatizados, simples, de bajo coste y de respuesta rápida están marcando el presente y futuro de la Química Analítica [2-5].

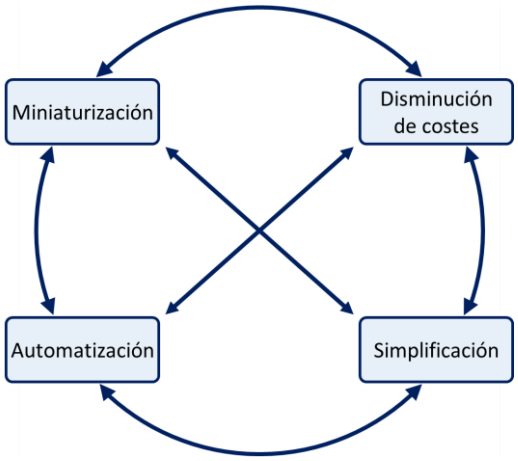

Figura 1.1. Esquema de la interrelación entre las tendencias actuales de la Química Analítica: simplificación, automatización, miniaturización y disminución de costes.

Por tanto, las tendencias actuales en Química Analítica se pueden concretar en los siguientes conceptos (**Figura 1.1**): **automatización** (reducción de la intervención humana en el proceso analítico), **simplificación** (reducción de la complejidad de dicho proceso), **miniaturización** (reducción del tamaño de las herramientas analíticas) y **disminución de costes** (tanto de las herramientas como de los procesos analíticos). Estas tendencias están interrelacionadas entre sí: por ejemplo, cuando un sistema se automatiza, casi siempre implica un grado de miniaturización y sobre todo de simplificación; por otro lado, la simplificación generalmente implica la reducción de la intervención humana y también la integración de módulos, y por tanto cierto grado de miniaturización. Todas ellas también están relacionadas con la disminución del coste, sobre todo la miniaturización, ya que a menor tamaño de las

herramientas, menor cantidad de materiales es necesaria para la fabricación de estas y además, se precisa un menor consumo de reactivos y de muestra, lo que al mismo tiempo conlleva una menor generación de residuos. Además, la combinación de todas estas tendencias hace posible el desarrollo de dispositivos **portables** y sistemas de respuesta rápida para su uso rutinario (sensores, sistemas de *screening*,…) que respondan a la creciente necesidad de obtener información analítica *in situ* (fuera del laboratorio) [1,6]. Esta necesidad está presente en campos tan diversos como el alimentario (para la detección de contaminantes tóxicos en alimentos o la evaluación de ciertos parámetros relacionados con la calidad de estos), el medioambiental (para la determinación de contaminantes en el medioambiente) o el clínico (para la determinación de marcadores que permitan el diagnóstico o seguimiento de enfermedades a pie de cama del paciente, en ambulatorios o farmacias) [2,7-9]. La necesidad de estos sistemas portables y de respuesta rápida se hace aún más evidente cuando hablamos de cualquiera de los ámbitos antes mencionados en zonas sub-desarrolladas, en vías de desarrollo o de acceso remoto [2,6,10].

Esta Tesis Doctoral se basa principalmente en el desarrollo de **biosensores** electroquímicos utilizando transductores de carbono. Idealmente los biosensores son herramientas de pequeño tamaño, portables, de bajo coste y fáciles de usar que permiten la detección directa, rápida y fiable de uno o más analitos en una muestra sin necesidad de pretratarla. Por lo tanto, un biosensor ideal seguiría todas las tendencias actuales en Química Analítica. Es evidente que desarrollar un biosensor que cumpla todas estas características ideales es muy difícil, pero también es cierto que una herramienta de este tipo sería de gran utilidad en diversos campos (clínico, medioambiental, industrial, etc.), ya que, aunque a día de hoy se dispone de un gran arsenal de técnicas analíticas de laboratorio, la gran mayoría implican un elevado consumo de tiempo (debido por ejemplo a los laboriosos y costosos pretratamientos necesarios en muchas ocasiones) y además, estas técnicas no suelen ser adecuadas para casos en los que el análisis debe realizarse de manera continua, en tiempo real y/o fuera del laboratorio. De ahí que el desarrollo de biosensores haya sido objeto de intensa investigación durante los últimos años como muestra la **Figura 1.2**.

En cuanto a transductores, actualmente una de las plataformas preferidas para el desarrollo de sensores portables y de bajo coste son los electrodos serigrafiados, que en los últimos años se están desarrollando sobre soportes diferentes a los cerámicos y poliméricos, como es el caso de los electrodos serigrafiados basados en papel o transparencia. De ahí que en la mayor parte de esta Tesis Doctoral, los transductores elegidos para la construcción de

biosensores fueran **electrodos serigrafiado**s, ya que son de pequeño tamaño y gracias a su bajo coste pueden ser desechados tras un solo uso.

En la parte final de este trabajo, avanzando en la tendencia de disminución de costes y adentrándose en la idea de la utilización de materiales baratos, producidos en masa y de uso común para el desarrollo de dispositivos analíticos, se plantea el uso de **alfileres de acero inoxidable** como electrodos. Estos alfileres, modificados con tinta de carbono, se utilizan como transductores en un sensor enzimático y también se integran en un sistema de inyección en flujo como base del sistema de detección.

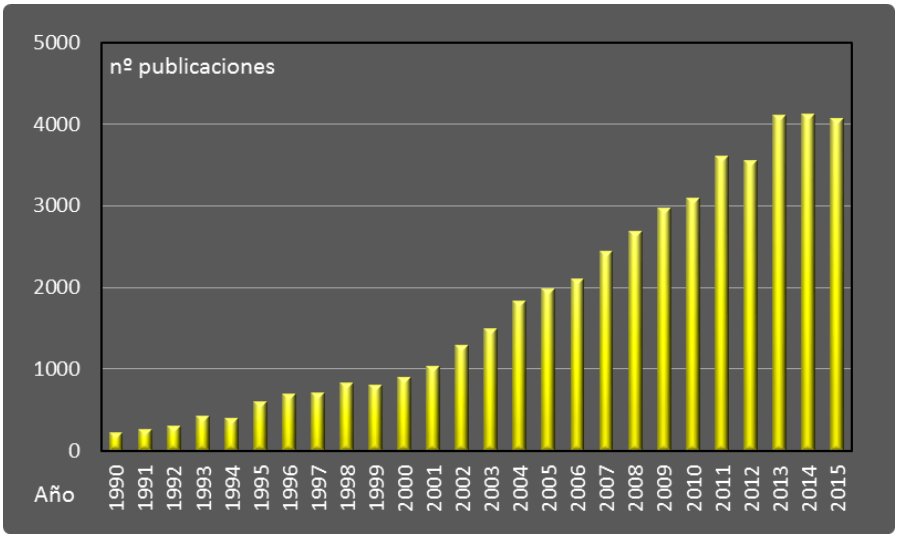

Figura 1.2. Número de publicaciones que se obtienen cuando se busca el término "*biosensor*" en Scopus entre los años 1990 y 2015.

Otro, aspecto importante de esta Tesis Doctoral es la aplicación de la **nanotecnología**, que en los últimos años ha experimentado un gran interés. En el campo de los biosensores, se utilizan nanopartículas con el fin de mejorar características como la estabilidad, la sensibilidad o la selectividad. En esta Tesis Doctoral se utilizaron nanopartículas de oro para mejorar el comportamiento de los electrodos serigrafiados como transductores para el desarrollo de los inmunosensores. También se evalúa la utilización de nanotubos de carbono en la tinta usada para la modificación de los alfileres de acero inoxidable.

Por lo tanto, en la introducción de esta Tesis Doctoral se recoge un resumen sobre las técnicas electroquímicas utilizadas como detección en los dispositivos desarrollados y una descripción sobre los diferentes tipos de biosensores que existen haciendo especial hincapié en los electroquímicos, así como un resumen sobre las enzimas utilizadas en los sensores

enzimáticos y los fundamentos de los inmunosensores. También se incluye una sección que trata sobre los electrodos serigrafiados como herramienta electródica y contextualiza la utilización de alfileres como transductores electroquímicos, y una sección sobre los sistemas de análisis por inyección en flujo y sus componentes. Finalmente, se tratan brevemente los analitos para los que se desarrollaron los diferentes biosensores.

1.2. La electroquímica como método de detección

Según indican Bockris y Reddy [11], existen dos tipos de electroquímica: la electroquímica iónica y la electroquímica electródica. La primera es la parte de la electroquímica que trata del transporte de las especies cargadas en el seno de disoluciones de electrolitos. La electroquímica electródica trata de las reacciones electroquímicas, es decir, de las transformaciones químicas que sufren las sustancias como consecuencia del intercambio de electrones que se produce en la interfase electrodo/disolución. Por tanto, la electroquímica electródica es de gran importancia ya que da lugar a técnicas analíticas de identificación y determinación de especies químicas, y junto con otros métodos como los ópticos, los térmicos, etc. forman los métodos de análisis instrumental [12].

Las técnicas electroquímicas se pueden dividir en dos grupos: estáticas o de equilibrio y dinámicas. Las técnicas de equilibrio o control termodinámico se basan en procesos electroquímicos que ocurren cuando no se aplica una fuente de excitación externa (procesos en los que la velocidad total de la reacción es cero). Las técnicas dinámicas se basan en procesos impulsados por la aplicación de una excitación externa que causa una reacción electroquímica en un sentido concreto: se consumen los reactivos generándose productos mediante una transferencia electrónica en la interfase electrodo-disolución. Los dos procesos redox que puede sufrir una especie electroactiva en disolución cuando se aplica una excitación perturbando el equilibrio son oxidación y reducción. En un proceso de oxidación la especie electroactiva cede electrones al electrodo, mientras que en un proceso de reducción, es el electrodo quien proporciona electrones a la especie electroactiva. Las diferentes posibilidades en el tipo y la magnitud de la excitación determinan la amplia variedad existente de técnicas electroquímicas [13].

La corriente generada en una reacción electroquímica tiene dos contribuciones: la corriente faradaica (que proviene de las reacciones electroquímicas) y la corriente capacitiva (debida a modificaciones de la doble capa iónica).

La corriente faradaica depende de la velocidad de cada una de las etapas de la reacción electroquímicas. Estas etapas son (**Figura 1.3**):

- Transferencia de masa de la especie electroactiva desde el seno de la disolución a la superficie electródica.
- Transferencia electrónica en la interfase electrodo-disolución entre la especie electroactiva y el electrodo.
- Transferencia de masa del producto de la reacción de transferencia electrónica hasta el seno de la disolución.

En algunos casos pueden producirse procesos de adsorción/desorción de las especies en la superficie electródica o reacciones químicas acopladas.

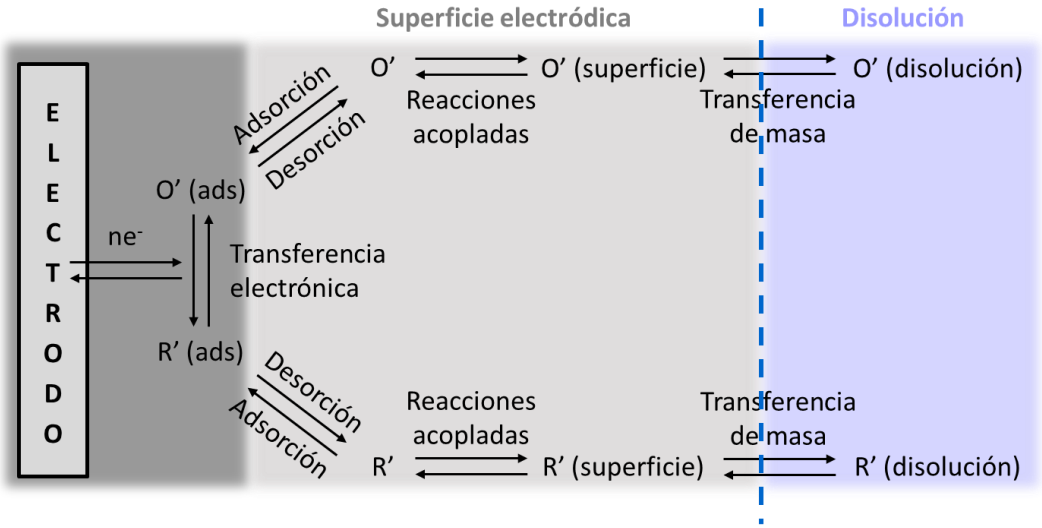

Figura 1.3. Etapas generales de una reacción electroquímica. Adaptada de la referencia [13].

La velocidad de la reacción electroquímica depende de la velocidad de cada una de estas etapas, pero una de ellas será el paso limitante de la reacción y por tanto, será la que determine la velocidad de la misma. En las condiciones más típicas (sin procesos acoplados), la velocidad de una reacción electroquímica está controlada por dos factores principales: la velocidad de la transferencia electrónica y la velocidad con la que las especies se mueven en la disolución hacia y desde la superficie electródica. De esta manera, si una reacción electroquímica está limitada por la transferencia de masa, es decir, la velocidad de transferencia electrónica es alta, se dice que es una reacción reversible (el equilibrio termodinámico se establece rápidamente tras la aplicación del sobrepotencial). Mientras que si la reacción está limitada por la velocidad de la transferencia electrónica, se habla de un proceso irreversible (se requiere un sobrepotencial mayor y el equilibrio termodinámico tarda más en establecerse).

La transferencia de masa en una celda electroquímica puede estar compuesta por tres factores:

- **Convección**: movimiento de especies debido a una fuerza mecánica, externa (agitación de la disolución) o natural (dada por diferencias de densidad en la disolución debidas a gradientes térmicos que se pueden generar en experimentos electroquímicos de tiempos largos).

- **Migración**: movimiento de especies cargadas debido a un gradiente de potenciales. Si se utiliza un electrolito de fondo inerte en gran exceso, la influencia de este transporte de masa de la especie electroactiva de interés se suprime.
- **Difusión**: movimiento de las especies generado por un gradiente de concentraciones (la especie difunde desde una zona con una mayor concentración hacia una zona con menor concentración).

Generalmente, en los experimentos electroquímicos la migración y la convección pueden minimizarse trabajando en una disolución en reposo y con una alta concentración de electrolito de fondo. Así, el único factor que influye en la transferencia de masa es la difusión.

La corriente capacitiva es debida a la distribución de cargas que se produce en la interfase electrodo-disolución. En esta interfase se genera una doble capa eléctrica cuyo funcionamiento es análogo al de un condensador eléctrico de manera que parte de la corriente en la celda electroquímica es utilizada para cargar el condensador y no para llevar a cabo la reacción electroquímica. Esta doble capa se produce porque, tras la aplicación de un potencial, la superficie del electrodo de trabajo se carga y se produce una reorganización de las cargas eléctricas de la disolución para mantener el balance neutro en la interfase. Entonces, iones presentes en la disolución migran para compensar la densidad de carga local de la superficie, generándose así un flujo de corriente no faradaica. En la capa cargada de la disolución cercana a la interfase, se pueden distinguir dos regiones o capas. Un modelo comúnmente utilizado para explicar la interfase electrodo-disolución es el modelo Gouy-Chapman-Stern [13] (**Figura 1.4**). Según este modelo, la primera capa, que está en contacto cercano con el electrodo, está formada por iones compactos solvatados por el disolvente con una carga contraria a la del electrodo. Esta capa cercana a la interfase electrodo/disolución es la llamada capa compacta o plano interno de Helmholtz (IHP) y su tamaño es similar al tamaño de los iones hidratados (unos pocos Angstroms). En la segunda capa, que está más alejada del electrodo, las fuerzas electrostáticas son más débiles y la distribución iónica está afectada por la agitación térmica aleatoria. Esta segunda capa es la capa difusa o plano externo de Helmholtz (OHP) y puede llegar a tener una longitud de nanómetros. Se compone principalmente de iones hidratados de carga contraria al electrodo (aunque ya puede encontrarse algún ion de la misma carga que el electrodo) y que interaccionan por fuerzas electrostáticas de largo alcance. El exceso de carga de esta capa disminuye gradualmente con la distancia al electrodo hasta llegar al seno de la disolución. La corriente capacitiva siempre va estar presente y, como el sistema de medida no puede separar las corrientes según su

naturaleza, la corriente medida será la suma de la corriente faradaica y de la capacitiva (o no faradaica).

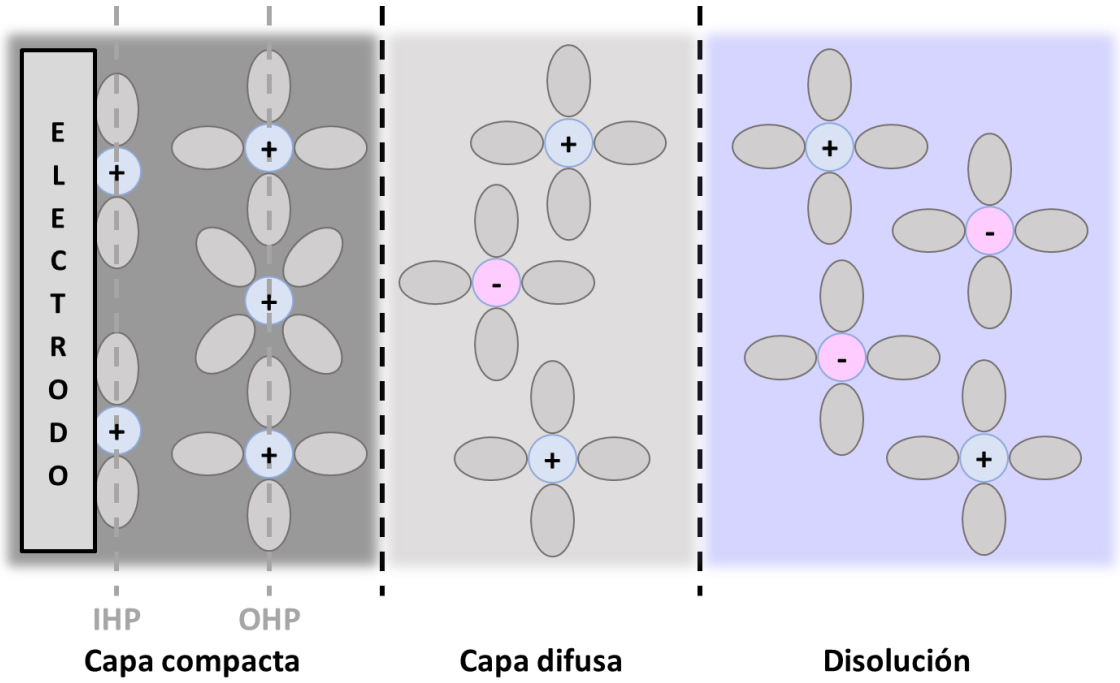

Figura 1.4. Esquema de la doble capa eléctrica según el modelo de Gouy-Chapman-Stern.

1.2.1. Celda electroquímica

Los componentes básicos necesarios para llevar a cabo una medida electroquímica son la celda electroquímica y el circuito electrónico que controla y mide la corriente o el potencial según la técnica electroquímica empleada (potenciostato).

La celda electroquímica puede ser de dos o de tres electrodos. En el primer caso, la celda está formada por un electrodo de trabajo y un electrodo de referencia. El de trabajo es el electrodo en el que ocurre la reacción electroquímica de interés. Por su parte, la función del electrodo de referencia es proporcionar un potencial estable frente al cual se monitoriza el potencial aplicado al electrodo de trabajo. El principal problema de este tipo de celdas es que se produce una disminución en el potencial aplicado (caída óhmica) debido a que parte del potencial tiene que traspasar la resistencia de la disolución, por lo que en ocasiones no es posible controlar adecuadamente el potencial del electrodo de trabajo.

Las celdas electroquímicas de tres electrodos están formadas por un electrodo de trabajo, uno de referencia y uno auxiliar (o contraelectrodo). En estas celdas la corriente

electrolítica fluye entre el electrodo de trabajo y el auxiliar, mientras que el potencial del electrodo de trabajo se controla frente al de referencia, de manera que entre el electrodo de trabajo y el de referencia no fluye corriente. Según la de Ohm la diferencia de potencial, *V*, es igual al producto de la resistencia, *R*, por la intensidad, *i* ($V = i \cdot R$). Por tanto, la presencia del electrodo auxiliar para evitar el flujo de corriente entre el electrodo de trabajo y el referencia, además de mejorar la estabilidad experimental del electrodo de referencia, minimiza la caída óhmica por lo que el potencial aplicado está mejor controlado. Aun así, incluso en los sistemas de tres electrodos la caída óhmica no puede ser eliminada por completo, ya que existe una resistencia incompensada en la celda (Ru) debida a la distancia física entre el electrodo de trabajo y el de referencia.

Las celdas de tres electrodos son por tanto las más utilizadas en estudios electroquímicos. Como electrodo auxiliar se escoge generalmente un material inerte bajo las condiciones de la reacción electroquímica (por ejemplo, un hilo de platino [14]) con un área mayor que la del electrodo de trabajo. El electrodo de trabajo suele ser metálico (oro, platino, plata,...), de carbono (pasta de carbono, carbono pirolítico, carbono vítreo, nanotubos de carbono,…), o de materiales semiconductores (silicio, óxido de indio y estaño,…) y puede tener diferentes geometrías. En cuanto al electrodo de referencia, el más utilizado es el electrodo de plata/cloruro de plata (Ag/AgCl) basado en la reacción redox:

$$\mathrm{AgCl}\ (s) + \mathrm{e^-} \leftrightarrow \mathrm{Ag}\ (s) + \mathrm{Cl^-}\ (aq)$$

Este electrodo de referencia consiste en un hilo de plata anodizado con una fina capa de AgCl y sumergido en una disolución saturada de cloruro potásico (KCl) donde un tapón poroso actúa como puente salino.

1.2.2. Técnicas electroquímicas

Como ya se ha indicado anteriormente, existe una amplia variedad de técnicas electroquímicas según el tipo y magnitud de la excitación aplicada para producir la reacción electroquímica, y la magnitud medida como señal electroquímica. A continuación se explicarán brevemente las técnicas electroquímicas empleadas lo largo de este trabajo como técnicas de detección: la voltamperometría cíclica, la voltamperometría de redisolución anódica y la cronoamperometría.

1.2.2.1. Voltamperometría cíclica

La voltamperometría cíclica es la técnica electroquímica más utilizada tanto para estudiar procesos redox como para caracterizar el comportamiento de un electrodo. Esta técnica se basa en la medida de la intensidad de la corriente generada cuando se realiza un barrido de potencial. Este se aplica en sentido directo (desde un potencial inicial E_0 hasta un potencial final E_i) e inverso (desde el potencial E_i hasta un potencial E_{ii} que suele ser igual, aunque no necesariamente, a E_0), realizando lo que se denomina un barrido triangular de potencial como muestra la **Figura 1.5**. La pendiente correspondiente a la variación del potencial con el tiempo es la velocidad de barrido (v). La voltamperometría lineal es una técnica similar a la cíclica en la que sólo se realiza el barrido de potencial en sentido directo. Los parámetros más importantes en la voltamperometría cíclica son las intensidades de corriente del pico anódico (i_{pa}) y catódico (i_{pc}), los potenciales del pico anódico (E_{pa}) y catódico (E_{pc}), y la velocidad de barrido (v).

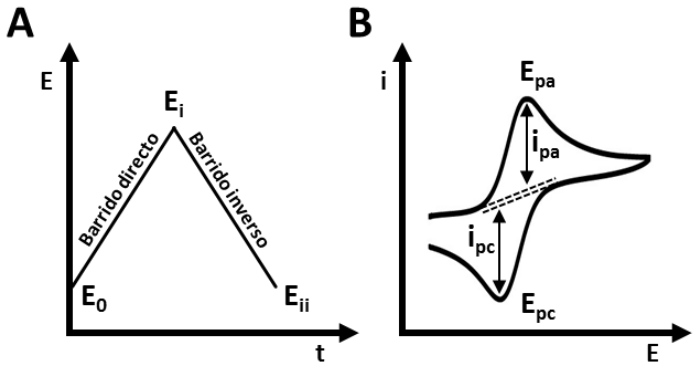

Figura 1.5. Formato de excitación (A) y respuesta (B) en voltamperometría cíclica. E_0 es el potencial inicial, E_i el potencial de inflexión, E_{ii} el potencial final, E_{pa} el potencial del pico anódico, E_{pc} el potencial del pico catódico, i_{pa} la intensidad de corriente de pico anódico y i_{pc} la intensidad de corriente del pico catódico.

La diferencia entre los potenciales E_{pa} y E_{pc} (ΔE_p) se puede usar para estimar la reversibilidad de un proceso redox. Para una transferencia electrónica reversible, el valor de ΔE_p es independiente de la velocidad de barrido y se calcula como:

$$\Delta E_p = \frac{59\ mV}{n} \qquad (\mathbf{1})$$

donde n es el número de electrones intercambiados en la reacción electroquímica. Este es un valor teórico que puede variar según las condiciones experimentales, pero, para similares condiciones experimentales, el valor de ΔE_p puede ser usado para comparar la reversibilidad

de diferentes procesos redox. Normalmente cuanto menor es el valor de ΔE_p, mayor es la reversibilidad (la transferencia electrónica es más rápida). Además, en sistemas redox con baja reversibilidad, ΔE_p aumenta con la velocidad de barrido. Por otra parte, la relación entre la intensidad del pico anódico y la del pico catódico (i_{pa}/i_{pc}) también se puede usar como estimación de la reversibilidad de un sistema redox. Si las especies generadas en el barrido de E_0 a E_i son estables con el tiempo, los picos de intensidad de corriente deberían ser iguales (por tanto el cociente i_{pa}/i_{pc} sería 1) y la transferencia electrónica es reversible en ambas direcciones. Si la transferencia electrónica muestra una reversibilidad menor, el valor de i_{pa}/i_{pc} se va alejando de 1 (puede ser mayor o menor que 1). Este cociente se ve fuertemente afectado por reacciones acopladas al proceso redox.

La corriente faradaica generada en una voltamperometría cíclica (la intensidad de corriente del pico) de un sistema electroquímico controlado por difusión es proporcional a la raíz cuadrada de la velocidad de barrido de acuerdo con la *ecuación de Randles-Sevcik* (para un electrodo plano a 25^0C y un proceso reversible) [13]:

$$i_p = (2.69 \cdot 10^5)\, n^{3/2}\, A\, C^* D^{1/2}\, v^{1/2} \qquad (\mathbf{2})$$

donde i_p es la intensidad de corriente del pico (A), n el número de electrones intercambiados en la reacción electroquímica, A el área del electrodo (cm^2), C^* la concentración de la especie electroactiva en la disolución ($mol \cdot cm^{-3}$), D el coeficiente de difusión de la especie electroactiva ($cm^2 \cdot s^{-1}$) y v la velocidad de barrido de potencial ($V \cdot s^{-1}$).

En el caso de un sistema electroquímico controlado por adsorción, la corriente faradaica sigue la siguiente ecuación que muestra su dependencia lineal con la velocidad de barrido (v):

$$i_p = \frac{n^2\, F^2\, A\, \Gamma^*}{4\, R\, T}\, v \qquad (\mathbf{3})$$

donde F es la constante de Faraday ($C \cdot mol^{-1}$), Γ^* la concentración de la especie adsorbida, R la constante universal de los gases ideales ($J \cdot mol^{-1} \cdot K^{-1}$) y T la temperatura (K)

1.2.2.2. Voltamperometría de redisolución anódica

La voltamperometría de redisolución anódica es especialmente utilizada en la determinación de metales (o complejos metálicos) ya que permite su preconcentración en la superficie del electrodo y su posterior redisolución. Esta técnica consiste básicamente en dos etapas que se describen brevemente a continuación (**Figura 1.6**):

1. **Preconcentración**: en esta etapa se aplica, durante un tiempo determinado, un potencial al que la especie electroactiva se reduce, de manera que se preconcentra sobre la superficie electródica.
2. **Redisolución**: en esta etapa se aplica un barrido de potenciales desde el potencial de reducción empleado para la preconcentración, hasta un potencial donde se produce la reoxidación (y redisolución) de la especie. En condiciones normales, la corriente generada es proporcional a la cantidad de especie preconcentrada en el electrodo, y por tanto, a la concentración de esta en disolución.

Debido a la preconcentración de la especie sobre el electrodo, la intensidad de corriente que se obtiene en la reoxidación es mayor que la que se obtendría en la reducción (que estaría limitada por la difusión de la especie al electrodo). De esta manera, se obtienen mejores límites de detección en comparación con la determinación directa de la especie.

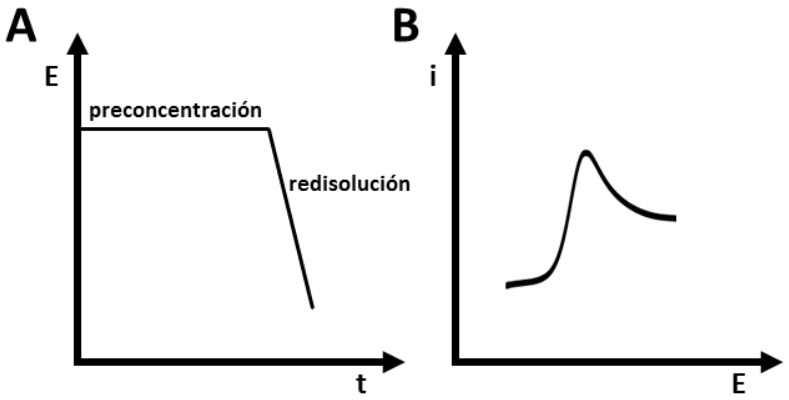

Figura 1.6. Perfil de la variación de potencial *vs*. tiempo que se aplica (A), y forma de la curva intensidad *vs*. potencial (B) que se obtiene, en voltamperometría de redisolución anódica.

1.2.2.3. Cronoamperometría

La cronoamperometría se basa en la medida de la corriente electrolítica en función del tiempo cuando se aplica un potencial (**Figura 1.7**). Este potencial puede ser constante durante toda la medida o, en experimentos más complicados, se pueden aplicar diferentes potenciales durante diferentes tiempos a lo largo de toda la medida.

En una cronoamperometría la intensidad faradaica decae exponencialmente desde un valor teórico de infinito a $t = 0$ y tiende a cero a medida que aumenta el tiempo. Para un electrodo plano, cuando el transporte de masa es controlado por difusión, la relación entre la corriente y el tiempo viene dada por la *ecuación de Cottrell*:

$$i = \frac{nFAD^{1/2}C^*}{\pi^{1/2}t^{1/2}} \qquad (\mathbf{4})$$

donde *i* es la intensidad de corriente (A), n el número de electrones intercambiados en la reacción electroquímica, *F* la constante de Faraday ($C \cdot mol^{-1}$), *A* el área del electrodo (cm^2), *D* el coeficiente de difusión de la especie electroactiva ($cm^2 \cdot s^{-1}$), *C** la concentración de la especie electroactiva en la disolución ($mol \cdot cm^{-3}$) y *t* el tiempo (s). Esta ecuación indica que la intensidad de corriente faradaica es inversamente proporcional a la raíz cuadrada del tiempo.

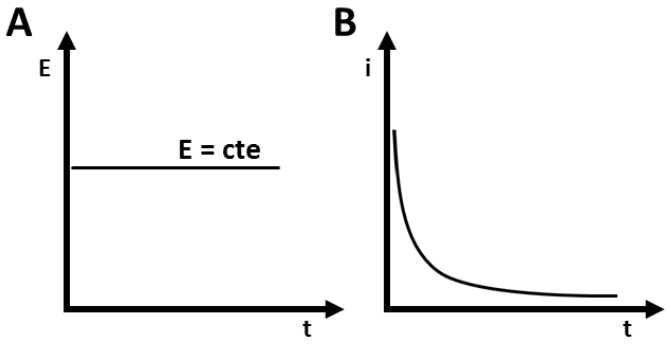

Figura 1.7. Formato de excitación (A) y respuesta (B) para una cronoamperometría.

1.3. Biosensores electroquímicos

Un sensor químico se puede definir como un dispositivo que transforma información química, que puede ir desde la concentración de un componente específico de una muestra hasta el análisis total de la composición de esta, en una señal analíticamente útil [15]. Un sensor químico consta principalmente de dos componentes básicos conectados en serie: un receptor o elemento de reconocimiento del analito y un transductor (**Figura 1.8**). La función del elemento de reconocimiento consiste, como su propio nombre indica, en reconocer de manera específica al analito de interés en la matriz de una muestra. El transductor se encarga de interpretar la reacción de reconocimiento transformándola en una señal cuantificable.

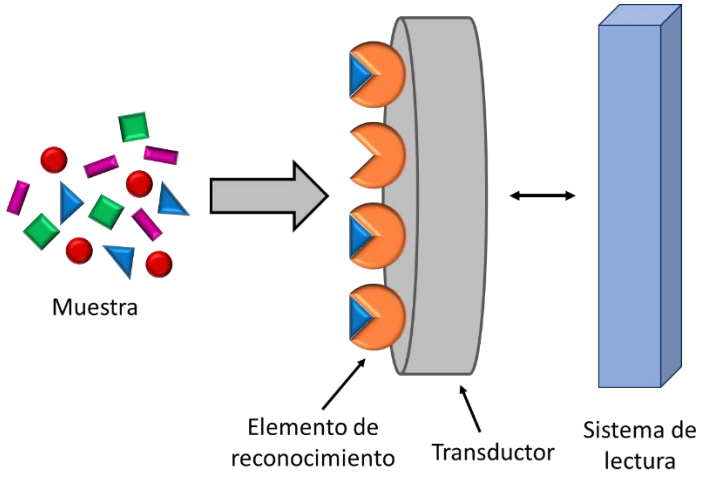

Figura 1.8. Esquema de los principales componentes de un sensor químico.

Dentro de los sensores químicos se encuentran los **biosensores**, en los cuales el sistema de reconocimiento utiliza mecanismos o principios biológicos. Este sistema de reconocimiento biológico (o bioreceptor) tiene como misión aportar al sensor un alto grado de selectividad hacia el analito. Idealmente, el bioreceptor debería detectar únicamente el analito de interés y no reaccionar ante otras especies. No obstante, hay que decir que, en realidad, habitualmente no se cumple esta situación ideal, sino que en general el bioreceptor actúa, en mayor o menor medida, sobre un conjunto de especies similares. El primer biosensor fue descrito por Clark y Lyons en 1962 y consistía en un sensor enzimático electroquímico para la determinación de glucosa. Estaba basado en el atrapamiento de la enzima glucosa oxidasa mediante una membrana de diálisis sobre un electrodo de O_2 [16]. Esta invención fue el germen del sensor de glucosa tan utilizado a día de hoy por personas diabéticas para su control en sangre.

Los biosensores se pueden clasificar, principalmente, de acuerdo al mecanismo biológico de reconocimiento o al modo de transducción de la señal [17]. Según el tipo de elemento de reconocimiento, los biosensores pueden ser [15,18,19]:

- **catalíticos**, cuando el reconocimiento del analito está basado en una reacción catalizada ya sea por enzimas (lo más habitual) o por células, tejidos o microorganismos que pueden contener enzimas que actúen como elemento de reconocimiento;
- **de afinidad** entre los que se encuentran los inmunosensores (el elemento de reconocimiento es un anticuerpo o un antígeno), los genosensores (usan ácidos nucleicos como elemento de reconocimiento), los aptasensores (donde el elemento de reconocimiento es un aptámero), los basados en quimiorreceptores (la reacción de reconocimiento consiste en una interacción entre el analito o ligando y un receptor biológico) y los basados en polímeros molecularmente impresos (*molecularly imprinted polymers*, MIPs).

Según el transductor, los biosensores pueden ser principalmente electroquímicos, ópticos, piezoeléctricos o térmicos. Los métodos de detección más usados en biosensores son los electroquímicos, seguidos por los ópticos y los piezoeléctricos. Más de la mitad de los biosensores desarrollados en la bibliografía son electroquímicos debido a su alta sensibilidad, sencillez, competitividad en costes y fácil miniaturización [18,20].

Los biosensores electroquímicos miden cambios electroquímicos que ocurren cuando una especie química interacciona con el elemento de reconocimiento conectado con el transductor. Estos cambios suelen ser variaciones en el potencial (potenciometría), en la corriente (amperometría), en la resistencia al paso de corriente (de impedancia) o en la conductividad del medio (conductimetría) [15].

Los transductores electroquímicos son los más utilizados para el desarrollo de biosensores debido a una serie de importantes ventajas [18,21]:

- La señal obtenida es eléctrica y por tanto es factible la transducción directa de la velocidad de reacción en la señal de lectura.
- Las medidas electroquímicas pueden llevarse a cabo en volúmenes pequeños de muestra con relativa facilidad gracias a la naturaleza interfacial de la medida electroquímica, lo que hace que estos dispositivos sean especialmente adecuados para la monitorización *in vivo*.
- La sensibilidad de los métodos electroquímicos no depende del volumen, lo que permite trabajar con pequeños volúmenes de muestra.

- Los límites de detección que se obtienen son suficientes y adecuados para la detección de un gran número de analitos de interés.
- La relativa simplicidad y el bajo coste de la instrumentación necesaria permite una fácil disponibilidad de estos dispositivos. Además, su fácil miniaturización hace posible el desarrollo de sensores portables para su aplicación *in situ*.
- Los transductores electroquímicos permiten la detección en muestras turbias o coloreadas, lo que implica una gran ventaja frente a la transducción óptica.

1.3.1. Características analíticas de los biosensores

Las características analíticas de los biosensores se pueden determinar mediante los parámetros típicos para la caracterización de un método analítico convencional. Estos parámetros son útiles para comparar biosensores diferentes en términos de calidad de resultados, robustez de operación, estabilidad de respuesta y almacenamiento. En la bibliografía se pueden encontrar libros que tratan extensamente estos parámetros [22,23]. A continuación se van a introducir brevemente los más importantes:

- **Exactitud**: grado de concordancia entre el resultado de una determinación (o la media de *n* resultados) dado por el biosensor y la concentración real del analito en la muestra.
- **Precisión**: grado de concordancia entre un grupo de medidas independientes y repetitivas realizadas en diferentes alícuotas de la misma muestra. Dentro de la precisión se pueden distinguir dos términos: repetitibilidad, cuando las medidas son realizadas en las mismas condiciones (mismo operador, aparatos y laboratorio, y en un intervalo corto de tiempo) y reproducibilidad, cuando las condiciones bajo las que se realizan las medidas son diferentes (diferente operador, aparatos, laboratorios y en largos periodos de tiempo).
- **Selectividad**: indica la capacidad del biosensor para determinar un analito en una muestra sin que otras especies presentes en la muestra interfieran en la medida.
- **Intervalo dinámico**: es el rango de concentraciones que el biosensor es capaz de detectar.
- **Sensibilidad**: indica el cambio en la respuesta del biosensor producido por una variación (en una unidad) en la concentración del analito. Para una concentración de analito fija, la sensibilidad será mayor cuanto mayor sea el cambio en la respuesta dada por el biosensor. Si la respuesta del biosensor se relaciona con la concentración del analito de forma lineal, es decir, mediante una recta de calibrado, la pendiente de esa recta es la sensibilidad.

- **Límite de detección (*limit of detection*, LOD)**: es la mínima concentración (o cantidad) de analito que el biosensor es capaz de detectar con un grado de incertidumbre aceptable.
- **Límite de cuantificación (*limit of quantification*, LOQ)**: es la mínima cantidad de analito que el biosensor es capaz de cuantificar con un grado de incertidumbre aceptable.

1.3.2. Inmovilización del elemento de reconocimiento

Desde el desarrollo del primer sensor (el sensor de glucosa de Clark en 1962 [16]) en el que la enzima glucosa oxidasa estaba retenida entre dos membranas, se han descrito numerosos método de inmovilización del material biológico para el desarrollo de biosensores. Este proceso es el más importante en la fabricación de un biosensor ya que de él dependen características tan cruciales como el tiempo de vida o la sensibilidad del mismo. El principal problema que puede acarrear el proceso de inmovilización es la alteración de la conformación del material biológico respecto a su estado nativo implicando una pérdida en su capacidad de reconocer al analito. En general, los métodos de inmovilización se pueden clasificar en dos grupos: **físicos**, donde se incluye la adsorción y el atrapamiento; y **químicos**, entre los que se encuentran el entrecruzamiento y las monocapas autoensambladas [15,18,24]. En la bibliografía se pueden encontrar varias revisiones en las que se recogen los diferentes métodos de inmovilización [25-27], por lo que a continuación solo se comentarán de manera resumida algunos de ellos.

Adsorción física

La adsorción se basa en interacciones de tipo no covalente como fuerzas electroestáticas, hidrofóbicas, enlaces de hidrógeno o de Van der Walls. El procedimiento habitual consiste en incubar una disolución del receptor biológico sobre la superficie electródica durante un tiempo. La adsorción es un método de inmovilización sencillo, rápido y de bajo coste que no implica cambios en la conformación del material biológico, pero tiene como inconvenientes su poca estabilidad mecánica y la debilidad de la unión al soporte.

Atrapamiento

El atrapamiento consiste en la inclusión del elemento de reconocimiento dentro de una matriz de un polímero altamente entrecruzado (o un gel) o de una membrana semipermeable. La matriz polimérica o la membrana pueden ser, en cierta medida, selectivos permitiendo el

paso del analito pero no de algunas especies que puedan ser interferentes. Otra forma de atrapamiento es la inclusión del elemento de reconocimiento en la propia matriz del transductor (es decir, del electrodo en el caso de biosensores electroquímicos).

Unión covalente

La unión covalente consiste en la unión de grupos funcionales del elemento de reconocimiento (que no participan en el reconocimiento del analito) con la superficie activada del transductor. Por esta razón, la elección de la superficie del transductor es crucial ya que determinará la reacción de inmovilización y la estabilidad de esta.

Entrecruzamiento

El entrecruzamiento o *cross-linking* es un tipo de inmovilización covalente que consiste en la unión entre el elemento de reconocimiento y la superficie del transductor mediante espaciadores con dos (o más) grupos funcionales reactivos. Si los dos grupos funcionales son iguales se habla de *crosslinkers* homobifuncionales como es el caso del glutaraldehido (muy común); si son diferentes se dice que el *crosslinker* es heterobifuncional. Estos últimos son menos usados aunque proporcionan una mayor selectividad en cuanto a la inmovilización debido a la diferente reactividad de los grupos funcionales. Este método es muy utilizado ya que es bastante rápido y simple. Su mayor desventaja es la posibilidad de que el elemento de reconocimiento sufra alteraciones químicas o conformacionales disminuyendo su capacidad de reconocimiento.

Monocapas autoensambladas

Las monocapas autoensambladas (*self-assembled monolayers*, SAMs) son monocapas de un compuesto generadas sobre la superficie del transductor. Este compuesto muestra, por un extremo, una alta afinidad por la superficie del transductor, mientras que por el otro posee un grupo funcional que puede interaccionar con el elemento de reconocimiento (generalmente mediante un enlace covalente). Un ejemplo típico de este método de inmovilización son las SAMs de tioles sobre superficies de oro.

Unión de afinidad

Este método consiste en modificar el transductor con alguna especie que se una por afinidad al elemento de reconocimiento (la interacción debe darse en alguna posición del elemento de reconocimiento que no influya en su función). El sistema más utilizado es el

complejo estreptavidina-biotina: el transductor está modificado con estreptavidina y el elemento de reconocimiento con biotina, de manera que, tras su interacción el elemento de reconocimiento queda unido al transductor. Si el elemento de reconocimiento está funcionalizado con biotina en una posición determinada, se puede conseguir que este quede unido al transductor con una orientación determinada dejando la zona de interacción con el analito más disponible para la reacción de reconocimiento.

1.3.3. Biosensores enzimáticos electroquímicos

Los biosensores electroquímicos enzimáticos se basan en el acoplamiento de una o varias enzimas con un transductor electroquímico, combinando la especificidad de la(s) enzima(s) hacia el(los) sustrato(s) con la alta sensibilidad de las técnicas electroquímicas.

Las enzimas son proteínas que catalizan reacciones bioquímicas en los sistemas vivos. Estos catalizadores además de eficientes, muestran una alta selectividad por su sustrato. Las enzimas son utilizadas habitualmente como elemento de reconocimiento biológico en biosensores debido a su disponibilidad comercial y a su facilidad de aislamiento y purificación. Su mayor inconveniente es su estabilidad, de manera que la gradual pérdida de actividad de la enzima generalmente es lo que determina la vida útil del biosensor [25].

La reacción enzimática, que además del sustrato en muchas ocasiones requiere el uso de otro reactivo (cofactor), es un proceso dinámico que consta de varias etapas que se pueden resumir como sigue: i) el sustrato es enlazado al sitio de unión de la enzima formando el complejo enzima-sustrato; ii) el sustrato experimenta una reacción química generalmente con la participación del cofactor; iii) el producto generado es liberado y el sitio activo de la enzima vuelve al estado inicial para comenzar un nuevo ciclo de reacción. La detección en el biosensor puede ser del producto de la reacción o del cofactor. Pero también se puede detectar el sustrato o alguna especie inhibidora de la reacción enzimática.

En los biosensores enzimáticos, el uso de dos o más enzimas puede aportar ventajas como [28]: i) aumento de la sensibilidad al utilizar una enzima auxiliar que regenere el analito dando lugar por tanto a un “reciclado” del sustrato; ii) generación de una especie más fácilmente detectable que los productos de la reacción enzimática principal, al emplear una enzima auxiliar que actúe sobre alguno de estos productos; iii) eliminación de interferencias ya que puede ocurrir que alguno de los productos de la reacción enzimática principal inhiba la actividad enzimática o que existan inhibidores en disolución, de manera que la enzima auxiliar

puede reaccionar con esos interferentes eliminando su efecto en la reacción enzimática de interés.

1.3.3.1. Enzimas

El mecanismo de las reacciones enzimáticas se puede encontrar detalladamente explicado en diversos libros de bioquímica y biosensores [24,29], por lo que aquí se va a tratar de manera muy resumida. El modelo cinético se basa en la formación del complejo enzima-sustrato como se muestra a continuación:

$$S + E \underset{k_{-1}}{\overset{k_1}{\rightleftharpoons}} ES \xrightarrow{k_2} E + P$$

Donde *S* es el sustrato, *E* la enzima, *ES* el complejo enzima-sustrato y k_1, k_{-1} y k_2 las constantes de velocidad de las reacciones correspondientes. Considerando el modelo cinético que sigue la aproximación del estado estacionario, la concentración del complejo enzima-sustrato es constante, por lo que la velocidad de formación del complejo es compensada por la velocidad de su disociación en enzima y sustrato y por la velocidad de formación del producto. La velocidad de la reacción, es decir, de la formación del producto vendrá dada por la ecuación de Michaelis-Menten:

$$v = \frac{d[P]}{dt} = \frac{-d[S]}{dt} = k_2[ES] = k_2[E_0]\frac{[S]}{K_m + [S]} = V_{max}\frac{[S]}{K_m + [S]} \qquad (\mathbf{5})$$

donde $[E_0]$ es la concentración inicial de enzima, V_{max} la velocidad máxima de la reacción y K_m la constante de Michaelis-Menten:

$$K_m = \frac{k_{-1} + k_2}{k_1} \qquad (\mathbf{6})$$

Para una enzima, la velocidad de la reacción, *v*, es función de la relación $[S]/K_m$:
Cuando $[S] << K_m$, $v \approx (V_{max}/K_m)[S]$ (cinética de primer orden respecto a $[S]$).
Cuando $[S] >> K_m$, $v \approx V_{max}$ (cinética de orden cero respecto a $[S]$). En este caso, $v = V_{max} = k_2[E_0]$.
Cuando $[S] = K_m$, $v = V_{max}/2$, es decir, K_m es la concentración de sustrato necesaria para alcanzar la mitad de la velocidad máxima.

La K_m da una idea sobre la afinidad que tiene el enzima por su sustrato, siendo esta mayor cuanto menor sea K_m.

A continuación se comentan brevemente algunas características de las enzimas que se han empleado a lo largo de este trabajo para el desarrollo de biosensores enzimáticos.

Enzimas oxidasas: glucosa oxidasa y alcohol oxidasa

Las enzimas oxidasas, dentro de las cuales se encuentran la glucosa oxidasa y la alcohol oxidasa, utilizan oxígeno molecular como agente de reoxidación en el ciclo catalítico. Dependiendo de que la enzima done dos o cuatro electrones al oxígeno, el producto final de la reacción es peróxido de hidrógeno (H_2O_2) o agua. De este modo, la reacción enzimática puede monitorizarse electroquímicamente o bien mediante la disminución del contenido de oxígeno en la disolución o, si el H_2O_2 es el producto final, mediante su oxidación (o reducción) electroquímica sobre el electrodo [28]. Aunque existen enzimas oxidasas que no tienen ni requieren cofactor [30], las más comunes sí que dependen de un cofactor fuertemente enlazado dentro de su estructura que media en la transferencia electrónica. La estructura de ese cofactor es o bien del tipo flavina (dinucleótido de flavina adenina (FAD) o mononucleótido deflavina (FMN)) o un grupo que contiene ion cobre [28,31].

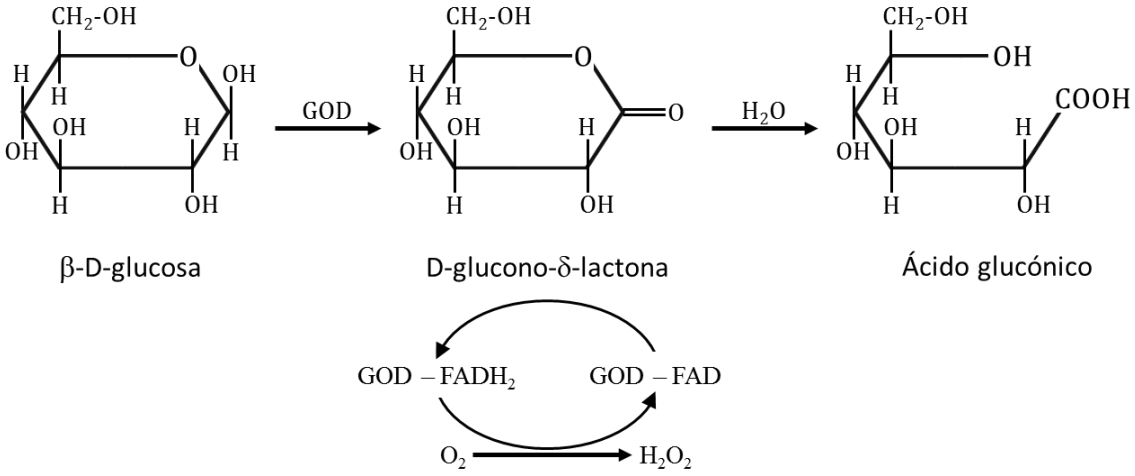

Figura 1.9. Esquema de la reacción de oxidación de la glucosa catalizada por la glucosa oxidasa. Figura adaptada de la referencia [32].

La **glucosa oxidasa** (GOx) es una enzima dimérica que habitualmente se extrae del hongo *Aspergillus niger*. Cataliza la oxidación de la *β-D*-glucosa a *D*-glucono-δ-lactona usando el

oxígeno molecular como aceptor electrónico, produciendo simultáneamente H_2O_2. En las oxidasas con cofactor del tipo flavina, la reacción de oxidación se produce mediante dos semi-reacciones: una de reducción y una de oxidación (**Figura 1.9**). En la semi-reacción de reducción, la *β-D*-glucosa se oxida a *D*-glucono-δ-lactona cuya hidrólisis no enzimática produce ácido glucónico. Mientras, el cofactor FAD de la GOx es reducido a $FADH_2$. En el paso oxidativo, el $FADH_2$ de la GOx reducida se regenera a través de su reoxidación por el oxígeno generando H_2O_2 [31-34].

La **alcohol oxidasa** (AOx) es una enzima oligomérica formada por ocho subunidades idénticas, cada una de las cuales posee el cofactor FAD fuertemente unido. La fuente más común de obtención de esta enzima son las levaduras metilotróficas como *Hansenula*, *Pichia* y *Candida*. LA AOx oxida alcoholes de bajo peso molecular (metanol, etanol, propanol,…) generando el correspondiente aldehído, utilizando el oxígeno molecular como aceptor electrónico (**Figura 1.10**). Al igual que en el caso de la GOx, la AOx es una oxidasa con cofactor de tipo flavina, y la reacción de oxidación que cataliza ser puede dividir en dos semi-reacciones: la de reducción, en la que el alcohol se oxida y el FAD se reduce a $FADH_2$, y la de oxidación, en la que el cofactor de la enzima se regenera mediante oxidación por oxígeno produciéndose H_2O_2 [31,35,36].

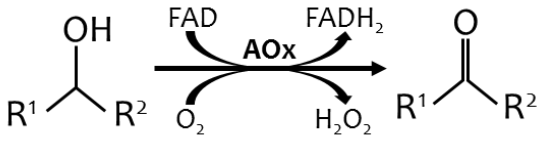

Figura 1.10. Esquema de la reacción de oxidación del alcohol catalizada por la alcohol oxidasa. R' puede ser un hidrógeno o un grupo alquilo o arilo. Figura adaptada de los artículos [31,35].

Deshidrogenasas: Fructosa deshidrogenasa

La enzima fructosa deshidrogenasa (FDH) fue aislada y parcialmente caracterizada por primera vez en 1966 por Yamada *et al*. [37]. Pertenece al grupo de las quinoproteínas, que son enzimas que contienen *o*-quinonas como cofactores y difieren completamente de aquellas enzimas que dependen de los nucleótidos de nicotina y flavina. En concreto, la FDH utiliza como cofactor quinona de pirroloquinolina (*pyrroloquinoline quinone*, PQQ), por lo que se dice que pertenece al grupo de las PQQ-deshidrogenasas [38,39]. Las bacterias acéticas (especialmente de las especies del género *Gluconobacter*) son la fuente más común de este tipo de enzimas [40].

Las PQQ-deshidrogrenasas poseen ciertas características que las hacen especialmente adecuadas para su aplicación en biosensores: la PQQ y su apoenzima forman un complejo estable por lo que el oxígeno no afecta a la actividad catalítica de la enzima y además no necesitan la presencia de un cofactor soluble que actúe como co-sustrato, a diferencia de las $NAD(P)^+$/NAD(PH) deshidrogenasas [38,41,42]. La FDH está formada por tres subunidades (la subunidad I es la que contiene el grupo PQQ) y cataliza la oxidación de *D*-fructosa para formar *5*-ceto-*D*-fructosa reduciéndose simultáneamente la PQQ a $PQQH_2$. La reacción se puede representar como [39,40,42,43]:

$$D-fructosa + aceptor\ (ox) \xrightarrow{FDH} 5-ceto-D-fructosa + aceptor\ (red)$$

Se pueden utilizar diferentes aceptores en esta reacción (mediadores electroquímicos, colorantes, etc.) para monitorizar la reacción y relacionarla con la cantidad de fructosa [18,19]. La FDH es específica para la D-fructosa y presenta baja afinidad por sustratos análogos como la *D*-glucosa, la *D*-fructosa-*6*-fosfato, la *D*-fructosa-*1,6*-bifosfato o la *5*-ceto-*D*-fructosa [39].

Peroxidasas: peroxidasa de rábano silvestre

Las peroxidasas son un grupo de oxidoreductasas que catalizan la reducción de peróxidos, como el H_2O_2, y la oxidación de una variedad de especies orgánicas e inorgánicas. Son enzimas que contienen hierro (III) y protoporfirina IX (ferriprotoporfirina IX) como grupo prostético. Las peroxidasas son muy utilizadas en bioquímica e inmunoensayos enzimáticos. Generalmente se usan para la determinación de H_2O_2 y pequeños peróxidos orgánicos [44]. Los tubérculos de raíz de rábano silvestre son la fuente habitual para la producción comercial de la peroxidasa conocida como HRP (peroxidasa de rábano silvestre).

En la reacción de una peroxidasa con el H_2O_2, la forma nativa de la enzima se oxida mediante la transferencia de dos electrones formando el denominado compuesto-I. La regeneración de la enzima en su forma nativa se lleva a cabo mediante dos etapas individuales de reducción en las que se intercambia un electrón con una especie intermedia llamada compuesto-II. Esta serie de reacciones se pueden representar así [45]:

$$\text{Peroxidasa nativa} + H_2O_2 \rightarrow \text{Compuesto-I} + H_2O$$
$$\text{Compuesto-I} + H_2A \rightarrow \text{Compuesto-II} + HA^*$$
$$\text{Compuesto-II} + H_2A \rightarrow \text{Peroxidasa nativa} + HA^* + H_2O$$

Como especies donoras de electrones pueden utilizarse aminas aromáticas, compuestos fenólicos, ferrocianuro, yoduro,… Los diseños electródicos más sencillos utilizan la

monitorización directa de la trasferencia electrónica de la peroxidasa a un potencial cercano a +0.6 V (*vs*. electrodo de calomelanos). La corriente que se genera es debida a la reducción electroquímica de los compuestos I y II que son reacciones cinéticamente lentas sobre la mayoría de los materiales electródicos. Con el fin de evitar esta transferencia electrónica lenta, los compuestos donadores de electrones que antes citamos se usan como mediadores que reaccionan rápidamente con la peroxidasa oxidada [46].

Los biosensores electroquímicos ofrecen un gran potencial para la aplicación de peroxidasas. La combinación de peroxidasa con enzimas que producen H_2O_2 (característica común de muchas oxidasas) para la fabricación de biosensores enzimáticos se ha propuesto como solución a los problemas asociados con el elevado valor del potencial requerido para la monitorización electroquímica directa de H_2O_2 [28].

1.3.3.2. Mediadores

Los mediadores son agentes artificiales de transferencia electrónica que participan en la reacción redox con el componente biológico facilitando la transferencia de electrones. Son especies de bajo peso molecular que dan lugar a reacciones redox de manera que son capaces de trasladar los electrones desde el centro redox de la enzima a la superficie del electrodo: durante la reacción catalítica, el mediador reacciona con la enzima y luego difunde hacia el electrodo para intercambiar los electrones [47]. Por ejemplo [48]:

$$\text{Glucosa} + \text{GOx (FAD)} \rightarrow \text{Glucolactona} + \text{GOx (FADH}_2\text{)}$$

$$\text{GOx (FADH}_2\text{)} + 2\ \text{Medidador (ox)} \rightarrow \text{GOx (FAD)} + 2\ \text{Mediador (red)} + 2H^+$$

$$\text{En el electrodo: 2 Mediador (red)} \rightarrow 2\ \text{Mediador (ox)} + 2\ e^-$$

La producción de mediador reducido es lo que se mide, mediante su oxidación, en el electrodo.

Las características que debería tener un mediador ideal son [47]:

- reaccionar rápidamente con la enzima.
- dar lugar a un proceso de transferencia electrónica reversible.
- ser estable en las formas oxidada y reducida.
- mostrar un bajo potencial formal e idealmente independiente del pH. El mediador debe ser escogido de manera que su potencial redox sea menor que el de las posibles interferencias electroactivas presentes en la muestra.

- no reaccionar con el oxígeno u otras especies (por lo que las medidas son menos dependientes de la concentración de oxígeno).
- no ser tóxico.

En la bibliografía se puede encontrar una amplia variedad de mediadores utilizados en biosensores enzimáticos [47] (ferroceno [48,49], azul de Prusia [50-52], tetratiofulvaleno [53],…). La incorporación de estos mediadores a un biosensor enzimático puede realizarse de diferentes formas. Por ejemplo, el mediador puede estar embebido o retenido mediante una membrana [40,53], inmovilizado mediante entrecruzamiento [54], incorporado en la matriz del electrodo de trabajo [49] o electrodepositado sobre este [50].

En los biosensores enzimáticos desarrollados a lo largo de esta Tesis Doctoral se utilizan como mediadores el ferrocianuro y la ftalocianina de cobalto. El ferrocianuro $[Fe^{II}(CN)_6]^{-4}$ tiene una geométrica octaédrica y es, junto al ferricianuro ($[Fe^{III}(CN)_6]^{-3}$) y al ferrocianuro férrico ($Fe_4^{III}[Fe^{II}(CN)_6]_3$ (azul de Prusia)), una de las formas más comunes en las que el cianuro se encuentra en la naturaleza [55].

Por otra parte, las ftalocianinas son compuestos aromáticos macrocíclicos de un intenso color verde azulado muy utilizadas como tintes. Poseen la capacidad de coordinar cationes metálicos en el centro de su estructura dando lugar a las metaloftalocianinas entre las que se encuentra la ftalocianina de cobalto (**Figura 1.11**) [56].

Tanto el ferrocianuro [57-59] como la ftalocianina de cobalto [60,61] han sido ampliamente utilizados como mediadores en biosensores enzimáticos.

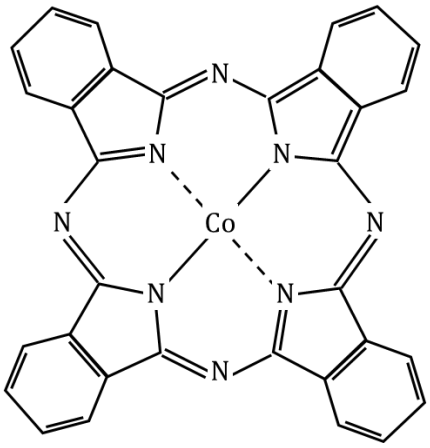

Figura 1.11. Estructura de la ftalocianina de cobalto.

1.3.4. Inmunosensores electroquímicos

Los inmunosensores son biosensores de afinidad que se basan en la reacción bioquímica que implica el reconocimiento de un antígeno por un anticuerpo, uniéndose por una zona concreta formando el complejo antígeno-anticuerpo. En el caso de los inmunosensores electroquímicos, la monitorización de esta reacción de reconocimiento se realiza mediante un transductor electroquímico. La gran selectividad de los anticuerpos viene dada por la estereoespecificidad de los puntos de unión con el antígeno (parátopos), lo que hace que estos sistemas sean sumamente interesantes para el desarrollo de biosensores, ya que permiten la detección y cuantificación de antígenos a niveles muy bajos (incluso picogramos) en muestras tan complejas como suero o plasma sanguíneo [28,62].

Generalmente es difícil de seguir de manera directa la reacción entre el anticuerpo y el antígeno, de ahí que lo más habitual sea el uso de marcas (especies unidas al anticuerpo o al antígeno que permiten saber si la reacción de afinidad ha tenido lugar). También existen inmunosensores "*label-free*" (sin marca) que, aunque suelen ser menos sensibles, cada vez están ganando más interés debido a su simplicidad [63,64]. En la bibliografía se pueden encontrar una gran variedad de marcas para inmunosensores electroquímicos como enzimas, especies electroactivas orgánicas y nanopartículas metálicas [65-68]. Las marcas más usadas tradicionalmente en inmunoensayos son las enzimas; su funcionamiento consiste en actuar sobre un sustrato añadido dando lugar a un producto detectable por el transductor, permitiendo relacionar la señal obtenida con la cantidad de antígeno unido al anticuerpo [28], que a su vez es proporcional al antígeno en disolución.

Existen varios formatos de inmunosensores según el formato de inmunoensayo en el que se basen: competitivo y no competitivo (siendo el tipo el tipo sándwich el más habitual). En un ensayo competitivo, el antígeno de la muestra y una cantidad fija de antígeno marcado compiten por los sitios de unión del anticuerpo que está presente en una cantidad fija y limitada. De esta manera, la señal que se obtiene es inversamente proporcional a la cantidad de analito que hay en la muestra. En un ensayo tipo sándwich, el antígeno se une a un anticuerpo (llamado de captura) que generalmente está inmovilizado en una superficie sólida. A su vez, el antígeno se une a un segundo anticuerpo (llamado de detección) que lleva unida una marca que es la que proporciona la señal analítica. En todos los inmunoensayos existen interacciones no específicas que se producen porque los anticuerpos o el antígeno interaccionan con otros componentes del ensayo o con la superficie de inmovilización. En general, estas interacciones hacen que se obtengan señales analíticas en ausencia de analito.

De ahí que esté extendido el uso de agentes bloqueantes con el fin de minimizar estas interacciones no específicas [69,70].

Los ensayos ELISA (*enzyme linked immunosorbent assay*), normalmente realizados en placa de pocillos, son el método más comúnmente aceptado para la detección de analitos mediante inmunoensayos. El uso de transductores electroquímicos para el desarrollo de inmunosensores muestra importantes ventajas respecto a los ELISAs como son el empleo de pequeños volúmenes de muestra, la posibilidad de análisis en tiempo real gracias a la transducción directa de la señal eléctrica en una señal medible y la obtención de bajos límites de detección. Estas ventajas junto con la posibilidad de miniaturización de la instrumentación, hace que los inmunosensores electroquímicos se postulen como una interesante alternativa a los inmunoensayos convencionales.

En el Capítulo II de esta Memoria se puede encontrar una revisión bibliográfica sobre inmunosensores basados en electrodos serigrafiados para la detección de biomarcadores en el que se da más información sobre este tipo de biosensores.

1.3.4.1. Anticuerpos

Los anticuerpos son una familia de glicoproteínas conocidas como inmunoglobulinas (Ig) producidas por los mamíferos como respuesta a la entrada en el organismo de moléculas extrañas. Son el producto de la respuesta humoral del organismo para luchar contra posibles patógenos. Existen diferentes clases de inmunoglobulinas humanas: IgG, IgM, IgA, IgD y IgE, ordenadas de mayor a menor abundancia en suero. La IgG, además de ser la más abundante, es la más utilizada en técnicas inmunoanalíticas.

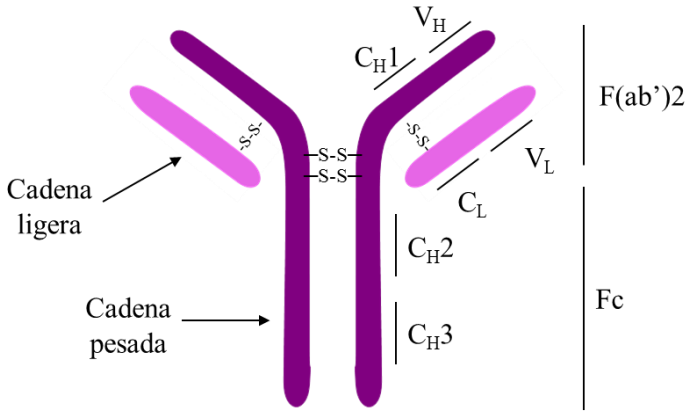

Figura 1.12. Esquema de la estructura de un anticuerpo.

Los anticuerpos se suelen representar como una molécula en forma de "Y" con dos tipos distintos de cadenas polipeptídicas que se diferencian en su peso molecular (**Figura 1.12**). La cadena más pequeña se conoce como cadena ligera, con un peso molecular de aproximadamente 25 kDa; la cadena más grande es la cadena pesada, cuyo peso molecular ronda los 50 kDa. En cada Ig hay dos cadenas pesadas y dos ligeras unidas por enlaces disulfuro. Tanto las cadenas ligeras como las pesadas tienen un dominio variable (V) y uno constante (C) denominadas así basándose en la variabilidad de su secuencia de aminoácidos. La cadena ligera posee un dominio variable (V_L) y uno constante (C_L), mientras que la cadena pesada consta de un dominio variable (V_H) y tres dominios constantes (C_H1, C_H2, C_H3; el C_H3 empieza en el carboxilo terminal de la proteína). Los dominios variables de ambas cadenas son las regiones más importantes del anticuerpo en cuanto al reconocimiento del antígeno, ya que la especificidad del anticuerpo depende de la secuencia de aminoácidos de esos dominios. En cada uno de los dominios V_L y V_H, hay tres subregiones con una mayor variabilidad, conocidas como regiones hipervariables. Por tanto, cada anticuerpo posee seis regiones que se conocen como regiones determinantes de complementariedad (*complementarity determining regions*, CDR) y que conjuntamente forman el sitio de unión al epítopo (zona del antígeno por donde se une al anticuerpo). La diversidad de las CDR es lo que permite la producción de anticuerpos con alta afinidad a casi cualquier antígeno [69,71].

Un anticuerpo se puede dividir en fragmentos por digestión con papaína: un fragmento Fc que es cristalizable, y dos fragmentos Fab que contienen los parátopos (zona de unión con el antígeno). Cuando la digestión se hace con pepsina se obtiene: un fragmento divalente F(ab')2 (dímero que contiene los dos Fab), y la parte Fc dividida en fragmentos pequeños.

Los anticuerpos pueden ser policlonales o monoclonales. Los primeros provienen de la purificación del suero de un animal que ha sido inmunizado con el antígeno (antisuero). De esta manera, linfocitos diferentes producen anticuerpos que serán diferentes, por lo que su respuesta frente al antígeno será diferente (reconocerán epítopos diferentes). Por el contrario, un anticuerpo monoclonal se obtiene aislando una a una las células que producen esos anticuerpos y haciéndolas inmortales fusionándolas con una línea celular de mieloma (linfocito canceroso) para obtener los hibridomas (líneas celulares híbridas). Estos hibridomas, al estar formados por células idénticas que son clones de una única célula, producen anticuerpos idénticos entre sí (misma afinidad, selectividad y especificidad). Aunque un anticuerpo se produce para su unión con un único antígeno, en ocasiones esto no ocurre así y un anticuerpo puede unirse a más de un antígeno (generalmente con estructuras similares) dando lugar a lo que se conoce como reactividad cruzada [69,71].

1.3.4.2. Antígeno

El **antígeno** es la molécula que penetra en el organismo y produce la respuesta inmune. El antígeno presenta inmunogenicidad (capacidad para producir la respuesta inmune) y antigenicidad (capacidad de interaccionar con los anticuerpos que su presencia ha generado). Existen moléculas pequeñas, conocidas como **haptenos**, que presentan antigenicidad pero no son capaces de generar por sí solas una respuesta inmune. Para poder generar anticuerpos, estas moléculas son conjugadas con una molécula transportadora. Hay que tener en cuenta que los anticuerpos son proteínas y también pueden generar respuesta inmune y por tanto ser antígenos que interaccionen con los anticuerpos generados. Las características del antígeno a detectar (naturaleza química, conformación, tamaños, número y accesibilidad de epítopos) son importantes a la hora de diseñar el inmunoensayo.

1.3.4.3. Fosfatasa alcalina como marca electroquímica

La fosfatasa alcalina (*alkaline phosphatase*, AP) es una enzima hidrolasa ampliamente utilizada como marca en inmunoensayos que cataliza la hidrólisis de grupos fosfato. Es un dímero con dos cationes Zn^{2+} y uno Mg^{2+} en cada sitio activo [72,73].

En inmunosensores electroquímicos, la función de la AP como marca suele consistir en generar productos electroactivos que puedan ser detectados y cuantificados electroquímicamente. Existen diversos sustratos para la AP útiles para la detección electroquímica como son el 3-indoxil fosfato (*3-indoxyl phosphate*, 3-IP) [74-76], la hidroquinona difosfato [77,78], el 4-nitrofenil fosfato [79] y el p-aminofenil fosfato [80] entre otros [81].

En nuestro grupo de investigación se desarrolló previamente un método para la utilización de la AP como marca enzimática utilizando una mezcla de 3-IP e iones plata (Ag^{+}) como sustrato [82], siendo este el método utilizado en los inmunosensores desarrollado en este trabajo. El 3-IP está formado básicamente por un anillo indólico con un grupo fosfato en la posición 3. En presencia de AP, el 3-IP se hidroliza en la posición 3 dando lugar a un intermedio indoxílico. Este intermedio sufre una tautomería ceto-enólica y en presencia del oxígeno atmosférico se oxida generando azul de índigo, un producto que es insoluble en medio acuoso y muestra un intenso color azul. A la vez que se produce esa oxidación, se reducen los iones plata presentes en la disolución, generándose plata metálica (Ag^{0}) que se deposita sobre el electrodo junto con el azul de índigo. Esa plata metálica depositada se puede detectar mediante voltamperometría de redisolución anódica (**Figura 1.13**). Como el producto

de la reacción enzimática que se mide, la plata metálica, se deposita sobre el electrodo donde estaba la AP, se evita la difusión del producto detectable a los electrodos vecinos, lo que permite la detección simultánea de dos o más analitos en electrodos colindantes utilizando la misma marca.

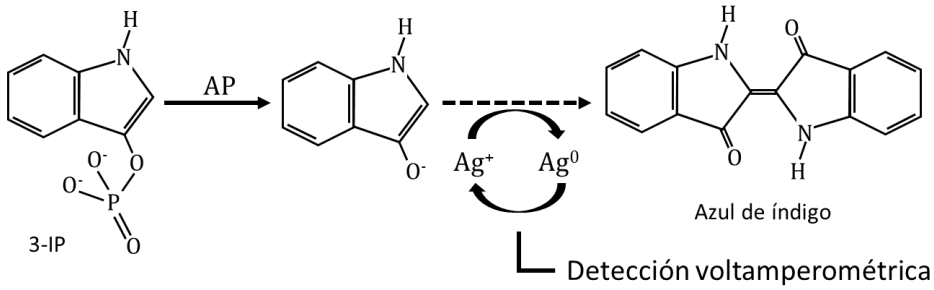

Figura 1.13. Esquema de la deposición enzimática de plata metálica catalizada por la fosfatasa alcalina para la detección electroquímica. Figura adaptada de la referencia [82].

1.4. Transductores electroquímicos

La miniaturización de los dispositivos analíticos, como ya se ha explicado, es una de las tendencias más importantes de la Química Analítica en la actualidad. De entre todas las ventajas del empleo de sistemas miniaturizados, pueden destacarse la reducción en el consumo de muestra y reactivos y por tanto, también en los productos de desecho generados, lo que permite realizar análisis en una simple gota de muestra o el desarrollo de sensores *in vivo*.

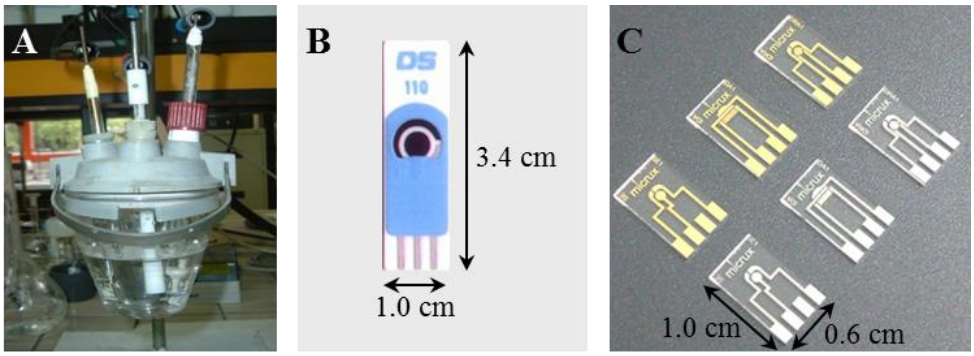

Figura 1.14. Diferentes celdas electroquímicas formadas por tres electrodos (de trabajo, auxiliar y referencia): (A) celda convencional (volumen 20-200 mL), (B) electrodo serigrafiado (*thick film*; volumen 50 µL) [83] y (C) electrodos *thin-film* (volumen 1-10 µL) [84].

Como ya se ha comentado, en los sistemas con detección electroquímica, la miniaturización es sencilla dado que la mayoría de las medidas son interfaciales y eléctricas, lo que significa que, por una parte, se registran procesos que suceden en la interfase electrodo–disolución, favoreciendo la monitorización *in vivo*, y por otra parte, no se requiere una posterior conversión de la señal obtenida. Además, los límites de detección que se suelen obtener son suficientes y adecuados para la detección de numerosos analitos de interés. Por otro lado, la relativa simplicidad y el bajo coste de la instrumentación permiten una fácil disponibilidad de estos dispositivos. No obstante, este tipo de detección presenta también inconvenientes como su baja selectividad en comparación con otras técnicas analíticas (lo que se puede minimizar drásticamente utilizando un elemento de reconocimiento que posea una alta especificidad) y la necesidad de utilizar un electrodo de referencia.

Esta tendencia de miniaturización de los dispositivos, junto con el desarrollo en técnicas de microfabricación como la de capa gruesa (o *thick-film*) y la de capa fina (o *thin-film*), han hecho que las celdas electroquímicas convencionales, en las que se trabaja con volúmenes del

orden de los "mL", se hayan ido reemplazando por celdas más pequeñas en las que el volumen de trabajo es del orden de los "µL" (**Figura 1.14**).

1.4.1. Electrodos serigrafiados

Desde los años 90, la tecnología de serigrafiado o *screen-printing* ha sido cada vez más utilizada para la producción de electrodos en serie de bajo coste y pequeñas dimensiones. Sus buenas características electroanalíticas, flexibilidad de diseño, posibilidad de incorporación a sistemas portátiles, además de su sencillez de manejo y bajo coste, han hecho que el uso de electrodos serigrafiados como transductores electroquímicos para el desarrollo de sensores y biosensores en diversos campos (alimentario, medioambiental, análisis clínico, etc.) sea cada vez mayor (**Figura 1.15**).

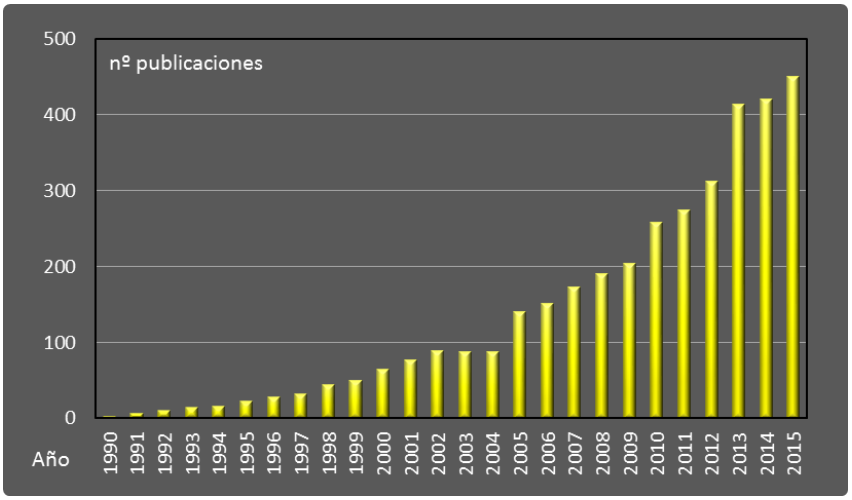

Figura 1.15. Número de publicaciones que se obtienen cuando se busca el término "*screen-printed electrode*" en Scopus entre los años 1990 y 2015.

Dentro del campo del análisis clínico, este tipo de electrodos presenta una serie de ventajas adicionales como la posibilidad de trabajar con pequeños volúmenes tanto de reactivos (muy importante dado el elevado coste de los reactivos biológicos) como de muestra, y además permite desarrollar sensores desechables gracias al bajo coste por unidad. Además de como transductores para biosensores [85-87], los electrodos serigrafiados (*screen-printed electrodes*, SPEs) han sido utilizados para aplicaciones tan diversas como la detección de metales pesados [88-90], la caracterización de nanopartículas [91,92] o espectroelectroquímica [93,94].

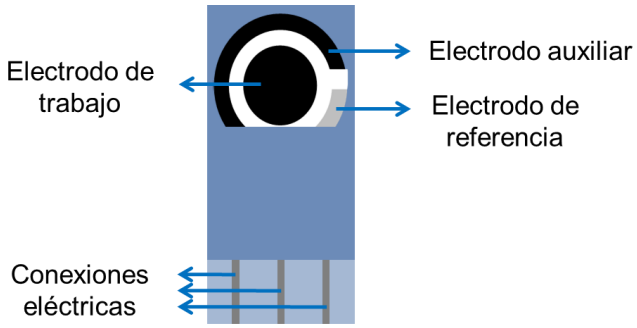

Figura 1.16. Esquema de un diseño típico de un electrodo serigrafiado.

La tecnología de serigrafiado se engloba dentro de la tecnología de capa gruesa o *thick-film*. Esta tecnología, que tiene su origen en la industria gráfica y se utiliza para la fabricación de circuitos electrónicos, permite la fabricación en masa de electrodos sólidos planos, mecánicamente robustos y de una gran versatilidad en cuanto a diseño. El diseño más habitual de los electrodos serigrafiados consiste en una celda electroquímica de tres electrodos: de trabajo, auxiliar y referencia (**Figura 1.16**). Aunque el proceso de fabricación puede variar según la aplicación final que se pretenda, este proceso consta de unas etapas básicas (**Figura 1.17**). En primer lugar es importante seleccionar el sustrato que suele ser de materiales cerámicos o poliméricos. La elección del material dependerá de la temperatura del posterior curado del electrodo y del medio en el que este va ser utilizado (por ejemplo el PVC en medio acuosos no presenta problemas mientras que en disolventes orgánicos el que mejores resultados proporciona es el poliéster) [95]. Por otro lado, el diseño y fabricación de la pantalla que se utilizará para el proceso de serigrafiado es crucial ya que definirá el tamaño y la geometría del electrodo final. Utilizando esa pantalla, que también controla el grosor de la capa de tinta, se deposita la tinta haciéndola pasar a su través. A continuación se realiza una etapa de secado y curado de la tinta a alta temperatura. Por último, se recubre con un material aislante para delimitar el área de trabajo y dejar libre una parte final para conectar con el potenciostato [85,86,96]. Las tintas para el serigrafiado suelen ser comerciales y de variada naturaleza (oro, plata, platino, carbono,…) con un amplio rango de propiedades como viscosidad, conductividad o resistencia térmica. Además, estas tintas se pueden combinar con otras especies químicas permitiendo obtener una enorme variedad. La tinta de carbono es la más utilizada gracias a su bajo coste y a que es relativamente inerte químicamente, mientras

que las tintas de oro o platino son menos usadas debido a su mayor coste. La tinta de plata es muy utilizada para los electrodos de referencia y las conexiones eléctricas.

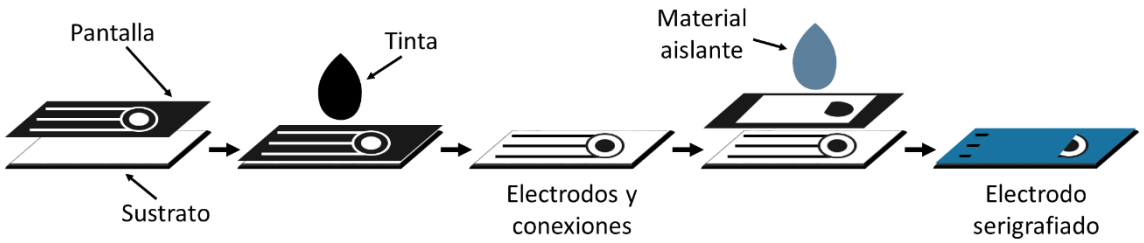

Figura 1.17. Esquema de las etapas de fabricación de electrodos serigrafiados.

Los SPEs han adquirido tanta popularidad en los últimos años debido a las importantes ventajas que muestran frente a los electrodos convencionales (ej. pasta de carbono, carbono vítreo, etc.) entre las que caben destacar las siguientes:

- **Bajo coste**: al ser producidos en masa el coste final es relativamente bajo lo que permite que puedan ser desechables tras un solo uso ("usar y tirar") evitando la necesidad de limpiar y regenerar la superficie electródica para una nueva medida (procedimientos necesarios cuando se utilizan electrodos convencionales). Otra ventaja derivada del bajo coste es la posibilidad de trabajar con varios electrodos serigrafiados simultáneamente permitiendo aumentar la cantidad de medidas realizadas en un tiempo determinado.
- **Pequeño tamaño**: las dimensiones de los SPEs son de pocos centímetros. Esto hace que puedan ser portátiles y que el volumen de muestra necesario sea de unos pocos microlitros.
- **Gran versatilidad en diseño y modificaciones**: es posible la fabricación de SPEs con diferentes diseños (diferentes tintas, uno o varios electrodos de trabajo, varias celdas electroquímicas en una misma tarjeta serigrafiada,…) según la aplicación para la que se quieran utilizar. Por ejemplo, el hecho de poder tener varios electrodos de trabajo en una misma tarjeta serigrafiada es muy útil a la hora de realizar análisis multianalito. Sin embargo, la gran versatilidad de los SPEs reside, no solo en sus amplias posibilidades en cuanto a diseño, sino también en su fácil modificación, ya sea para construir un (bio)sensor o para mejorar las propiedades electroquímicas. Estos electrodos pueden ser modificados por adición de diferentes especies o materiales a la tinta de serigrafiado (mediadores, polímeros, metales,…) o modificando su superficie una vez fabricados

depositando sobre ella diferentes materiales o elementos de reconocimiento (enzimas, anticuerpos, metales,…) [85,97,98].

Entre algunas limitaciones de los SPEs se puede destacar el hecho de que generalmente incorporan un electrodo de referencia sólido, habitualmente de plata, que actúa como electrodo de quasi-referencia por lo que el potencial podría no ser totalmente reproducible y estable a lo largo de un experimento o entre varios experimentos. Por otra parte, las tintas usadas para el serigrafiados pueden contener impurezas en su composición (por ejemplo plata [99]) que interfieran en el experimento a realizar, teniendo que reducir la ventana de potenciales a aplicar o haciendo necesaria alguna etapa de limpieza o tratamiento para eliminar esas impurezas.

Aunque en la bibliografía se pueden encontrar ya numerosos ejemplos de electrodos serigrafiados en papel, se ha decidido, debido a su singularidad e importancia, dedicar un epígrafe al papel como soporte de dispositivos electroanalíticos y electrodos.

1.4.2. Electrodos basados en papel y materiales similares

En el contexto de las tendencias en Química Analítica comentadas en la Sección 1.1 (simplificación, automatización, miniaturización y reducción de costes) ha emergido un nuevo concepto: el uso de materiales comunes, producidos en masa y de bajo coste para el desarrollo de dispositivos analíticos [100].

El papel es un material muy conocido y barato que ha sido utilizado como sustrato en test analíticos durante siglos [101]. El empleo del papel como sustrato muestra ventajas únicas frente a los materiales tradicionales: transporte de fluidos por capilaridad sin necesidad de emplear una fuente de energía, alta relación área superficial / volumen lo que mejora los límites de detección en los métodos colorimétricos y capacidad para almacenar reactivos en su forma activa dentro de su red de fibras. Además el papel es fácil de almacenar y transportar, es flexible, al ser de celulosa es compatible con muestras biológicas, suele ser blanco (útil en ensayos colorimétricos), y es inflamable por lo que puede ser desechado mediante incineración de una manera fácil y segura (muy útil para ensayos con muestras biológicas) [10,101]. Todo esto hace que el papel se haya utilizado con finalidades tan diversas como la síntesis química o los test clínicos cualitativos, siendo las tiras de flujo lateral el ejemplo más claro de este último [10,101-105]. Pero el papel como plataforma para la fabricación de dispositivos microfluídicos no se planteó hasta 2007, cuando Whitesides *et al*. describieron el primero de los que se conocen como dispositivos analíticos microfluídicos basados en papel

(*microfluidic paper-based analytical devices*, µPADs) para análisis químico [106]. Los µPADs son simples, de bajo coste, desechables y portables. Estas características se combinan además con la capacidad de realizar análisis multianalito y con las funciones de un dispositivo *lab-on-a-chip* convencional [107]. Hoy en día ya se pueden encontrar en la bibliografía una amplia variedad de µPADs para la detección de analitos tan diversos como metales o proteínas [101,107-109] (**Figura 1.18**). Paralelamente, y siguiendo la tendencia de usar materiales comunes y baratos, se han empleado también materiales como hilos o tejidos textiles para la fabricación de dispositivos analíticos [110-112].

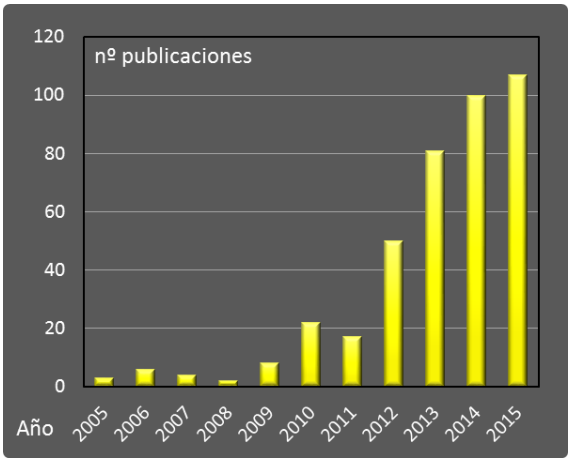

Figura 1.18. Número de publicaciones que se obtienen cuando se busca el término "*paper-based analytical device*" en Scopus entre los años 2005 y 2015.

Las técnicas de detección que se utilizan en los (µ)PADs son diversas [101]: colorimétricas [109,113], electroquímicas [108,110,114], (electro)quimioluminiscentes [115,116], etc. Por su parte, las técnicas electroquímicas son muy adecuadas para la detección en este tipo de dispositivos gracias a las ventajas ya comentadas anteriormente: portabilidad y bajo coste, capacidad de miniaturización, bajo consumo de muestra y reactivos, y alta sensibilidad para bajas concentraciones de analitos [117]. Esto explica el gran desarrollo y fabricación, en los últimos años, de electrodos miniaturizados utilizando materiales comunes, y su integración en los (µ)PADs. En la bibliografía se pueden encontrar diversos ejemplos: electrodos serigrafiados en papel y transparencias [118-120], electrodos basados en hilos cubiertos con tinta conductora [100,121] o pintados utilizando un bolígrafo cargado con una tinta conductora o un lápiz de grafito convencional [122-126].

1.4.3. Transductores nanoestructurados

Los nanomateriales se definen como materiales en los que alguna de sus dimensiones es de escala nanométrica (entre 1 y 100 nm). Los nanomateriales presentan propiedades físicas y químicas únicas y diferentes a las que posee el mismo material con dimensiones macroscópicas. Estas propiedades dependen del tamaño y forma de estos materiales así como de la ordenación de los átomos que lo componen y del comportamiento electrónico en su estructura energética. En comparación con los materiales macroscópicos, los nanomateriales presentan una mayor relación área/volumen lo que determina su mayor reactividad química.

Los nanomateriales se pueden clasificar según sus dimensiones en [127]:

- **0D**, cuando todas sus dimensiones se encuentran en la escala nanométrica; a este grupo pertenecen las nanopartículas.
- **1D**, cuando una de sus dimensiones está fuera de la escala nanométrica como por ejemplo los nanotubos, las nanofibras o los nanohilos.
- **2D**, cuando solo una de sus dimensiones está en el orden de los nanómetros (las otras lo superan) como pasa en las nanoláminas.

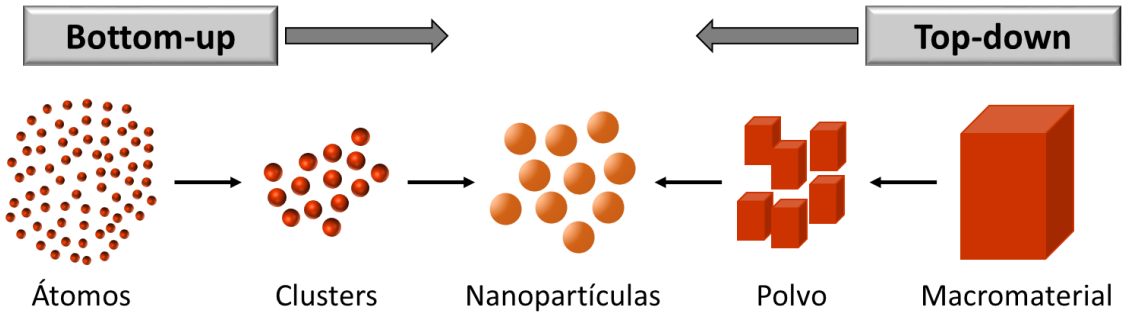

Figura 1.19. Esquema de las dos posibles estrategias que se pueden emplear para obtener nanomateriales: *bottom-up* y *top-down*.

Los métodos de fabricación de nanomateriales se pueden dividir en dos grandes grupos (**Figura 1.19**): de abajo-a-arriba (*bottom-up*) y de arriba-a-abajo (*top-down*). En los métodos *bottom-up* se parte de átomos o moléculas que son ensamblados para construir nanoestructuras mediante reacciones químicas controladas como el autoensamblaje o métodos de deposición (p. ej. de vapor o electrodeposición). En los métodos *top-down* la

fabricación se realiza a partir de materiales macroscópicos en los que alguna de sus dimensiones se reduce hasta la nanoescala (p. ej. técnicas litográficas o grabado químico).

Las atractivas propiedades que poseen los nanomateriales han hecho que la utilización de estos haya proporcionado interesantes posibilidades en muy diversos campos, entre ellos el análisis electroquímico. Además de marca en biosensores, otra gran aplicación de estos materiales es su uso para modificar electrodos con el fin de mejorar las propiedades electródicas de estos. Algunas de las principales ventajas que muestran los **electrodos nanoestructurados** se pueden resumir de la siguiente manera:

- Los nanomateriales, gracias a la alta relación área/volumen que presentan, proporcionan al electrodo un aumento del área superficial. De este hecho derivan otras ventajas como la posibilidad de inmovilizar sobre el transductor una mayor carga proteica o el aumento de la respuesta analítica.
- Muchos nanomateriales muestran una alta biocompatibilidad por lo que, la modificación de los electrodos con estos materiales mejora la inmovilización del elemento de reconocimiento biológico, por ejemplo, evitando la pérdida de funcionalidad o incrementando la estabilidad de la inmovilización.
- Algunos nanomateriales muestran propiedades electrocatalíticas a diferentes reacciones electroquímicas que normalmente presentan una velocidad de transferencia electrónica lenta o en las que participan especies que no son activas en la ventana de potenciales útil del electrodo sin modificar. Es decir, nanoestructurando los electrodos se puede disminuir el sobrepotencial necesario para producir una reacción electroquímica.
- La modificación de electrodos con nanomateriales supone un ahorro de costes frente al uso de un electrodo fabricado completamente con el material en cuestión, sobre todo cuando se trata de metales nobles como el oro o el platino. Se ha demostrado que un conjunto aleatorio de nanopartículas sobre un sustrato conductor puede funcionar como un electrodo macroscópico del mismo material, pero con un coste de fabricación significativamente menor.

Como ya se ha mencionado anteriormente, una de las cualidades de los electrodos serigrafiados es la facilidad con la que se puede modificar su superficie. Existen muy diversas formas para nanoestructurar electrodos serigrafiados entre las que se pueden destacar muy brevemente las siguientes [25,128]:

- **Dopado de la tinta**, operación que permite obtener dispositivos que, una vez fabricados, ya están modificados con el material, por lo que no es necesario una etapa posterior para la modificación.
- **Adsorción directa**, método muy sencillo que consiste en depositar una gota del nanomaterial dispersado en un disolvente adecuado y compatible con el material electródico, y dejarlo secar para que se evapore el disolvente.
- **Unión covalente** mediante la unión de grupos funcionales presentes en la superficie electródica y en el nanomaterial a inmovilizar.
- **Electrodeposición** del nanomaterial, generalmente nanopartículas metálicas, mediante la aplicación de un potencial o una corriente a una disolución que contenga un metal o complejo metálico.

Además, estas formas de modificación se pueden combinar y emplear para diferentes materiales obteniendo electrodos modificados con estructuras nanohíbridas, formadas por dos o más nanomateriales, que pueden aportar mejoras en las características de estos electrodos para aplicaciones analíticas [88,129].

1.4.3.1. Nanotubos de carbono

Los nanotubos de carbono (*carbon nanotubes*, CNTs) son tubos de tamaño nanométrico constituidos por unidades hexagonales de átomos de carbono con hibridación sp^2, resultado del enrollamiento de láminas de grafeno. Según su estructura, los CNTs pueden ser de pared simple (*single-walled carbon nanotubes*, SWCNTs), formados por una única lámina de grafeno enrollada de forma cilíndrica, o de pared múltiple (*multi-walled carbon nanotubes*, MWCNTs), formados por varias capas concéntricas de grafeno y dispuestas en forma tubular. La longitud de los CNTs puede variar desde decenas de nanómetros hasta micrómetros. Los diámetros suelen ir desde 0.4 a 3 nm para los SWCNTs y desde 2 a 100 nm para los MWCNTs [130].

Existen diferentes métodos para la síntesis de CNTs entre las que se pueden destacar la ablación láser, la descarga de arco eléctrico y la deposición química de vapor [131]. Los CNTs presentan mala solubilidad en medios acuosos por lo que, para solventar esto, pueden ser funcionalizados con diferentes grupos funcionales oxigenados, nitrogenados o sulfurados, ya sea mediante interacciones covalentes o no covalentes [132,133].

Los CNTs son uno de los nanomateriales más estudiados debido a sus interesantes propiedades como son su gran elasticidad, resistencia a la tracción, estabilidad térmica y alta conductividad eléctrica, lo que los convierte en un material muy atractivo para gran variedad

de aplicaciones, entre ellas aplicaciones electroquímicas. De manera general, los biosensores electroquímicos que emplean CNTs presentan: i) una elevada relación área/volumen, lo que se traduce en una alta capacidad de funcionalización y ii) una mejora de la transferencia electrónica de muchas reacciones electroquímicas [130,134]. Posibles inconvenientes del uso de electrodos modificados con CNTs son el aumento de las corrientes capacitivas (debido a las estructuras porosas con gran área efectiva que forman) o interferencias en los procesos faradaicos debido a los grupos funcionales que pueden presentar los CNTs.

1.4.3.2. Nanopartículas de oro

El carbono es el material más utilizado en los electrodos de trabajo de los SPEs debido a sus buenas cualidades: presenta una baja corriente de fondo y una amplia ventana de potenciales, y además es de bajo coste y relativamente inerte. Sin embargo, esto último se traduce en una baja capacidad para retener material proteico. La nanoestructuración de los electrodos serigrafiados de carbono (*screen-printed carbon electrodes*, SPCEs) con nanopartículas de oro (*gold nanoparticles*, AuNPs) mejora la biocompatibilidad del electrodo favoreciendo la inmovilización del elemento de reconocimiento, muy útil en el desarrollo de biosensores [135]. Además, las AuNPs presentan una alta relación superficie-volumen, una alta energía superficial, capacidad para disminuir la distancia entre las proteínas y la superficie del transductor y para actuar como conductor de los electrones entre los grupos prostéticos y la superficie del electrodo, facilitando la transferencia electrónica entre las proteínas y el electrodo [135,136].

Como ya se ha indicado, existen diversos métodos para la modificación de electrodos con AuNPs: se pueden unir las AuNPs covalentemente con grupos funcionales de monocapas autoensambladas, o bien depositar directamente sobre la superficie electródica, o incluso incorporarlas en la tinta con la que se va preparar el electrodo [86,135]. Pero también se puede utilizar la electrodeposición que permite una modificación rápida, simple, eficiente y reproducible.

La electrodeposición es uno de los métodos más utilizados para generar superficies con nanopartículas metálicas sobre superficies electródicas. El procedimiento consiste en aplicar una energía de excitación capaz de reducir un catión metálico al estado de oxidación elemental de manera que el metal reducido genera núcleos que crecen sobre la superficie del electrodo. La excitación para reducir el catión metálico puede realizarse aplicando un potencial (o pulsos de potencial), aplicando una corriente catódica o mediante técnicas

voltamperométricas. La electrodeposición de un metal sobre electrodos de carbono sigue normalmente un mecanismo de Volmer-Weber [137], según el cual sobre la superficie electródica se forman núcleos tridimensionales independientes de manera aleatoria que son los que luego crecen formando las nanopartículas.

La electrodeposición es una técnica válida para diferentes tipos de sustratos conductores. Además, permite un gran control sobre las nanopartículas generadas ya que cambios en los parámetros usados para la deposición como el tiempo, el potencial aplicado o la concentración de la especie precursora pueden dar lugar a nanopartículas con diferente morfología, distribución y propiedades electroquímicas [129,138].

1.5. Análisis por inyección en flujo con detección electroquímica

El análisis por inyección en flujo (*flow injection analysis*, FIA), propuesto originalmente por Ruzicka y Hansen en 1975 [139], es una técnica de análisis basada en la inyección de una muestra líquida en una corriente de flujo continua de una disolución portadora adecuada que la conduce a un detector sin la intervención de un operador. El FIA deriva del análisis en flujo continuo (*continous flow analysis*, CFA) en el que la muestra se introduce en el flujo de manera continua [140]. Otras técnicas de análisis en flujo son el análisis en flujo segmentado (*segmented flow analysis*, SFA) donde el flujo es separado (segmentado) por burbujas de aire [140-142]; o el análisis por inyección secuencial (*sequential injection analysis*, SIA) que consiste en un flujo discontinuo en el que la muestra y la disolución portadora son inyectados secuencialmente [143-145].

En un sistema FIA típico, la señal analítica se mide de manera continua y aparece cuando el flujo que contiene la muestra pasa por el detector. De esta manera, la medida de la señal analítica es muy rápida, lo que implica una mayor capacidad de muestreo frente a medidas hechas en sistemas "estáticos" [146]. Pero esto también implica que la técnica de detección debe ser lo suficientemente rápida como para recoger la señal en el tiempo que tarda la muestra en pasar por el detector. De ahí que las técnicas electroquímicas, gracias a su sencillez y rapidez, resulten muy adecuadas para su combinación con sistemas FIA. El electroanálisis en sistemas de flujo muestra una serie de ventajas frente a su uso en sistemas "estáticos":

- Mayor eficiencia y precisión. Al ser un sistema automático, se disminuyen los errores debidos al factor humano.
- Reducción del riesgo de contaminación durante el análisis.
- Combinación de buena precisión con alta sensibilidad utilizando instrumentación relativamente barata.
- Aumento del transporte de masa hacia el electrodo de trabajo permitiendo mejoras significativas en los límites de detección [71].

Además, el FIA combinado con técnicas electroquímicas muestra un gran potencial para la miniaturización de los sistemas, ya que tanto el tamaño de los electrodos como el de la instrumentación puede reducirse significativamente respecto al de los convencionales (por ejemplo, utilizando los electrodos serigrafiados comentados anteriormente) [71].

En un sistema FIA, donde el flujo se genera mediante presión, se produce un flujo laminar (las partículas se desplazan siguiendo trayectorias paralelas formando un conjunto de capas o lámina) en el que las partículas de las capas centrales fluyen con una velocidad mayor que las situadas en las capas más próximas a las paredes del tubo por el que fluyen, dando

lugar a un perfil parabólico (**Figura 1.20**). Cuando la muestra se inyecta, según va circulando a través del flujo, esta va dispersándose y mezclándose con la disolución portadora de manera que se forma un gradiente de concentración. La dispersión en un sistema FIA se cuantifica mediante el coeficiente de dispersión, *D*:

$$D = \frac{C^0}{C} \qquad (7)$$

donde C^0 es la concentración de la muestra antes de que se produzca la dispersión y *C* es la concentración de la muestra tras haber sufrido el proceso de dispersión. Se define como dispersión limitada cuando *D* está comprendido entre 1 y 2; esta dispersión se utiliza cuando la muestra se lleva hasta el detector sin diluir, es decir, el FIA solo sirve como mero transportador de la muestra al detector. Cuando *D* está comprendido entre 2 y 10 se considera dispersión media; esta se usa generalmente cuando la muestra debe mezclarse y/o reaccionar con la fase móvil o una corriente con reactivos para formar un producto detectable. Un coeficiente de dispersión $D > 10$ supone una gran dispersión, lo que se utiliza cuando es necesario diluir la muestra para que su concentración entre en el intervalo de medida del sistema [143,147]. La dispersión depende de diferentes factores como el volumen de muestra inyectado, la velocidad de flujo, la longitud y el diámetro del tubo que transporta la muestra del inyector al detector, de la viscosidad de la fase móvil y/o de la muestra y de la temperatura entre otros [147].

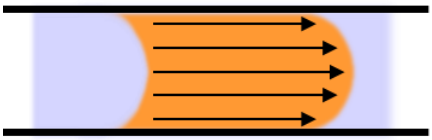

Figura 1.20. Perfil de velocidad de las partículas de un líquido en un flujo laminar generado por presión.

En los sistemas FIA es esencial la reproducibilidad de tres aspectos básicos: (i) la inyección de la muestra, tanto en el modo como se inyecta como en el volumen que se inyecta; (ii) la dispersión de la muestra; (iii) y el tiempo que tarda la muestra en ir desde el inyector hasta el detector. En un sistema FIA las medidas no se realizan en condiciones de equilibrio; no es necesario ya que, como hemos indicado, la configuración del sistema y las condiciones químicas y físicas no varían entre medidas. Habitualmente, la señal que se genera es transitoria ya que corresponde al paso de la muestra por el detector, por lo que las curvas

registradas tienen forma de pico; la anchura del mismo dependerá de la dispersión de la muestra en el flujo de la disolución portadora (**Figura 1.21**).

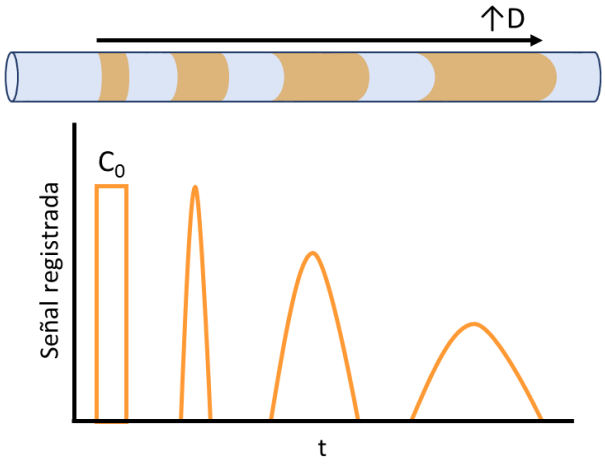

Figura 1.21. Esquema que indica cómo la dispersión de la muestra afecta a la señal registrada.

Los componentes básicos de un sistema FIA son: un sistema de propulsión, un sistema de inyección de muestra y un detector conectado a un sistema de adquisición de datos (normalmente un ordenador) (**Figura 1.22**).

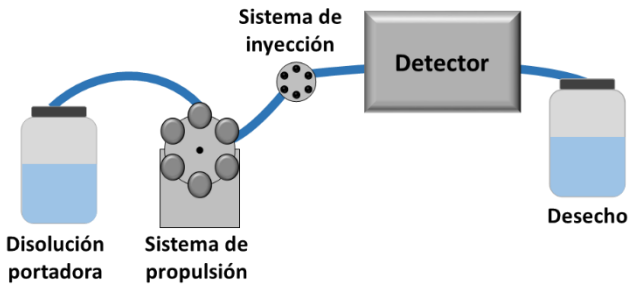

Figura 1.22. Esquema de un sistema FIA con sus componentes básicos.

Sistema de propulsión

En un sistema FIA, la unidad de propulsión sirve para transportar un fluido a través de los conductos del sistema mediante impulsos o aspiración [148]. El sistema de propulsión ideal para un sistema FIA debe cumplir los siguientes requisitos:

- Proporcionar velocidades de flujo reproducibles a corto (horas) y largo (días) plazo con el fin de mantener constante el tiempo de residencia (tiempo que tarda la muestra en llegar al detector desde el inyector) y la dispersión.
- Permitir un fácil ajuste dela velocidad de flujo.
- Capacidad multi-canal, es decir, que permita la posibilidad de tener varias fases móviles en paralelo para asegurar cierta versatilidad a la hora de diseñar el sistema.
- Generar un flujo continuo y sin pulsos. Algunos sistemas de propulsión pueden no satisfacer este requisito completamente pero cuando esto ocurre, los pulsos deben ser minimizados todo lo posible.
- Resistencia a reactivos y disolventes agresivos.

Existen varios mecanismos para propulsar el flujo en un sistema FIA: por gravedad, mediante bombas peristálticas, microbombas, pistones o bombas de jeringa entre otros. Las bombas peristálticas son las más utilizadas. En este caso, la fase móvil es propulsada a través de un tubo flexible; un rotor comprime el tubo de manera que al rotar la fase móvil es forzada a moverse a través del tubo. Generalmente estas bombas permiten la colocación de varios tubos pudiendo tener así varias corrientes de fase móvil paralelas. Los tubos flexibles que se usan con este tipo de bombas suele ser un tipo de PVC transparente y flexible. La velocidad de flujo se puede controlar fácilmente ajustando la velocidad de rotación de la bomba o cambiando el diámetro interno de los tubos que trasportan el flujo [71,148].

Sistema de inyección

El sistema de inyección de la muestra debe permitir introducir una cantidad conocida y reproducible dentro de la corriente de flujo provocando la mínima perturbación posible en dicha corriente. El sistema de inyección más común en los sistemas FIA son las válvulas rotatorias. Estas válvulas tienen dos posiciones: la posición de carga y la de inyección (**Figura 1.23**) En la posición de carga, un depósito de volumen definido (normalmente comprendido entre 10 y 500 µL [71,147]) se llena de muestra. En la posición de inyección, este volumen es arrastrado por la fase móvil introduciéndose así en la corriente de flujo. De esta manera el volumen de muestra inyectado es siempre el mismo para todas las medidas. Este se puede cambiar fácilmente reemplazando el depósito de la válvula por otro con un volumen diferente.

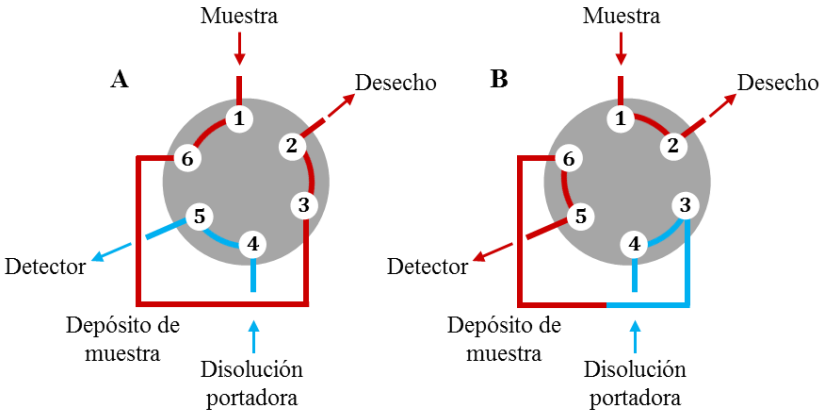

Figura 1.23. Esquema de una válvula rotatoria de inyección de seis vías en posición de carga (A) y en posición de inyección (B).

Detector y celda de flujo

Existe una gran variedad de celdas de flujo para la detección electroquímica en los sistemas FIA. Estas celdas deben cumplir ciertas características como facilidad de manejo y mantenimiento, mínimo volumen muerto, rapidez de análisis y capacidad para realizar medidas en pequeños volúmenes.

Desde hace años se han venido desarrollando celdas de flujo que incorporan electrodos miniaturizados. El uso de estos electrodos implica, además de miniaturización, simplificación y abaratamiento de los sistemas, cumpliendo así con las tendencias en Química Analítica que se han comentado. Actualmente, existen diversas celdas de flujo comerciales tanto para electrodos *thick-film* como *thin-film* (**Figura 1.24**).

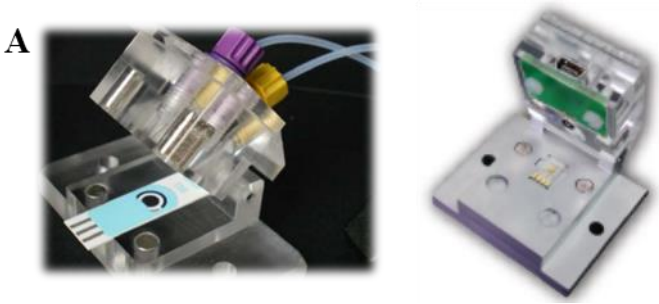

Figura 1.24. Fotografía de celdas de flujo para electrodos serigrafiado (*thick-film*, A) y para electrodos de capa fina (*thin-film*, B) de las casas comerciales DropSens y Micrux Technologies [83,84].

1.6. Analitos

Dado que en la introducción de cada publicación ya se comenta específicamente cada analito, en esta sección solo se recoge una breve descripción de algunos aspectos generales y del interés de su determinación.

1.6.1. Azúcares: glucosa y fructosa

Glucosa

La glucosa es un pentahidroxihexanal y pertenece por tanto a la clase de las aldohexosas (**Figura 1.25**) [149]. Su fórmula empírica es $C_6H_{12}O_6$ y su peso molecular 180 g/mol. Este azúcar posee dos enantiómeros, *D*-glucosa y *L*-glucosa, siendo el de configuración *D* el enantiómero natural. La glucosa, ya sea libre o combinada, es el compuesto orgánico más abundante de la naturaleza. Está presente en numerosos frutos y plantas y es el principal componente de polímeros como la celulosa, el almidón y el glucógeno. Además, mediante su oxidación catabólica, es la fuente primaria de energía de las células. En la sangre humana la concentración de glucosa oscila entre 80 y 120 mg/dL (4.4-6.6 mM) [150]. A nivel industrial se obtiene a partir de la hidrólisis enzimática de almidón de cereales.

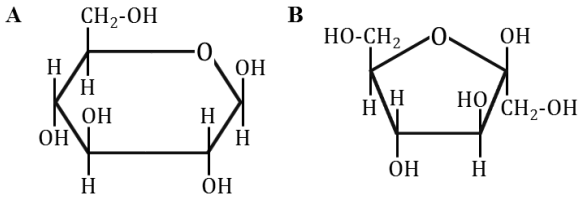

Figura 1.25. Estructura de la β-D-glucosa (A) y de la β-D-fructosa (B).

La determinación de glucosa es de gran importancia en campos como la bioquímica, la industria alimentaria, y el diagnóstico clínico. En la industria alimentaria, la determinación de glucosa es necesaria en el control de los procesos de fermentación y en el control de calidad para el cumplimiento de la legislación que regula la concentración de glucosa en algunos alimentos y bebidas [58]. En el ámbito clínico, el principal motivo por el que los análisis de glucosa son tan importantes es la enfermedad *diabetes mellitus*. Esta enfermedad es causada por una baja producción de insulina (la hormona generada por el páncreas para controlar la glucemia) por la resistencia a esta o por ambas causas combinadas [151]. Como las células necesitan la insulina para la absorber la glucosa de la sangre y cubrir sus necesidades de

energía, las células de los enfermos de diabetes sufren la escasez de glucosa, mientras que sus niveles en sangre aumentan [151]. Por tanto, es necesaria una determinación de glucosa en sangre, frecuente y rápida tanto para el diagnóstico como para el control de esta enfermedad. La diabetes es una de las principales causas de discapacidad y muerte en el mundo. Esta enfermedad puede acarrear numerosas complicaciones como enfermedades cardiovasculares, ceguera o insuficiencia renal [150]. Se estima que alrededor de 200 millones de personas en todo el mundo padecen diabetes, y se calcula que esta cifra superará los 300 millones en el año 2030 [152,153].

El sistema para la determinación de glucosa más conocido es el sensor de glucosa para diabéticos. Este es un sensor amperométrico enzimático basado generalmente en el empleo de electrodos fabricados con la tecnología de serigrafiado. La importancia de los biosensores de glucosa es tal que representa aproximadamente el 85% del total del mercado de los biosensores [150].

Por todo esto, el desarrollo de sensores de glucosa fiables, de alta sensibilidad y bajo coste ha sido objeto de intensa investigación durante décadas. En la bibliografía se pueden encontrar una gran cantidad de revisiones sobre sensores de glucosa [150-152,154-157].

Fructosa

La fructosa es un monosacárido con la misma fórmula empírica que la glucosa ($C_6H_{12}O_6$) pero con diferente estructura (**Figura 1.25**) [149]. Al igual que la glucosa, la fructosa posee dos enantiómeros, *D*-fructosa y *L*-fructosa. Está presente en numerosas frutas y vegetales, pero también en mieles, refrescos y bebidas alcohólicas.

Desde un punto de vista energético, la fructosa y la glucosa tienen el mismo valor calórico, pero el cuerpo humano los metaboliza de manera diferente. De ahí que se creyese que la fructosa podía ser un sustituto de la glucosa ya que además tiene mayor poder endulzante. Sin embargo, diversos estudios han asociado las dietas ricas en fructosa a la resistencia a la insulina, a la obesidad y al elevado colesterol [158,159].

La determinación de fructosa es importante sobre todo en el campo alimentario por ejemplo como indicador de la calidad de los alimentos; por ejemplo, la relación de concentraciones de azúcares en una miel puede determinar si esta está adulterada. La concentración de fructosa también es indicador del grado de maduración de las frutas [160]. En la bibliografía se pueden encontrar diversos sistemas para la determinación de fructosa

como espectrometría de masas [161,162], sensores ópticos [163,164] o sensores electroquímicos [165-167].

1.6.2. Etanol

El etanol, o alcohol etílico, es un alcohol de cadena corta cuya fórmula empírica es C_2H_5OH. Se presenta como un líquido incoloro e inflamable (en condiciones normales de presión y temperatura) y es miscible con el agua. El etanol es el alcohol mayoritario en las bebidas alcohólicas. Además, el etanol se emplea habitualmente como combustible (bioetanol obtenido a partir de biomasa), disolvente para lacas, barnices, perfumes, etc. y como medio o materia prima para reacción químicas [168,169].

La determinación de etanol es por tanto, de gran importancia en diversas áreas: en la industria alimentaria, para el control de los procesos de fermentación y el control de calidad, así como para un correcto etiquetado y cumplimiento de la legislación que regula el contenido de etanol y otros alcoholes en las bebidas, y también en el ámbito clínico, debido a sus efectos toxicológicos [36,168]. Tradicionalmente, los métodos más utilizados para la determinación de etanol se han basado en cromatografía de gases o cromatografía de líquidos de alta eficacia (*high performance liquid chromatography*, HPLC) acoplada a un detector de ionización de llama (*flame ionization detector,* FID), o en densimetrías. Muchos otros métodos para la determinación de etanol se pueden encontrar en la bibliografía (espectroscopía Raman, espectroscopía infrarroja, espectrometría de masas,…) [170], pero la mayoría de estos requieren grandes aparatos y procesos lentos y tediosos, de ahí el interés de desarrollar sensores de etanol. En la bibliografía se pueden encontrar diversos ejemplos de estos sensores tanto enzimáticos como basados en nanomateriales [36,171-174].

1.6.3. Proteína beta-amiloide 1-42

Actualmente, la demencia es uno de los mayores problemas de salud pública a nivel mundial. La tasa de incidencia de esta enfermedad aumenta con la edad, por lo que el aumento de la esperanza de vida supone un incremento progresivo en el número de enfermos. Hoy en día se estima que alrededor de 44 millones de personas padecen demencia en el mundo, y se calcula que este número sea el doble para el año 2030 y más del triple en el año 2050, si no se encuentra forma de tratar o prevenir esta enfermedad [175]. La demencia no es una enfermedad específica sino que es un término general que describe una amplia variedad de síntomas asociados con pérdidas de memoria y de la habilidad de pensar y

razonar, afectando a la capacidad del enfermo para llegar a cabo tareas cotidianas [176]. La demencia está causada por daños neuronales. El tipo de demencia más común es la enfermedad de Alzheimer (*Alzheimer's disease*, AD) que representa el 50-75% del total de las demencias [175,176].

La AD es una enfermedad neurodegenerativa crónica caracterizada por un deterioro global y gradual en las funciones cognitivas y ejecutivas hasta la total pérdida de independencia e incapacidad física. Alois Alzheimer habló del primer caso de esta enfermedad en noviembre de 1906 en un congreso de psiquiatría en Tübingen (Alemania) [177,178]. Aunque la AD se descubrió hace más de 100 años y se han hecho grandes avances en cuanto a sus causas, factores de riesgo, diagnóstico y tratamiento, a día de hoy no están claros los cambios biológicos que la causan, las diferentes progresiones que presenta o cómo prevenirla y curarla [179,180]. La detección precoz es importante ya que la eficacia de los tratamientos existentes para disminuir la intensidad de los síntomas suele ser mayor cuando se aplican en las fases tempranas de la enfermedad [181].

El diagnóstico de AD, que combina criterios clínicos con estudios histológicos y de neuroimagen, suele ser tardío debido al comienzo insidioso y variable de la enfermedad; cuando los pacientes cumplen los criterios establecidos para dar un diagnóstico con certeza, estos ya presentan un deterioro significativo en varias áreas cognitivas, por lo que el grado de patología presente en el cerebro ya es generalizado [176,181,182]. En 2011, el Instituto Nacional del Envejecimiento (*National Institute on Aging* (EEUU) NIA) y la Asociación del Alzheimer (*Alzheimer's Association*, EEUU) propusieron unos nuevos criterios y guías para el diagnóstico de la AD, actualizando los publicados en 1984 [176]. En cuanto al diagnóstico, la novedad más destacable que incluyen es la incorporación de los tests de biomarcadores. Un biomarcador es un factor biológico que puede ser medido y su cantidad indica la presencia o el riesgo de desarrollar una enfermedad [183]. Entre los factores a estudiar como posibles biomarcadores del Alzheimer están los niveles de ciertas proteínas, como la beta-amiloide o la tau, en líquido cerebroespinal (*cerebrospinal fluid*, CSF) y sangre. Estos nuevos criterios aún son solo una propuesta y es necesaria más investigación antes de que sean establecidos como herramienta de diagnóstico [180].

Las principales características histopatológicas de la AD son la progresiva acumulación de placas seniles extracelulares que contienen beta-amiloide (Aβ), y los ovillos neurofibrilares asociados a la proteína tau. Estos cambios patológicos se presentan incluso antes del comienzo de la demencia clínica. Además, la AD conduce a una dramática pérdida de neuronas y sinapsis; con el tiempo los cerebros de pacientes con AD sufren drásticas disminuciones de

tamaño [184,185]. Los péptidos beta-amiloide, que son el componente principal de esas placas seniles, se generan mayoritariamente en el cerebro y están presentes en el CSF y en el plasma. Pueden tener entre 15 y 43 amino ácidos; el péptido de 40 aminoácidos es el más abundante mientras que el de 42 (Aβ1-42) parece ser esencial para que se inicie la agregación de estos, y se considera central en la hipótesis de la cascada de amiloide de la AD [186]. Esta hipótesis postula que la AD comienza con el procesamiento anormal de la proteína precursora del amiloide (APP) y, mediante diferentes mecanismos, la Aβ produce las características patológicas de la AD incluyendo neuroinflamación, fosforilación de la proteína tau, disfunción sináptica, muerte celular y atrofia cerebral [181,187]. Además de la Aβ1-42 y la tau, la tau fosforilada es otro de los biomarcadores que se consideran para la AD. La combinación de baja concentración de Aβ y alta de tau en líquido cerebroespinal predice con buena precisión la presencia de los cambios patológicos típicos del Alzheimer. Varios estudios indican que la sensibilidad y especificidad de esos tres biomarcadores por separado para diferenciar enfermos de AD de controles es del 80-90% [179,184,188].

La identificación en el cerebro de las placas seniles formadas por Aβ se lleva a cabo mediante diferentes técnicas de neuroimagen [189] (resonancia mágnetica, resonancia de plasmones de superficie, espectroscopía de infarrojo cercano, etc.). Por otra parte, para la determinación de Aβ1-42 en CSF se pueden encontrar diversos kits ELISA comerciales [190-192], mientras que, en cuanto al desarrollo de sensores, a día de hoy la bibliografía es aún escasa [189,193,194].

1.6.4. Biomarcadores del cáncer de mama: HER2 y CA15-3

El cáncer de mama es el segundo tipo de cáncer más común en todo el mundo. En las mujeres, este tipo de cáncer es el más frecuente tanto en los países desarrollados como en los en vías de desarrollo [195]. La detección precoz es de suma importancia ya que puede aumentar la calidad y la expectativa de vida de los pacientes. Los biomarcadores como el receptor 2 del factor de crecimiento epidérmico humano (*human epidermal growth factor receptor 2*, HER2), y el antígeno carbohidratado (*cancer antigen*, CA 15-3) son de gran utilidad para el diagnóstico y seguimiento de esta enfermedad.

La determinación de HER2 se suele hacer en tejidos mediante técnicas de hibridación *in situ* o inmunohistoquímicas, mientras que el CA 15-3 se determina en suero mediante inmunoensayos enzimáticos. En la revisión del Capítulo II se pueden encontrar ejemplos de sensores electroquímicos para la determinación de estos biomarcadores.

HER2

El receptor del factor de crecimiento epidérmico (*epidermal growth factor receptor*, EGFR) forma parte de una familia de receptores tirosina quinasa. Esta familia de receptores, también designada como ErbB o HER (*human epidermal growth factor receptor*) está envuelta en la señalización celular y juega un papel importante en la proliferación, crecimiento, apoptosis y diferenciación celular. Estos procesos son esenciales para la vida, pero cuando están fuera de control generalmente dan lugar a enfermedades como el cáncer. Dentro de esta familia de receptores se incluyen el EGFR (ErbB-1 o HER1), el HER2 (ErbB-2), el HER3 (ErbB-3) y el HER4 (ErbB-4). Todas estas proteínas son receptores del factor de crecimiento transmembranales con similares estructuras pero diferentes funciones biológicas [196,197].

En el cromosoma 17 se encuentra el gen que codifica la proteína HER2. Esta proteína presenta tres dominios: una región extracelular similar a la de las otras EGFRs, una región transmembranal hidrofóbica, y una zona intracelular con actividad tirosina quinasa. El dominio extracelular (*extracellular domain*, ECD) puede separarse indicando un aumento de la fosforilación de la región tirosina quinasa y aumentando por tanto los niveles de señalización celular. El ECD entra en el torrente sanguíneo convirtiéndose en un indicador de la sobreexpresión del HER2, que se relaciona con la existencia de metástasis y con un bajo índice de supervivencia. Esta proteína es sobreexpresada en el 20-30% de los cánceres de mama [197,198].

Actualmente, existen terapias aprobadas por la FDA (*Food and Drug Administration*, EEUU) para pacientes con cáncer que muestren una sobrexpresión de HER2, diseñadas contra el ECD del HER2 o contra el dominio intracelular con tirosina quinasa. Ejemplo de ello son los fármacos *Trastuzumab*, que es un anticuerpo monoclonal recombinante específico para el ECD del HER2 aprobado en 1998 por la FDA para el tratamiento del cáncer de mama metastásico, y *Lapatinib*, un inhibidor de la tirosina quinada específico para EGRF y HER2 [199,200].

CA 15-3

La MUC-1 es una proteína transmembranal que pertenece al grupo de las mucinas. Sus funciones normales son de protección celular y lubricación. En condiciones normales la MUC-1 se expresa en la membrana plasmática apical de las células epiteliales. Pero cuando se produce una transformación maligna, la MUC-1 se puede expresar a niveles elevados por toda la superficie de la membrana así como en el citoplasma. Además de esto, también se pueden

dar cambios en la glicosilación. Así, tanto la sobreexpresión como la alteración en la glicosilación hacen que la MUC-1 pueda usarse como marcador del cáncer [198,201,202].

El CA 15-3 es la forma soluble de la MUC-1, por lo que su determinación es posible en sangre. La mayoría de pacientes con cáncer de mama metastásico muestran niveles elevados de CA 15-3. Pero también se pueden encontrar concentraciones altas de este marcador en enfermos con otro tipo de adenocarcinomas avanzados como el de ovarios, el de páncreas, el de pulmón o el gástrico. Enfermedades benignas como la hepatitis o la cirrosis también pueden producir un aumento de este marcador aunque en estos casos dicho aumento suele ser leve. Aunque su valor diagnóstico es relativamente pequeño, el CA 15-3 está establecido como biomarcador del cáncer de mama para la monitorización de la enfermedad y la respuesta del paciente al tratamiento [201,203].

1.7. Bibliografía

[1] M. Valcárcel and M. S. Cárdenas, *Automatización y miniaturización en Química Analítica*, 1ª ed., Springer-Verlag Ibérica, 2000.

[2] B. Srinivasan, S. Tung, "Development and Applications of Portable Biosensors", *J. Lab. Autom.*, 2015, 20, 365–389.

[3] B. Derkus, "Applying the Miniaturization technologies for biosensor design", *Biosens. Bioelectron.*, 2016, 79, 901-913.

[4] J. Wang, "Portable electrochemical systems", *TrAC - Trends Anal. Chem.*, 2002, 21, 226-232.

[5] M. Ryvolová, J. Preisler, D. Brabazon, M. Macka, "Portable capillary-based (non-chip) capillary electrophoresis", *TrAC - Trends Anal. Chem.*, 2010, 29, 339-353.

[6] E. Petryayeva, W. R. Algar, "Toward point-of-care diagnostics with consumer electronic devices: the expanding role of nanoparticles", *RSC Adv.*, 2015, 5, 22256-22282.

[7] G. Bülbül, A. Hayat, S. Andreescu, "Portable nanoparticle-based sensors for food safety assessment", *Sensors*, 2015, 15, 30736-30758.

[8] D. Zhang, Q. Liu, "Biosensors and bioelectronics on smartphone for portable biochemical detection", *Biosens. Bioelectron.*, 2016, 75, 273-284.

[9] P. B. Luppa, C. Müller, A. Schlichtiger, H. Schlebusch, "Point-of-care testing (POCT): Current techniques and future perspectives", *TrAC - Trends Anal. Chem.*, 2011, 30, 887-898.

[10] A. W. Martinez, S. T. Phillips, G. M. Whitesides, E. Carrilho, "Diagnostics for the developing world: microfluidic paper-based analytical devices", *Anal. Chem.*, 2010, 82, 3-10.

[11] J. O. Bockris, A. K. N. Reddy, *Volume 1: Modern Electrochemistry. Ionics*, 2ª ed., vol. 1. Springer US, 1998.

[12] D. A. Skoog, F. J. Holler, T. A. Nieman, *Principios de análisis instrumental*, 5ª ed. McGraw-Hill, 2001.

[13] A. J. Bard, L. R. Faulkner, *Electrochemical Methods. Fundamentals and Applications*, 2ª ed. John Wiley & Sons, Inc., 2001.

[14] C. G. Zoski, *Handbook of Electrochemistry*, 1ª ed. Elsevier, 2007.

[15] D. R. Thevenot, K. Toth, R. A. Durst, G. S. Wilson, D. R. Thévenot, K. Toth, R. A. Durst, G. S. Wilson, "Electrochemical biosensors: recommended definitions and classification", *Biosens. Bioelectron.*, 2001, 16, 121-131.

[16] L. C. Clark, C. Lyons, "Electrode systems for continuous monitoring in cardiovascular surgery", *Ann. N. Y. Acad. Sci.*, 1962, 102, 29-45.

[17] D. R. Thévenot, K. Toth, R. A. Durst, G. S. Wilson, "Electrochemical biosensors: Recommended definitions and classification", *Pure Appl. Chem.*, 1999, 71, 2333-2348.

[18] J. M. Pingarrón Carrazón, P. S. Batanero, *Química electroanalítica. Fundamentos y aplicaciones*, 1ª ed. Síntesis S.A., 1999.

[19] S. M. Borisov, O. S. Wolfbeis, "Optical biosensors", *Chem. Rev.*, 2008, 108, 423-461.

[20] J. H. T. Luong, K. B. Male, J. D. Glennon, "Biosensor technology: technology push versus market pull", *Biotechnol. Adv.*, 2008, 26, 492-500.

[21] N. J. Ronkainen-Matsuno, J. H. Thomas, H. B. Halsall, W. R. Heineman, "Electrochemical immunoassay moving into the fast lane", *TrAC - Trends Anal. Chem.*, 2002, 21, 213-225.

[22] J. Miller, J. C. Miller, *Statistics and Chemometrics for Analytical Chemistry*, 6ª ed. Pearson Education Canada, 2010.

[23] E. Prichard, V. Barwick, *Quality assurance in analytical Chemistry*, 1ª ed. John Wiley & Sons, Ltd., 2007.

[24] S. R. Mikkelsen, E. Cortón, *Bioanalytical chemistry*, 1ª ed. John Wiley & Sons, Inc., 2004.

[25] W. Putzbach, N. J. Ronkainen, "Immobilization techniques in the fabrication of nanomaterial-based electrochemical biosensors: a review", *Sensors*, 2013, 13, 4811-4840.

[26] N. R. Mohamad, N. H. C. Marzuki, N. A. Buang, F. Huyop, R. A. Wahab, "An overview of technologies for immobilization of enzymes and surface analysis techniques for immobilized enzymes", *Biotechnol. Biotechnol. Equip.*, 2015, 29, 205-220.

[27] A. Sassolas, L. J. Blum, B. D. Leca-Bouvier, "Immobilization strategies to develop enzymatic biosensors", *Biotechnol. Adv.*, 2012, 30,489-511.

[28] A. J. Reviejo, J. M. Pingarrón, A. Julio Reviejo, José M. Pingarrón, "Biosensores electroquímicos. Una herramienta útil para el análisis medioambiental, alimentario y clínico", *Anales de la Real Sociedad Española de Química*, 2000, 2, 5-15.

[29] B. R. Eggins, *Chemical Sensors and Biosensors*, 1ª ed. John Wiley & Sons, Ltd., 2002.

[30] S. Fetzner, R. A. Steiner, "Cofactor-independent oxidases and oxygenases", *Appl. Microbiol. Biotechnol.*, 2010, 86, 791-804.

[31] M. Pickl, M. Fuchs, S. M. Glueck, K. Faber, "The substrate tolerance of alcohol oxidases", *Appl. Microbiol. Biotechnol.*, 2015, 99, 6617-6642.

[32] S. Witt, G. Wohlfahrt, D. Schomburg, H. J. Hecht, H. M. Kalisz, "Conserved arginine-516 of Penicillium amagasakiense glucose oxidase is essential for the efficient binding of beta-D-glucose", *Biochem. J.*, 2000, 347, 553-559.

[33] A. L. Galant, R. C. Kaufman, J. D. Wilson, "Glucose: Detection and analysis", *Food Chem.*, 2015, 188, 149-160.

[34] S. B. Bankar, M. V Bule, R. S. Singhal, L. Ananthanarayan, "Glucose oxidase-an overview", *Biotechnol. Adv.*, 2009, 27, 489-501.

[35] P. Goswami, S. S. R. Chinnadayyala, M. Chakraborty, A. K. Kumar, A. Kakoti, "An overview on alcohol oxidases and their potential applications", *Appl. Microbiol. Biotechnol.*, 2013, 97, 4259-4275.

[36] A. M. Azevedo, D. M. F. Prazeres, J. M. S. Cabral, L. P. Fonseca, "Ethanol biosensors based on alcohol oxidase", *Biosens. Bioelectron.*, 2005, 21, 235-247.

[37] Y. Yamada, K. Aida, T. Uemura, "A new enzyme, D-Fructose Dehydrogenase", *Agric. Biol. Chem.*, 1966, 30, 95-96.

[38] V. L. Davidson, L. H. Jones, "Intermolecular electron transfer from quinoproteins and its relevance to biosensor technology", *Anal. Chim. Acta*, 1991, 249, 235-240.

[39] M. Flores-Encarnación, M. Sánchez-Cuevas, F. Ortiz-Gutiérrez, "Las PQQ-deshidrogenasas. Un novedoso ejemplo de quinoproteínas bacterianas", *Rev. Latinoam. Microbiol.*, 2004, 46, 47-59.

[40] J. Tkáč, I. Voštiar, E. Šturdík, P. Gemeiner, V. V. Mastihuba, J. J. Annus, J. Tkac, I. Voštiar, E. Šturdik, P. Gemeiner, V. V. Mastihuba, J. J. Annus, "Fructose biosensor based on d-fructose dehydrogenase immobilised on a ferrocene-embedded cellulose acetate membrane", *Anal. Chim. Acta*, 2001, 439, 39-46.

[41] M. Smolander, G. Marko-Varga, L. Gorton, "Aldose dehydrogenase-modified carbon paste electrodes as amperometric aldose sensors", *Anal. Chim. Acta*, 1995, 302, 233-240.

[42] C. A. B. Garcia, G. De Oliveira Neto, L. T. Kubota, "New fructose biosensors utilizing a polypyrrole film and D-fructose 5-dehydrogenase immobilized by different processes", *Anal. Chim. Acta*, 1998, 374, 201-208.

[43] C. A. B. Garcia, G. D. O. Neto, L. T. Kubota, L. A. Grandin, "A new amperometric biosensor for fructose using a carbon paste electrode modified with silica gel coated with Meldola ' s Blue and fructose 5-dehydrogenase", *Carbon N. Y.*, 1996, 418, 147-151.

[44] M. Hamid, "Potential applications of peroxidases", *Food Chem.*, 2009, 115, 1177-1186.

[45] T. Ruzgasa, E. Csregib, J. Emn, L. Gortonb, T. Ruzgas, E. Csoregi, J. Emneus, L. Gorton, G. Marko-Varga, "Peroxidase-modified electrodes: Fundamentals and application", *Anal. Chim. Acta*, 1996, 330, 123-138.

[46] L. Gorton, "Carbon paste electrodes modified with enzymes, tissues, and cells", *Electroanalysis*, 1995, 7, 23-45.

[47] A. Chaubey B. D. Malhotra, "Mediated biosensors", *Biosens. Bioelectron.*, 2002, 17, 441-456.

[48] M. Saleem, H. Yu, L. Wang, Zain-ul-Abdin, H. Khalid, M. Akram, N. M. Abbasi, J. Huang, "Review on synthesis of ferrocene-based redox polymers and derivatives and their application in glucose sensing", *Anal. Chim. Acta*, 2015, 876, 9-25.

[49] A. G.-V. de Prada, N. Peña, M. L. Mena, a. J. Reviejo, J. M. Pingarrón, "Graphite–Teflon composite bienzyme amperometric biosensors for monitoring of alcohols", *Biosens. Bioelectron.*, 2003, 18, 1279-1288.

[50] I. L. de Mattos, L. Gorton, T. Ruzgas, A. A. Karyakin, "Sensor for Hydrogen Peroxide Based on Prussian Blue Modified Electrode : Improvement of the Operational Stability", *Anal. Sci.*, 2000, 16, 795-798.

[51] I. L. De Mattos, L. Gorton, T. Ruzgas, "Sensor and biosensor based on Prussian Blue modified gold and platinum screen printed electrodes", *Biosens. Bioelectron.*, 2006, 18, 193-200.

[52] S. Cinti, F. Arduini, D. Moscone, G. Palleschi, L. Gonzalez-Macia, A. J. Killard, "Cholesterol

biosensor based on inkjet-printed Prussian blue nanoparticle-modified screen-printed electrodes", *Sens. Actuators B.*, 2015, 221, 187-190.

[53] M. Gamella, S. Campuzano, A. J. Reviejo, J. M. Pingarrón, "Integrated multienzyme electrochemical biosensors for the determination of glycerol in wines", *Anal. Chim. Acta*, 2008, 609, 201-209.

[54] S. Campuzano, O. A. Loaiza, M. Pedrero, F. J. M. de Villena, J. M. Pingarrón, "An integrated bienzyme glucose oxidase-fructose dehydrogenase-tetrathiafulvalene-3-mercaptopropionic acid-gold electrode for the simultaneous determination of glucose and fructose", *Bioelectrochemistry*,2004, 63, 199-206.

[55] X.Z. Yu, J.D. Gu, T.P. Li, "Availability of ferrocyanide and ferricyanide complexes as a nitrogen source to cyanogenic plants", *Arch. Environ. Contam. Toxicol.*, 2008, 55, 229-237.

[56] J. K. F. Van Staden, "Application of phthalocyanines in flow- and sequential-injection analysis and microfluidics systems: A review", *Talanta*, 2015, 139, 75-88.

[57] M. A. Alonso Lomillo, J. Ruiz, F. Pascual, J. Gonzalo Ruiz, F. J. Muñoz Pascual, "Biosensor based on platinum chips for glucose determination", *Anal. Chim. Acta*, 2005, 547, 209-214.

[58] J. Gonzalo-Ruíz, M. Asunción Alonso-Lomillo, F. Javier Muñoz, "Screen-printed biosensors for glucose determination in grape juice", *Biosens. Bioelectron.*, 2007, 22, 1517-1521.

[59] N. Peña, G. Ruiz, A. J. Reviejo, J. M. Pingarrón, "Graphite-teflon composite bienzyme electrodes for the determination of cholesterol in reversed micelles. Application to food samples", *Anal. Chem.*, 2001, 73, 1190-1195.

[60] K. Wang, J. J. Xu, H. Y. Chen, "A novel glucose biosensor based on the nanoscaled cobalt phthalocyanine-glucose oxidase biocomposite", *Biosens. Bioelectron.*, 2005, 20, 1388-1396.

[61] H. Wang, Y. Bu, W. Dai, K. Li, H. Wang, X. Zuo, "Well-dispersed cobalt phthalocyanine nanorods on graphene for the electrochemical detection of hydrogen peroxide and glucose sensing" *Sens. Actuators B.*, 2015, 216, 298-306.

[62] E. Burcu Bahadir, M. Kemal Sezgintürk, "Applications of electrochemical immunosensors for early clinical diagnostics," *Talanta*, vol. 132, pp. 162–174, 2015.

[63] I. Diaconu, C. Cristea, V. Hârceagă, G. Marrazza, I. Berindan-Neagoe, R. Săndulescu, V. Hârceagă, G. Marrazza, I. Berindan-Neagoe, R. Săndulescu, "Electrochemical immunosensors in breast and ovarian cancer", *Clin. Chim. Acta*, 2013, 425, 128-138.

[64] P. B. Luppa, L. J. Sokoll, D. W. Chan, "Immunosensors-principles and applications to clinical chemistry", *Clin. Chim. Acta*, 2001, 314, 1-26.

[65] G. Liu, Y. Lin, "Nanomaterial labels in electrochemical immunosensors and immunoassays", *Talanta*, 2007, 74, 308-317.

[66] J. Tang, D. Tang, "Non-enzymatic electrochemical immunoassay using noble metal nanoparticles: a review", *Microchim. Acta*, 2015, 182, 2077-2089.

[67] Y. Wan, Y. Su, X. Zhu, G. Liu, C. Fan, "Development of electrochemical immunosensors towards

point of care diagnostics", *Biosens. Bioelectron.*, 2013, 47, 1-11.

[68] M. D. Gonzalez, M. B. González-Garcia, A. C. Garcia, "Recent Advances in Electrochemical Enzyme Immunoassays", *Electroanalysis*, 2005, 17, 1901-1918.

[69] X. Zhang, H. Ju, J. Wang, *Electrochemical sensors biosensors and their biomedical applications*, 1ª ed., Elsevier Inc., 2008.

[70] F. Ricci, G. Adornetto, G. Palleschi, "A review of experimental aspects of electrochemical immunosensors", *Electrochim. Acta*, 2012, 84, 74-83.

[71] A. Escarpa, M. C. González, M. Á. López, *Agricultural and food electroanalysis*, 1ª ed. John Wiley & Sons, Ltd., 2015.

[72] E. E. Kim, H. W. Wyckoff, "Reaction mechanism of alkaline phosphatase based on crystal structures", *J. Mol. Biol.*, 1991, 218, 449-464.

[73] J. E. Coleman, "Structure and mechanism of alkaline phosphatase" *Annu Rev Biophys.*, 1992, 21, 441-483.

[74] P. Fanjul-Bolado, M. B. González-García, A. Costa-García, "Voltammetric determination of alkaline phosphatase and horseradish peroxidase activity using 3-indoxyl phosphate as substrate: Application to enzyme immunoassay", *Talanta*, 2004, 64, 452-457.

[75] M. Díaz-González, M. B. González-García, A. Costa-García, "Immunosensor for Mycobacterium tuberculosis on screen-printed carbon electrodes", *Biosens. Bioelectron.*, 2005, 20, 2035-2043.

[76] P. Fanjul-Bolado, M. B. González-García, A. Costa-García, "Detection of leucoindigo in alkaline phosphatase and peroxidase based assays using 3-indoxyl phosphate as substrate", *Anal. Chim. Acta*, 2005, 534, 231-238.

[77] M. S. Wilson, R. D. Rauh, "Hydroquinone diphosphate: An alkaline phosphatase substrate that does not produce electrode fouling in electrochemical immunoassays", *Biosens. Bioelectron.*, 2004, 20, 276-283.

[78] M. M. P. da Silva Neves, M. B. G. García, D. H. Santos, P. Fanjul-Bolado, "Hydroquinone diphosphate/Ag^+ as an enzymatic substrate for alkaline phosphatase catalyzed silver deposition", *Electrochem. commun.*, 2015, 60, 1-4.

[79] P. Fanjul-Bolado, M. B. González-García, A. Costa-García, "Flow screen-printed amperometric detection of p-nitrophenol in alkaline phosphatase-based assays", *Anal. Bioanal. Chem.*, 2006, 385, 1202-1208.

[80] H. Dong, C. M. Li, W. Chen, Q. Zhou, Z. X. Zeng, J. H. T. Luong, "Sensitive amperometric immunosensing using polypyrrolepropylic acid films for biomolecule immobilization", *Anal. Chem.*, 2006, 78, 7424-7431.

[81] A. Preechaworapun, Z. Dai, Y. Xiang, O. Chailapakul, J. Wang, "Investigation of the enzyme hydrolysis products of the substrates of alkaline phosphatase in electrochemical immunosensing", *Talanta*, 2008, 76, 424-431.

[82] P. Fanjul-Bolado, D. Hernández-Santos, M. B. González-García, A. Costa-García, "Alkaline

phosphatase-catalyzed silver deposition for electrochemical detection", *Anal. Chem.*, 2007, 79, 5272-5277.

[83] "Dropsens, www.dropsens.com". Fecha de consulta: 15 de Mayo de 2016

[84] "Micrux Technologies, www.micruxfluidic.com". Fecha de consulta: 15 de Mayo de 2016

[85] Z. Taleat, A. Khoshroo, M. Mazloum-Ardakani, "Screen-printed electrodes for biosensing: a review (2008–2013)", *Microchim. Acta*, 2014, 181, 865-891.

[86] R. A. S. Couto, J. L. F. C. Lima, M. B. Quinaz, "Recent developments, characteristics and potential applications of screen-printed electrodes in pharmaceutical and biological analysis", *Talanta*, 2016, 146, 801-814.

[87] M. Pedrero, S. Campuzano, J. M. Pingarrón, "Electrochemical Biosensors for the Determination of Cardiovascular Markers: a Review", *Electroanalysis*, 2014, 26, 1132-1153.

[88] D. Martín-Yerga, M. B. González-García, A. Costa-García, "Use of nanohybrid materials as electrochemical transducers for mercury sensors", *Sens. Actuators B.*, 2012, 165, 143-150.

[89] J. Wang, B. Tian, "Screen-printed stripping voltammetric/potentiometric electrodes for decentralized testing of trace lead", *Anal. Chem.*, 1992, 64, 1706-1709.

[90] M. Á. G. Rico, M. Olivares-Marín, E. P. Gil, "Modification of carbon screen-printed electrodes by adsorption of chemically synthesized Bi nanoparticles for the voltammetric stripping detection of Zn(II), Cd(II) and Pb(II)", *Talanta*, 2009, 80, 631-635.

[91] M. Giovanni, A. Ambrosi, Z. Sofer, M. Pumera, "Impact electrochemistry of individual molybdenum nanoparticles", *Electrochem. commun.*, 2015, 56, 16-19.

[92] C. S. Lim, S. M. Tan, Z. Sofer, M. Pumera, "Impact Electrochemistry of Layered Transition Metal Dichalcogenides", *ACS Nano*, 2015, 9, 8474-8483.

[93] N. González-Diéguez, A. Colina, J. López-Palacios, A. Heras, "Spectroelectrochemistry at screen-printed electrodes: determination of dopamine", *Anal. Chem.*, 2012, 84, 9146-9153.

[94] C. N. Hernández, M. B. G. García, D. H. Santos, M. A. Heras, A. Colina, P. Fanjul-Bolado, "Aqueous UV–VIS spectroelectrochemical study of the voltammetric reduction of graphene oxide on screen-printed carbon electrodes", *Electrochem. commun.*, 2016, 64, 65-68.

[95] S. Kröger, A. P. F. Turner, "Solvent-resistant carbon electrodes screen printed onto plastic for use in biosensors", *Anal. Chim. Acta*, 1997, 347, 9-18.

[96] C. M. Elliott, R. W. Murray, "Chemically Modified Carbon Electrodes", *Anal. Chem.*, 1992, 48, 1281-1286.

[97] O. D. Renedo, M. a Alonso-Lomillo, M. J. A. Martínez, "Recent developments in the field of screen-printed electrodes and their related applications", *Talanta*, 2007, 73, 202-219.

[98] J. P. Hart, A. Crew, E. Crouch, K. C. Honeychurch, R. M. Pemberton, "Some Recent Designs and Developments of Screen-Printed Carbon Electrochemical Sensors/Biosensors for Biomedical, Environmental, and Industrial Analyses", *Anal. Lett.*, 2004, 37, 789-830.

[99] P. T. Lee, D. Lowinsohn, R. G. Compton, "The use of screen-printed electrodes in a proof of

concept electrochemical estimation of homocysteine and glutathione in the presence of cysteine using catechol", *Sensors*, 2014, 14, 10395-10411.

[100] N. C. Sekar, S. A. Mousavi Shaegh, S. H. Ng, L. Ge, S. N. Tan, "Simple thick-film thread-based voltammetric sensors", *Electrochem. commun.*, 2014, 46, 128-131.

[101] D. M. Cate, J. A. Adkins, J. Mettakoonpitak, C. S. Henry, "Recent developments in paper-based microfluidic devices", *Anal. Chem.*, 2015, 87, 19-41.

[102] P. Von Lode, "Point-of-care immunotesting: Approaching the analytical performance of central laboratory methods", *Clin. Biochem.*, 2005, 38, 591-606.

[103] S. Su, M. M. Ali, C. D. M. Filipe, Y. Li, R. Pelton, "Microgel-based inks for paper-supported biosensing applications", *Biomacromolecules*, 2008, 9, 935-941.

[104] M. D. Bowman, R. C. Jeske, H. E. Blackwell, "Microwave-accelerated SPOT-synthesis on cellulose supports", *Org. Lett.*, 2004, 6, 2019-2022.

[105] K. Hilpert, D. F. H. Winkler, R. E. W. Hancock, "Peptide arrays on cellulose support: SPOT synthesis, a time and cost efficient method for synthesis of large numbers of peptides in a parallel and addressable fashion", *Nat. Protoc.*, 2007, 6, 133-1349.

[106] A. W. Martinez, S. T. Phillips, M. J. Butte, G. M. Whitesides, "Patterned paper as a platform for inexpensive, low-volume, portable bioassays" *Angew. Chemie*, 2007, 46, 1318-1320.

[107] Y. Wu, P. Xue, Y. Kang, K. M. Hui, "Paper-based microfluidic electrochemical immunodevice integrated with nanobioprobes onto graphene film for ultrasensitive multiplexed detection of cancer biomarkers", *Anal. Chem.*, 2013, 125, 8661-8668.

[108] Z. Nie, C. A. Nijhuis, J. Gong, X. Chen, A. Kumachev, A. W. Martinez, M. Narovlyansky, G. M. Whitesides, "Electrochemical sensing in paper-based microfluidic devices", *Lab Chip*, 2010, 10, 477-483.

[109] M. Zhou, M. Yang, F. Zhou, "Paper based colorimetric biosensing platform utilizing cross-linked siloxane as probe", *Biosens. Bioelectron.*, 2014, 55, 39-43.

[110] Y. C. Wei, L. M. Fu, C. H. Lin, "Electrophoresis separation and electrochemical detection on a novel thread-based microfluidic device", *Microfluid. Nanofluidics*, 2013, 14, 583-590.

[111] M. Reches, K. A. Mirica, R. Dasgupta, M. D. Dickey, M. J. Butte, G. M. Whitesides, "Thread as a Matrix for Biomedical Assays", *Appl. Mater. interfaces*, 2010, 2, 1722-1728.

[112] A. Nilghaz, D. H. B. Wicaksono, D. Gustiono, F. A. Abdul Majid, E. Supriyanto, M. R. Abdul Kadir, "Flexible microfluidic cloth-based analytical devices using a low-cost wax patterning technique", *Lab Chip*, 2012, 12, 209-218.

[113] W. Dungchai, O. Chailapakul, C. S. Henry, "Use of multiple colorimetric indicators for paper-based microfluidic devices", *Anal. Chim. Acta*, 2010, 674, 227-233.

[114] Y. Wu, P. Xue, Y. Kang, K. M. Hui, "Paper-Based Microfluidic electrochemical immunodevice integrated with nanobioprobes onto graphene film for ultrasensitive multiplexed detection of cancer biomarkers", *Anal. Chem*. 2013, 125, 8661-8668.

[115] L. Li, W. Li, C. Ma, H. Yang, S. Ge, J. Yu, "Paper-based electrochemiluminescence immunodevice for carcinoembryonic antigen using nanoporous gold-chitosan hybrids and graphene quantum dots functionalized Au@Pt", *Sens. Actuators B.*, 2014,202, 314-322.

[116] J. Yu, L. Ge, J. Huang, S. Wang, S. Ge, "Microfluidic paper-based chemiluminescence biosensor for simultaneous determination of glucose and uric acid", *Lab Chip*, 2011, 11, 1286-1291.

[117] T. Rungsawang, E. Punrat, J. Adkins, C. Henry, O. Chailapakul, "Development of electrochemical paper-based glucose sensor using cellulose-4-aminophenylboronic acid-modified screen-printed carbon electrode", *Electroanalysis*, 2015, 27.

[118] K. E. Berg, J. A. Adkins, S. E. Boyle, C. S. Henry, "Manganese detection using stencil-printed carbon ink electrodes on transparency film", *Electroanalysis*, 2015, 27.

[119] W. Dungchai, O. Chailapakul, C. S. Henry, "Electrochemical detection for paper-based microfluidics", *Anal. Chem.*, 2009, 81, 5821-5826.

[120] W. Dungchai, O. Chailapakul, C. S. Henry, "A low-cost, simple, and rapid fabrication method for paper-based microfluidics using wax screen-printing", *Analyst*, 2011, 136, 77-82.

[121] D. Dendukuri, T. Choudhary, G. P. Rajamanickam, "Woven Electrochemical Fabric-based Test Sensors (WEFTS): A new class of multiplexed electrochemical sensors", *Lab Chip*, 2015, 15, 2064-2072.

[122] H. Yang, Q. Kong, S. Wang, J. Xu, Z. Bian, X. Zheng, C. Ma, S. Ge, J. Yu, "Hand-drawn&written pen-on-paper electrochemiluminescence immunodevice powered by rechargeable battery for low-cost point-of-care testing", *Biosens. Bioelectron.*, 2014, 61, 21-27.

[123] A. C. Glavan, D. C. Christodouleas, B. Mosadegh, H. D. Yu, B. S. Smith, J. Lessing, M. T. Fernández-Abedul, G. M. Whitesides, "Folding analytical devices for electrochemical ELISA in hydrophobic R^F paper", *Anal. Chem.*, 2014, 86, 11999-12007.

[124] K. C. Honeychurch, "The voltammetric behaviour of lead at a hand drawn pencil electrode and its trace determination in water by stripping voltammetry", *Anal. Methods*, 2015, 7, 2437-2443.

[125] J. Zhang, L. Huang, Y. Lin, L. Chen, Z. Zeng, L. Shen, Q. Chen, "Pencil-trace on printed silver interdigitated electrodes for paper-based NO_2 gas sensors", *Appl. Phys. Lett.*, 2015, 106, 143101.

[126] N. Dossi, R. Toniolo, F. Impellizzieri, G. Bontempelli, "Doped pencil leads for drawing modified electrodes on paper-based electrochemical devices", *J. Electroanal. Chem.*, 2014,723,90-94.

[127] B. Rezaei, M. Ghani, A. M. Shoushtari, M. Rabiee, "Electrochemical biosensors based on nanofibres for cardiac biomarker detection: A comprehensive review", *Biosens. Bioelectron.*, 2016, 78, 513-523.

[128] L. Reverté, B. Prieto-Simón, M. Campàs, "New advances in electrochemical biosensors for the detection of toxins: Nanomaterials, magnetic beads and microfluidics systems. A review", *Anal. Chim. Acta*, 2016, 908, 8-21.

[129] M. M. Pereira da Silva Neves, M. B. G. García, C. Delerue-Matos, A. C. García, "Nanohybrid materials as transducer surfaces for electrochemical sensing applications", *Electroanalysis*, 2011, 23, 63-71.

[130] S. N. Kim, J. F. Rusling, F. Papadimitrakopoulos, "Carbon nanotubes for electronic and electrochemical detection of biomolecules", *Adv. Mater.*, 2007, 19, 3214-3228.

[131] J. Prasek, J. Drbohlavova, J. Chomoucka, J. Hubalek, O. Jasek, V. Adam, R. Kizek, "Methods for carbon nanotubes synthesis-review", *J. Mater. Chem.*, 2011, 21, 15872.

[132] Y.-L. Zhao, J. F. Stoddart, "Noncovalent Functionalization of Single-Walled Carbon Nanotubes", *Acc. Chem. Res.*, 2009, 42, 1161-1171.

[133] K. Balasubramanian, M. Burghard, "Chemically functionalized carbon nanotubes", *Small*, 2005, 1, 180-192.

[134] A. K. Sarma, P. Vatsyayan, P. Goswami, S. D. Minteer, "Recent advances in material science for developing enzyme electrodes", *Biosens. Bioelectron.*, 2009, 24, 2313-2322.

[135] J. M. Pingarrón, P. Yáñez-Sedeño, A. González-Cortés, "Gold nanoparticle-based electrochemical biosensors", *Electrochim. Acta*, 2008, 53, 5848-5866.

[136] S. Liu, D. Leech, H. Ju, "Application of colloidal gold in protein Immobilization, electron transfer, and biosensing", *Anal. Lett.*, 2003,36, 1-19.

[137] R. T. Pötzschke, C. A. Gervasi, S. Vinzelberg, G. Staikov, W. J. Lorenz, "Nanoscale studies of Ag electrodeposition on HOPG (0001)", *Electrochim. Acta*, 1995, 40, 1469-1474.

[138] G. Martínez-Paredes, M. B. González-García, A. Costa-García, "In situ electrochemical generation of gold nanostructured screen-printed carbon electrodes. Application to the detection of lead underpotential deposition", *Electrochim. Acta*, 2009, 54, 4801-4808.

[139] J. Ruzicka, E. H. Hansen, "Flow injection analyses. Part I. A new concept of fast continuous flow analysis", *Anal. Chim. Acta*, 1975, 78, 145-157.

[140] C. Vakh, M. Falkova, I. Timofeeva, A. Moskvin, A. Bulatov, "Flow analysis : A novel approach for classification", *Crit. Rev. Anal. Chem.*, 2016.

[141] B. Shu, C. Zhang, D. Xing, "Segmented continuous-flow multiplex polymerase chain reaction microfluidics for high-throughput and rapid foodborne pathogen detection", *Anal. Chim. Acta*, 2014, 826, 51-60.

[142] R. Sánchez, J. L. Todolí, C.P. Lienemann, J.M. Mermet, "Universal calibration for metal determination in fuels and biofuels by inductively coupled plasma atomic emission spectrometry based on segmented flow injection and a 350°C heated chamber", *J. Anal. At. Spectrom.*, 2012, 27, 937-945.

[143] J. Cazes, *Ewing's Analytical Instrumentation Handbook*, 3ª ed. Dekker, 2009.

[144] J. Kozak, J. Paluch, A. Węgrzecka, M. Kozak, M. Wieczorek, J. Kochana, P. Kościelniak, "Single peak parameters technique for simultaneous measurements: Spectrophotometric sequential injection determination of Fe(II) and Fe(III)", *Talanta*, 2016, 148, 626-632.

[145] G. Shao, D. Lu, Z. Fu, D. Du, R. M. Ozanich, W. Wang, Y. Lin, "Design, fabrication and test of a pneumatically controlled, renewable, microfluidic bead trapping device for sequential injection analysis applications", *Analyst*, 2016, 141, 206-215.

[146] M. Trojanowicz, K. Kolacinska, "Recent advances in flow injection analysis", *Analyst*, 2016.

[147] A. A. Kulkarni, I. S. Vaidya, "Flow injection analysis: an overview", *J. Crit. Rev.*, 2015, 2, 19-24.

[148] R. C. Prados-Rosales, J. L. Luque-García, M. D. L. de Castro, "Propelling devices: the heart of flow injection approaches", *Anal. Chim. Acta*, 2002, 461, 169-180.

[149] M. Ibrahim, M. Alaam, H. El-Haes, A. F. Jalbout, A. De Leon, "Analysis of the structure and vibrational spectra of glucose and fructose", *Eclética Química*, 2006, 31, 15-21.

[150] J. Wang, "Electrochemical glucose biosensors", *Chem. Rev.*, 2008, 108, 814-825.

[151] J. D. Newman, A. P. F. Turner, "Home blood glucose biosensors: A commercial perspective", *Biosens. Bioelectron.*, 2005, 20, 2435-2453.

[152] M. M. Rahman, A. J. S. Ahammad, J. H. Jin, S. J. Ahn, J. J. Lee, "A Comprehensive Review of Glucose Biosensors Based on Nanostructured Metal-Oxides", *Sensors*, 2010, 10, 4855-4886.

[153] S. Wild, G. Roglic, A. Green, R. Sicree, H. King, "Global prevalence of diabetes. Estimates for the year 2000 and projections for 2030", *Diabetes Care*, 2004, 27, 1047-1053.

[154] G. S. Wilson, R. Gifford, "Biosensors for real-time in vivo measurements", *Biosens. Bioelectron.*, 2005, 20, 2388-2403.

[155] S. A. Zaidi, J. H. Shin, "Recent developments in nanostructure based electrochemical glucose sensors", *Talanta*, 2016, 149, 30-42.

[156] K. Tian, M. Prestgard, A. Tiwari, "A review of recent advances in nonenzymatic glucose sensors", *Mater. Sci. Eng. C*, 2014, 41, 100-118.

[157] H.C. Wang, A.R. Lee, "Recent developments in blood glucose sensors", *J. Food Drug Anal.*, 2015, 23, 191-200.

[158] C. A. Lyssiotis, L. C. Cantley, "Metabolic syndrome: F stands for fructose and fat", *Nature*, 2013, 502, 181-182.

[159] J. L. Sievenpiper, R. J. de Souza, A. Mirrahimi, M. E. Yu, A. J. Carleton, J. Beyene, L. Chiavaroli, M. Di Buono, A. L. Jenkins, L. A. Leiter, T. M. S. Wolever, C. W. C. Kendall, D. J. A. Jenkins, "Effect of Fructose on Body Weight in Controlled Feeding Trials", *Ann. Intern. Med.*, 2012, 156, 291-304.

[160] P. A. Paredes, J. Parellada, V. M. Fernández, L. Katakis, E. Domínguez, "Amperometric mediated carbon paste biosensor based on D-fructose dehydrogenase for the determination of fructose in food analysis", *Biosens. Bioelectron.*, 1997, 12, 1233-1243.

[161] P. N. Wahjudi, M. E. Patterson, S. Lim, J. K. Yee, C. S. Mao, W. N. P. Lee, "Measurement of glucose and fructose in clinical samples using gas chromatography/mass spectrometry", *Clin. Biochem.*, 2010, 43, 198-207.

[162] C. W. Wang, W. T. Chen, H. T. Chang, "Quantification of saccharides in honey samples through surface-assisted laser desorption/ionization mass spectrometry using HgTe nanostructures", *J. Am. Soc. Mass Spectrom.*, 2014, 25, 1247-1252.

[163] W. Tan, D. Zhang, Z. Wang, C. Liu, D. Zhu, "4-(N,N-Dimethylamine)benzonitrile (DMABN) derivatives with boronic acid and boronate groups: new fluorescent sensors for saccharides and

fluoride ion", *J. Mater. Chem.*, 2007, 17, 1964-1968.

[164] S. Qian, Y. Liang, J. Ma, Y. Zhang, J. Zhao, W. Peng, "Boronic acid modified fiber optic SPR sensor and its application in saccharide detection", *Sens. Actuators B.*, 2015, 220, 1217-1223.

[165] R. Antiochia, L. Gorton, "A new osmium-polymer modified screen-printed graphene electrode for fructose detection", *Sens. Actuators B.*, 2014, 195, 287-293.

[166] U. B. Trivedi, D. Lakshminarayana, I. L. Kothari, P. B. Patel, C. J. Panchal, "Amperometric fructose biosensor based on fructose dehydrogenase enzyme", *Sens. Actuators B.*, 2009, 136, 45-51.

[167] S. Campuzano, V. Escamilla-Gómez, M. Ángeles Herranz, M. Pedrero, J. M. Pingarrón, "Development of amperometric biosensors using thiolated tetrathiafulvalene-derivatised self-assembled monolayer modified electrodes", *Sens. Actuators B.*, 2008, 134, 974-980.

[168] B. Bucur, G. L. Radu, C. N. Toader, "Analysis of methanol–ethanol mixtures from falsified beverages using a dual biosensors amperometric system based on alcohol dehydrogenase and alcohol oxidase", *Eur. Food Res. Technol.*, 2007, 226, 1335-1342.

[169] Y. Lin, S. Tanaka, "Ethanol fermentation from biomass resources: Current state and prospects", *Appl. Microbiol. Biotechnol.*, 2006, 69, 627-642.

[170] G. Wen, Y. Zhang, S. Shuang, C. Dong, M. M. F. Choi, "Application of a biosensor for monitoring of ethanol", *Biosens. Bioelectron.*, 2007, 23, 121-129.

[171] A. L. Zou, Y. Qiu, J. J. Yu, B. Yin, G. Y. Cao, H. Q. Zhang, L. Z. Hu, "Ethanol sensing with Au-modified ZnO microwires", *Sens. Actuators B.*, 2016,227, 65-72.

[172] B. Tao, J. Zhang, S. Hui, L. Wan, "An amperometric ethanol sensor based on a Pd–Ni/SiNWs electrode", *Sens. Actuators B.*, 2009, 142, 298-303.

[173] M. Hnaien, F. Lagarde, N. Jaffrezic-Renault, "A rapid and sensitive alcohol oxidase/catalase conductometric biosensor for alcohol determination", *Talanta*, 2010, 81, 222-227.

[174] T. Gessei, H. Sato, E. Kazawa, H. Kudo, H. Saito, K. Mitsubayashi, "Bio-sniffers for ethanol and acetaldehyde using carbon and Ag/AgCl coated electrodes", *Microchim. Acta*, 2009, 165, 179-186.

[175] M. Prince, E. Albanese, M. Guerchet, M. Prina, "World Alzheimer Report 2014, Dementia and risk reduction, An analysis of protective and modifiable factors," London, 2014.

[176] W. Thies, L. Bleiler, "2013 Alzheimer's disease facts and figures", *Alzheimer's Dement.*, 2013, 9, 208-245.

[177] M. B. Graeber, "The case described by Alois Alzheimer in 1911", *Eur. Arch. Psychiatry Clin. Neurosci.*, 1998, 248, 111-122.

[178] H. Hippius, G. Neundorfer, "The discovery of Alzheimer's disease", *Dialogues Clin. Neurosci.*, 2003, 5, 101-108.

[179] C. L. Allan, C. E. Sexton, D. Welchew, K. P. Ebmeier, "Imaging and biomarkers for Alzheimer's disease", *Maturitas*, 2010, 65, 138-142.

[180] Alzheimer's Association, "Alzheimer's disease facts and figures", *Alzheimer's Dement.*, 2016, 12,

459-509.

[181] C. Valls-pedret, J. L. Molinuevo, L. Rami, "Diagnóstico precoz de la enfermedad de Alzheime : fase prodrómica y preclínica", 2010, 51, 471-480.

[182] E. Arana Fernández de Moya, "Demencias e imagen: lo basico", *Radiologia*, 2010, 52, 4-17.

[183] J. Atkinson A.J., W. A. Colburn, V. G. DeGruttola, D. L. DeMets, G. J. Downing, D. F. Hoth, J. A. Oates, C. C. Peck, R. T. Schooley, B. A. Spilker, J. Woodcock, S. L. Zeger, "Biomarkers and surrogate endpoints: Preferred definitions and conceptual framework", *Clin. Pharmacol. Ther.*, 2001, 69, 89-95.

[184] F. H. Bouwman, S. N. M. Schoonenboom, W. M. van der Flier, E. J. van Elk, A. Kok, F. Barkhof, M. a Blankenstein, P. Scheltens, "CSF biomarkers and medial temporal lobe atrophy predict dementia in mild cognitive impairment", *Neurobiol. Aging*, 2007, 28, 1070-1074.

[185] M. G. Spillantini, M. Goedert, "Tau protein pathology in neurodegenerative diseases", *Trends Neurosci.*, 1998, 2236, 428- 433.

[186] A. M. Fagan, D. M. Holtzman, "Cerebrospinal fluid biomarkers of Alzheimer's disease" *Biomark. Med.*, 2010, 4, 51-63.

[187] J. Hardy, D. J. Selkoe, "The Amyloid Hypothesis of Alzheimer's Disease: Progress and Problems on the Road to Therapeutics" *Science*, 2002, 297, 184-185.

[188] J. A. Monge-Argilés, J. Sánchez-Payá, C. Muñoz-Ruíz, A. Pampliega-Pérez, J. Montoya-Gutiérrez, C. Leiva-Santana, "Biomarcadores en el líquido cefalorraquídeo de pacientes con deterioro cognitivo leve: metaanálisis de su capacidad predictiva para el diagnóstico de la enfermedad de Alzheimer", *Neurologia*, 2010, 50, 193-200.

[189] A. Kaushik, R. D. Jayant, S. Tiwari, A. Vashist, M. Nair, "Nano-biosensors to detect beta-amyloid for Alzheimer's disease management", *Biosens. Bioelectron.*, 2016, 80, 273-287.

[190] "AnaSpec, Inc., www.anaspec.com". Fecha de consulta: 20 de Mayo de 2016

[191] "Thermo Fisher Scientific Inc., www.thermofisher.com". Fecha de consulta: 20 de Mayo de 2016

[192] "Fujirebio, www.fujirebio-europe.com". Fecha de consulta: 20 de Mayo de 2016

[193] M. Yang, X. Yi, J. Wang, F. Zhou, "Electroanalytical and surface plasmon resonance sensors for detection of breast cancer and Alzheimer's disease biomarkers in cells and body fluids", *Analyst*, 2014, 139, 1814-1825.

[194] S. Chen, L. Zhang, Y. Long, F. Zhou, "Electroanalytical Sensors and Methods for Assays and Studies of Neurological Biomarkers", *Electroanalysis*, 2014, 26, 1236-1248.

[195] "World Health Organization, International Agency for Research on Cancer, GLOBOCAN 2012, http://globocan.iarc.fr. Fecha de consulta: 10 de Mayo de 2016

[196] K. D. Cole, H. J. He, L. Wang, "Breast cancer biomarker measurements and standards", *Proteomics - Clin. Appl.*, 2013, 7, 17-29.

[197] Q. A. M. Al Khafaji, M. Harris, S. Tombelli, S. Laschi, A. P. F. Turner, M. Mascini, G. Marrazza, "An Electrochemical Immunoassay for HER2 Detection", *Electroanalysis*, 2012, 24, 735-742.

[198] A. Ravelli, J. M. Reuben, F. Lanza, S. Anfossi, M. R. Cappelletti, L. Zanotti, A. Gobbi, C. Senti, P. Brambilla, M. Milani, D. Spada, P. Pedrazzoli, M. Martino, A. Bottini, D. Generali, "Breast cancer circulating biomarkers: advantages, drawbacks, and new insights", *Tumor Biol.*, 2015, 36, 6653-6665.

[199] L. Lam, N. McAndrew, M. Yee, T. Fu, J. C. Tchou, H. Zhang, "Challenges in the clinical utility of the serum test for HER2 ECD", *Biochim. Biophys. Acta,* 2012, 826, 199-208.

[200] L. J. Tafe, G. J. Tsongalis, "The human epidermal growth factor receptor 2 (HER2)", *Clin. Chem. Lab. Med.*, 2012, 50, 23-30.

[201] M. J. Duffy, D. Evoy, E. W. McDermott, "CA 15-3: Uses and limitation as a biomarker for breast cancer", *Clin. Chim. Acta*, 2010, 411, 1869-18874.

[202] A. N. Bhatt, R. Mathur, A. Farooque, A. Verma, B. S. Dwarakanath, "Cancer biomarkers - current perspectives", *Indian J. Med. Res.*, 2010, 132, 129-149.

[203] J. A. Ludwig, J. N. Weinstein, "Biomarkers in cancer staging, prognosis and treatment selection", *Nat. Rev. Cancer*, 2005, 5, 845-856.

2. OBJETIVOS

El objetivo de esta Tesis Doctoral es el desarrollo de diferentes dispositivos analíticos (principalmente biosensores e inmunosensores) con detección electroquímica utilizando transductores de carbono. Para ello se escogieron primeramente como tales transductores los electrodos serigrafiados debido a las grandes ventajas que aportan al desarrollo de sensores. Además, gracias a la gran variedad de diseños comerciales disponibles, fue posible utilizar diferentes electrodos adecuándose a la aplicación final pretendida.

En la última parte de esta Tesis se decidió, siguiendo las tendencias actuales en cuanto a detección electroquímica, utilizar alfileres como transductores ya que son materiales de uso común, producidos en masa y de muy bajo coste.

Este objetivo tan amplio se puede desglosar en los siguientes objetivos parciales:

- Objetivo específico 1: construcción y puesta a punto de sensores enzimáticos miniaturizados, desechables, de fabricación simple y fácil utilización para la determinación de glucosa, fructosa y etanol utilizando electrodos serigrafiados de carbono modificados con mediadores redox.
- Objetivo específico 2: desarrollo de un immunosensor miniaturizado y desechable para la determinación de beta-amiloide 1-42 (biomarcador de la enfermedad de Alzheimer) basado en electrodos serigrafiados de carbono.
- Objetivo específico 3: desarrollo de un bi-immunosensor miniaturizado y desechable para la determinación de CA 15-3 y HER2 (biomarcadores del cáncer de mama) basado en electrodos serigrafiados con dos electrodos de trabajo de carbono.
- Objetivo específico 4: diseño y fabricación de un biosensor electroquímico para la determinación de glucosa utilizando alfileres modificados con tinta de carbono como transductores.
- Objetivo específico 5: diseño de un dispositivo multidetección basado en alfileres.
- Objetivo específico 6: diseño, construcción y evaluación de un sistema de inyección en flujo con detección electroquímica utilizando alfileres como electrodos.

3. RESULTADOS Y DISCUSIÓN

3.1. Capítulo I: Sensores enzimáticos basados en electrodos serigrafiados

- Artículo 1: "*Enzymatic sensor using mediator-screen-printed carbon electrodes*"
- Artículo 2: "*Amperometric fructose sensor based on ferrocyanide modified screen-printed carbon electrode*"
- Artículo 3: "*Comparative study of different alcohol sensors based on screen-printed carbon electrodes*"

3.1.1. Introducción

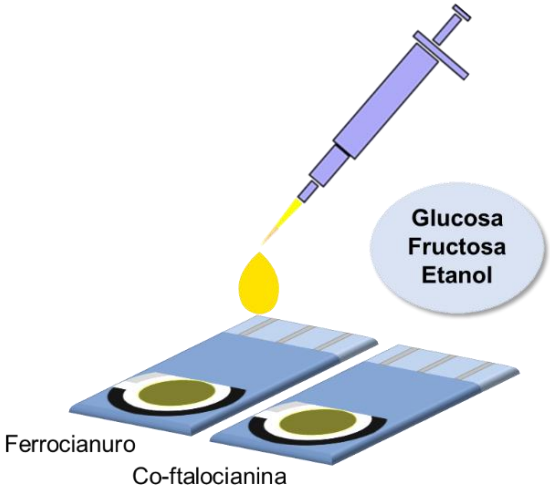

Como se ha mencionado anteriormente, la glucosa, la fructosa y el etanol son analitos de gran interés. En este capítulo se desarrollan y ponen a punto metodologías para la construcción de biosensores para estos analitos utilizando electrodos serigrafiados de carbono como transductores. El objetivo es obtener biosensores lo más simple posibles pero con características analíticas adecuadas para su aplicación a muestras reales.

Los electrodos serigrafiados de carbono que se utilizan a lo largo de este capítulo están modificados con mediadores redox incluidos en la tinta de carbono del electrodo de trabajo. Los mediadores redox, como ya se ha indicado, son especies que facilitan la transferencia electrónica entre la especie a oxidar (o reducir) y la superficie electródica. Aunque en la bibliografía hay varios ejemplos de electrocatálisis directa, el alto potencial necesario (que disminuye la selectividad del sensor) y las bajas corrientes que se obtienen (lo que afecta a la sensibilidad), hacen que el uso de un mediador como aceptor de electrones sea habitual en los biosensores enzimáticos.

Existen diferentes métodos para incluir un mediador en un biosensor: entrecruzamiento, electrodeposición, retención mediante membrana,… Sin embargo, en este capítulo se opta por emplear electrodos serigrafiados comerciales que contienen el mediador ya incluido en la tinta del electrodo de trabajo, a fin de simplificar lo más posible la fabricación de los biosensores. Además, como la inmovilización de las enzimas se realiza por adsorción, se obtienen dispositivos desechables con una fabricación muy rápida y sencilla.

3.1.2. Artículo 1: "*Enzymatic sensor using mediator-screen-printed carbon electrodes*"

Electroanalysis 2011, 23, 209-214

Full Paper ELECTROANALYSIS

Electroanalysis 2011, 23 (1) 209 - 214

Enzymatic Sensor Using Mediator-Screen-Printed Carbon Electrode

Julien Biscay[a], Estefanía Costa Rama[a], María Begoña González García[a], José Manuel Pingarrón Carrazón[b], Agustín Costa García[a]*

[a]Departamento de Química Física y Analítica, Facultad de Química, Universidad de Oviedo, 33006 Oviedo, España

[b]Departamento de Química Analítica, Facultad de Química, Universidad Complutense de Madrid, 28040 Madrid, España

Presented at the 13th International Conference on Electroanalysis, ESEAC 2010, Gijón, Spain

ABSTRACT

A new glucose sensor was developed using screen-printed ferrocyanide/carbon electrodes. The ferrocyanide is included in the carbon ink of the commercial screen-printed electrode. The immobilization of enzymes glucose oxidase (GOx) and horseradish peroxidase (HRP) was carried out in a very easy way. An aliquot of 10 µL of a GOx/HRP mixture was deposited on the electrode surface and left there until dried (approximately 1 h) at room temperature. The ferricyanide generated enzymatically was detected amperometrically applying a potential of -0.1 V (*vs*. Ag pseudo reference electrode). The sensor, so constructed, shows a good sensitivity to glucose (-2.12 µA/mM) with a slope deviation of ±0.06 µA/mM and a linear range comprised between 0.05 and 1 mM of glucose, with a limit of detection of 0.025 mM. These sensors show good intersensors reproducibility and a high stability. When they are stored at 4°C, no significant changes in the slope value of the glucose calibration plot were found after 3 months. Glucose was determined in real samples as honey, blood, drink for babies and glucosed drink with a great accuracy.

Keywords: Ferrocyanide, Glucose Oxidase, Glucose Sensors, Peroxidase, Screen-Printed Carbon Electrodes.

1. Introduction

In recent years, electrochemical detection, based on amperometric enzyme electrodes using oxido-reductase enzymes, has been developed combining the selectivity of the enzymes for its natural substrate with the sensitivity of the electrochemical detection.

Electrochemical biosensors have been applied successfully for the determination of glucose. In general, glucose oxidase (GOx) is selected as a model enzyme due to its inexpensive, stable, and practical use [1,2]. The detection of glucose by electrochemical biosensors is based on the electrochemical oxidation of hydrogen peroxide generated by enzyme-catalyzed oxidation of glucose at anodic potentials (higher than 0.6 V vs. Ag/AgCl) [1,3,4]. Consequently, the co-oxidations of others electrochemically active substances such as ascorbic acid (AA), uric acid (UA) may produce undesirable interfering currents. In order to overcome this interference problem, some improved biosensors have been used to detect hydrogen peroxide at low potentials [5,6], and nonconducting polymers have been employed as selective membranes [2]. Another strategy to measure at lower potential consists to use other mediators as Prussian Blue [7,8], Meldola Blue [9], ferrocene [10, 11] or ferrocyanide [12,13]. Nanomaterials such as gold nanoparticles [14, 15] or carbon nanotubes [16] have also been used in order to improve the electronic transfer between the electroactive center of the enzyme and the surface electrode (3rd generation sensor) [17]. These sensors would not need any mediator but in most of the cases, those sensors with nanoparticles or nanotubes need some compound as mediator [18,19], which can offer an improvement of sensitivity. The immobilization of the enzyme and the mediator is a very important step. Both stability and the biological function of the enzyme mainly depend of the immobilization. Thus different enzyme immobilization techniques are possible [20]: adsorption [21], cross-linking [22,23], entrapment [24,25] or electropolymerization [26,27] are carried out in order to ensure the stability of the sensor.

The present work describes the design of a glucose sensor, using a screen-printed ferrocyanide/carbon electrode (SPFCE). Screen-printing is a well-established technique to fabricate electrochemical transducers because of its low cost and the possibility of their massive production [28,29]. Moreover it allows using different inks that includes compounds that can act as mediators. These advantages, together with the ones associated to the enzymatic biosensors, convert these devices in a tool of great interest in food industry [28,30], clinical [31] and environmental analysis [32]. The glucose sensor developed in this work was obtained by the adsorption of a GOx/HRP mixture on the SPFCE surface.

2. Experimental

2.1. Chemicals

Glucose oxidase (GOx; ref. G2133), horseradish peroxidase (HRP; ref. 6782), trizma base, minimum 99.9% titration (ref. T1503) were purchased from Sigma (Spain) and both, *D-(+)*-Glucose anhydrous for biochemistry (ref. 8582146) and the nitric acid 65% were delivered by Merck (Spain). All chemicals were of analytical reagent grade, and the water used was obtained from a Millipore Milli-Q purification system. Stock solutions of glucose and GOx/HRP mixture were prepared daily in 0.1 M Tris-HNO_3 buffer of pH 7 and stored at 4^0C in a refrigerator. Britton-Robinson buffer solutions of pH values between 3 and 9 were used for pH studies.

2.2. Apparatus and measurements

Chronoamperometric measurements were performed using an ECO Chemie µAutolab type II potentiostat interfaced with a Pentium 166 computer system and controlled by the Autolab GPES software version 4.8 for Windows 98. All measurements were carried out at room temperature. Screen-printed ferrocyanide/carbon electrodes (ref DRP-F10) and an edge connector (ref. DRPDSC) were purchased from DropSens, S.L (Oviedo, Spain). These sensors consist in a Ferrocyanide/Carbon working (4 mm diameter), carbon auxiliary and silver pseudo reference electrodes printed on an alumina substrate. An insulating layer serves to delimit the electrochemical cell and electric contacts.

2.3. Electrode modification

After a first step of washing, 10 µL of a mixture of GOx (1.6 U/µL) and HRP (2.5 U/µL) were deposited on the SPFCE to construct a single-use glucose sensor. The mixture of enzymes was prepared in a 0.1 M Tris-HNO_3 buffer (pH 7) and leaving to dry 1 h onto the electrode. After a second washing step, the sensor can be used or kept into a refrigerator at 4^0C and protected from light.

2.4. Analytical signal recording

To obtain the analytical signal, an aliquot of 40 µL of glucose solution was deposited on the sensor. The chronoamperogram was recorded applying a potential of -0.1 V during 50 s. A different sensor was used for each measurement.

2.5. Real sample measurements

The sensor developed in this work was tested in different real samples (blood, honey, drinks for babies and glucose drink). In the case of blood, the sample was centrifuged at 5000 rpm during 5 min. Then, the serum was diluted 10 times in the buffer. 1 g of honey was diluted in 50 mL of Milli-Q water and diluted 100 times in the buffer solution. 20 g of glucosed drink were dissolved in 100 mL of Milli-Q water and next, this solution was diluted 10000 times in the buffer solution. Finally, the drink for babies was diluted 100 times in the buffer solution. 40 µL of each sample were put on different sensors and the chronoamperogram was recorded during 50 s applying a potential of -0.1 V.

3. Results and Discussion

3.1. Optimization of parameters that affect the enzymatic rate

The enzyme reaction was monitored by the reduction of the ferricyanide enzymatically generated (**Figure 1**).

As following, different parameters were optimized as the concentration of the enzymes and the buffer pH.

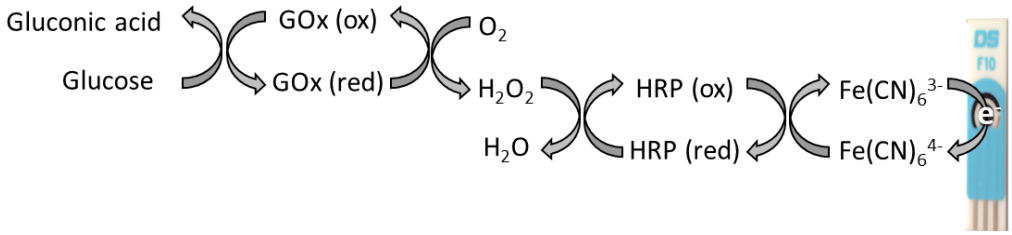

Fig. 1. Enzymatic reactions at the electrode surface.

3.1.1. Concentration of the enzymes

Different sensors were prepared, according **Section 2.3**, dropping GOx/HRP mixtures with different concentrations of enzymes. For each concentration of enzymes, a chronoamperogram for a glucose concentration of 0.10 mM was recorded as described in **Section 2.4**. The result of this study is reported in **Figure 2**.

It can be noted that the analytical signal increases with the concentration of GOx, whereas the response of the sensor is constant for HRP concentrations comprised between

2.5 and 10.7 U/µL. A concentration of 1.6 U/µL and 2.5 U/µL of GOx and HRP respectively were chosen because for these ones, higher and more reproducibility signal was obtained.

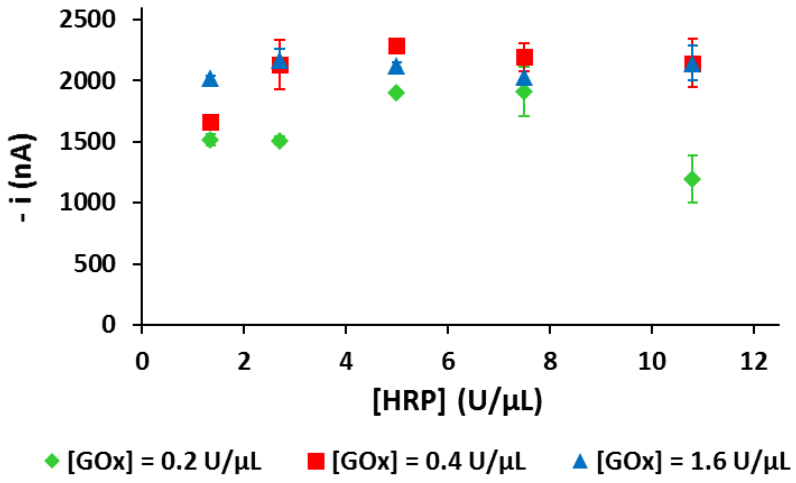

Fig. 2. Effect of the concentration of GOx and HRP on the analytical signal. Glucose concentration 0.10 mM; E applied -0.1 V. Data are given as average *±SD* (n = 3).

3.1.2. Effect of the pH

The influence of the pH on the sensor response was studied. The GOx/HRP mixture was prepared in different Britton-Robinson solutions of different pHs (3 < pH < 9). Sensors were prepared as explained in **Section 2.3** and the chronoamperometric signal was recorded as described in **Section 2.4**. All the results are summarized in the **Figure 3**.

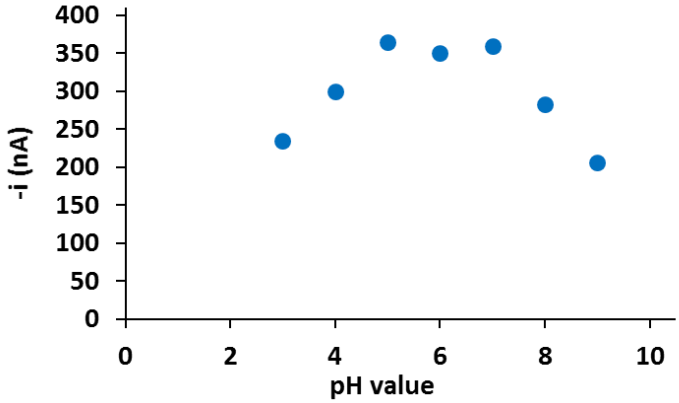

Fig. 3. Effect of pH value on response of sensors for 0.10 mM glucose (1.6 U/µL GOx and 2.5 U/µL HRP).

The analytical signal increases with pH until a value of 5 when a plateau was reached between 5 and 7. Then stabilization can be observed in the pH range 5 - 7. At higher pH values the sensor response decreases. Those results are as expected because they correspond to the optimal pH range of the enzymes. For further studies a pH of 7 was chosen which corresponds to the pH commonly used.

3.2. Calibration of the sensor

Chronoamperograms corresponding to an addition of 40 µL of different concentrations of glucose were recorded to check the response of the electrodes in presence of glucose. **Figure 4A** shows the calibration curve obtained. The sensor shows Michaelis-Menten kinetics. Using the Lineweaver-Burk linearization, the Michaelis-Menten constant (K_m) was calculated and the value was 1.7 ± 0.3 mM. This data was lower than previously reported values using GOx/Au_{nano}/Pt_{nano}/gold electrode (11.89 mM) [33], using Pt_{nano}-CNT electrode (14.4 mM) [34] or using Prussian Blue as mediator (3.73 mM) [8], suggesting the high affinity of the GOx/HRP glucose biosensor [35,36]. It can be explained by the simplicity of the enzyme immobilization. It reveals that the biosensor remains GOx activity and a high affinity to glucose. The linear range is represented in the **Figure 4B**. A linear relationship between current and glucose concentration in the range of 0.05 and 1 mM was obtained with a correlation coefficient of 0.998 (n = 3) according to the following equation:

$$i\ (\mu A) = -2.10\ [glucose]\ (mM) - 0.06$$

This linear range is similar to the sensors found in the literature using a bienzymatic system based in GOx and HRP [36,37] but in these works the biosensor preparation is much more laborious. Concerning the sensitivity, it is close to the sensors based on Prussian Blue and modified with carbon nanotubes (2.67 µA/mM) [38] and superior in comparison with the sensor using ferrocyanide which needs chitosan oligomers (0.677 µA/mM) [39].

In order to evaluate the reproducibility of the sensor, a series of 33 electrodes was prepared and tested the same day. This operation was repeated 4 times in different days. A calibration plot of each series was carried out with solutions of glucose prepared the day of the measurement. **Table 1** shows the different calibration plot equations obtained with all series. Then, the slopes of subsequent calibrations were used to calculate the reproducibility in terms of *RSD* (**Table 1**).

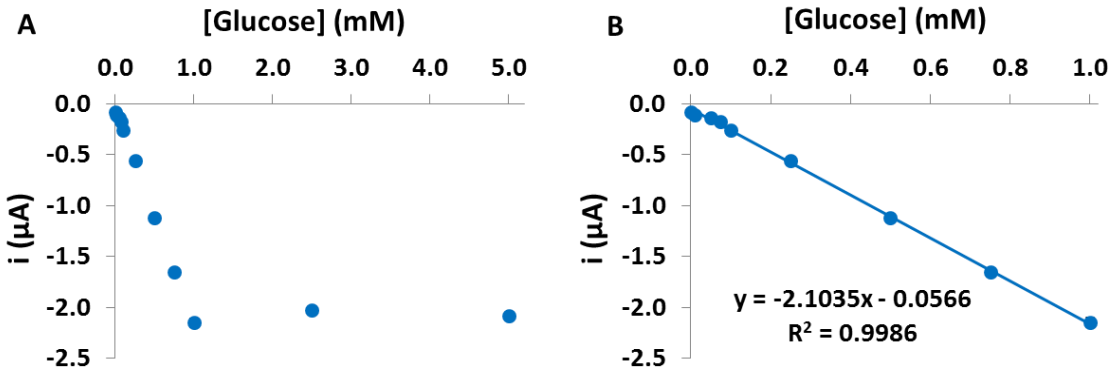

Fig. 4. Calibration curve and calibration plot of the proposed glucose sensor in the concentration range 0.05 - 1 mM. Detection potential = -0.1 V (*vs*. Ag pseudoreference electrode). Data are given as average ±*SD* (n = 3)

The sensor presents an excellent reproducibility and a slope of -2.12 ± 0.06 µA/mM (R^2 = 0.997). This reproducibility allows the detection of glucose with a simple measurement (one standard and the sample). The relative standard deviation of the different slopes is 2.6% (n = 4). The sensor presents a very good reproducibility in comparison of the other sensors and particularly those using mixture of GOx/HRP with bovine serum albumin (BSA) as cross-linker (6.47%) [12].

Table 1. Calibration plot equations of four glucose sensor series. n = 9 in all calibration plots. Each point was measured three times.

	Equation	R^2
Calibration plot 1	i (µA) = -2.19 [glucose] (mM) - 0.06	0.9973
Calibration plot 2	i (µA) = -2.12 [glucose] (mM) - 0.04	0.9994
Calibration plot 3	i (µA) = -2.04 [glucose] (mM) - 0.04	0.9990
Calibration plot 4	i (µA) = -2.14 [glucose] (mM) - 0.07	0.9940
Mean slope	-2.12 ± 0.06 µA/mM	

3.3. Specificity of the sensor

Potential interferences for the amperometric response of the sensor were checked. For example, glucose and fructose are the most important sugars presents in honey. Also during the fermentation of wine it is important to know the level of glucose and the ascorbic acid

may interference in the measurement. To evaluate these interferences, solutions of 0.10 mM of glucose, fructose and ascorbic acid, mixture of fructose (0.10 mM) and glucose (0.10 mM), and another one of ascorbic acid (0.10 mM) and glucose (0.10 mM) were prepared. 40 µL of those solutions were dropped on the sensor and chronoamperograms were recorded as explained in the **Section 2.4**. **Table 2** sumarizes the results obtained. It can be seen that the sensor does not give any response in the presence of fructose, due to the enzyme specificity. The presence of ascorbic acid does not interfere in the analytical signal.

Table 2. Study of the interferences caused by fructose and ascorbic acid. Data are given as average *±SD* (n = 3).

Background	Glucose	Fructose	Ascorbic acid	Glucose-fructose	Glucose-ascorbic acid
-97 ± 6 nA	-580 ± 17 nA	-70 ± 0 nA	-163 ± 15 nA	-590 ± 17 nA	-595 ± 21 nA

3.4. Stability of the sensor

Several glucose sensors were prepared and kept into the refrigerator (4^0C) and light protected until their use. A calibration plot was carried out in the range of 0.01 to 5 mM at different times (1, 15, 30, 60 and 90 days). The calibrations plots are shown in the **Table 3**.

Table 3. Calibration plots of electrodes stored during different times. n = 9 in all calibration plots. Each point was measured three times.

	Equation	R^2
1 day	i (µA) = -2.14 [glucose] (mM) - 0.07	0.994
15 days	i (µA) = -2.16 [glucose] (mM) - 0.06	0.997
30 days	i (µA) = -2.09 [glucose] (mM) - 0.08	0.9990
60 days	i (µA) = -2.32 [glucose] (mM) - 0.07	0.9994
90 days	i (µA) = -2.11 [glucose] (mM) - 0.10	0.996
Mean slope	-2.16 ± 0.09 µA/mM	

As can be seen, the sensors are stable at least 3 months without a loose of sensitivity and the slope is -2.16 ± 0.09 µA/mM. This life-time is quite long for a glucose sensor based on screen-printed electrodes [27,28]. In the literature, a previous study was performed by

adsorbing the enzyme and the stability obtained was 12 months [40] but the preparation of this biosensor required more steps. This life time is similar to the stability of the commercialized glucose sensor (12 - 18 months) [41]. So, in our case, it could be expected a similar stability.

3.5. Application to real samples

Real samples as blood, honey, drink for babies and glucosed drink were studied using the glucose sensor. The level of glucose in blood is in the range of 4.4 - 6.6 mM (80 - 120 mg/dL) for normal people and between 8.3 and 16.6 mM (150 - 300 mg/dL) for diabetes mellitus patients [42]. The samples were prepared as explained in the **Section 2.5** and the analytical signal was recorded as described in the **Section 2.4**. The results were compared with the apparatus One Touch used by the diabetes. All the results are resumed in the **Table 4**. For the entire sample used, the sensor showed a good accuracy with the results given by the references. The standard deviation of all the measurements is also very good.

Table 4. Measurement of glucose with the proposed sensor in real samples; E applied -0.1 V (*vs*. Ag pseudoreference electrode). Data are given as average *±SD* (n = 3).

Real sample	Reference	Glucose sensor
Honey (g/100 g)	30	29.3 ± 0.4
Drink for babies (g/100 mL)	5	5.8 ± 0.2
Blood (mg/dL)	90 ± 9	85 ± 6
	137 ± 14	128 ± 1
Glucose drink (g/L)	20	19 ± 2

4. Conclusions

Glucose biosensors account for about 85% of the entire biosensors market. Such huge market size makes necessary constant investigation for developing new biosensors easy to prepare, which give cheap, reliable and tight results. In this work, a single-use glucose sensor was designed which can operate under air by immobilizing a mixture of GOx and HRP on a screen-printed ferrocyanide/carbon electrode. The biosensor transducer is a commercial screen-printed electrode which has the mediator included in the working electrode; this screen-printed electrode does not need a pretreatment to be used as transducer. Moreover,

the biosensor is very easily obtained by simple adsorption of the mixture of enzymes onto the working electrode with no need of cross-linking agents or covalent bindings. The resulting sensor displays low detection limits, high reproducibility and long term stability for glucose determination and wide linear response range from 0.05 to 1.00 mM with sensitivity of -2.12 ± 0.06 μA/mM. Furthermore this bienzymatic GOx/HRP glucose sensor can be used for the selective determination of glucose in different samples with a minimum sample preparation in most of the cases.

Acknowledgement

This work has been supported by the Spanish Ministry of Science and Innovation Project MICINN-09-PET2008-0174-02.

References

[1] K. Xinhuang, M. Zhibin, Z. Xiaoyong, C. Peixiang, M. Jinyuan, *Anal. Biochem.* 2007, 369, 71.

[2] S. Hrapovic, Y. Liu, K. B. Male, J. H. T. Luong, *Anal. Chem.* 2004, 76, 1083.

[3] R. M. Ianniello, A. M. Yacynyeh, *Anal. Chem.* 1981, 53, 2090.

[4] J. Wang, N. Naser, L. Anges, W. Hui, L. Chen, *Anal. Chem.* 1992, 64, 1285.

[5] M. Yang, Y. Yang, Y. Liu, G. Shen, R. Yu, *Biosens. Bioelectron.* 2006, 21, 1125.

[6] Y. Sun, F. Yan, W. Yang, C. Sun, *Biomaterials* 2006, 27, 4042.

[7] C. Jing-Yang, Y. Ching-Mu, Y. Miao-Ju, C. Lin Chi, *Biosens. Bioelectron.* 2009, 24, 2015.

[8] W. Xueying, G. Haifang, Y. Fan, T. Yifeng, *Biosens. Bioelectron.* 2009, 24, 1527.

[9] M. Langun, Y. Katsunobu, *Talanta* 2000, 51, 187.

[10] S. J. Dong, B. X. Wang, B. F. Liu, *Biosens. Bioelectron.* 1992, 7, 215.

[11] M. E. Ghica, C. M.A. Brett, *Anal. Lett.* 2005, 38, 907.

[12] J. Gonzalo Ruiz, M. Asunción Alonso Lomillo, F. Javier Muñoz, *Biosens. Bioelectron.* 2007, 22, 1517.

[13] N. Peña, G. Ruiz, A. J. Reviejo, J. M. Pingarrón, *Anal. Chem.* 2001, 73, 1190.

[14] C. Zhang, N. Wang, Y. Niu, C. Sun, *Sens. Actuators B* 2005, 109(2) 367.

[15] K. Xinhuang, M. Zhibin, Z. Xiaoyong, C. Peixiang, M. Jinyuan, *Anal. Biochem.* 2007, 369, 71.

[16] G. Wen-Jun, L. Yi, Q. Yu, Z. Xiao-Bin, H. Gui-Quan, *Biosens. Bioelectron.* 2005, 21, 508.

[17] M. Viticoli, A. Curulli, A. Cusma, S. Kaciulis, S. Nunziante, L. Pandolfi, F. Valentini, G. Padeletti, *Mater. Sci. Eng.* 2006, 26C, 947.

[18] C. Zhijun, J. Xueqin, X. Qingji, Y. Shouzhuo, *Biosens. Bioelectron.* 2008, 24, 222.

[19] M. Cano, J. L. Ávila, M. Mayén, M. L. Mena, J. Pingarrón, R. Rodríguez-Amaro, *J. Electroanal. Chem.* 2008, 615, 69.

[20] M. Albareda-Sirvent, A. Merkoçi, S. Alegret, *Sens. Actuators B* 2000, 69, 153.

[21] B.W. Lu, W.C Chen, *J. Magn. Mater.* 2006, 304, e400.

[22] S. Campuzano, O. A. Loaiza, M. Pedrero, F. de Villena, J. M. Pingarrón, *Bioelectrochem.* 2004, 63, 199.

[23] F. Ricci, D. Moscone, C.S Tutra, G. Palleshi, A. Amine, A. Poscia, F. Valgimini, D. Messeri, *Biosens. Bioelectron.* 2005, 20, 1993.

[24] P. C. Nien, T. S. Tung, K. C. Ho, *Electroanalysis* 2006, 18, 1408.

[25] G. A. M. Mersal, M. Khodari, U. Bilitewski, *Biosens. Biolectron.* 2004, 20, 305.

[26] T. Faming, Z. Guoyi, *Anal. Chim. Acta* 2002, 451, 251.

[27] M. A. Alonso Lomillo, J. G. Ruiz, F. J. Muños Pascual, *Anal. Chim. Acta* 2005, 547, 209.

[28] G. S. Wilson y R. Gifford, *Biosens. Bioelectron.* 2005, 20, 2388.

[29] C. A. Galán-Vidal, J. Muñoz, C. Domínguez, S. Alegret, *Trends. Anal. Chem.* 1995, 14, 225.

[30] A. Lupu, D. Compagnone, G. Palleschi, *Anal. Chim. Acta.* 2004, 513, 67.

[31] A. Heller, B. Feldman, *Chem. Rev.* 2008, 108, 2482.

[32] R. Güell, G. Aragay, C. Fontàs, E. Anticó, A. Merkoçi, *Anal. Chim Acta.* 2008, 627, 219.

[33] X. Chu, D. Duan, G. Shen, R. Yu, *Talanta* 2007, 71, 2040.

[34] Y. Zou, C. Xiang, L. X. Sun, F. Xu, *Biosens. Bioelectron.* 2008, 23, 1010.

[35] T.W. Yi, Y. Lei, Z. Zi-Qiang, Z. Jian, Z. Jian-Zhong, F. Chun-hai, *Sens. Actuators B* 2009, 136, 332.

[36] T. Faming, Z. Guoyi, *Anal. Chim. Acta* 2002, 451, 251.

[37] G. Ming, W. Jianwen, T. Yifeng, D. Junwei, *Sens. Actuators B* 2010, 148, 486.

[38] C. Jing-Yang, Y. Chung-Mu, Y. Miao-Ju, C. Lin-Chen, *Biosens. Bioelectron.* 2009, 2015.

[39] L. Shyh-Hwang, F. Hung-Yuan, C. Wen-Chang, *Sens. Actuators B* 2006, 117, 236.

[40] S. Kröger, S. J. Setford, A. P. F. Turner, *Anal. Chim. Acta* 1998, 368, 219.

[41] J. Hu, *Biosens. Bioelectron.* 2009, 24, 1083.

[42] J. Wang, *Chem. Rev.* 2008, 108, 814.

3.1.3. Artículo 2: "*Amperometric fructose sensor based on ferrocyanide modified screen-printed carbon electrode*"

Talanta 2012, 88, 432-438

Talanta 88 (2012) 432–438

Contents lists available at SciVerse ScienceDirect

Talanta

journal homepage: www.elsevier.com/locate/talanta

Amperometric fructose sensor based on ferrocyanide modified screen-printed carbon electrode

Julien Biscay[a], Estefanía Costa Rama[a], María Begoña González García[a], A. Julio Reviejo[b], José Manuel Pingarrón Carrazón[b], Agustín Costa García[a]*

[a]Departamento de Química Física y Analítica, Facultad de Química, Universidad de Oviedo, 33006 Oviedo, España

[b]Departamento de Química Analítica, Facultad de Química, Universidad Complutense de Madrid, 28040 Madrid, España

ABSTRACT

The first fructose sensor using a commercial screen-printed ferrocyanide/carbon electrodes (SPFCE) is reported here. The ferrocyanide is included in the carbon ink of the commercial screen-printed carbon electrode. The immobilization of enzyme *D*-fructose dehydrogenase (FDH) was carried out in an easy way. An aliquot of 10 µL FDH was deposited on the electrode surface and left there until dried (approximately 1 h) at room temperature. The sensor, so constructed, shows a good sensitivity to fructose (1.25 µA/mM) with a slope deviation of ± 0.02 µA/mM and a linear range comprised between 0.1 and 1.0 mM of fructose, with a limit of detection of 0.05 mM. These sensors show good intersensors reproducibility after a previous pretreatment and a high stability. Fructose was determined in real samples as honey, cola, fruit juices (orange, tomato, apple and pineapple), red wine, red and white grapes, musts and liquor of peach with a good accuracy.

Keywords: Ferrocyanide, Fructose dehydrogenase, Fructose sensor, Screen-Printed Carbon Electrode.

1. Introduction

Determination of sugars in food [1] and biological fluids [2,3] for quality control and disease diagnostics is of paramount importance. *D*-Fructose, one of the principal sugar components, is a widely distributed monosaccharide and an important sweetener. Several analytical methods for the determination of *D*-fructose such as fluorometric [4,5], gas chromatography [6], liquid chromatography [7], Fourier transform mid infrared spectroscopy [8] and near infrared spectroscopy [9], electrochemistry [10,11] have been described in the literature. These methods often are expensive, time consuming and require elaborate sample pretreatment [7]. Enzyme kits are also available for fructose determination using a coupled-enzyme system. The advantage of the enzymatic determination relies on the inherent selectivity of enzymes and the short analysis time. The enzyme *D*-fructose dehydrogenase (FDH) was isolated and characterized for the first time by Yamada *et al*. who confirmed that the enzyme catalyzes the oxidation of *D*-fructose to 5-keto-fructose in the presence of mediator [12] as for example, ferrocene [13], Meldola Blue [14], and ferricyanide [15]. FDH is an enzyme containing pyrroloquinoline quinone (PQQ) and belongs to a group of quinoproteins that have been described as a good alternative for the construction of enzymes electrodes [16]. The stability and the biological function of the enzyme depend of the immobilization of the mediator and the enzyme. Thus, different enzyme immobilization techniques as adsorption [17], cross-linking [18,19], entrapment [20,21] or electropolymerization [22] are carried out in order to ensure the stability of the sensor.

Considering the disadvantages of the classical methods, the development of a portable, rapid, accurate and reproducible sensor is of a great interest. In the literature, few articles about fructose sensor using the screen-printing technique have been found [23,24]. The pretreatment and the modification of the electrodes are more complicated and longer. In those cases, the screen-printed electrode was fabricated in the laboratory and ferricyanide or phenazine methansulfate were used as mediators. The present work describes the design of the first fructose sensor using a commercial screen-printed ferrocyanide/carbon electrode (SPFCE). The sensor developed in this work was obtained by the simple adsorption of FDH on the SPFCE surface. Experimental parameters, as applied potential, pH of the buffer solution and the concentration of the enzyme have been optimized. Analytical performances, in terms of reproducibility, limit of detection, linear range, stability and viability to measure in real sample have been reported too and are acceptable in comparison to other fructose sensors based on SPE.

2. Experimental

2.1. Chemicals

D-Fructose dehydrogenase from *Gluconobacter industrius* (FDH; ref. F4892), *D-(−)*-fructose (F0127), fructose assay kit (ref. FA-20) and glucose assay kit (ref. GAGO-20) were purchased from Sigma (Madrid, Spain). Potassium chloride (ref. 596470), sodium hydroxide, sulfuric acid (ref. 1.00731.1011) and copper sulfate (ref. 102780) were delivered by Merck (Spain). All chemicals were of analytical reagent grade, and the Milli-Q water used was obtained from a Millipore Direct-Q^{TM} 5 purification system. Stock solutions of fructose and FDH were prepared daily in 0.1 M phosphate buffer solution (PBS) of pH 4.5 for an immediate use. Britton Robinson buffer solutions of pH values 3 and 9 were used for pH studies.

2.2. Apparatus and measurements

Chronoamperometric measurements were performed using an ECO Chemie µAutolab type II potentiostat interfaced with a Pentium 166 computer system and controlled by the Autolab GPES software version 4.8 for Windows 98. All measurements were carried out at room temperature. Screen-printed ferrocyanide/carbon electrodes (ref. DRP-F10) and an edge connector (ref. DRP-DSC) were purchased from DropSens, S.L. (Oviedo, Spain). These sensors consist in a ferrocyanide/carbon working (4 mm diameter), carbon auxiliary and silver pseudoreference electrodes printed on an alumina substrate. An insulating layer serves to delimit the electrochemical cell and electric contacts. Spectrophotometric measurements were performed using a spectrophotometer Spectronic 20 Genesis.

2.3. Electrode modification

After a first step of washing, 40 µL of the buffer (0.1 M PBS, pH 4.5) was deposited on the SPFCE and a potential of +0.25 V was applied to reach an intensity of 1.8 µA. Then, an aliquot of 10 µL of FDH (0.125 U/µL) was put onto the electrode surface and leaving there until dryness (1 h). After a second washing step, the sensor can be used or kept into a freezer at -20^{0}C and protected from light**.**

2.4. Analytical signal recording

To obtain the analytical signal, an aliquot of 40 µL of fructose solution was deposited on the sensor. The chronoamperogram was recorded applying a potential of +0.25 V during 100 s. A different sensor was used for each measurement.

2.5. Real sample measurement

The sensor developed in this work was tested in different real samples (red wine, musts, honey, cola, orange juice, pineapple juice, tomato juice, and apple juice). 1 g of honey was diluted in 50 mL of deionized water and diluted 100 times in the buffer solution. The fruit juices were diluted 200 times while the cola, the musts have been diluted 2000 times, the red wine 100 times and the liquor of peach 1000 times. In the case of the grapes, a pretreatment was necessary, centrifugating them during 5 min at 5000 rpm. Then the supernatant was diluted 1000 times with the buffer. 40 µL of each sample was dropped on different sensors and the chronoamperogram was recorded as explained in **Section 2.4**. The obtained results with these food samples were compared with those obtained with two enzymatic spectrophotometric commercial kits. Samples were also prepared and tested following the instructions of the fructose and glucose enzymatic kits. Fructose kit is based on the phosphorylation of the *D-(−)*-fructose by adenosine trisphosphate to *D-(−)*-fructose 6-phosphate with the formation of adenosine-5V-diphosphate (ADP). Fructose 6-phosphate is converted to glucose-6-phosphate by phosphoglucose isomerase (PGI) and this later is oxidized to 6-phosphogluconate in the presence of nicotinamide adenine dinucleotide (NAD) catalyzed by glucose-6-phosphate dehydrogenase (G6PDH). The reduced form of NAD, NADH, formed during the oxidation of *D*-glucose-6-phosphate is measured at 340 nm. Glucose kit is based on the spectrophotometric detection of the reaction product formed in the reaction between H_2O_2 and the reduced form of the *o*-dianisidine. Then the reaction of the sulfuric acid with the oxidized *o*-dianisidine formed a pink colored and more stable product. The intensity of the pink color is proportional to the original glucose concentration and measured at 540 nm.

3. Results and discussion

3.1. Optimization of parameters that affect the analytical signal

3.1.1. Study of the applied potential

First of all, the potential applied to detect fructose is a critical parameter due to two reasons: the potential applied must oxidize the ferrocyanide to ferricyanide which reacts with the fructose according to the following reaction:

$$fructose + ferricyanide \xrightarrow{FDH} keto - fructose + ferrocyanide$$

Moreover, the potential applied must allow detecting the ferrocyanide enzymatically generated. This potential must be high enough to oxidize the ferrocyanide and in the same time must allow discriminating the ferrocyanide enzymatically generated from the ferrocyanide electrochemically oxidized. The mechanism of the reaction is summarized in **Fig.1**.

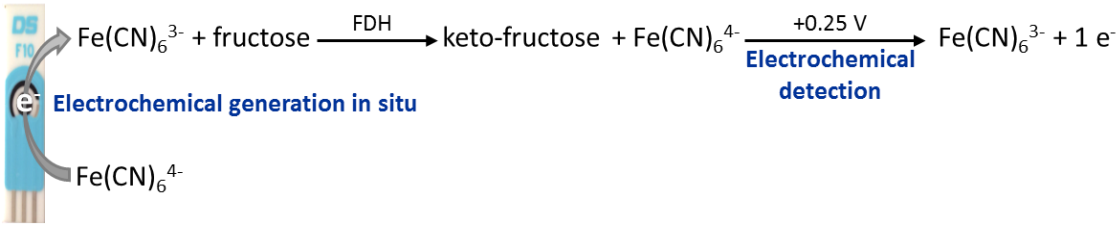

Fig 1. Enzymatic reactions at the electrode surface.

After a first washing step, 10 µL of FDH (0.5 U/µL) were deposited and left to dry 1 h. After a second washing step, the analytical signal was recorded according to **Section 2.4** with 40 µL of 1 mM of fructose, applying to each sensor a different potential (from +0.1 to +0.4 V). The results obtained are shown in **Fig. 2**.

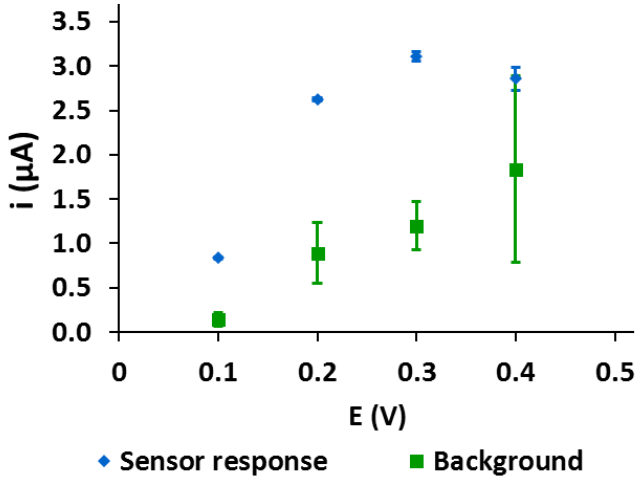

Fig. 2. Effect of the applied potential on the analytical signal. [Fructose] = 1 mM in 0.1 M PBS (pH 6); [FDH] = 0.5 U/µL in 0.1 M PBS (pH 4.5), t recording = 100 s. Data are given as average ± *SD* (n = 3).

The analytical signal increased with potential until +0.3 V, but the background signals became more important at more positive values of potentials, because more ferrocyanide was oxidized to ferricyanide. For higher potentials, the response decreased and the background

was more important. The best potentials for the measurement were between +0.2 and +0.3 V where the highest signal recorded and the lowest value of the background were obtained. For further experiments, the applied potential was +0.25 V. For lower values of potential than +0.2 V, the analytical response was lower due to the reduction of the ferricyanide to ferrocyanide. However, despite the response/background ratio obtained at chosen potential was (+0.25 V) high enough, the background signal was very high and gave rise a bad intersensor reproducibility. In order to decrease the background signal and improve the intersensor reproducibility, an electrochemical pretreatment was carried out. After a washing step, an aliquot of 40 µL of 0.1 M PBS (pH 4.5) was deposited on the sensor and a chronoamperogram was recorded applying +0.25 V (during ca. 80 s) until to obtain a basal signal of 1.8 µA. In that way, all the electrodes were similar because part of ferrocyanide has been oxidized and removed of the electrode surface and consequently, lower backgrounds were obtained. The results of the pretreatment on the background and on the signal recorded are resumed in **Table 1**.

Table 1. Effect of pretreatment on the analytical and background signal. Fructose concentration, 1 mM; [FDH] = 0.125 U/µL in 0.1 M PBS (pH 4.5), E applied +0.25 V (*vs*. Ag pseudoreference electrode), t recording = 100 s. Data are given as average, each point was measured three times.

	Without pretreatment		With pretreatment	
	Current (µA)	RSD (%)	Current (µA)	RSD (%)
Background	0.97	45	0.05	20
Signal	3.7	36	1.4	8
Signal/background	3.8		28.0	

Although the analytical signal obtained with pretreatment was lower, the signal/background ratio was 7-fold times higher. In all cases of fructose sensor using SPE reported, a longer pretreatment was necessary (**Table 2**).

3.1.2. Optimization concentration of the enzyme

Different sensors were prepared, dropping different FDH concentrations. For each concentration of enzymes, a chronoamperogram with a fructose concentration of 1 mM was recorded as described in **Section 2.4**. The result of this study is reported in **Fig. 3**.

It can be noted that the analytical signal increased when concentration of FDH increased. The background, after an initial increase, kept constant for a concentration of FDH

comprised between 0.125 and 0.500 U/µL. It was chosen a concentration of FDH of 0.125 U/µL, because the analytical signal was considered quite high with excellent intersensor reproducibility and moreover, cost of the sensor was lower.

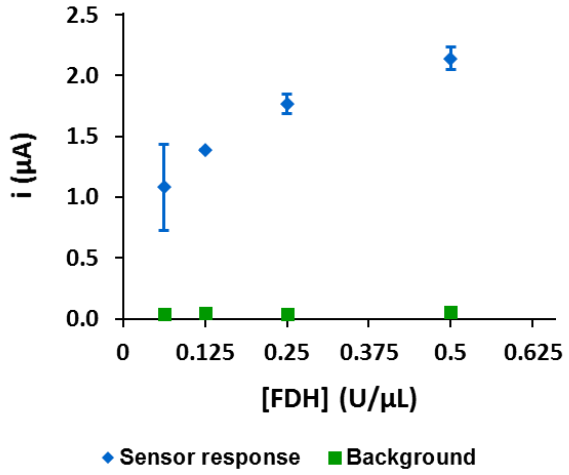

Fig. 3. Effect of the concentration of enzyme FDH on the analytical signal and on the background. [Fructose] = 1 mM in 0.1 M PBS (pH 4.5); E applied +0.25 V (*vs*. Ag pseudoreference electrode), t recording 100 s. Data are given as average ± *SD* (n = 3).

3.1.3. Effect of the pH

The influence of the pH of the substrate was tested. Fructose solutions were prepared in Britton-Robinson solutions for the pH values 3 and 9. For the pH values between 3 and 9, fructose was prepared in 0.1 M PBS buffer. Sensors were prepared as explained in **Section 2.3** and the chronoamperometric signal was recorded as described in **Section 2.4**. The results obtained are shown in **Fig. 4**. The analytical signal increased with pH until a pH value of 4 when a plateau was reached between 4 and 5. At higher pH values the sensor response decreased. Moreover, the background was smaller in the range of better response. To complete the study, glucose response was checked between pH values 3 and 9. So glucose solutions were prepared in Britton-Robinson solutions for the pH values 3 and 9. For the pH values between 3 and 9, glucose was prepared in 0.1 M PBS buffer. The results are resumed in **Fig. 4**. The response of the sensor to the presence of glucose increased between pH values 4 and 9. For further studies a pH of 4.5 was chosen, because it corresponds to the optimal pH of the enzyme and to the soluble FDH with ferricyanide and at the same time the interference caused by the glucose is smaller [25].

Table 2. Analytical characteristics of some fructose sensors.

Electrode modification	Mediator	Type of electrode	Pretreatment	Potential (V)	Sensitivity	Detection limit (mM)	Linear range	K_m (mM)	Reproducibility	Stability	Ref.
Adsorption of FDH	Ferrocyanide	SPFCE	Applying +0.25 V to reach 1.8 mA (80 s)	+0.25	1.25 mA mM^{-1}	0.05	(0.1-1) mM	0.9	1.9	No lost of sensitivity after 60 days at -20ºC	Present work
Entrapment of FDH in a polymer matrix	Ferricyanide	SPE	Applying +1.2 V during 240 s	+0.4	0.62 mA mM^{-1}	0.65	(3-13) mM	Not reported	Not reported	More than 50% of sensitivity lost after 30 days	[23]
Adsorption of FDH/BSA/ glutaraldehyde mixture	Phenazine methansulfate	Bare graphite SPE	Applying +1.7 V during 180 s	+0.07	Not reported	Not reported	(0.05-0.5) mM	Not reported	7	10% of sensitivity lost after 15 days	[24]
Adsorption of FDH	none	MWCNT modified platinum electrode	None	-0.15	Not reported	5	Up to 40 mM	11	Not reported	3 days	[26]
FDH coated on ferrocene-embedded cellulose acetate membrane	Ferrocene	Glassy carbon electrode	None	+0.300	20 mA mM^{-1}	7	Not reported	Not reported	Not reported	9 hours	[13]
FDH coated with Meldola Blue onto a silica gel	Meldola Blue	Silica gel modified carbon electrode	None	+0.02	0.618mA mM^{-1} cm^{-2}	Not reported	(0.1-0.8) mM	Not reported	0.68	2 months	[14]
Cross linking with glutaraldehyde	Tetrathiafulvalene	Gold electrode	Polishment, sonification, immersion in KOH, H_2SO_4 and HNO_3	+0.2	1.7 mA mM^{-1}	0.002	(0.01-1) mM	5.4	Not reported	30 days	[29]

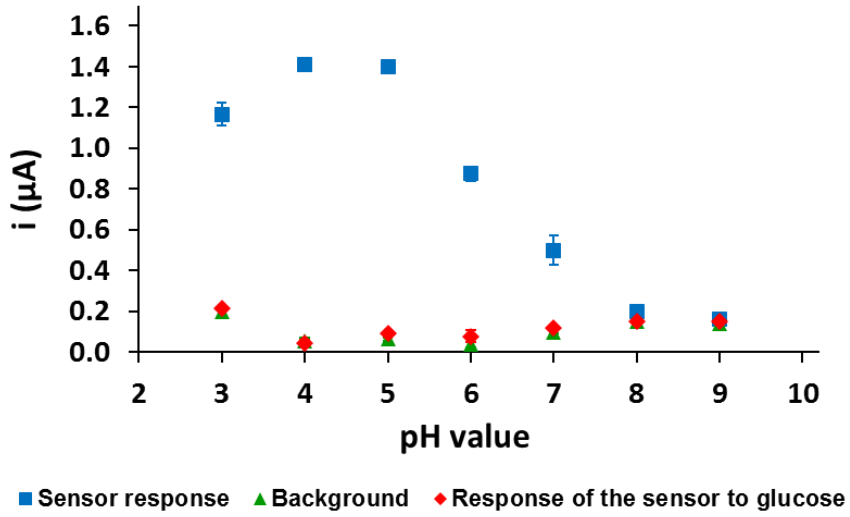

Fig. 4. Effect of the pH value of the substrate and glucose on the response of sensors to 1 mM fructose and 1 mM glucose, [FDH] = 0.125 U/µL; E applied +0.25 V (*vs*. Ag pseudoreference electrode), t recording 100 s, each point was measured three times.

3.2. Calibration of the sensor

Chronoamperograms corresponding to aliquots of 40 µL of different concentration of fructose were recorded to check the response of the electrodes in presence of fructose. **Fig. 5A** shows the calibration curve obtained. The sensor shows Michaelis-Menten kinetics. Using the Lineweaver-Burk linearization, the Michaelis-Menten constant (K_m) was calculated and the value was 0.9 ± 0.1 mM. This value is lower than the value obtained with FDH immobilized on a multi-walled carbon nanotubes modified platinum electrode [26] and in the same range of sensors using a cellulose acetate membrane [13]. The linear range is displayed in **Fig. 5B**. A linear relationship between current and FDH concentration in the range of 0.1 and 1.0 mM was obtained with a coefficient of determination of 0.998 according to the following equation:

$$i\ (\mu A) = 1.27\ [\text{fructose}]\ (\text{mM}) + 0.15$$

The present sensor shows a linear range similar or better than the other sensor in the same category (**Table 2**).

In order to evaluate the reproducibility of the sensor, series of 18 electrodes were prepared and tested the same day. This operation was repeated on three different days. A calibration plot of each series was carried out with solutions of fructose prepared the day of the measurement. The results are shown in **Table 3**. The sensor has a good reproducibility and a slope of 1.25 ± 0.02 µA/mM. This reproducibility allows the detection of fructose with a

simple measurement (one standard and the sample). The relative standard deviation of the different slopes and the sensitivity obtained (1.9% and 1.25 µA/mM) are excellent in comparison with the other fructose sensor based on screen-printed electrodes or fructose sensors in general (**Table 2**).

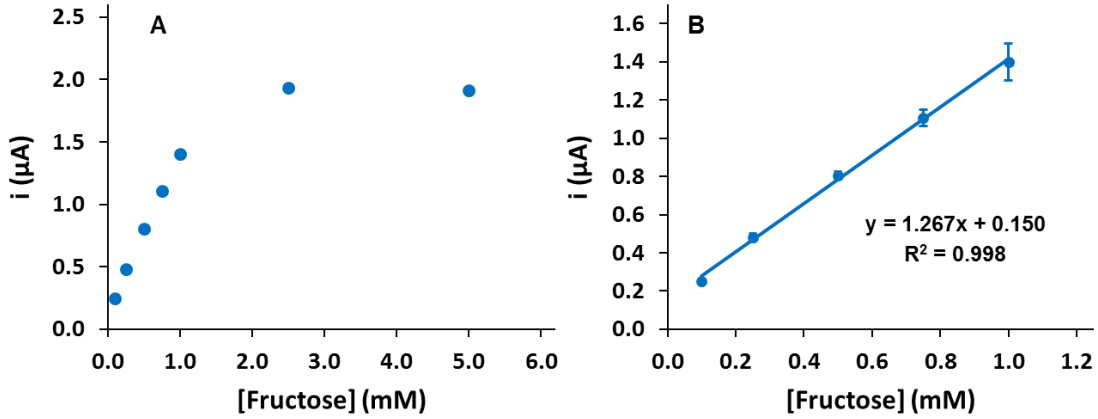

Fig. 5. Calibration curve and calibration plot of the proposed fructose sensor in the concentration range 0.1 to 5 mM. E applied +0.25 V (*vs*. Ag pseudo reference electrode), t recording 100 s. Data are given as average ± *SD* (n = 3).

Table 3. Calibration plot equations of three fructose sensor series, [FDH] = 0.125 U/µL in 0.1 M PBS (pH 4.5), E applied +0.25 V (*vs*. Ag pseudoreference electrode), t recording 100 s, n = 6 in all calibration plots; each point was measured three times.

	Equation	R^2
Calibration plot 1	i (µA) = 1.27 [fructose] (mM) + 0.15	0.998
Calibration plot 2	i (µA) = 1.23 [fructose] (mM) + 0.16	0.995
Calibration plot 3	i (µA) = 1.26 [fructose] (mM) + 0.17	0.992
Calibration plot 4	i (µA) = 1.22 [fructose] (mM) + 0.18	0.990
Mean slope	1.25 ± 0.02 µA/mM	

3.3. Specificity of the sensor

The specificity of the sensor was checked under the experimental conditions explained in **Section 2.4**. The potential interferences tested were ascorbic acid and another sugar such

as glucose. To evaluate these interferences, solutions of 0.50 mM of glucose and fructose and another one of 0.025 mM of ascorbic acid, mixture of fructose (0.50 mM) and glucose (0.50 mM) and another one of ascorbic acid (0.025 mM) and fructose (0.50 mM) were prepared. To eliminate interferences caused by the ascorbic acid, solutions containing this interfering agent were prepared and treated with copper sulfate. So mixture of ascorbic acid (0.025 mM) and copper sulfate (0.025 mM) and fructose (0.5 mM) and another mixture of ascorbic acid (0.025 mM) and copper sulfate (0.025 mM) were prepared. 40 µL of those solutions were dropped on the sensor and chronoamperograms were recorded as explained in **Section 2.4**. The different results obtained are resumed in **Table 4**. The present sensor shows a good specificity for the fructose. In presence of glucose and ascorbic acid no measurable amperometric response could be observed. The signals recorded for the glucose and ascorbic acid measurements are equal as the recorded for the background.

Table 4. Study of the interferences caused by glucose and ascorbic acid. [FDH] = 0.125 U/µL, [glucose] = 0.50 mM, [ascorbic acid] = 0.025 mM, [fructose] = 0.50 mM, all the solutions are prepared in 0.1 M PBS (pH 4.5), E applied +0.25 V (*vs*. Ag pseudoreference electrode), t recording 100 s, each point was measured three times. Data are given as average *±SD* (n = 3).

Background	Fructose	Glucose	Fructose/glucose	Pretreated ascorbic acid	Fructose/pretreated ascorbic acid
45 ± 7 nA	810 ± 20 nA	47 ± 6 nA	825 ± 50 nA	50 ± 5 nA	810 ± 30 nA

3.4. Stability of the sensor

Several fructose sensors were prepared as described in **Section 2.3**, kept into the refrigerator (4^0C) or a freezer (-20^0C) and light protected until their use. A calibration plot was carried out in the range of 0.1-1.0 mM after one and two months. The calibration plots are summarized in **Table 5**. When the sensor is kept in refrigerator, it can be observed after one month a decrease of 20% of the slope. On the other hand, when sensors are kept at -20^0C, the sensitivity decreased about 5% after two months. This stability is very good compared with other works and the best regarding the other screen printed fructose sensors already published.

Table 5. Calibration plot of electrodes stored during different times. n = 6 in all calibration plots. [FDH] = 0.125 U/µL in 0.1 M PBS (pH 4.5), E applied +0.25 V (*vs*. Ag pseudoreference electrode), t recording 100 s, each point was measured three times.

	Freezer		Refrigerator	
	Equation	R^2	Equation	R^2
Calibration plot (1 day)	i (µA) = 1.25 [fructose] (mM) + 0.17	0.994	i (µA) = 1.25 [fructose] (mM) + 0.17	0.994
Calibration plot (1 month)	i (µA) = 1.18 [fructose] (mM) + 0.14	0.996	i (µA) = 0.99 [fructose] (mM) – 0.05	0.999
Calibration plot (2 months)	i (µA) = 1.18 [fructose] (mM) + 0.17	0.995	–	–

4. Application to real sample

The proposed fructose sensor was used to measure fructose in real samples as honey, some fruit juices (apple, pineapple, orange, and tomato), red wine, musts, liquor of peach and grapes. The samples were prepared as explained in **Section 2.5** and the analytical signal was recorded as described in **Section 2.4**. In all of the tested samples, the reference value indicated the amount of the addition of fructose and glucose. Recently, we have reported the construction of an amperometric sensor for glucose in which a mixture of glucose oxidase (GOx) and horseradish peroxidase (HRP) was immobilized by adsorption on a SPFCE [27]. The results were compared to a volumetric method using ferricyanide for the qualitative determination of reducing sugars [28] and with two enzymatic commercial kits. In the case of the cola, pineapple and orange juice, the volumetric method could not be used. In that samples it has been used the value given on the bottle as reference. So fructose and glucose were determined in the samples exposed above and the results obtained were summarized in **Table 6**. In all the cases, the proposed sensor shows a good accuracy with the results obtained with the reference and with the kits in a large range of sugars concentration. Seeing those results, it could be studied the eventuality of the construction of a very simple biosensor for the simultaneous detection of fructose and glucose by the immobilization of a mixture glucose oxidase and horseradish peroxidase, and fructose dehydrogenase onto the surface of a ferrocyanide/carbon screen printed electrode.

Table 6. Measurement of fructose and glucose with the proposed sensor and a previously published glucose sensor in real samples. [FDH] = 0.125 U/µL in 0.1 M PBS (pH 4.5), E applied +0.25 V (*vs*. Ag pseudoreference electrode), t recording 100 s. Data are given as average *±SD* (n = 3).

Real sample	Fructose sensor	Fructose kit	Glucose sensor	Glucose kit	∑glucose and fructose (sensor)	∑glucose and fructose (kit)	Reference (volumetric method)
Honey (g/100g)	29.1 ± 0.4	31	34 ± 1	35	63 ± 1	66	69
Tomato juice (g/100 mL)	1.7 ± 0.2	1.5	1.10 ± 0.01	1.0	2.8 ± 0.2	2.5	2.8
Pineapple juice (g/100 mL)	3.22 ± 0.08	3.3	1.50 ± 0.03	1.6	4.72 ± 0.09	4.9	5.2
Orange juice (g/100 mL)	3.4 ± 0.2	3.4	1.60 ± 0.05	1.5	5 ± 0.2	4.9	5.2
Red wine (g/L)	5.3 ± 0.1	5.5	2.3 ± 0.1	2.4	7.6 ± 0.2	7.9	7.7 ± 0.6
Apple juice (g/100 mL)	7.68 ± 0.01	7.4	2.7 ± 0.2	2.8	10.4 ± 0.1	10.2	11.85
Cola (g/100 mL)	8.0 ± 0.1	8.3	2.80 ± 0.05	3.0	10.8 ± 0.1	11.3	10.6
Red must (g/L)	41 ± 1	40	73 ± 1	73	114 ± 1	113	130 ± 8
White must (g/L)	43 ± 1	42	84 ± 1	81	127 ± 1	123	126 ± 13
Red grapes (g/L)	62 ± 4	63	89 ± 2	92	151 ± 5	155	147 ± 10
White grapes (g/L)	53 ± 2	55	116 ± 2	113	169 ± 3	168	160 ± 7
Liquor of peach (g/L)	74 ± 2	80	170 ± 10	183	244 ± 9	263	283 ± 9

5. Conclusion

In this work, the first fructose sensor based on a commercial screen-printed electrodes is reported. This single-use fructose sensor can operate under air by immobilizing FDH on a screen-printed ferrocyanide/carbon electrode. The biosensor transducer is a commercial

screen-printed electrode which has the mediator included in the working electrode; this SPFCE needs a pretreatment to be used as transducer. Moreover, the biosensor is very easily obtained by simple adsorption of the enzyme onto the working electrode with no need of cross-linking agents or polymers. The resulting sensor displays low detection limits, high reproducibility, long-term stability for fructose determination and linear response range from 0.1 to 1.0 mM with sensitivity of 1.25 ± 0.02 μA/mM. Furthermore the sensor can analyze fructose in sample containing glucose without its elimination and with a minimum sample preparation. Finally, interferences provocated by the presence of the ascorbic acid was not a problem with the studied samples.

Acknowledgement

This work has been supported by the Spanish Ministry of Science and Innovation Project MICINN-09-PET2008-0174-02.

References

[1] P.A. Paredes, J. Parellada, V.M. Fernandez, I. Katakis, E. Dominguez, Biosens. Bioelectron. 12 (1997) 1233-1243.

[2] A. Lindqvist, A. Baelemans, C. Erlanson-Albertsson, Regul. Pept. 150 (2008) 26-32.

[3] K. Mellor, R.H. Ritchie, G. Meredith, O.L. Woodman, M.J. Morris, L.M.D. Delbridge, Nutrition 26 (2010) 842-848.

[4] N.D. Danielson, C.A. Heenan, F. Haddadian, A. Numan, Microchem. J. 63 (1999) 405-414.

[5] W. Tan, D. Zhang, Z. Wang, C. Liu, D. Zhu, J. Mater. Chem. 17 (2007) 1964-1968.

[6] P.N. Wahjudi, M.E. Patterson, S. Lim, J.K. Yee, C.S. Mao, W.-N.P. Lee, Clin. Biochem. 43 (2010) 198-207.

[7] J.H. Han, H.N. Choi, S. Park, T.D. Chung, W.-Y. Lee, Anal. Sci. 26 (2010) 995-1000.

[8] S. Bureau, D. Ruiz, M. Reich, B. Gouble, D. Bertrand, J.M. Audergon, C.M.G.C. Renard, Food Chem. 115 (2009) 1133-1140.

[9] L. Xie, X. Ye, D. Liu, Y. Ying, Food Chem. 114 (2009) 1135-1140.

[10] S. Tsujimura, A. Nishina, Y. Kamitaka, K. Kano, Anal. Chem. 81 (2009) 9383-9387.

[11] S. Campuzano, V. Escamilla-Gomez, M.A. Herranz, M. Pedreroa, J.M. Pingarron, Sens. Actuators B 134 (2008) 974-980.

[12] Y. Yamada, K. Aida, T. Uemura, Agric. Biol. Chem. 30 (1996) 95-96.

[13] J. Tkác, I. Vostiar, E. Sturdík, P. Gemeiner, V. Mastihuba, J. Annus, Anal. Chim. Acta 439 (2001) 39-46.

[14] C.A.B. García, G. de Oliveira Neto, L.T. Kubota, L.A. Grandin, J. Electroanal. Chem. 418 (1996) 147-151.

[15] C.A.B. García, G. De Oliveira Neto, L.T. Kubota, Anal. Chim. Acta 374 (1998) 201-208.

[16] M. Smolander, G.M. Varga, L. Gorton, Anal. Chim. Acta 302 (1995) 233-240.

[17] A. Kusakari, M. Izumi, H. Ohnuki, Colloids Surf. A: Physicochem. Eng. Aspects 321 (2008) 47-51.

[18] R. Rajkumar, A. Warsinke, H. Mohwald, F.W. Scheller, M. Katterle, Talanta 76 (2008) 1119-1123.

[19] S. Campuzano, O.A. Loaiza, M. Pedrero, F.J.M. de Villena, J.M. Pingarrón, Bioelectrochemistry 63 (2004) 199-206.

[20] S.M. Reddy, P. Vadgama, Anal. Chim. Acta 461 (2002) 57-64.

[21] R. Ben-Knaz, D. Avnir, Biomaterials 30 (2009) 1263-1267.

[22] A.S. Bassi, E. Lee, J.X. Zhu, Food Res. Int. 31 (1998) 119-127.

[23] U.B. Trivedi, D. Lakshminarayana, I.L. Kothari, P.B. Patel, C.J. Panchal, Sens. Actuators B 136 (2009) 45-51.

[24] S. Piermarini, G. Volpe, M. Esti, M. Simonetti, G. Palleschi, Food Chem. 127 (2011) 749-754.

[25] M. Ameyama, E. Shinagawa, K. Matsushima, O. Adachi, J. Bacteriol. 145 (1981) 814-823.

[26] M. Tominaga, S. Nomura, I. Taniguchi, Biosens. Bioelectron. 24 (2009) 1184-1188.

[27] J. Biscay, E. Costa Rama, M.B. González García, J.M. Pingarrón Carrazón, A. Costa García, Electroanalysis 23 (2011) 209-214.

[28] S.W. Cole, Biochem. J. 27 (3) (1933) 723-726.

[29] S. Campuzano, R. Gálvez, M. Pedrero, F.J.M. de Villena, J.M. Pingarrón, Anal Bioanal Chem. 377 (2003) 600-607.

3.1.4. Artículo 3: "Comparative study of different alcohol sensors based on screen-printed carbon electrodes"

Analytica Chimica Acta 2012, 728, 69-76

Analytica Chimica Acta 728 (2012) 69–76

Contents lists available at SciVerse ScienceDirect

Analytica Chimica Acta

journal homepage: www.elsevier.com/locate/aca

Comparative study of different alcohol sensors based on screen-printed carbon electrodes

Estefanía Costa Rama[a], Julien Biscay[a], María Begoña González García[a], A. Julio Reviejo[b], José Manuel Pingarrón Carrazón[b], Agustín Costa García[a]*

[a]Departamento de Química Física y Analítica, Facultad de Química, Universidad de Oviedo, 33006 Oviedo, España

[b]Departamento de Química Analítica, Facultad de Química, Universidad Complutense de Madrid, 28040 Madrid, España

ABSTRACT

Different very simple single-use alcohol enzyme sensors were developed using alcohol oxidase (AOx) from three different yeast, *Hansenula sp*., *Pichia pastoris* and *Candida boidinii*, and employing three different commercial mediator-based screen-printed carbon electrodes as transducers. The mediators tested, Prussian Blue, ferrocyanide and co-phthalocyanine were included into the ink of the working electrode. The procedure to obtain these sensors consists of the immobilization of the enzyme on the electrode surface by adsorption. For the immobilization, an AOx solution is deposited on the working electrode and left until dried (1 h) at room temperature. The best results were obtained with the biosensor using screen-printed co-phthalocyanine/carbon electrode and AOx from *Hansenula sp*. The reduced cobalt–phthalocyanine form is amperometrically detected at +0.4 V (*vs*. Ag pseudo reference electrode). This sensor shows good sensitivity (1211 nA mM^{-1}), high precision (2.1% RSD value for the slope value of the calibration plot) and wide linear response (0.05-1.00 mM) for ethanol determination. The sensor provides also accurate results for ethanol quantification in alcoholic drinks.

Abbreviations: AOx, alcohol oxidase; SPPBCEs, Screen-Printed Prussian Blue/Carbon Electrodes; SPFCEs, Screen-Printed Ferrocyanide/Carbon Electrodes; SPCPCEs, Screen-Printed Co-phthalocyanine/Carbon Electrodes.

Keywords: Ferrocyanide, Prussian Blue, Co-phthalocyanine, Screen-Printed Carbon Electrode, Alcohol Oxidase.

1. Introduction

The determination of ethanol is of great importance in food industry, medicine and biotechnology because of its toxicological and psychological effects [1]. The food, beverage and pulp industries need fast, simple and economic analytical methods to control fermentation processes and product quality [2]. Several methods and strategies have been reported for the determination of ethanol, e.g. gas chromatography, liquid chromatography, refractometry and spectrophotometry, among others [2].

The use of enzymes for the detection and quantification of ethanol in complex samples offers a better specificity and therefore, a simpler sample treatment. Alcohol oxidase (AOx) [3,4], NAD^+-dependent alcohol dehydrogenase (ADH) [1,5,6] and PQQ-dependent alcohol dehydrogenases [7,8] have been used as bioselective elements in ethanol biosensors. In this work, AOx produced by three methylotrophic yeasts [9], *Hansenula polymorpha*, *Pichia pastoris*, *Candida boidinii*, have been used.

Alcohol oxidase oxidizes low molecular weight alcohols to the corresponding aldehyde, using molecular oxygen (O_2) as the electron acceptor, according to the following reaction:

$$RCH_2OH + O_2 \xrightarrow{AOx} RCHO + H_2O_2$$

The oxidation of alcohol by AOx is irreversible due to the strong oxidizing character of O_2 and can be monitored by measuring either the decrease in O_2 concentration or the increase in H_2O_2 concentration [9].

The electrochemical determination of ethanol is based on the oxidation or reduction of H_2O_2 generated by the enzyme-catalyzed reaction. In order to shuttle electrons involved in the electrochemical oxidation or reduction of H_2O_2 at low potential values, the use of mediators such as Meldola Blue [10–12], ferrocene [13–15], ferrocyanide [10,16,17], Prussian Blue [18,19] or Co-phthalocyanine [20,21], is a well-known strategy. There are several ways to incorporate a mediator in an enzymatic biosensor e.g. by a membrane [22,23], into a Nafion gel [24], by cross-linking [25], by electrodeposition [26] or inclusion in the working electrode [16,27].

Screen-printing is a well-established technique to fabricate electrochemical biosensors because of inherent advantages such as miniaturization, versatility, low cost and the

possibility of mass production [28]. All these advantages make these devices interesting tools in biosensors design [28]. Moreover, screen-printed carbon electrodes (SPCEs) with mediators incorporated in the carbon ink are commercially available.

In this paper, three commercial SPCEs modified with different mediators included in the carbon ink, Prussian Blue, ferrocyanide and Co-phthalocyanine, and AOx from three different sources, *Hansenula sp*., *P. pastoris* and *C. boidinii*, were evaluated and compared in order to design simple, disposable and reliable alcohol sensors.

2. Experimental

2.1. Chemicals

Alcohol oxidase from *Hansenula Polymorpha* (AOx; ref. A0438), alcohol oxidase solution from *P. pastoris* (AOx; ref. A2404), alcohol oxidase from *C. boidinii* (AOx; ref. A6941), Horseradish Peroxidase, Type VI-A (HRP; ref. 6782), ascorbic acid (ref. A5960), gallic acid (ref. G7384) and l-cysteine (ref. W326305) were purchased from Sigma (Spain). Ethanol absolute, methanol, ortho-phosphoric acid 85% and sodium hydroxide (pellets) were delivered by Merck (Spain). All chemicals were of analytical reagent grade. The Milli-Q water used was obtained from a Millipore Direct-QTM 5 purification system. Stock solutions of ethanol, AOx and AOx/HRP were prepared daily in 0.1 M phosphate buffer of suitable pH and stored at 4^0C in refrigerator. Britton-Robinson buffer solutions of pH 3 and 9, and 0.1 M phosphate buffer solutions of pH values between 4 and 8 were used for pH studies.

2.2. Apparatus and measurements

Chronoamperometric measurements were carried out using an ECO Chemie μAutolab type II potentiostat interfaced with a Pentium 166 computer system and controlled by the Autolab GPES software version 4.8 for Windows 98. All measurements were performed at room temperature. Screen-printed Prussian Blue/carbon electrodes (SPPBCEs; DRP-710), screen-printed ferrocyanide/carbon electrodes (SPFCEs; ref DRP-F10), screen-printed Co-phthalocyanine/carbon electrodes (SPCPCEs; ref DRP-410), and an edge connector (ref. DRP-DSC) were purchased from DropSens, S.L. (Oviedo, Spain). These devices consist of a working electrode (4 mm diameter), a carbon auxiliary electrode and a silver pseudoreference electrode printed on an alumina substrate. The working electrode is made of Prussian Blue/carbon, ferrocyanide/carbon or co-phthalocyanine/carbon in each case. An insulating layer delimits the electrochemical cell and the electric contacts.

For comparison purposes, real samples were also analyzed by gas chromatography with HP6890 chromatograph composed of an injector, a 2-m long packed column and a flame ionization detector (FID).

2.3. Electrode modification with enzymes

The used procedure is the same in all cases. After a first washing step with Milli-Q water, 10 µL of a mixture of AOx/HRP solution was deposited on the SPCE, and left to dry 1 h onto the electrode. The mixture of enzymes was prepared in phosphate buffer 0.1 M pH 6 in an adequate concentration. For the screen-printed co-phthalocyanine/carbon electrodes, HRP was not included in the mixture.

2.4. Analytical signal recording

A 40-µL aliquot of the ethanol solution was deposited on the sensor and chronoamperometry by applying a potential of -0.1 V during 100 s for SPPBCEs, -0.1 V during 170 s for SPFCEs, and +0.4 V during 170 s for SPCPCEs was employed to record the analytical signals. A different sensor was used for each measurement.

2.5. Interferences measurement

Methanol, gallic acid, cysteine and ascorbic acid were checked as potential interferences for the amperometric response of the biosensor. For all of them, an adequate dilution in 0.1 M phosphate buffer pH 6 was the only sample treatment needed. 40 µL of each solution were dropped on different sensors and the chronoamperogram was recorded using the experimental conditions mentioned in **Section 2.4**.

2.6. Real samples measurement

The developed SPCPCEs, biosensor was used to analyze different alcoholic beverages (Rioja wine, hazelnut liqueur and tequila). In all cases, a 1:10000 dilution in 0.1 M phosphate buffer pH 6 was the only sample treatment needed. Then, the chronoamperogram was recorded upon deposition of 40 µL of each sample solution on the sensor surface using the experimental conditions mentioned in **Section 2.4**.

2.7. Gas chromatographic measurements

In order to compare the results obtained with the enzymatic sensor, the alcoholic beverages were also analyzed by gas chromatographic (GC) using an internal standard method. A calibration plot for ethanol in concentrations ranging between 0 and 10% (v/v) was

constructed using 5% of propanol as internal standard. The samples were previously diluted to obtain an adequate ethanol concentration.

3. Results and discussion

In the case of the SPPBCEs and SPFCEs, the enzymatic reaction is monitored by the electrochemical reduction of the $Fe(CN)_6^{3-}$ (**Fig. 1A**) generated in the enzyme reaction with HRP, while in the case of the SPCPCEs, the reaction is monitored by the electrochemical oxidation of Co^{2+} (**Fig. 1B**).

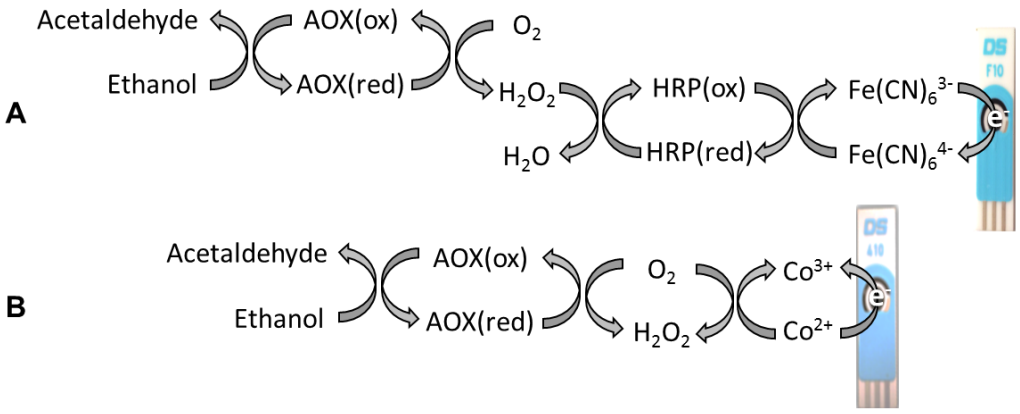

Fig. 1. Enzymatic reactions at the surface of SPPBCEs and SPFCEs (A), and SPCPCEs (B).

3.1. Comparison of enzymes using the different screen-printed electrodes

Following the methodology described in **Section 2.3**, different SPFCEs and SPPBCEs biosensors were prepared with 0.05 U μL^{-1} of each AOx and HRP. Regarding SPCPCEs, the same methodology was used but without HRP. The three enzymes sources, *Hansenula sp*., *P. pastoris* and *C. boidinii*, were tested in all cases.

Calibration plots for ethanol were constructed with each enzymatic sensor. **Fig. 2** shows the comparison of these calibrations using the three AOx enzymes as recognition element in SPPBCEs (**Fig. 2A**), SPFCEs (**Fig. 2B**) and SPCPCEs (**Fig. 2C**). The analytical parameters for the calibration plots are summarized in **Table 1**.

Although the highest slope value was obtained with SPPBCEs and AOx from *Hansenula sp*., the blank responses were very high and affected seriously the reproducibility of the slope values obtained with different biosensors. However, the slope values found in the case of

SPFCEs and AOx from *P. pastoris* were lower but more reproducible. Nevertheless, the SPCPCEs modified with AOx from *Hansenula sp*. showed the best results with a good correlation coefficient and a wide linear range. Moreover, in this case, HRP is not necessary to achieve an adequate performance of the sensor with the subsequent lower cost. The reason why different sources of enzymes gave rise to so different results is not clear at present.

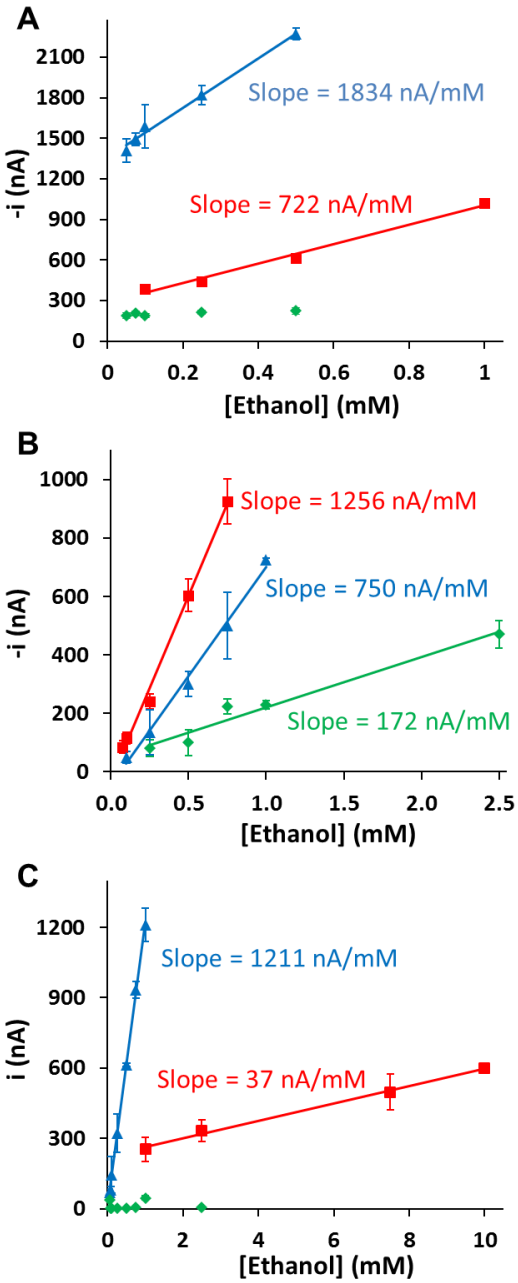

Fig. 2. Calibration plots for ethanol obtained with SPPBCEs (A), SPFCEs (B) and SPCPCEs (C) based biosensors. AOx from *Hansenula sp.* (▲), *Pichia pastoris* (■) and *Candida boidinii* (♦). Ethanol diluted in phosphate buffer 0.1 M pH 6. Data are given as average *±SD* (n = 3).

Table 1. Characteristics of the calibration plots for ethanol obtained with SPPBCEs, SPFCEs and SPCPCEs-based biosensors using AOx from *Hansenula sp*., *Pichia pastoris* and Candida *boidinii*.

		Equation	R^2	Linear range (mM)
SPPBCEs	*Hansenula sp.*	-i (nA) = 1834 [ethanol] (mM) + 1359	0.992	0.05-0.50
	Pichia pastoris	-i (nA) = 722 [ethanol] (mM) + 282	0.990	0.1-1.0
	Candida boidinii	–	–	–
SPFCEs	*Hansenula sp.*	-i (nA) = 750 [ethanol] (mM) - 48	0.993	0.1-1.0
	Pichia pastoris	-i (nA) = 1256 [ethanol] (mM) - 27	0.994	0.075-0.750
	Candida boidinii	-i (nA) = 172 [ethanol] (mM) + 48	0.96	0.25-2.50
SPCPCEs	*Hansenula sp.*	i (nA) = 1211 [ethanol] (mM) + 11	0.9991	0.05-1.00
	Pichia pastoris	i (nA) = 37 [ethanol] (mM) + 226	0.995	1-10
	Candida boidinii	–	–	–

3.2. Optimization of parameters for the biosensor design

3.2.1. Enzymes concentration

In order to evaluate this experimental variable, different biosensors were prepared by depositing, on SPCPCEs, solutions of AOx from *Hansenula sp*. with different concentrations. For each concentration, chronoamperograms for 1 mM ethanol solution, prepared in phosphate buffer 0.1 M pH 6, were recorded. The obtained results are summarized in **Fig. 3**. The biosensor response increased with the AOx concentration until a plateau was reached at 0.15 $U \cdot \mu L^{-1}$, value that was chosen for further studies.

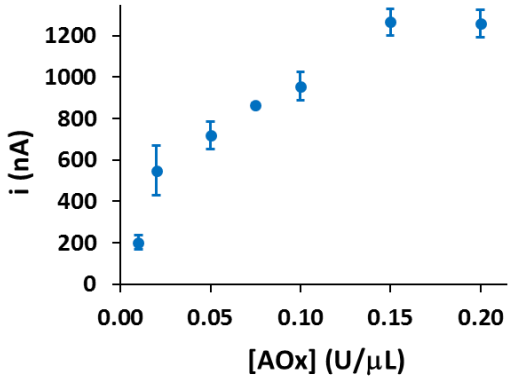

Fig. 3. Effect of the enzyme concentration on the responses for 1 mM ethanol of different biosensors prepared with SPCPEs and AOx from *Hansenula sp.* Data are given as average *±SD* (n = 3).

3.2.2. Effect of pH

The pH effect on the analytical signal was checked by recording chronoamperograms upon deposition of 40 µL of 1 mM ethanol solution and by applying a potential of +0.4 V during 170 s. The ethanol stock solution was diluted using buffers with pH values between 3 and 9 and the results are displayed in **Fig. 4**.

As it can be seen, the higher responses were obtained at pH values between 5 and 6. However, considering the better reproducibility achieved at pH 6, this pH value was chosen for further studies.

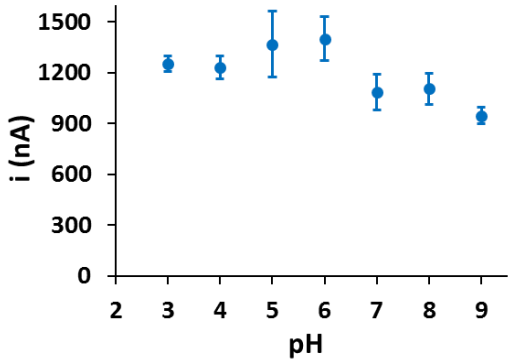

Fig. 4. Effect of the pH value on the response of the biosensor constructed with SPCPEs and AOx from *Hansenula sp.* (0.15 U·µL^{-1}). Ethanol concentration, 1 mM. Data are given as average *±SD* (n = 3).

3.3. Analytical characteristics of the biosensor

Chronoamperometry at +0.4 V during 170 s allowed a calibration plot for ethanol to be obtained with the equation, i (nA) = 1211 [ethanol] (mM) + 11, and the linear range, 0.05-1.00 mM, given in **Table 1**. The detection limit (LOD) was calculated according to the $3s_b/m$ criteria, where m is the slope of the linear range of the corresponding calibration plot, and s_b was estimated as the standard deviation of the intercept. The LOD value thus obtained was 0.02 mM. It is interesting to remark that this simple biosensor design shows sensitivity, detection limit and range of linearity values comparable, or in some cases better, than those for other alcohol sensors developed in the last years which need the use of polymers, membranes or cross-linkers (**Table 2**). Moreover, the time of fabrication of this sensor is one of the shortest, in spite of some of the fabrication time estimated are shorter than they really are because these fabrication times were estimated adding the times indicated in the articles for some of the manufacturing stages for each sensor.

Furthermore, the sensor showed a Michaelis-Menten kinetics behavior. The apparent Michaelis–Menten constant (K_m) was calculated using the Lineweaver-Burk linearization, and the value obtained was 2.4 ± 0.7 mM. This K_m value resulted to be lower than those calculated with other enzyme sensors using polymers, membranes or cross-linkers, as well as with many sensors based on screen-printed electrodes (see **Table 2**) indicating a high bioaffinity to ethanol with the developed design as a consequence of the simplicity of the AOx immobilization strategy.

In order to evaluate the reproducibility of the sensors, several sensors were prepared in different days to carry out four different calibration plots for ethanol. Each sensor was used for only one measurement (single-use). Each calibration plot was constructed using ethanol solutions prepared the same day of the measurement. **Table 3** shows the equations calculated for each calibration plot and the reproducibility was estimated in terms of the *RSD* value calculated from the corresponding slope values. The biosensor exhibited an excellent reproducibility with a mean slope value of 1205 ± 26 nA·mM^{-1} and a *RSD* of 2.1% (n = 5). The achieved reproducibility can be advantageously compared with other alcohol sensors previously reported involving many more steps in their fabrication (**Table 2**). This low *RSD* value is very important taking into account that the biosensor construction relies on the use of a commercial screen-printed electrode and is a single-use sensor. Therefore, the high reproducibility achieved allows ethanol determination to be carried out with a very simple and rapid procedure (just one standard and the sample).

Table 3. Calibration plot equations for five different alcohol sensors (n = 7 in all calibration plots). Each point was measured three times.

	Equation	R^2
Calibration plot 1	i (nA) = 1211 [ethanol] (mM) + 11	0.9991
Calibration plot 2	i (nA) = 1180 [ethanol] (mM) + 40	0.993
Calibration plot 3	i (nA) = 1210 [ethanol] (mM) – 11	0.990
Calibration plot 4	i (nA) = 1242 [ethanol] (mM) + 2	0.9997
Calibration plot 5	i (nA) = 1182 [ethanol] (mM) + 30	0.998
Mean slope	1205 ± 26 nA mM^{-1}	

Table 2. Analytical characteristics of some alcohol sensors.

Analytical performance		Sensitivity	Detection limit (mM)	Linear range	K_M	Reproducibility (*RSD*)	Stability	Fabrication time	Reference
AOx immobilization by adsorption on SPCPCEs		1211 nA mM^{-1}	0.02	0.05-1 mM	2.4 mM	2.1%	No loss after 2 months	≈ 1 h	Present work
AOx and bovine liver catalase immobilization in a photoreticulated poly(vinyl alcohol) membrane at surface of interdigitated microelectrodes		363 µS mM^{-1}	0.001	Up to 0.07 mM	–	1.5 - 4%	5% signal decrease after 4 months	≈ 50 min	[29]
Conducting polymers to AOx immobilization	Polypyrrole	21.4 nA mM^{-1} cm^{-2}	170	–	12300 mM	–	50% activity lost after 28 days	–	[30]
	Poly(3,4-ethylenedioxythiophene)	21.4 nA mM^{-1} cm^{-2}	170	–	7800 mM	–	20% activity lost after 28 days	–	
	Poly(3,4-ethylenedioxypyrrole)	22.2 nA mM^{-1} cm^{-2}	170	–	6000 mM	–	23% activity lost after 28 days	–	
AOx immobilization by electrochemical polymerization in poly(3,4-ethylenedioxythiphene) on platinum printed electrodes		–	0.3	0.3-20 mM	–	4.2%	No loss after 2 months	≈ 15 min	[31]
AOx immobilization by cross-linking with glutaraldehyde using bovine serum albumin and poly(neutral red) as redox mediator		171.8 nA mM^{-1}	0.03	Up to 0.7 mM	1.96 mM	8.6%	12% of sensitivity lost after 6 weeks	≈ 1 h 10 min	[32]
AOx/chitosan immobilization by eggshell membrane		–	0.03	0.06 - 0.8 mM	3.89 mM	3.4%	13.4% sensitivity lost after 3 months	≈ 6 h 40 min	[33]
AOx immobilized by glutaraldehyde co-crosslinking with bovine serum albumin on a electropolymerized film modified gold electrode		4100 nA mM^{-1} cm^{-2}	0.0023	Up to 0.75 mM	5.30 mM	–	–	≈ 1 h 20 min	[34]
Os complex-modified redox hydrogel to crosslinking peroxidase and electrodeposition paint entrapping the AOx	Royal palm tree peroxidase	98000 nA mM^{-1}	0.02	–	9.5 mM	–	–	≈ 20 h	[35]
	HRP	60000 nA mM^{-1}	0.02	–	9.6 mM	–	–		

Table 2. (*Continued*)

Analytical performance		Sensitivity	Detection limit (mM)	Linear range	K_M	Reproducibility (*RSD*)	Stability	Fabrication time	Reference
Graphite-Teflon-alcohol oxidase-HRP-ferrocene electrode		551 nA mM^{-1}	0.0053	0.02 - 2 mM	0.0138 s^{-1}	6.5%	No loss of enzymes activity after 3 months	≈ 3 h 25 min	[13]
Alcohol dehydrogenase with 4-ferrocenylphenol and 2,4,7-trinitro-9-fluorenone electrochemically polymerized on screen-printed		–	–	0 - 1 mM	1.05 mM	–	–	≈ 34 min	[8]
Poly(carbamoyl)sulfonate hydrogel to AOX immobilization on screen-printed	*Hansenula sp.*	30.2 nA mM^{-1}	–	0.01 - 3.0 mM	–	–	40 - 50% signal decrease after 18 days	≈ 22 h	[2]
	P. pastoris	10.6 nA mM^{-1}	–	0.02 - 3.75 mM	–	–			
	C. boidinii	6.2 nA mM^{-1}	–	0.04 - 3.75 mM	–	–			
Enzymes immobilized by entrapment in a photocrosslinkable polyvinyl alcohol containing stilbazolium groups on screen-printed	Meldola blue and ADH	5.282 nA mM^{-1}	0.1	0.3 - 8 mM	7 mM	47%	1 month	≈ 4 h	[36]
	Co-phthalocyanine and AOX	1.01 nA mM^{-1}	10	15 - 110 mM	80 mM	41%			
Quinohemoprotein ADH (QH-ADH), Poly(ethylene glycol) diglycidyl ether (PEGDGE) and Os-complexed poly(1-vinylimidazole) redox polymer ($PVI_{13}dmeOs$)	QH-ADH/PEGDGE/graphite	1570 nA mM^{-1} cm^{-2}	0.01	0.01 – 0.2 mM	0.45 mM	–	–	≈ 20 h	[37]
	QH-ADH/$PVI_{13}dmeOs$/PEGDGE/graphite	7280 nA mM^{-1} cm^{-2}	0.001	0.005 - 1 mM	1.27 mM	–	–		
	QH-ADH/PEGDGE/screen-printed	50000 nA mM^{-1} cm^{-2}	0.005	0.005 - 1 mM	62 mM	–	–		
	QH-ADH/$PVI_{13}dmeOs$/PEGDGE/screen-printed	336000 nA mM^{-1} cm^{-2}	0.001	0.001 – 0.25 mM	183 mM	–	–		
PQQ-dependent alcohol dehydrogenase	Carbon electrodes	4630 nA mM^{-1} cm^{-2}	0.0018	–	4.75 mM	–	–	≈ 20 h	[38]
	Graphite electrodes	6830 nA mM^{-1} cm^{-2}	0.005	–	0.71 mM	–	–		
	Screen-printed electrodes	179000 nA mM^{-1} cm^{-2}	0.001	–	1.19 mM	–	10% signal decrease after 5 days. Stable for the next 6 days		

3.4. Specificity of the sensor

The specificity of the sensor was checked under the experimental conditions explained in **Section 2.4**. The potential interfering agents tested were methanol, ascorbic acid, gallic acid and cysteine. The concentration of these interferents in red wine is: methanol 38-200 mg L^{-1} [13,33], ascorbic acid 20 mg L^{-1} [39,40], polyphenols like gallic acid 2000 mg L^{-1} [41,42] and amino acids like cysteine 2000 mg L^{-1} [43]. According to this, to evaluate those interferences, solutions of 500 µM of ethanol, 1 µM of methanol, 0.1 µM of acid ascorbic, 10 µM of gallic acid and 10 µM of cysteine were prepared. 40 µL of those solutions were dropped on the sensor and chronoamperograms were recorded as explained in **Section 2.4**. The different results obtained are resumed in **Table 4**. The present sensor shows a good specificity for the ethanol. The signals recorded for the methanol, ascorbic acid, gallic acid and cysteine measurements are equal as the recorded for the background.

Table 4. Study of the interferences caused by methanol, ascorbic acid, gallic acid and cysteine. [ethanol] = 500 µM, [methanol] = 1 µM, [ascorbic acid] = 0.1 µM, [galic acid] = 10 µM and [cysteine] = 10 µM. Each point was measured three times. Data are given as average *±SD* (n = 3).

Background	Ethanol	Methanol	Ascorbic acid	Gallic acid	Cysteine
155 ± 7 nA	805 ± 42 nA	135 ± 11 nA	175 ± 7 nA	185 ± 9 nA	125 ± 8 nA

3.5. Storage ability

In order to evaluate the storage stability of the ethanol biosensor, two sets of sensors was prepared and light protected stored at -20^{0}C during 30 days and 60 days, respectively. In the calibration plot of **Figure 5** each concentration was measured using 9 sensors: 3 sensors prepared and used in the same day, 3 sensors stored 30 days at -20^{0}C and 3 sensors stored 60 days at -20^{0}C. The slope and the correlation coefficient obtained was 1219 ± 160 nA mM^{-1}, and 0.997, respectively. These data are better than those reported for others sensors that need the use of polymers, membranes or cross-linkers (**Table 2**), including the alcohol sensor based on screen-printed electrodes modified with alcohol dehydrogenase by physical adsorption [38] where a sensitivity loss of 10% after 5 days is observed.

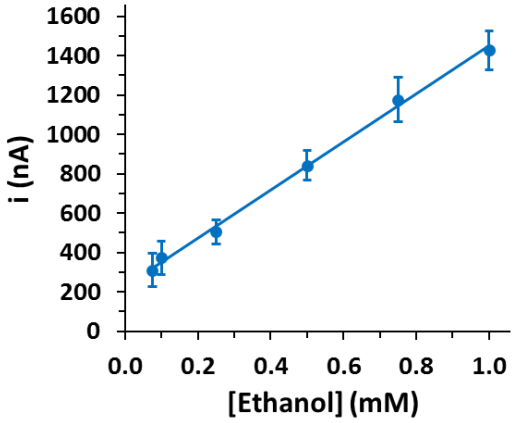

Figure 5. Calibration plot using 9 sensors for each concentration: 3 prepared and used the same day, 3 stored 30 days at -20^{0}C and 3 stored 60 days at -20^{0}C.

3.6. Application to real samples

Different alcoholic drinks were analyzed using the developed alcohol sensor. The samples were treated as described in **Section 2.6** and the analytical signal was recorded according to **Section 2.4.** The samples were also analyzed by GC to compare the results, which are summarized in **Table 5**.

The application of the Student's *t*-test demonstrated that there were no significant differences between the values labeled, those obtained with the biosensor and those obtained with GC, at a 0.05 significance level, thus demonstrating the good accuracy and precision achieved.

Table 5. Determination of ethanol in real samples with the develop biosensor and by applying GC. Data are given as average *±SD* (n = 3).

	[Ethanol] labeled (%)	GC			Sensor of this work		
		[Ethanol] (%)	SD	RSD (%)	[Ethanol] (%)	SD	RSD (%)
Rioja wine	12.5	13.9	0.7	4.7	12.2	0.4	2.8
Hazelnut liqueur	20	20.2	0.5	2.4	20.1	0.8	3.9
Tequila	38	38	1	2.8	38.0	0.7	1.8

4. Conclusions

From all assayed alcohol sensors the better results obtained was with the sensor developed using a commercial screen-printed carbon electrode containing co-phthalocyanine as redox mediator into the working electrode. This sensor does not need a pretreatment step to be used as transducer in this sensor. Moreover, the sensor fabrication was extremely simple consisting on the immobilization by adsorption on the SPCPCE of only one enzyme, AOx from *Hansenula sp*. Therefore, the use of other reagents such as cross-linkers or polymers or the need for covalent bindings, are avoided. The developed biosensor shows high sensitivity (1211 $nA \cdot mM^{-1}$), low detection limit (0.02 mM), high reproducibility (2.1%) and a wide linear response (0.05 - 1.00 mM), characteristics that can be advantageously compared with others alcohol sensors previously reported. Furthermore this enzymatic alcohol sensor is able to determine ethanol in alcoholic drinks with just a dilution with Mili-Q water as sample treatment.

Acknowledgement

This work has been supported by the Spanish Ministry of Science and Innovation Project MICINN-09-PET2008-0174-02.

References

[1] C. X. Cai, K.H. Xue, Y.-M. Zhou, H. Yang, Talanta 44 (1997) 339-347.

[2] N.G. Patel, S. Meier, K. Cammann, G.C. Chemnitius, Sens. Actuators B 75 (2001) 101-110.

[3] A.R. Vijayakumar, E. Csöregi, A. Heller, L. Gorton, Anal. Chim. Acta 327 (1996) 223-234.

[4] A. Morales, F. Céspedes, E. Martínez-Fàbregas, S. Alegret, Electrochim. Acta 43 (1998) 3575-3579.

[5] M. Boujtita, M. Chapleau, N. El Murr, Anal. Chim. Acta 319 (1996) 91-96.

[6] J. K. Park, H.J. Yee, K.S. Lee, W.Y. Lee, M.C. Shin, T.H. Kim, S.R. Kim, Anal. Chim. Acta 390 (1999) 83-91.

[7] A. Ramanavicius, K. Habermüller, E. Csöregi, V. Laurinavicius, W. Schuhmann, Anal. Chem. 71 (1999) 3581-3586.

[8] J. Razumiene, V. Gureviciene, V. Laurinavicius, J.V. Grazulevicius, Sens. Actuators B 78 (2001) 243-248.

[9] A.M. Azevedo, D. Miguel, F. Prazeres, J.M.S. Cabral, L.P. Fonseca, Biosens. Bioelectron. 21 (2005) 235-247.

[10] M. Asunción Alonso Lomillo, J. Gonzalo Ruiz, F. Javier Muñoz Pascual, Anal. Chim. Acta 547 (2005) 209-214.

[11] C.A.B. Garcia, G. de Oliveira Neto, L.T. Kubota, L.A. Grandin, J. Electroanal. Chem. 418 (1996) 147-151.

[12] L. Mao, K. Yamamoto, Talanta 51 (2000) 187-195.

[13] A. Guzmán-Vázquez de Prada, N. Peña, M.L. Mena, A.J. Reviejo, J.M. Pingarrón, Biosens. Bioelectron. 18 (2003) 1279-1288.

[14] J. Tkác, I. Vostiar, P. Gemeiner, E. Sturdík, Bioelectrochemistry 55 (2002) 149-151.

[15] M.E. Ghica, C.M.A. Brett, Anal. Lett. 38 (2005) 907-920.

[16] J. Biscay, E.C. Rama, M.B.G. García, J.M.P. Carrazón, A.C. García, Electroanalysis 23 (2011) 209-214.

[17] J. Gonzalo-Ruiz, M. Asunción Alonso-Lomillo, F. Javier Muñoz, Biosens. Bioelectron. 22 (2007) 1517-1521.

[18] J.Y. Chiu, C.M. Yu, M.J. Yen, L.C. Chen, Biosens. Bioelectron. 24 (2009) 2015-2020.

[19] D. Lowinsohn, M. Bertotti, Anal. Biochem. 365 (2007) 260-265.

[20] N. Sehlotho, S. Griveau, N. Ruillé, M. Boujtita, T. Nyokong, F. Bedioui, Mater. Sci. Eng. C 28 (2008) 606-612.

[21] K. Wang, J.-J. Xu, H.-Y. Chen, Biosens. Bioelectron. 20 (2005) 1388-1396.

[22] J. Tkác, I. Vostiar, E. Sturdik, P. Gemeiner, V. Mastihuba, J. Annus, Anal. Chim. Acta 439 (2001) 39-46.

[23] M. Gamella, S. Campuzano, A.J. Reviejo, J.M. Pingarrón, Anal. Chim. Acta 609 (2008) 201-209.

[24] H. Liu, J. Deng, Anal. Chim. Acta 300 (1995) 65-70.

[25] S. Susana Campuzano, Ó.A. Loaiza, M. María Pedrero, F. Javier Manuel de Villena, J.M. Pingarrón, Bioelectrochemistry 63 (2004) 199-206.

[26] A. Curulli, F. Valentini, S. Orlanduci, M.L. Terranova, G. Palleschi, Biosens. Bioelectron. 20 (2004) 1223-1232.

[27] S.D. Sprules, J.P. Hart, S.A. Wring, R. Pittson, Anal. Chim. Acta 304 (1995) 17-24.

[28] M. Albareda-Sirvent, A. Merkoçi, S. Alegret, Sens. Actuators B 69 (2000) 153-163.

[29] M. Hnaien, F. Lagarde, N. Jaffrezic-Renault, Talanta 81 (2010) 222-227.

[30] Ö. Türkarslan, A. Elif Böyükbayram, L. Toppare, Synth. Met. 160 (2010) 808-813.

[31] T.B. Goriushkina, A.P. Soldatkin, S.V. Dzyadevych, J. Agric. Food Chem. 57 (2009) 6528-6535.

[32] M.M. Barsan, C.M.A. Brett, Talanta 74 (2008) 1505-1510.

[33] G. Wen, Y. Zhang, S. Shuang, C. Dong, M.M.F. Choi, Biosens. Bioelectron. 23 (2007) 121-129.

[34] D. Carelli, D. Centonze, A. De Giglio, M. Quinto, P.G. Zambonin, Anal. Chim. Acta 565 (2006) 27-35.

[35] I.S. Alpeeva, A. Vilkanauskyte, B. Ngounou, E. Csöregi, I.Y. Sakharov, M. Gonchar, W. Schumhmann, Microchim. Acta 152 (2005) 21-27.

[36] B. Bucur, G.L. Radu, C.N. Toader, Eur. Food Res. Technol. 226 (2008) 1335–-1342.

[37] M. Niculescu, T. Erichsen, V. Sukharev, Z. Kerenyi, E. Csöregi, W. Schuhmann, Anal. Chim. Acta 463 (2002) 39-51.

[38] J. Razumiene, M. Niculescu, A. Ramanavicius, V. Laurinavicius, E. Csöregi, Electroanalysis 14 (2002) 43-49.

[39] T.J. Cardwell, M.J. Christophersen, Anal. Chim. Acta 416 (2000) 105-110.

[40] L. Campanell, A. Bonanni, E. Finotti, M. Tomassetti, Biosens. Bioelectron. 19 (2004) 641-651.

[41] V. Carralero Sanz, M.L. Mena, A. González-Cortés, P. Yáñez-Sedeño, J.M. Pingarrón, Anal. Chim. Acta 582 (2005) 1-8.

[42] I. Tedesco, M. Russo, P. Russo, G. Iacomino, G.L. Russo, A. Carraturo, C. Faruolo, L. Moio, R. Palumbo, J. Nutr. Biochem. 11 (2000) 114-119.

[43] P.M. Izquierdo Cañas, E. García Romero, S. Gómez Alonso, M. Fernández González, M.L.L. Palop Herreros, J. Food Compos. Anal. 21 (2008) 731-735

3.2. Capítulo II: Immunosensores basados en electrodos serigrafiados

- Artículo 4: "*Screen-printed electrochemical immunosensors for the detection of cancer and cardiovascular biomarkers*"
- Artículo 5: "*Competitive electrochemical immunosensor for amyloid-beta 1-42 detection based on gold nanostructurated screen-printed carbon electrodes*"
- Artículo 6: "*Multiplexed electrochemical immunosensor for detection of breast cancer biomarkers*"

3.2.1. Introducción

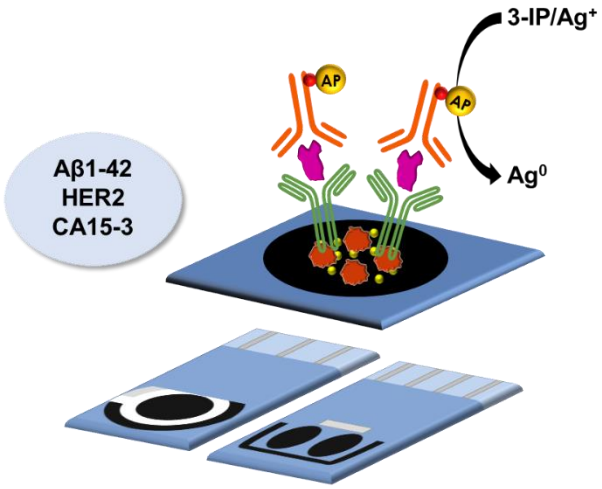

Los inmunosensores electroquímicos, gracias a su selectividad y sensibilidad, resultan muy interesantes como herramientas para el diagnóstico o seguimiento de enfermedades mediante la determinación de biomarcadores.

En este capítulo se desarrollan dos inmunosensores utilizando electrodos serigrafiados nanoestructurados con nanopartículas de oro como transductor, y la enzima fosfatasa alcalina como marca. El primero de ellos es un immunosensor para la detección de un biomarcador de la enfermedad de Alzheimer: la beta amiloide 1-42. El segundo es un immunosensor multianalito que permite la detección simultánea de dos biomarcadores del cáncer de mama: el CA 15-3 y el HER2. Para este último se escoge un diseño de electrodo serigrafiado con dos electrodos de trabajo.

En este capítulo también se presenta, a modo de introducción, una revisión bibliográfica de inmunosensores basados en electrodos serigrafiados para la determinación de biomarcadores de los dos tipos de enfermedades que suponen una mayor amenaza para la población mundial: el cáncer y las enfermedades cardiovasculares.

3.2.2. Artículo 4: "Screen-printed electrochemical immunosensors for the detection of cancer and cardiovascular biomarkers"

Electroanalysis 2016 (aceptado)

Full Paper Wiley Online Library ELECTROANALYSIS

Electroanalysis

Screen-printed electrochemical immunosensors for the detection of cancer and cardiovascular biomarkers

Estefanía Costa Rama, Agustín Costa García*

Departamento de Química Física y Analítica, Facultad de Química, Universidad de Oviedo, 33006 Oviedo, Spain

ABSTRACT

Electrochemical immunosensors (EIs) for the determination of disease biomarkers has attracted a wide interest due to its high sensitivity, low cost, and possible integration in compact analytical devices. The use of screen-printed electrodes (SPEs) to develop EIs contribute to the great potential they have in point of care (POC) test, since SPEs show good electrical properties and allow the reduction of the electrochemical instrumentation down to small pocket-size devices. Moreover, during the last years, SPEs have gone through significant improvements related to both their design and printing materials. Since cancer and cardiovascular diseases are the major threats of global health, there is a growing demand for the development of portable, rapid, simple and inexpensive devices for the detection of these diseases. This article presents an overview about the main biomarkers of cancer and cardiovascular diseases and the EIs based on SPEs for the detection of these biomarkers.

Keywords: Screen-printed electrode, Electrochemical, Immunosensors, Cardiovascular biomarkers, Cancer biomarkers.

1. Introduction

A biomarker (biological marker) can be defined as a characteristic that is objectively measured and evaluated as an indicator of normal biological processes, pathogenic processes or pharmacologic responses to a therapeutic intervention [1]. Sensitive and selective detection of disease biomarkers is of great importance for early diagnosis, staging of disease, prediction and monitoring of clinical response to a treatment and even for the development of molecularly targeted therapy [1-3]. Biomarkers can be specific cells, molecules, genes, gene products, enzymes or hormones and can be measured in biological media such as tissues, cells or fluids [1,4]. To maximize the usefulness and minimize the cost and time for screening, it is advantageous that these biomarkers could be measurable in biological fluids which allow a non- or minimally invasive sample collection such as serum, urine or saliva.

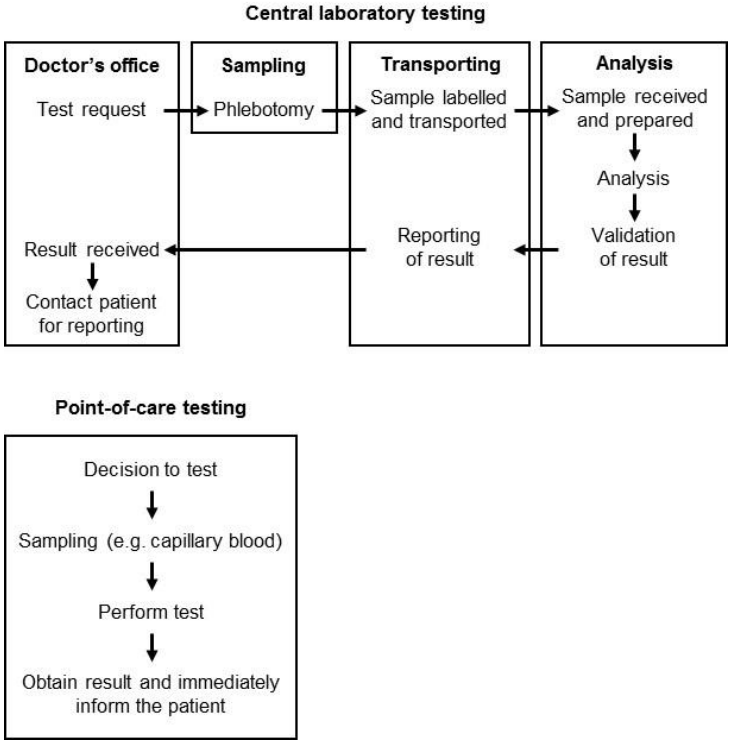

Fig. 1. Simplified scheme of the process of clinical testing using central laboratory versus POC testing. Adapted from [10].

During last years, the need to save time and money gaining simultaneously in efficacy, implies the decentralization of analytical operations to point-of-care (POC) system platforms (**Figure 1**) [5-7]. POC testing can be described as ancillary, bedside, near-patient, remote and

decentralized laboratory testing, which is performed at the site of patient care [8]. POC testing can be performed in a hospital, in a doctor's office or even at home; moreover, this devices can also be very useful in resource-limited settings [8,9].

So, the realization of POC testing requires not only fast, sensitive and selective detection, but also miniaturized, inexpensive and integrated device. Electrochemical immunosensors (EIs) with its high specificity and sensitivity, low cost, and potential of automatization and miniaturization has been a promising approach for POC testing [10,11]. Screen-printed electrodes (SPEs), with low cost and mass production, have been extensively employed for developing novel EIs providing advantages such as portability and low sample consumption [12-14]. Moreover, due to its great versatility of design, SPEs allow for development multiplexing analysis. The possibility of simultaneous determination of different analytes saving time and money has a high importance in critical clinical situations since it can discard different pathologies and conduct the patient to the correct treatment.

There are several reviews about EIs [11,12,15-20]; however only a few of them are focusing on the biomarkers detected [21-23]. In addition, although the bibliography about biosensors based on SPEs is extensive, there are few reviews about this [12,14,24,25]. This review summarizes the main biomarkers of cancer and cardiovascular diseases and recount publications about EIs based on SPEs for these biomarkers focusing on their final analytical application.

2. Electrochemical immunosensors

The International Union of Pure and Applied Chemistry (IUPAC) defines biosensor as 'a device that uses specific biochemical reactions mediated by isolated enzymes, immunosystems, tissues, organelles or whole cells to detect chemical compounds usually by electrical, thermal or optical signals' (International Union of Pure and Applied Chemistry, http://goldbook.iupac.org/, 2016). The development of a biosensor was first reported by Clark and Lyons in 1962 whereby they demonstrated enzyme electrodes for glucose determination [26]. The term 'biosensor' was coined by Cammann in 1977 [27]. A biosensor has two major components: a biological detector or sensor molecule (bioelement) and a signal transducer that provides a signal that the ligand has bound to the receptor molecule [28,29].

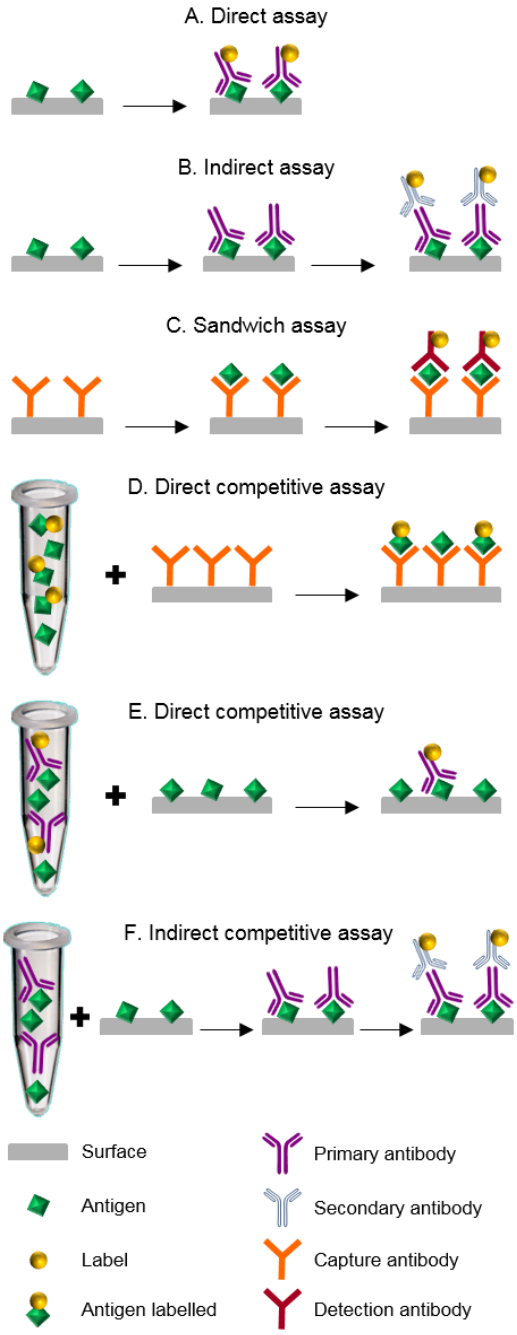

Fig. 2. Scheme of immunoassay formats.

An immunosensor is a class of biosensor that comprises an antigen or antibody species coupled to a signal transducer which detects the binding of the complementary species [29]. Regarding the detection, there are four main types of immunosensors: electrochemical (potentiometric, amperometric, conductimetric, capacitive and impedimetric), optical, microgravimetric and thermometric [30]. In relation to the immunoreactions, there are four

main types of immunoassays in which an immunosensor can be based on: direct, indirect, sandwich and competitive (**Figure 2**). The basic principles for the assay are similar and they generally include the following steps: capture of the analyte (usually the antigen), blocking of non-reacted surface and recognition of the analyte. Direct immunoassay is the simplest assay. It lies in immobilizing the antigen to the surface and, after washing and blocking steps, a specific labelled antibody is added for detection (**Figure 2A**). In an indirect immunoassay the antigen is immobilized onto the surface and then it is bound to a specific antibody. Then, a labelled secondary antibody against this primary antibody is incubated for detection purposes (**Figure 2B**) [31]. In the sandwich assay, after antigens have bound with antibodies immobilized onto the surface, labelled antibodies directed toward a second binding site of the antigen are added. Thus, the antigen is "sandwiched" between two antibodies (**Figure 2C**) [12,32]. In the case of competitive assays, two approaches can be followed: a first one in which immobilized antibodies react with the free antigens in competition with labelled antigens (**Figure 2D**) or a second one in which immobilized antigens compete with free antigens for labelled free antibodies (**Figure 2E**). Both these approaches are denoted as direct competitive immunoassay. The second format is generally preferred and avoids the problems related to antibody immobilization (correct orientation of the antibody and loss of affinity). It is also used when labelled primary antibodies are not available for the analyte of interest. In this case, a labelled secondary antibody is used to binding with the primary antibody for detection purposes. This format is defined as indirect competitive immunoassay (**Figure 2F**) [31,32]. Most of the developed immunosensors are based either on a competitive or sandwich assay. Methodologies that utilise a single recognition phase (antibody-antigen complex) suffer from reduced specificity compared to dual recognition phase (sandwich complex) strategies [33]. Moreover, the sandwich format can be between 2 and 5 times more sensitive than those in which antigen is directly bound to the solid surface [34].

All the immunoassays represented in **Figure 2** are based on the use of a label, but the immunosensors can also be label-free. A label-free immunosensor is able to detect the physical changes during the immune complex formation, while an immunosensor based on the use of a label measures the signal generated by the label for detect the immune complex formation allowing more sensitive and versatile detection [21]. There is a great variety of labels which can be used for electrochemical immunosensors (EIs) development such as enzymes, electroactive compounds, metal nanoparticles or quantum dots [11,16,17,35-37]. Although immunosensors based on the use of labels show higher sensitivity, the label-free immunosensors represent a true alternative for the development of immunosensors due to

their simplicity [30]. Currently, in the literature there is a great number of EIs reported for real sample analysis. The two main types of EIs used in clinical analysis are amperometric and potentiometric [38]. Impedimetric and capacitive immunosensors have started to gain interest due to their direct use to determinate the antibody-antigen interaction without the need of other reagents and the separation step, but their sensitivities are still limited [21].

3. Screen-printed electrodes

The screen-printing technology, adapted from the microelectronics industry, offers high volume production of solid, planar, inexpensive and highly reliable electrodes; moreover, this technique holds great promise for sensors on-site monitoring [25,39]. The fabrication of screen-printed electrodes (SPEs) consists of a series of basic stages: selection of the screen which will defines the geometry and size of the SPE, selection and preparation of the inks, selection of the substrate, and printing, drying and curing steps. In summary, a SPE is fabricated by a sequential layer-by-layer deposition of ink onto a substrate through the use of a screen or mesh which controls the film layer thickness and the geometry of the final electrode [12-14]. The substrate is commonly a solid surface made of an insulating material such as glass, ceramic, plastic, etc. and the conducting path of the electrode usually are made of carbon ink/paste, or platinum, gold or other metal pastes. For the working electrode, the material mostly used is carbon (or modifications of carbon such as graphene, graphite, fullerene or carbon nanotubes) because it is relatively inexpensive, easy to modify and chemically inert; metals such as gold, silver or platinum are also employed but less than carbon because of their higher cost. The reference electrode material is mostly Ag/AgCl and the counter electrode usually is fabricated from the same material as the working electrode [12,14,24].

Of note, SPEs present a great versatility in the way they can be modified; these modifications give different properties to SPEs making them suitable for diverse applications. In fact, there are very few works related to the use of unmodified SPEs in the determination of interesting analytes [13,40]. SPEs can be modified by the addition of very different substances (mediators, polymers, complexing agents, metals, metal oxides, etc.) to the inks, or modifying their surface (with substances such as polymers, enzymes, metal films, etc.) [14,25,41]. Enzymes, microorganisms, proteins (antibodies or antigens) and nucleic acids have commonly been employed in the construction of biosensors based on SPEs [11,24]. These biomolecules can be immobilized onto the surface of the working electrode employing a variety of immobilization strategies such as adsorption, covalent binding, entrapment,

crosslinking or affinity binding [42,43]. Great advancement has been achieved modifying SPEs with nanomaterials such as metal nanoparticles or carbon nanomaterials that improve the electrochemical behavior of the SPEs and enhanced the immobilization efficiency of biological molecules [44-48]. Moreover, the planar nature of the SPEs makes easy the modification of their surface and, through the help of an automatic dispenser, this can be done in a mass-producible way [18].

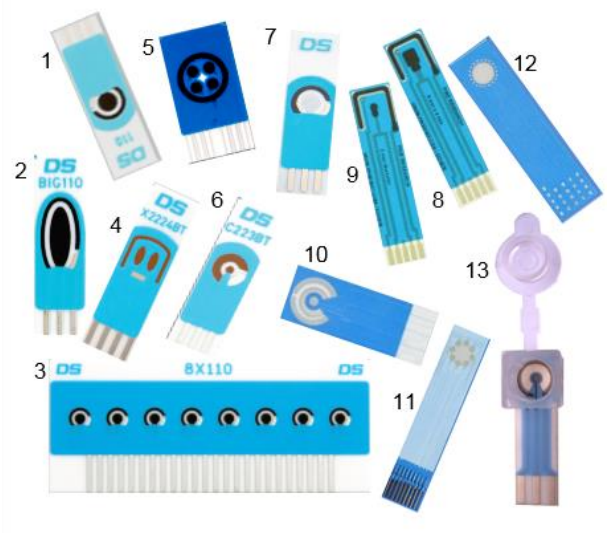

Fig. 3. Examples of commercial SPEs. Commercialised by DropSens: 1-carbon SPE, ref. DRP-110; 2-carbon SPE, ref. DRP-110BIG; 3-card with 8 carbon SPEs, ref. DRP-8X110; 4-dual gold SPEs, ref. DRP-X2224BT; 5-SPE with 4 working electrodes, ref. DRP-4W110; 6-gold SPEs, ref. DRP-223BT; 7-optically transparent SPEs, Ref. DRP-P10. Commercialised by Pine Research Instrumentation: 8,9-carbon SPE, ref. RRPE1002C, ref. RRPE1001C. Commercialised by BVT Technologies: 10-SPE with two counter electrodes, ref. AC6; 11-SPE with 8 working electrodes, ref. AC9; 12-SPE with 20 working electrodes, ref. AC10; 13-SPE with microreactor, ref. MAC.

SPEs can be designed as systems of two electrodes (working and reference electrodes; known as first-generation SPEs), but usually include a three electrodes configuration (working, reference and auxiliary electrodes; known as second-generation SPEs) [14,24]. The versatility of design of the SPEs is another interesting characteristic since it allows customize the production of SPEs for special applications and multiplex analysis (**Figure 3**). There are many commercial sources of SPEs in different configuration (e.g. Pine Research Instrumentation, http://www.pineinst.com/echem/; BVT Technologies, http://www.bvt.cz/; Rusens Ltd., http://www.rusens.com/speng.html; DropSens, http://www.dropsens.com/; Gwent Group,

http://www.gwent.org). SPEs with two or four working electrodes, arrays of 8 SPEs and of 96 SPEs in a 96-well plate are commercially available making the use of these electrode even more advantageous.

As it has been previously mentioned, the substrate used for fabricating SPEs is commonly a rigid one, but during the last years paper has become increasingly attractive as substrate for the development of electroanalytical devices. There are many examples of SPEs based on paper or transparency to detect a wide variety of analytes [49-52]. There are examples too of SPEs fabricated on textiles or even skin-worn tattoo-based SPEs for developing wearable electrochemical devices [53-54]. This shows the great potential of the screen-printed technology for developing electroanalytical devices.

3.1. Screen-printed electrochemical immunosensors

EIs based on electrochemical detection offer several potential advantages over the more widely used spectrophotometric/fluorescence techniques, especially when sensitivity is needed [16]. Besides the sensitivity and high accuracy at low analyte concentrations, other important advantages of the electrochemical detection are its low cost, ability for miniaturization, portability, low reagent and sample consumption and the lack of interferences caused by the turbid or coloured samples [16,52].

The choice of the electrode for developing an EI is a crucial step because not only affects the cost, but also the sensitivity of the assay. Conventional electrodes, such as carbon paste or glassy carbon among others, are widely used in electrochemical laboratories because they behave very well from an electrochemical point of view [18]. But, this kind of electrodes are not well suited for developing EIs because they are not intended for single use, and often before each use their surfaces must to be regenerated consuming time and reagents. Another disadvantage of conventional electrodes to be used as transducers in EIs is that these electrodes need an external reference electrode, and often a counter electrode, so the measurement step is not too practical [18]. Moreover, they require a quite large volume of sample for the measurement. In this context, screen-printed electrodes (SPEs) are much better suited as transducer in EIs. SPEs offer mass-production, low-cost fabrication and its miniaturized dimensions allow perform all immunological steps in a drop of few microliters of solution reducing the reagent and sample volume consumption. In addition, the decrease in the diffusion distances for the analytes to reach their surface-bound receptor partners allows shorter incubation periods and, thus, faster assays [32]. Moreover, since SPEs are disposable, they avoid others common problems of classical solid electrodes such as memory effects and

tedious cleaning processes [14]. The electrochemical instrumentation used with SPEs has been reduced to small pocket-size devices which make them applicable for both personal and professional use. Thus, these electrodes have successfully been employed in the development of analytical methodologies that respond to the growing need to perform rapid *in situ* analyses [25].

Table 1. Types of cancer and tumour-associated biomarkers [22,56,59,62]. PSA: prostate specific antigen; PAP: prostatic acid phosphatase; AFP: α-fetoprotein; hCG: human chorionic gonadotropin; CAGE-1: cancer antigen gene 1; CA: cancer antigen; CEA: carcinoembryonic antigen; SCC: squamous cell carcinoma; NSE: neuron specific enolase; BTA: bladder tumour associated antigen; FDP: fibrin degradation protein; NMP22: nuclear matrix protein 22; HA: hyaluronic acid; HAase: hyaluronidase; HER2: human epidermal growth factor receptor 2.

Cancer type	Biomarkers
Prostate	PSA, PAP
Testicular	AFP, β-hCG, CAGE-1, ESO-1
Ovarian	CA125, AFP, hCG, p53, CEA
Colon and pancreatic	CEA, CA19-9, CA24-2, p53
Lung	NY-ESO-1/ESO-1, CEA, CA19-9, SCC, CYFRA21-1, NSE
Melanoma	Tyrosinase, NY-ESO-1/ESO-1
Liver	AFP, CEA
Gastric carcinoma	CA72-4, CEA, CA19-9
Esophagus carcinoma	SCC
Trophoblastic	SCC, hCG
Bladder	BTA, BAT, FDP, NMP22, HA, HAase, BLCA-4, CYFRA21-1
Breast	CA15-3, CA125, CA27-29, CEA, BRCA1, BRCA2, MUC-1, NY-BR-1, ING-1, HER2/NEU
Leukaemia	BCR, ABL, PML, BCL1, BCL2, ETO

4. Cancer biomarkers detection

Cancer can be defined as an abnormal and uncontrolled growth and development of normal cells beyond their natural boundaries [21,55]. Cancer can take over 200 distinct forms including lung, prostate, breast, ovarian, skin, colon, hematologic and leukaemia cancer [55]. Environmental factors (e.g. tobacco smoke, alcohol, radiation and carcinogenic chemicals),

genetic factors (e.g. inherited mutations and autoimmune dysfunction) and bacterial (associated with stomach cancers) or viral infections (associated with cervical cancer) are associated with an increased risk of developing cancer [55-57]. In 2004, cancer killed 7.4 million people, and this number is estimated to reach 12 million by 2030 [58]. Early detection and treatment of cancer increase the chance of being cured of this disease.

Table 2. Normal levels for some of cancer biomarkers [62]. PSA: prostate specific antigen; hCG: human chorionic gonadotropin; AFP: α-fetoprotein; CEA: carcinoembryonic antigen; CA: cancer antigen.

Biomarker	Thresholds
tPSA	4 ng/mL
hCG	5.0 mIU/mL
AFP	10 ng/mL
CEA	3 ng/mL
CA125	35 U/mL
CA15-3	25 U/mL
CA27-29	36.4 U/mL
CA19-9	37 U/mL
CA242	20 U/mL
CA72-4	6 U/mL

Existing methods of screening cancer based on cell morphology using staining and microscopy that are invasive techniques that involve taking a biopsy and then examining the tissue to identify and detect cancer cells [56]. The analysis of biomarkers in blood, urine and other body fluids (their collection is non- or minimally invasive in comparison with biopsies) is other method applied in cancer diagnosis and staging, and in monitoring response to cancer therapy. The biomarkers can also be present in or on tumour cells but the isolation of proteins from fixed tissue samples is much more difficult than those of nucleic acids, so proteins which are expressed on the cell surface are analysed by immunohistochemical assays in the fixed tumour tissue [55,59]. Due to the fact that most cancer diseases are associated with the presence of more than one tumour marker (see **Table 1**), multi-marker profiles (presence and concentration level; **Table 2**) can be essential for the early diagnosis of disease onset and be associated with the stages of tumours [55,56,59]. Cancer biomarkers can be used in several ways (**Table 3**) [22,57,58,60,61] :

- Diagnostic biomarker can be used for screening healthy population or high-risk individuals and assist in early detection of the disease.
- Prognostic biomarkers allow for predicting the natural course of an individual cancer assessing the malignant potential of tumours; these biomarkers guide the decision of whom to treat and how aggressively to treat.
- Predictive biomarkers can be used to monitoring the course of cancer in a patient in remission or while receiving a treatment.
- Pharmacodynamic biomarkers measure the near-term treatment effects of a drug on the tumour or on the host, and can be used to guide dose selection in the early stages of clinical development of a new anticancer drug.

The first electrochemical immunosensor for tumor marker detection was reported in the late 1970s [64]. It was an amperometric sensor based on a competitive assay using catalase as label for hCG (human chorionic gonadotropin) detection. Thereafter, many immunosensors for cancer biomarkers have been reported in the literature [4,14,21,22,59]. Discussion of EIs based on SPEs for some of the major cancer biomarkers is presented below (**Table 4**).

Table 3. Selection of US Food and Drug Administration (FDA) approved cancer biomarkers [62,63]. AFP: *α*-fetoprotein; β-hCG: *β*-human chorionic gonadotropin; CA: cancer antigen; CEA: carcinoembryonic antigen; PSA: prostate specific antigen; HER2: human epidermal growth factor receptor 2; NMP22: nuclear matrix protein 22; FDP: fibrin degradation protein; BTA: bladder tumour associated antigen; IHC: immunohistochemistry; FISH: fluorescent *in-situ* hybridization.

Biomarker	Type	Source	Cancer type	Clinical use
AFP	Glycoprotein	Serum	Non-seminomatous testicular	Staging
β-hCG	Glycoprotein	Serum	Testicular	Staging
CA19-9	Carbohydrate	Serum	Pancreatic	Monitoring
CA125	Glycoprotein	Serum	Ovarian	Monitoring
CEA	Protein	Serum	Colon	Monitoring
tPSA	Protein	Serum	Prostate	Screening and monitoring
PSA complexed	Protein	Serum	Prostate	Screening and monitoring
fPSA (%)	Protein	Serum	Prostate	Benign prostatic hyperplasia versus cancer diagnosis
CA15-3	Glycoprotein	Serum	Breast	Monitoring
CA27-29	Glycoprotein	Serum	Breast	Monitoring
HER2/NEU	Protein (IHC)	Breast tumor	Breast	Prognosis and selection of therapy
HER2/NEU	Protein	Serum	Breast	Monitoring
HER2/NEU	DNA (FISH)	Breast tumor	Breast	Prognosis and selection of therapy
NMP22	Protein	Urine	Bladder	Screening and monitoring
Fibrin/FDP	Protein	Urine	Bladder	Monitoring
BTA	Protein	Urine	Bladder	Monitoring
High molecular weight CEA and mucin	Protein (Immunofluorescence)	Urine	Bladder	Monitoring

Table 4. Main characteristics of some EIs based on SPEs for cancer biomarkers. PSA: prostate specific antigen; IL-8: interleukin; CA: cancer antigen; CEA: carcinoembryonic antigen; HER2: human epidermal growth factor receptor 2; AFP: α-fetoprotein; SPCE: screen-printed carbon electrode; WE: working electrode; LOD: limit of detection; Ab: antibody LSV: linear sweep voltammetry; DPV: differential pulse voltammetry; CV: cyclic voltammetry; EIS: electrochemical impedance spectroscopy; SWV: square wave voltammetry; AuNPs: gold nanoparticles; AgNPs: silver nanoparticles; HRP: horseradish peroxidase; SAM: self-assembly monolayer; CNTs: carbon nanotubes; MWCNTs: multiwalled carbon nanotubes; 8; QD: quantum dots; PLA: proximity ligation assay; GOx: glucose oxidase; GO: graphene oxide; HER: hydrogen evolution reaction.

Biomarker	Methodology	Transduction technique	Sample	Concentration range	LOD	Ref.
tPSA, fPSA	Simultaneous determination in SPCE with two WEs nanostructured with AuNPs. Sandwich-type immunoassay. Ab immobilization by adsorption. Alkaline phosphatase as label.	LSV	Serum	tPSA: 1-10 ng/mL fPSA: 1-10 ng/mL	-	[65]
fPSA	Electroactive silver-mediated poly(amidoamine) dendrimer nanostructures as label. AuNPs nanostructured SPEs.	LSV	Serum	0.005-5.0 ng/mL	1.0 pg/mL	[66]
tPSA	Re-usable 8-channel SPCEs. Magnetic beads as support for a sandwich-type immunoassay using HRP as label.	Amperometry	Serum	5-100 ng/mL	1.86 ng/mL	[67]
tPSA	SPEs based on sheets of vegetable parchment. Graphene nanosheets and HRP-labelled detecting Ab functionalized with AuNPs.	LSV	Serum	2 pg/mL - 2 µg/mL	0.45 pg/mL	[68]
tPSA	Label-free. Ab immobilization by two ways tested: entrapment and affinity reaction by avidin-biotin affinity approach.	EIS	-	Entrapment: 1-10 ng/mL; Affinity: 1-10 pg/mL	Entrapment: 1 ng/mL; Affinity: 1 pg/mL	[69]
tPSA, IL-8	16 SPEs array. Detecting ab and HRP (label) loading onto MWCNTs.	CV	-	tPSA: 5-4000 pg/mL; IL-8: 8-1000 pg/mL	tPSA: < 5 pg/mL; IL-8: 8 pg/mL	[70]
tPSA	3D origami paper SPEs. MnO_2 nanowires electrodeposited on carbon working electrode with AuNPs layer. Sandwich-type immunoassay. GOx as label.	DPV	Serum	0.005-100 ng/mL	0.0012 ng/mL	[71]
CEA	Carbon nanoparticle/poly(ethylene imine) modified SPEs. Sandwich assay. Detecting Ab labelled with CdS nanocrystal QD sensitized.	SWV	Urine	0.032-10 ng/mL	32 pg/mL	[72]

Table 4 (Continued)

Biomarker	Methodology	Transduction technique	Sample	Concentration range	LOD	Ref.
CEA	Nanosilver-doped DNA polyion complex membrane as sensing interface on thionine/Nafion-modified SPCE. Sandwich assay. AuNPs conjugated with Ab-HRP.	DPV	Serum	0.03-32 ng/mL	10 pg/mL	[73]
CEA	PLA using assembling single-stranded DNA modified AuNPs on GO modified SPCE and tow DNA-labelled antibodies.	DPV	Serum	0.01-100 ng/mL	3.9 pg/mL	[74]
CA125	Label-free. SAM formation on AuNPs modified SPE.	EIS	Serum	0-100 U/mL	6.7 U/mL	[75]
CA15-3	Sandwich assay on graphene oxide modified SPCE using peroxidase-like magnetic silica nanoparticles/graphene oxide composite as label.	DPV	Serum	0.001-200 U/mL	0.28 mU/mL	[76]
CA19-9	Sandwich assay with detecting Ab functionalized with nanogold-encapsulated poly(amidoamine) dendrimer. Signal based on HER.	Amperometry	Serum	0.01-300 U/mL	6.3 U/mL	[77]
HER2	Label-free sensor using affibody immobilized on AuNPs modified SPE as bioreceptor.	EIS	Serum	0-40 ng/mL	6.0 ng/mL	[78]
HER2	Sandwich-type immunoassay on AuNPs nanostructured SPCE. Ab immobilization by adsorption. Alkaline phosphatase as label	LSV	Serum	15-100 ng/mL	4.4 ng/mL	[79]
AFP	Sandwich-type assay on gold SPEs. Invertase as label to catalysed sucrose to glucose. Re-usable immunosensor.	Personal glucose meter	Serum	0.5-50 ng/mL	0.18 ng/mL	[80]
CEA, AFP	Sandwich assay on AuNPs CNTs-chitosan modified SPCEs with two WE. GOx as label attached on silica nanospheres.	DPV	Serum	CEA: 5.0 pg/mL - 2.0 ng/mL; AFP: 5.0 pg/mL – 1.0 ng/mL	CEA: 3.2 pg/mL; AFP: 4.0 pg/mL	[81]
CEA, AFP	Sandwich assay on prussian blue and AuNPs modified SPCEs. Glucose oxidase as label attached on antibody and AuNPs modified CNTs.	DPV	Serum	CEA: 2.5 pg/mL - 2.0 ng/mL; AFP: 2.5 pg/mL - 2.5 ng/mL	CEA: 1.4 pg/m; AFP: 2.2 pg/mL	[82]
CEA, AFP	Sandwich assay on two WE SPCE. Streptavidin-functionalized AgNPs-modified CNT to link with biotinylated detecting Ab. Signal amplification by AgNP-promoted deposition of Ag using a silver enhancer solution.	LSV	Serum	CEA, AFP: 0.1 pg/mL - 5.0 ng/mL	CEA: 0.093 pg/mL; AFP: 0.061 pg/mL	[83]

Table 4 (Continued)

Biomarker	Methodology	Transduction technique	Sample	Concentration range	LOD	Ref.
CA125, CA19-9	Simultaneous detection based on competitive assay using SPCE with two WEs. Cellulose acetate membrane to immobilize thionine as mediator. HRP as label.	DPV	Serum	CA125: 0-25 U/mL; CA19-9: 0-24 U/mL	CA125: 0.4 U/mL; CA19-9: 0.2U/mL	[84]
CA15-3, CA125, CEA	Simultaneous determination in SPCE with three WEs nanostructured with AuNPs. Sandwich-type immunoassay. Alkaline phosphatase labelled antibody functionalized Au cluster with graphene for detection.	LSV	Serum	CA15-3: 0.005-50 U/mL; CA125: 0.001-100 U/mL; CEA: 0.004-200 ng/mL	CA15-3: 1.5 mU/mL; CA125: 0.34 mU/mL; CEA: 1.2 pg/mL	[85]
CA15-3, CA125, CEA	Simultaneous detection based sandwich-type assay on graphene modified SPCEs with three WE. Platinum nanoparticles as label.	DPV	Serum	CA15-3: 0.008-24 U/mL; CA125: 0.05-20 U/mL; CEA: 0.02 -20 ng/mL	CA15-3: 1 mU/mL; CA125: 2 mU/mL; CEA: 7 pg/mL	[86]
CEA, AFP, CA125, CA15-3	Paper-based device with 8 WE. Sandwich-type assay. Radical polymerization as signal amplification.	DPV	-	CEA: 0.01-100 ng/mL; AFP: 0.01-100 ng/mL; CA125: 0.05-100 ng/mL; CA15-3: 0.05-100 ng/mL	CEA: 0.01 ng/mL; AFP: 0.01 ng/mL; CA125: 0.05 ng/mL; CA15-3: 0.05 ng/mL	[87]
CA15-3, CA125, CA19-9, CEA	AuNPs with HRP-labelled antibodies immobilized by biopolymer/sol-gel on SPCEs with 4 WE. Formation of HRP-Ab/antigen complex blocked electron transfer decreasing the signal.	DPV	Serum	CA15-3: 0.4-140 U/mL; CA125: 0.5-330 U/mL; CA19-9:0.8-190 U/mL; CEA: 0.1-44 ng/mL	CA15-3: 0.2 U/mL; CA125: 0.5 U/mL; CA19-9:0.3 U/mL; CEA: 0.1 ng/mL	[88]

4.1. Prostate specific antigen (PSA)

Prostate specific antigen (PSA) is a serine protease belonging to the human kallikrein family [89,90]. It is synthesized specifically in the epithelial cells of the prostate gland and its expression therein is regulated by the androgen receptor. Due to its high tissue specificity, PSA is one of (if not the) most widely used tumor marker [22]. It is used extensively as a biomarker to screen and diagnose prostate cancer, to detect recurrence after definite therapy

and to follow response to treatment in the metastatic disease setting [89]. The normal reference range for PSA is 0-4 ng/mL, but benign conditions such as benign prostatic hypertrophy, acute prostatitis and infarction may be correlated with elevated PSA levels [22]. This is the main drawback of PSA as biomarker, the lack of specificity in distinguishing prostate cancer from non-malignant prostate disease. PSA has two forms in human serum: free PSA (fPSA) and PSA complexed, being the predominant one the complex with α-1-antichymotrypsin (PSA-ACT) [90]. Total PSA (tPSA) refers to the sum of fPSA and PSA complexed, and it is used to determine some cut off. A value of tPSA above 10.0 ng/mL is regarded as positive and indicates high probability of prostate cancer; a value below 4.0 ng/mL is considered negative and indicates low probability of prostate cancer. Between 4.0 and 10.0 ng/mL the result is in the so-called "grey zone" [65,67]. fPSA determination is performed when the value of tPSA is in the grey zone to distinguish prostate cancer from other causes of PSA elevation considering that men with prostate cancer have elevated levels of PSA complexed and low levels of fPSA [22,91].

In 2009, a dual sensor for fPSA and tPSA using disposable commercial SPEs containing two working carbon electrodes was developed [65]. Specific antibodies for tPSA and fPSA were immobilized by physical adsorption in each working electrode previously nanostructured with gold nanoparticles (AuNPs) generated *in situ*. The immunosensor was based in a sandwich-type immunoassay performed step by step taking 3 h. The enzyme alkaline phosphatase (AP) was used as label and a mixture of 3-indoxyl phosphate disodium salt (3-IP) and silver nitrate as substrate [92]. AP hydrolyses 3-IP resulting an indoxyl intermediate which reduces the silver ions to give metallic silver (Ag^0) and indigo blue. Thus, the silver enzymatically is deposited on the electrode surface and can be detected through the redissolution peak when an anodic stripping scan is carried out. Since the enzymatic product is metallic silver that is deposited on the electrode surface, no cross talk between electrodes is produced and it is possible to use the same label for the detection of both analytes. This bi-sensor showed a linear range very suitable for PSA detection in real samples; it is able to detect fPSA and tPSA in the linear range 1-10 ng/mL. More recently, Pei *et al*. [66] developed an immunosensor for fPSA based on a sandwich-type immunoassay using SPEs nanostructured with AuNPs as transducer and a signal amplification by electroactive silver-mediated poly(amidoamine) dendrimer nanostructures for detection. In this case the assay takes 25 min and enzymes are not necessary since the silver nanoparticles can directly catalyse the reduction of H_2O_2 without the participation of bioactive enzymes. Using linear sweep voltammetry as technique for measure the analytical signal, a wide quantification range between 0.005 and 5 ng/mL was achieved. Using sheets of

vegetable parchment, Yan *et al*. [68] fabricated stable and inexpensive carbon SPEs (SPCEs) for developing a sandwich-type immunosensor for the detection of tPSA. Using graphene nanosheets for coating the SPEs and HRP-labelled detecting antibody functionalized with AuNPs, an immunosensor with a quantification range of 2 pg/mL - 2 µg/mL was achieved. This wide linear range is possible since the graphene nanosheets increase the conductivity and the AuNPs provide a large surface area for the immobilization of the HRP-labelled detection antibody HRP-labelled and also enhance the electroreduction between HRP and H_2O_2 amplifying the analytical signal. The use of sheets of vegetable parchment for fabricating SPEs decreases the cost of the final sensor and, since the vegetable parchment is flammable, allow the easy and safe disposability of the immunosensor by incineration.

4.2. Carcinoembryonic Antigen (CEA)

Carcinoembryonic antigen (CEA), described in 1965, is a glycoprotein belonging to the immunoglobulin family [21]. It was among the first identified tumour antigens and is found in many carcinomas such as colon, lung, ovarian and breast cancer (**Table 1**) [14,72]. The clinical value of CEA detection is limited by a high false positive rate in healthy populations and by low diagnostic sensitivity and specificity, so clinical decisions regarding disease management is not based only on CEA levels [21,22]. For example, since CEA is metabolized in the liver, damage therein can elevate the CEA levels in the circulation and lead to false positive results. Moreover, CEA levels can be elevated in some patients after radiation and chemotherapy [22]. Despite these limitations, CEA is used as marker to monitor cancer recurrence after surgery and to follow patients during therapy [72].

Wu *et al*. [73] developed an immunosensor for CEA detection using a nanosilver-doped DNA polyion complex membrane (PIC) on the surface of the SPCEs as sensing interface. To construct this membrane, double-stranded DNA was assembled onto the surface of thionine/Nafion-modified SPCE to adsorb silver ions with positive charges and then, the silver ions were reduced to silver nanoparticles by $NaBH_4$. The capture antibody was immobilized on this surface in order to perform a sandwich-type assay using AuNPs conjugated with HRP-labelled antibody for the detection of CEA. The assay was performed in two steps taking 44 min. The use of nanosilver-doped DNA PIC membrane as immunosensing probe and HRP-anti-CEA-labelled AuNPs for signal amplification allowed to obtain a low LOD value of 10 pg/mL and a linear range of 0.03-32 ng/mL. Recently, a wider quantification range for CEA was achieved using an immunosensor based on a proximity ligation assay (PLA) [74]. The analytical signal of this sensor consisted in the electrochemical stripping of silver regulated by proximity

hybridization of single-stranded DNA. The device was prepared by assembling single-stranded DNA modified with AuNPs (ssDNA@AuNPs) on graphene oxide modified SPCE. In presence of the antigen and two DNA-labelled antibodies, the proximate complex is formed and can hybridize with the DNA assembled on the SPCE taking away the AuNPs. Thus, the silver deposition catalysed by the AuNPs decreases, and therefore the silver anodic stripping signal (**Figure 4**). The homogeneous proximity ligation and the hybridization of the product with the immobilized ssDNA were completed in a single step (40 min). With this strategy, a quantification range of four orders of magnitude for CEA detection was achieved (0.01 to 100 ng/mL).

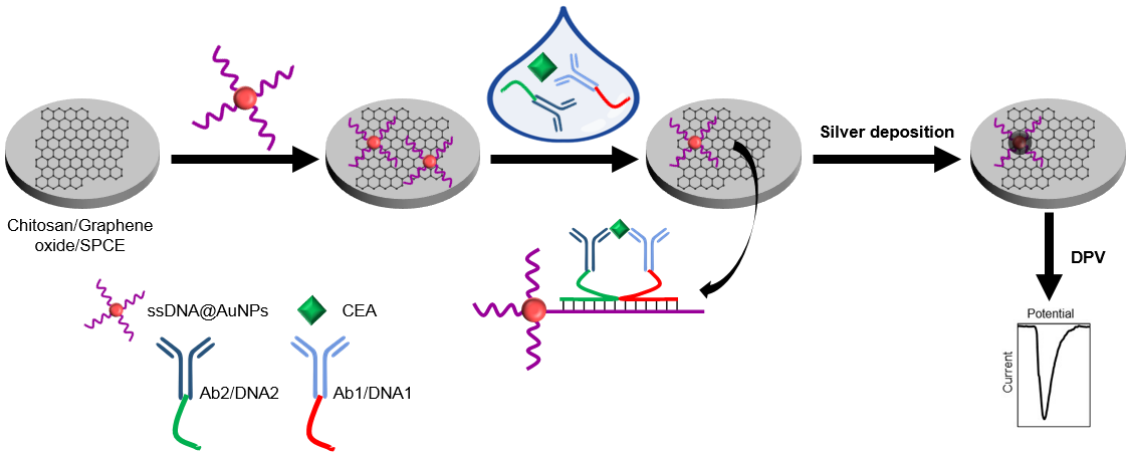

Fig. 4. Scheme of the immunosensor for CEA detection using a proximity ligation assay developed by Li *et al*. [74].

4.3. Other cancer biomarkers

Carbohydrate antigens, also called cancer antigens, are mainly produced in cancer cells, but rarely produced in normal tissues or benign lesions of tissues. The cancer antigens commonly detected are CA125, CA15-3, CA19-9, etc. (**Table 2**) [4,21,93]. Among them, CA125 is a high molecular weight protein most commonly associated with ovarian cancer but it is also linked to uterus, cervix, pancreas, liver, colon, breast, lung and digestive cancer [55,94]. CA125 has a very low sensitivity for early stage ovarian cancer since in Stage 1, 50% of patients have normal CA125 levels [55,95]. Moreover, several non-pathological conditions such as menstruation and pregnancy can increase levels of CA125 in healthy individuals [94]. But,

more than 90% of women have high levels of CA125 when the ovarian cancer is advanced, so CA125 is a valuable biomarker not only for cancer diagnosis, but also for monitoring cancer progression and treatment [14,55,95]. Normal blood levels are usually less than 35 U/mL: CA125 levels above this value is found in 1% of healthy population, 6% of patients with benign disease, 28% of patients with non-gynaecological malignancy and 82% of individuals with ovarian cancer [14,95].

CA15-3 is also an important carbohydrate antigen analysed in breast cancer patients (**Table 2**). It is overexpressed on the external layer of malignant glandular cells such as those seen in breast cancer [22,96]. In patients with breast cancer, CA15-3 levels increase by 10% in Stage 1, 20% in Stage 2, 40% in Stage 3 and 75% in Stage 4 of breast cancer [55]. But the diagnostic value of CA15-3 is relatively low because of an intrinsic lack of both sensitivity and specificity since high CA15-3 levels can be detected also in presence of other kinds of cancer disease such as gastric or ovarian cancers or even in presence of hepatic cirrhosis, hepatitis or hypothyroidism [96,97]. So, CA15-3 is used clinically most often to monitor patient therapy and it is considered along with tumor size, cancer stage and negative risk factors in determining treatment protocols [55]. Of note, CA27-29 is a slightly more sensitive breast cancer biomarker than CA15-3, so the US Food and Drug Administration (FDA) has approved both cancer antigens for monitoring therapy in breast cancer [22]. HER2/NEU protein belongs to the epidermal growth factor receptor (EGFR) family. This protein is amplified and/or overexpressed in approximately 20-30% of breast cancers [2]. Rising serum levels of HER2/NEU has been associated with progressive metastatic disease and poor response to therapies. In fact, HER2/NEU overexpression has been related with a poor rate of disease-free survival [21].

Taking into account that determining the concentration of a single biomarker is almost never enough, the possibility of determining several cancer biomarker simultaneously is very interesting since it can provide more information about the diagnosis or evolution of the disease. Wu *et al*. [84] developed a multiplex immunosensor to determine CA125 and CA19-9 based on a direct competitive assay using a SPCE with two working electrodes. A cellulose acetate membrane was used to co-immobilize thionine as mediator and the two antigen on the surface of each working electrode. With two simultaneous direct competitive immunoreactions (1 h) the corresponding HRP labelled antibodies were captured on the respective electrode surface on which the immobilized thionine shuttled electrons between HRP and the electrode for enzymatic reduction of H2O2 to produce detectable signals. The use of thionine as mediator that is immobilized on the electrodes instead of added to the

detection solution avoids the electrochemical "cross-talk" between the working electrodes. With this device LOD of 0.4 U/mL and 0.2 U/mL for CA125 and CA19-9 respectively were achieved (**Table 4**). More recently, Cui *et al*. [86] constructed a multiplex immunosensor for CA125, CA15-3 and CEA detection using platinum nanoparticles as label. The device is based on graphene modified SPCEs with three working electrodes where sandwich-type immunoassays (performed in two steps of 1 h) were carried out using mesoporous platinum nanoparticles labelled antibodies detection to catalyze the electro-reduction of H_2O_2 obtaining negligible cross-talk (LOD of 1 mU/mL, 2 mU/mL and 7 pg/mL for CA15-3, CA125 and CEA respectively). Another interesting work about multiplexed cancer biomarker detection is the device developed by Wu *et al*. [87] for CEA, AFP, CA125 and CA15-3 detection. They designed a paper-based electrochemical immunodevice with 8 carbon working electrodes screen-printed sharing the same Ag/AgCl reference and carbon counter electrodes. A sandwich-type assay was carried out on the graphene modified working electrodes. A radical polymerization reaction was used as signal amplification strategy: the antibodies detection were coupled with an initiator of the polymerization (*N*-hydroxysuccinmidyl bromoisobutyrate) and once the immunoassay is over, the polymerization is performed and then, the HRP solution was dropped onto each working electrode prior to electrochemical detection. Although the sensor is very promising since it is based on paper device and achieved a wide linear range (**Table 4**), it is a laborious and very long-time assay (only HRP dropping takes 10 h). In the context of portable devices development, Zhu *et al*. [80] developed an immunosensor based on gold SPEs for AFP detection using a personal glucose meter as signal transducer. The sensor was based on a sandwich-type assay in which the detecting antibody was labelled with the enzyme invertase. Once the reaction antibody-antigen was over, sucrose was added. Thus, in presence of invertase, the sucrose is catalyzed to generate glucose and fructose, and the glucose generated is detected using the personal glucose meter. Moreover, the immunosensor can be re-usable after a regeneration step using a glycine-HCl buffer solution in order to break the antibody-antigen binding. Others similar devices using personal glucose-meter (and magnetics beads) can be found in the literature for CEA and PSA detection [98,99].

5. Cardiovascular biomarkers

Cardiovascular diseases (CVDs) are the most prevalent cause of human death in both developing and developed countries [100]. According to the World Health Organization

(WHO), an estimated 17.5 million (31%) of all global deaths in 2012 are related to CVDs (WHO, http://www.who.int/). CVDs are a group of disorders of the heart and blood vessels including: coronary heart disease, cerebrovascular disease, peripheral arterial disease, rheumatic heart disease, congenital heart disease, deep vein thrombosis and pulmonary embolism. CVDs can be caused by a quite diverse factors including genetic, age, gender and hypertension, cholesterol, diabetes, obesity and overweight, smoking and stress [15,101]. Early and quick diagnosis of CVDs is crucial not only for patient survival but also for saving a great deal of cost and time in patient treatment [102].

Myocardial infarction (MI), which is defined as the necrosis of cardiac myocytes following prolonged ischemia, is one of the most immediately life threatening forms of acute coronary syndrome (ACS) [33]. The diagnosis of AMI has been based on the WHO criteria, whereby must meet at least two of the three conditions: characteristic chest pain, diagnosis electrocardiogram (ECG) changes and elevation of the biochemical markers in their blood [102]. Although EGG is an important management tool for guiding therapy [103,104], it is a poor diagnostic test for ACS since about half of the ACS-related patients admissions in hospitals demonstrate normal or ambiguous ECG readings [102,105]. Therefore, the assessment of cardiac marker elevation is critical to make a truly informed decision on a suitable treatment [15]. The levels of such markers can give information about the type of ACS, the time of first incidence of the attack and, for certain markers, the location of the damaged cells (**Figure 5**) [33].

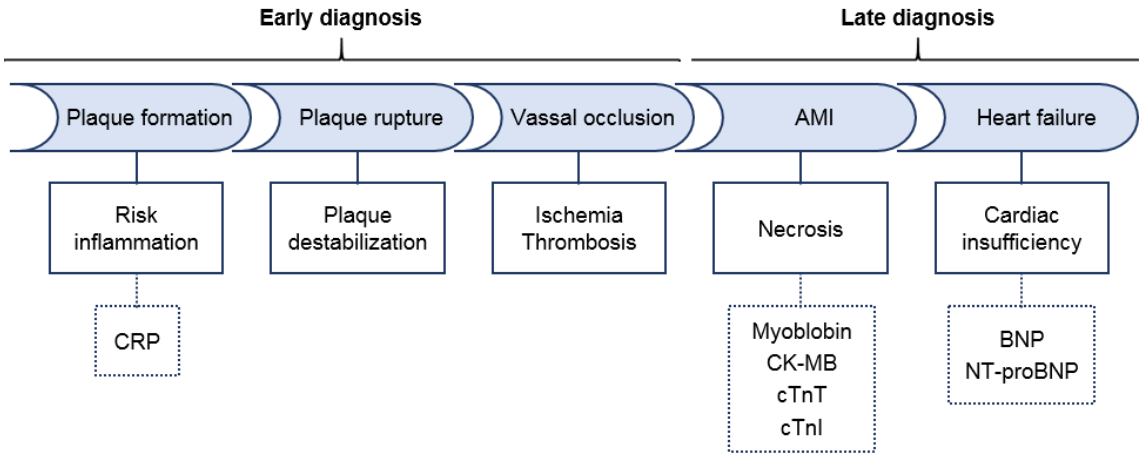

Fig. 5. Most frequently studied biomarkers in relation to the different mechanism involved in ACS. Adapted from [15,106].

The three main biomarkers for the diagnosis of AMI are: cardiac troponins (cardiac troponin T, cTnT, and cardiac troponin I, cTnI), creatine kinase MB (CK-MB) and myoglobin. Official organisms such as the European Society of Cardiology (ESC), the American Heart Association (AHA) or the International Federation of Clinical Chemistry (IFCC) define the biochemical criteria for detecting myocardial necrosis either as: (I) "a maximal concentration of cTnI or cTnT exceeding the 99th percentile of a reference control group on at least one occasion during the first 24 hours" or as (II) " a maximal value of CK-MB exceeding the 99th percentile of a reference control group on two successive samples, or a maximal value exceeding twice the upper limit of normal for the specific institution on one occasion during the first 24 hours" [106]. Cardiac troponins have been suggested by the guidelines as the preferred markers, with CK-MB as an acceptable alternative when troponins are not available. Due to their high sensitivity and specificity, human cardiac troponins are known as the "gold standard" for diagnosis and prognosis of AMI [23]. Cardiac troponins consist of a complex of troponin C (cTnC), I (cTnI) and T (cTnT) regulating the contraction of striated and cardiac muscle [107]. The complex dissociates with time in blood into free cTnT and I/C complex. Both cTnT and cTnI are recommended as the markers of choice because cTnC is unspecific [108]. Like CK-MB, cTnT and cTnI cannot be used as early markers because they show a similar early release kinetic following AMI in that it takes several hours for both of them to be released into circulation before being detectable [102]. However, cardiac troponins are the most specific cardiac biomarkers, and offer the widest temporal diagnostic window since their levels remain abnormal for 4-10 days after the onset of AMI with the peak concentration closely related to the infarct size [15,23]. Their cut-off levels range from 0.01 to 0.1 ng/mL for cTnI and from 0.05 to 0.1 ng/mL for cTnT [15,33,100].

Creatinine kinase (CK) is a dimeric molecule composed of two subunits (M and B) which exists in three molecular forms: MM, MB and BB. When the heart muscle dies during MI, one of the more abundant molecules released into the circulation is CK, but among the three isoenzyme forms, CK-MB offers better sensitivity and specificity compared with total CK as marker of myocardial damage. However, CK-MB diagnostic specificity is compromised when skeletal muscle is involved, such as in the case of trauma, cardiac surgery or extreme exercise. CK-MB cannot be used as an early marker because its narrow window: once released into the blood stream, CK-MB doubles its concentration within 5-6 hours after the onset of chest pain and exhibits peaks in 12-24 hours. But it can be useful for diagnosis of re-infarction and, therefore, in the evaluation of AMI. CK-MB cut-off level is defined at 10 ng/mL [15,100,102,106].

Table 5. Main characteristics of some CVDs biomarkers [15,23,31,33,100,111]. cTnI: cardiac troponin I; cTnT: cardiac troponin T; CK-MB: creatine kinase MB; CRP: C-reactive protein; BNP: B-type natriuretic peptide; NT-proBNP: N-terminal pro-B-type natriuretic peptide; HFABP: heart type fatty acid protein.

Biomarker	CVD indicator type	MW (kDa)	Cut-off levels (ng/mL)	Specificity level	Initial elevation (h)	Time to peak (h)	Duration of elevation
cTnI	Detection of AMI	23.5	0.01-0.1	High	4-6	12-24	4-8 days
cTnT	Detection of AMI	37	0.05-0.1	High	3-6	12-24	7-14 days
Myoglobin	Early detection of AMI	18	70-200	Low	1-3	6-12	12-48 hours
CK-MB	Early detection of AMI	85	10	Medium	4-6	12-24	3-4 days
CRP	Early detection of inflammation. Cardiac risk factor	125	$<10^3$, low risk; $1x10^3$-$3x10^3$, intermediate risk; $>3x10^3$-$15x10^3$, high risk (no definitive)	Medium	4-6	12-24	3-4 days
BNP	Acute coronary syndromes. Diagnosis of heart failure. Ventricular overload	3.4	-	High	No clinical consensus	No clinical consensus	No clinical consensus
NT-proBNP	Acute coronary syndromes. Diagnosis of heart failure. Ventricular overload	8.5	0.25-2	High	No clinical consensus	No clinical consensus	No clinical consensus
HFABP	Early detection of AMI	15	6	Low	1-3	6-10	18-36 hours

Myoglobin is a non-enzymatic protein useful in the diagnosis of AMI. Because of its small size (17.8 kDa), it is quickly released into circulation (1 hour) upon symptom onset with high sensitivity and high negative predictive value. However, myoglobin shows low clinical specificity because of its abundant presence not only in myocardial but also in skeletal muscle cells. So, injury in skeletal muscle can also increases the concentration of myoglobin. The cut-off level for myoglobin is defined in the range 70-200 ng/mL [15,23,102].

Several other cardiac biomarkers [106] have emerged such as C-reactive protein (CRP) which is an inflammatory marker and it has been the most frequently used single biomarker

for CVD risk [100]. This protein is indicator of a viral and bacterial infection, however whose level can increase due to the inflammation induced by infection or injury often leading to a heart attack or stroke. The CRP level is usually less than 2 mg/L for healthy individuals, and when it is higher than 3 mg/L the person is considered at high risk of developing CVD [15,23,33,109]. B-type natriuretic peptide (BNP) and its precursor, N-terminal pro-BNP (NT-proBNP), are neurohormones synthesized primarily in arterial or ventricular myocardium, and both have shown a significant value in diagnosis and prognosis of cardiac disease [102]. Other marker to consider is the heart type fatty acid protein (HFABP), which is a stable and small protein abundantly found in the cytoplasm of myocardial cells. It is not found in the circulation under non-pathological conditions, but it is rapidly released after AMI. Thus, HFABP show potential as sensitive biomarker for early detection of AMI as well as prognosis utility in risk stratification of ACS [15,106,110]. **Table 5** summarizes some of the main characteristics of most of the cardiac biomarkers.

5.1. EIs based on SPEs for cardiac biomarkers

During last years, many different biosensing devices have been reported for the detection of CVD biomarkers, and there are several recent reviews about sensors developed with these aim [15,31,33,100,112]. This section is focused on EIs based on SPEs for CVD biomarkers.

For cTnT detection, Silva *et al*. [113] developed an immunosensor using a conducting carbon silver-epoxy composite SPEs. The rigid conducting carbon polymer composite showed to be compatible to integrate streptavidin microspheres through glutaraldehyde allowing a stable immobilization of biotinylated capture antibody on the electrode surface. Using a sandwich-type assay and an anti-cTnT antibody labelled with HRP to perform the peroxidase reaction using H_2O_2 as enzyme substrate, a LOD of 0.2 ng/mL was achieved. More recently, the same author achieved a lower LOD for cTnT developing a label-free immunosensor based on amine-functionalized CNTs-SPE [114]. This device was fabricated by tightly squeezing an adhesive carbon ink containing CNTs onto a polyethylene terephthalate substrate forming a thin film. The antibody-antigen interactions at CNT-SPE surface were monitored by DPV measurements; the difference between the peak current in presence or absence of cTnT was used as analytical signal (**Figure 6**). The amine-functionalized CNTs incorporated into the carbon ink enabled stable measurement and oriented capture Ab immobilization, and moreover improve the electro-transfer reactions and increase the electrode surface area. The

LOD achieved by this label-free device was 0.0035 ng/mL This LOD is lower than this for the immunosensor previously indicated that needed a label for cTnT detection (HRP enzyme).

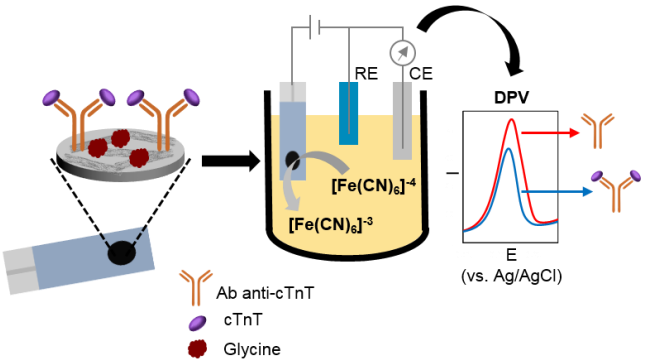

Fig. 6. Scheme of the immunosensor and the electrochemical principle of detection developed by Silva *et al*. [114].

For myoglobin determination there are few EIs based on SPEs. O'Regan *et al*. [115] developed an amperometric immunosensor for the detection of myoglobin in whole blood. It consisted on a one-step indirect sandwich-type assay using a secondary antibody labelled with alkaline phosphatase and immobilising the capture antibody by adsorption on the SPCE. The current response was measured by amperometry upon the addition of *p*-aminophenylphosphate. The quantification range achieved for myoglobin in spiked whole blood samples was 85-925 ng/mL. The simultaneous incubation of myoglobin in whole blood with the two detecting antibodies allowed to perform the assay in a shorter time than if the assay were performed step by step, maintaining the sensitivity of the sandwich assay. A wider quantification range was achieved by a label-free immunosensor developed by Suprun *et al*. [116]. It was based on the use of AuNPs as electrocatalysts of Fe(III)/Fe(II) electrode reaction of myoglobin. For fabricating this label-free immunosensor, the SPEs were modified with AuNPs/didodecyldimetrhylammonium bromide and the capture antibody. Once the experimental conditions were optimized, the square wave voltammetric cathodic peak of cardiac myoglobin reduction measurements gives a quantification concentration range of 10-1780 ng/mL. This sensor allows direct measurement of binding events without amplification stages or cover layers of labelled antibodies, needs small sample volumes (1-2 µL) and express detection in 30 min.

Table 6. Main characteristics of some EIs based on SPEs for CVD. cTnI: cardiac troponin I; cTnT: cardiac troponin T; CRP: C-reactive protein; HFABP: heart type fatty acid protein; MWCNTs: multiwalled carbon nanotubes; CNTs: carbon nanotubes; HRP: horseradish peroxidase; Ab: antibody; AP: alkaline phosphatase; AuNPs: gold nanoparticles; QD: quantum dots DPV: differential pulse voltammetry; ASV: anodic stripping voltammetry; SWV: square wave voltammetry.

Biomarker	Methodology	Transduction technique	Sample	Concentration range	LOD	Ref.
cTnT	Sandwich-type assay on graphite-epoxy silver SPE. Immobilization of capture Ab by integrated streptavidin microspheres	Amperometry	Serum	0.1-10 ng/mL	0.2 ng/mL	[113]
cTnT	Sandwich-type assay on SPCE modified with amino-functionalized MWCNTs. HRP as label.	Amperometry	Serum	0.02-0.32 ng/mL	0.016 ng/mL	[119]
cTnT	Label-free immunosensor based on amine-functionalised CNT-SPEs platforms.	DPV	Serum	0.0025-0.5 ng/mL	0.0035 ng/mL	[114]
cTnI	Sandwich-type assay using AP labelled detection Ab. Capture Ab immobilized by adsorption.	Amperometry	Blood	2-100 ng/mL	1-2 ng/mL	[120]
Myoglobin	One-step indirect sandwich-type assay using AP as label- Capture Ab immobilized by adsorption.	Amperometry	Whole blood	85-925 ng/mL	-	[115]
Myoglobin	Label-free immunosensor based using AuNPs as electrocatalysts of Fe(III)/Fe(II) electrode reaction of myoglobin.	SWV	Plasma	10-1780 ng/mL	10 ng/mL	[116]
CRP	HRP-labelled antibody functionalized Fe_3O_4@Au magnetic nanoparticles attracted to a Fe(III) phthalocyanine/chitosan membrane modified SPCE by an external magnetic field. After incubation, activity centre of HRP decreases linearly with CRP concentration. Reusable SPCEs.	Amperometry	Serum	1.2-200 ng/mL	0.5 ng/mL	[117]
CRP	Sandwich-type assay on bismuth citrate-modified SPE. Quantification through acidic dissolution of PbS QDs and ASV detection of Pb(II).	ASV	Serum	0.2-100 ng/mL	0.05 ng/mL	[118]
HFABP	Sandwich-type assay using AP labelled detection Ab. Capture Ab immobilized by adsorption on SPE.	Amperometry	Whole blood	4-250 ng/mL	4 ng/mL	[121]

Related to CRP, Gan *et al*. [117] developed an amperometric immunosensor for CRP determination in human serum. HRP-labelled anti-CRP antibody functionalized Fe_3O_4@Au magnetic nanoparticles were attracted to a Fe(III) phthalocyanine (FePc)/chitosan membrane-

modified SPCE by an external magnetic field. After the incubation of the sensor with CRP, the access of the activity center of the HRP to the electrode was partially inhibited leading to a linear decrease in the catalytic efficiency of the HRP to the reduction of immobilized FePc by H_2O_2 in the CRP concentration range from 1.2 to 200 ng/mL with a LOD of 0.5 ng/mL. Moreover, the SPCE was reusable since the magnetic nanoparticles can be washed from the electrode removing the magnet, which make the basal electrode renewable for next determination by adding new modified nanoparticles on its surface. Recently, a lower LOD was achieved using an immunosensor based on bismuth citrate-modified graphite SPE [118]. This device was based on a sandwich-type assay immobilizing the capture antibody by adsorption on the surface of the electrode, using a biotinylated detection antibody and streptavidin-conjugated PbS quantum dots. The assay was performed step by step and took nearly 3 h. The quantification of CRP was performed through acidic dissolution of the PbS QDs and anodic stripping voltammetric detection of Pb(II) released at the bismuth precursor modified transducer. Under optimal conditions, the linear range of concentrations showed by the sensor was 0.2-100 ng/mL and the LOD was 0.05 ng/ml.

In **Table 6** the main characteristics of EIs based on SPEs for the detection of cardiovascular diseases markers are summarized.

6. Conclusions

EIs are one of the most widely used analytical techniques in the quantitative detection of biomarkers diseases due to the specific binding of antibody to its corresponding antigen. Unlike spectroscopic and chromatographic instruments, electrochemical sensors can be easily adapted for detecting a wide range of analytes while remaining inexpensive. Since SPEs show advantages such as miniaturization, mass production, customization, portability and low cost, the replacement of conventional electrodes by SPEs is making possible to explore other options in the development of EIs. Taking this into account, this review summarizes researches on biomarkers used for detecting cancer and cardiovascular diseases and on the EIs based on SPEs developed for determinate these biomarkers.

The sensitivity of biomarkers is important for detection of diseases. Thus, the choice of the antibody immobilization is a crucial step because antibody acts as the recognition element for antibody-antigen reaction, and the performance of the detection of antigen binding capacity can be improved using a proper antibody surface. Moreover, the use of nanomaterials for electrode surface modification, for signal amplification or for use as label,

allows the improvement of the sensitivity. In addition, the great versatility of design of the SPEs offers multiplexing capability for simultaneous measurements of biomarkers.

Nonetheless, relevant and not yet totally controlled aspects such as storage and stability of EIs developed has to be improved for their use as clinical diagnosis routine tool. In one hand, the storage and transportation conditions of biosensors play an important role in their functionality and shelf life: environmental factors such as humidity, temperature and air exposure all offer potential obstacles in the functionality of biomaterials. In the other hand, the stability of proteins on the immunosensor is crucial to the feasibility of any commercialization prospects; low stability breaks the business viability of any biosensor product. Another challenge EIs must face for their consideration as a reliable option for diagnosis or monitoring of diseases is their validation using real samples. Many times the validation of the EIs developed in the bibliography is limited to doped samples (blood, serum, urine, ...). Other times, although the samples used are real patient samples, the number of samples tested is not enough to assure a reliable validation of the immunosensor. In addition, this validation must be performed not only in terms of sensibility, selectivity and accuracy, but also of rapidity, simplicity and cost with respect to other competitive methodologies existing. Moreover, since a POC test is desirable to encapsulate all the required instrumentation in a suitable portable format, additional research efforts are needed toward the full integration of EIs in automated and miniaturized systems in order to achieved EI-based POC systems. Therefore, further efforts in immunosensor stability and validation together with continuous miniaturization and automatization of EIs are the key to the success of the use of EIs in POC testing for making clinical results available at patient bedside or physician office.

Acknowledgement

This work has been supported by the FC-15-GRUPIN-021 project from the Asturias Regional Government.

References

[1] Biomarkers definitons working group, *Clin. Pharmacol. Ther.* 2001, 69, 89.

[2] M. Yang, X. Yi, J. Wang, F. Zhou, *Analyst* 2014, 139, 1814.

[3] R. S. Vasan, *Circulation* 2006, 113, 2335.

[4] J. Li, S. Li, C. F. Yang, *Electroanalysis* 2012, 24, 2213.

[5] E. Aguilera-Herrador, M. Cruz-Vera, M. Valcárcel, *Analyst* 2010, 135, 2220.

[6] E. Schleicher, *Anal. Bioanal. Chem.* 2006 384 124.

[7] G. J. Kost, N. K. Tran, *Cardiol. Clin.* 2005, 23, 467.

[8] A. Warsinke, *Anal. Bioanal. Chem.* 2009, 393, 1393.

[9] E. Petryayeva, W. R. Algar, *RSC Adv.* 2015, 5, 22256.

[10] P. Von Lode, *Clin. Biochem.* 2005, 38, 591.

[11] Y. Wan, Y. Su, X. Zhu, G. Liu, C. Fan, *Biosens. Bioelectron.* 2013, 47 1

[12] K. K. Mistry, K. Layek, A. Mahapatra, C. RoyChaudhuri, H. Saha, *Analyst* 2014, 139, 2289.

[13] R. A. S. Couto, J. L. F. C. Lima, M. B. Quinaz, *Talanta* 2016, 146, 801.

[14] Z. Taleat, A. Khoshroo, M. Mazloum-Ardakani, *Microchim. Acta* 2014, 181, 865.

[15] M. Pedrero, S. Campuzano, J. M. Pingarrón, *Electroanalysis* 2014, 26, 1132.

[16] M. D. González, M. B. González-Garcia, A. C. García, *Electroanalysis* 2005, 17, 1901.

[17] J. Tang, D. Tang, *Microchim. Acta* 2015, 182, 2077.

[18] F. Ricci, G. Adornetto, G. Palleschi, *Electrochim. Acta* 2012, 84, 74.

[19] C. K. Dixit, K. Kadimisetty, B. A. Otieno, C. Tang, S. Malla, C. E. Krause, J. F. Rusling, *Analyst* 2015, 141, 536.

[20] B. V. Chikkaveeraiah, A. A. Bhirde, N. Y. Morgan, H. S. Eden, X. Chen, *ACS Nano*, 2012, 6, 6546.

[21] I. Diaconu, C. Cristea, V. Hârceagă, G. Marrazza, I. Berindan-Neagoe, R. Săndulescu, *Clin. Chim. Acta* 2013, 425, 128.

[22] N. J. Ronkainen, S. L. Okon, *Materials* 2014, 7, 4669.

[23] E. Burcu Bahadir, M. Kemal Sezgintürk, *Talanta* 2015, 132, 162.

[24] M. Tudorache, C. Bala, *Anal. Bioanal. Chem*, 2007, 388, 565.

[25] O. D. Renedo, M. a Alonso-Lomillo, M. J. A. Martínez, *Talanta* 2007, 73, 202.

[26] L. C. Clark, C. Lyons, *Ann. N. Y. Acad. Sci.* 1962, 102, 29.

[27] K. Cammann, *Fresenius' Zeitschrift für Anal. Chemie* 1977, 287, 1.

[28] S. P. Mohanty, E. Kougianos, *IEEE Potentials* 2015, 25, 35.

[29] C. L. Morgan, D. J. Newman, C. P. Price, *Clin. Chem.* 1996, 42, 193.

[30] P. B. Luppa, L. J. Sokoll, D. W. Chan, *Clin. Chim. Acta*, 2001, 314, 1.

[31] Z. Altintas, W. M. Fakanya, I. E. Tothill, *Talanta*, 2014, 128, 177.

[32] F. Ricci, G. Volpe, L. Micheli, G. Palleschi, *Anal. Chim. Acta* 2007, 605, 111.

[33] M.I. Mohammed, M. P. Y. Desmulliez, *Lab Chip* 2011, 11, 569.

[34] Sino Biological Inc., ELISA encyclopedia, www.elisa-antibody.com (accessed 25 April 2016).

[35] G. Liu, Y. Lin, *Talanta* 2007, 74, 308.

[36] D. Martín-Yerga, M. B. González-García, A. Costa-García, *Talanta* 2014, 130, 598.

[37] M. M. P. S. Neves, M. B. González-García, C. Delerue-Matos, A. Costa-García, *Sens. Actuators B.* 2013,187, 33.

[38] R. I. Stefan, J. F. van Staden, H. Y. Aboul-Enein, *Fresenius. J. Anal. Chem.* 2000, 366, 659.

[39] U. Bilitewski, G. C. Chemnitius, P. Rüger, R. D. Schmid, *Sens. Actuators B.* 1992, 7, 351.

[40] K. C. Honeychurch, J. P. Hart, *TrAC - Trends Anal. Chem.* 2003, 22, 456.

[41] J. P. Hart, A. Crew, E. Crouch, K. C. Honeychurch, R. M. Pemberton, *Anal. Lett.* 2004, 37, 789.

[42] W. Putzbach, N. J. Ronkainen, *Sensors* 2013, 13, 4811.

[43] A. Sassolas, L. J. Blum, B. D. Leca-Bouvier, *Biotechnol. Adv.* 2012, 30, 489.

[44] P. Fanjul-Bolado, P. Queipo, P. J. Lamas-Ardisana, A. Costa-García, *Talanta* 2007, 74, 427.

[45] A. S. Calvo, C. Botas, D. Martín-Yerga, P. Álvarez, R. Menéndez, A. Costa-García, *J. Electrochem. Soc. 2015, 162, B282.*

[46] G. Martínez-Paredes, M. B. González-García, A. Costa-García, *Electrochim. Acta* 2009, 54, 4801.

[47] M. M. Pereira da Silva Neves, M. B. G. García, C. Delerue-Matos, A. C. García, *Electroanalysis* 2011, 23, 63.

[48] E. C. Rama, M. B. González-García, A. Costa-garcía, *Sens. Actuators B.* 2014, 201, 567.

[49] D. M. Cate, J. A. Adkins, J. Mettakoonpitak, C. S. Henry, *Anal. Chem.* 2015, 87, 19.

[50] K. E. Berg, J. A. Adkins, S. E. Boyle, C. S. Henry, *Electroanalysis*, 2015.

[51] N. Ruecha, N. Rodthongkum, D. M. Cate, J. Volckens, O. Chailapakul, and C. S. Henry, *Anal. Chim. Acta* 2015, 874, 40.

[52] T. Rungsawang, E. Punrat, J. Adkins, C. Henry, O. Chailapakul, *Electroanalysis*, 2015.

[53] J. R. Windmiller, J. Wang, *Electroanalysis*, 2013, 25, 29.

[54] A. J. Bandodkar, W. Jia, J. Wang, *Electroanalysis* 2015, 27, 562.

[55] B. Bohunicky, S. A. Mousa, *Nanotechnol. Sci. Appl.* 2011, 4, 1.

[56] I. E. Tothill, *Semin. Cell Dev. Biol.* 2009, 20, 55.

[57] A. Rasooly, J. Jacobson, *Biosens. Bioelectron.* 2006, 21, 1851.

[58] M. Perfézou, A. Turner, A. Merkoçi, *Chem. Soc. Rev.* 2012, 41, 2606.

[59] E. Simon, *Meas. Sci. Technol.* 2010, 21, 112002.

[60] C. L. Sawyers, *Nature* 2008, 452, 548.

[61] N. L. Henry, D. F. Hayes, *Mol. Oncol.* 2012, 6, 140.

[62] J. Wu, Z. Fu, F. Yan, H. Ju, *TrAC - Trends Anal. Chem.* 2007, 26, 679.

[63] J. a Ludwig, J. N. Weinstein, *Nat. Rev. Cancer* 2005, 5, 845.

[64] M. Aizawa, A. Morioka, S. Suzuki, Y. Nagamura, *Anal. Biochem.* 1979, 94, 22.

[65] V. Escamilla-Gómez, D. Hernández-Santos, M. B. González-García, J. M. Pingarrón-Carrazón, A. Costa-García, *Biosens. Bioelectron.* 2009, 24, 2678.

[66] X. Pei, Z. Xu, J. Zhang, Z. Liu, J. Tian, *Anal. Methods* 2013, 5, 3235.

[67] J. Biscay, M. B. González García, A. C. García, *Electroanalysis* 2015, 27, 2773.

[68] M. Yan, D. Zang, S. Ge, L. Ge, J. Yu, *Biosens. Bioelectron.* 2012, 38, 355.

[69] A. C. Barton, F. Davis, S. P. J. Higson, *Anal. Chem.* 2008, 80, 6198.

[70] Y. Wan, W. Deng, Y. Su, X. Zhu, C. Peng, H. Hu, H. Peng, S. Song, C. Fan, *Biosens. Bioelectron.* 2011, 30, 93.

[71] L. Li, J. Xu, X. Zheng, C. Ma, X. Song, S. Ge, J. Yu, M. Yan, *Biosens. Bioelectron.* 2014, 61, 76.

[72] J. A. Ho, Y. C. Lin, L. S. Wang, K. C. Hwang, P. T. Chou, *Anal. Chem.* 2009, 81, 1340.

[73] W. Wu, P. Yi, P. He, T. Jing, K. Liao, K. Yang, H. Wang, *Anal. Chim. Acta* 2010, 673, 126.

[74] J. Li, J. Wu, L. Cui, M. Liu, F. Yan, H. Ju, *Analyst* 2016, 141, 131.

[75] A. Ravalli, G. Pilon Dos Santos, M. Ferroni, G. Faglia, H. Yamanaka, G. Marrazza, *Sensors Actuators, B Chem.* 2013, 179, 194.

[76] S. Ge, M. Sun, W. Liu, S. Li, X. Wang, C. Chu, M. Yan, J. Yu, *Sens. Actuators B.* 2014, 192, 317.

[77] A. L. Sun, *Analyst* 2015, 140, 7948.

[78] A. Ravalli, C. G. da Rocha, H. Yamanaka, G. Marrazza, *Bioelectrochemistry* 2015, 106, 268.

[79] R. C. B. Marques, S. Viswanathan, H. P. a Nouws, C. Delerue-Matos, M. B. González-García, *Talanta* 2014, 129, 594.

[80] X. Zhu, H. Zheng, H. Xu, R. Lin, Y. Han, G. Yang, Z. Lin, L. Guo, B. Qiu, G. Chen, *Anal. Methods* 2014, 6, 5264.

[81] G. Lai, J. Wu, C. Leng, H. Ju, F. Yan, *Biosens. Bioelectron.* 2011, 26, 3782.

[82] G. Lai, F. Yan, H. Ju, *Anal. Chem.* 2009, 81, 9730.

[83] G. Lai, J. Wu, H. Ju, F. Yan, *Adv. Funct. Mater.* 2011, 21, 2938.

[84] J. Wu, Z. Zhang, Z. Fu, H. Ju, *Biosens. Bioelectron.* 2007, 23, 114.

[85] S. Ge, F. Yu, L. Ge, M. Yan, J. Yu, D. Chen, *Analyst* 2012, 137, 4727.

[86] Z. Cui, D. Wu, Y. Zhang, H. Ma, H. Li, B. Du, Q. Wei, H. Ju, *Anal. Chim. Acta* 2014, 807, 44.

[87] Y. Wu, P. Xue, K. M. Hui, Y. Kang, *Biosens. Bioelectron.* 2014, 52, 180.

[88] J. Wu, F. Yan, X. Zhang, Y. Yan, J. Tang, H. Ju, *Clin. Chem.* 2008, 54, 1481.

[89] A. M. LeBeau, P. Singh, J. T. Isaacs, S. R. Denmeade, *Biochemistry* 2009, 48, 3490.

[90] U. H. Stenman, J. Leinonen, H. Alfthan, S. Rannikko, K. Tuhkanen, O. Alfthan, *Cancer Res.* 1991, 51, 222.

[91] M. F. Ullah, M. Aatif, *Cancer Treat. Rev.* 2009, 35, 193.

[92] P. Fanjul-Bolado, D. Hernández-Santos, M. B. González-García, A. Costa-García, *Anal. Chem.* 2007, 79, 5272.

[93] M. H. Schlageter, J. Larghero, B. Cassinat, M. E. Toubert, C. Borschneck, J. D. Rain, *Clin. Chem.* 1998, 44, 1995.

[94] M. K. Tuxen, G. Sölétormos, P. Dombernowsky, *Cancer Treat. Rev.* 1995, 21, 215.

[95] T. Meyer, G. J. S. Rustin, *Br. J. Cancer* 2000, 82, 1535.

[96] A. Ravelli, J. M. Reuben, F. Lanza, S. Anfossi, M. R. Cappelletti, L. Zanotti, A. Gobbi, C. Senti, P. Brambilla, M. Milani, D. Spada, P. Pedrazzoli, M. Martino, A. Bottini, D. Generali, *Tumor Biol.* 2015, 36, 6653.

[97] M. J. Duffy, D. Evoy, E. W. McDermott, *Clin. Chim. Acta* 2010, 411, 1869.

[98] Y. Xiang, Y. Lu, *Anal. Chem.* 2012, 84, 4174.

[99] J. Su, J. Xu, Y. Chen, Y. Xiang, R. Yuan, Y. Chai, *Chem. Commun.* 2012, 48, 6909.

[100] A. Qureshi, Y. Gurbuz, J. H. Niazi, *Sens. Actuators B.* 2012, 171-172, 62.

[101] R. K. Upadhyay, *J. Lipids*, 2015, 2015, 971453.

[102] Z. Yang, D. Min Zhou, *Clin. Biochem.* 2006, 39, 771.

[103] S. Yusuf, M. Pearson, H. Sterry, S. Parish, D. Ramsdale, P. Rossi, P. Sleight, *Eur. Heart J.* 1984, 5, 690.

[104] Y. Rozenman, M. S. Gotsman, *Annu. Rev. Med.* 1994, 45, 31.

[105] P. Stubbs, P. O. Collinson, *Clin. Chim. Acta* 2001, 311, 57.

[106] U. Friess, M. Stark, *Anal. Bioanal. Chem.* 2009, 393, 1453.

[107] F. T. C. Moreira, R. A. F. Dutra, J. P. C. Noronha, A. L. Cunha, M. G. F. Sales, *Biosens. Bioelectron.* 2011, 28, 243.

[108] B. E. F. de Ávila, V. Escamilla-Gómez, S. Campuzano, M. Pedrero, J. M. Pingarrón, *Electroanalysis* 2013, 25, 51.

[109] P. M. Ridker, *Circulation* 2003, 107, 363.

[110] A. Kakoti, P. Goswami, *Biosens. Bioelectron.* 2013, 43, 400.

[111] B. McDonnell, S. Hearty, P. Leonard, R. O'Kennedy, *Clin. Biochem.* 2009, 42, 549.

[112] M. Hasanzadeh, N. Shadjou, M. Eskandani, M. de la Guardia, E. Omidinia, *TrAC - Trends Anal. Chem.* 2013, 49, 20.

[113] B. V. M. Silva, I. T. Cavalcanti, A. B. Mattos, P. Moura, M. D. P. T. Sotomayor, R. F. Dutra, *Biosens. Bioelectron.* 2010, 26, 1062.

[114] B. V. M. Silva, I. T. Cavalcanti, M. M. S. Silva, R. F. Dutra, *Talanta* 2013, 117, 431.

[115] T. M. O'Regan, L. J. O'Riordan, M. Pravda, C. K. O'Sullivan, G. G. Guilbault, *Anal. Chim. Acta* 2002, 460, 141.

[116] E. Suprun, T. Bulko, A. Lisitsa, O. Gnedenko, A. Ivanov, V. Shumyantseva, A. Archakov, *Biosens. Bioelectron.* 2010, 25, 1694.

[117] N. Gan, L. H. Meng, F. T. Hu, Y. T. Cao, Y. Z. Wu, L. Y. Jia, L. Zheng, *Appl. Mech. Mater.* 2012, 110-116, 519.

[118] C. Kokkinos, M. Prodromidis, A. Economou, P. Petrou, S. Kakabakos, *Anal. Chim. Acta* 2015, 886, 29.

[119] T. A. Freitas, A. B. Mattos, B. V. M. Silva, R. F. Dutra, *Biomed Res. Int.* 2014, 2014, 929786.

[120] T. O'Regan, M. Pravda, C. K. O'Sullivan, G. G. Guilbault, *Anal Lett*. 2003, 36, 1903.

[121] T. O'Regan, *Talanta* 2002, 57, 501.

Biographies

Estefanía Costa Rama obtained her B.Sc. degree in Chemistry, focus on Analytical Chemistry, in 2009 (University of Oviedo) and the M.Sc. degree in Chemical, Biochemical and Structural Analysis in 2010 (University of Oviedo). At present, she is working toward her Ph.D. degree at the Nanobioanalysis Research Group of the University of Oviedo, supervised by Prof. A. Costa-García. She has been working in the development of biosensors based on screen-printed electrodes.

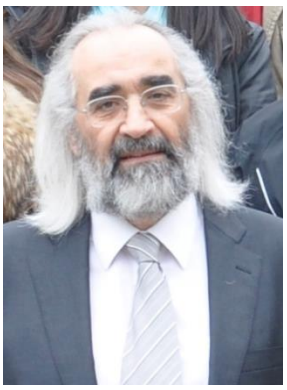

Agustín Costa-García obtained his degree in Chemistry, focused on Analytical Chemistry, in 1974 (University of Oviedo) and the Ph.D. in Chemistry in 1977 (University of Oviedo). Since February 2000 he is Professor in Analytical Chemistry (University of Oviedo). He leads the Nanobioanalysis Research Group of the University of Oviedo and has been supervisor of several research projects developed at the laboratories of the Department of Physical and Analytical Chemistry of the University of Oviedo. He has authored more than 200 research papers. Current research includes the development of nanostructured electrodic surfaces for its use as transducers for electrochemical (bio)sensors employing both enzymatic and non-enzymatic labels and the development of (bio)sensors based on paper.

3.2.3. Artículo 5: "Competitive electrochemical immunosensor for amyloid-beta 1-42 detection based on gold nanostructurated screen-printed carbon electrodes"

Sensors and Actuators B: Chemical 2014, 201, 567-571

Sensors and Actuators B 201 (2014) 567–571

Contents lists available at ScienceDirect

Sensors and Actuators B: Chemical

journal homepage: www.elsevier.com/locate/snb

Competitive electrochemical immunosensor for amyloid-beta 1-42 detection based on gold nanostructured screen-printed carbon electrodes

Estefanía Costa Rama, María Begoña González-García, Agustín Costa García*

Departamento de Química Física y Analítica, Facultad de Química, Universidad de Oviedo, España

ABSTRACT

Alzheimer's disease is the most common form of dementia, characterized by the progressive accumulation of plaques with amyloid-beta peptide of 42 amino acids as one of the primary constituents. A disposable electrochemical immunosensor for the detection of amyloid-beta 1-42 is developed. Screen-printed carbon electrodes nanostructured with gold nanoparticles generated "in situ" are used as the transducer surface. The immunosensing strategy consists in a competitive immunoassay: biotin-amyloid-beta 1-42 immobilized on the electrode surface and the analyte (amyloid-beta 1-42) compete for the anti-amyloid-beta 1-42 antibody. The electrochemical detection is carried out using an alkaline phosphatase labelled anti-rabbit IgG antibody. The analytical signal is based on the anodic stripping of enzymatically generated silver by cyclic voltammetry. The immunosensor achieved shows a low limit of detection (0.1 ng/mL) and a wide linear range (0.5-500 ng/mL).

Keywords: Amyloid-beta 1-42, Alzheimer's disease, Screen-Printed Carbon Electrode, Electrochemical immunosensor, Gold nanoparticles.

Abbreviations: AD, Alzheimer's disease; Aβ, amyloid-beta; SPCE, screen-printed carbon electrode; anti-IgG-AP, anti-rabbit IgG antibody labelled with alkaline phosphatase; biotin-Aβ1-42, amyloid-beta 1-42 labelled with biotin; anti-Aβ1-42, amyloid-beta 1-42 monoclonal antibody recombinant rabbit IgG; AuNP, gold nanoparticle, B-AP, biotin conjugated to alkaline phosphatase

1. Introduction

Today, over 35 million people worldwide currently live with dementia, and this number is expected to double by 2030 [1]. Alzheimer's disease (AD) represents 50–75% of all dementias [2]. The major histopathological hallmarks of AD are the progressive accumulation of plaques with amyloid-β (Aβ), and neurofibrillary tangles containing microtubuli-associated tau protein [3]. Aβ peptide comprising of 39–42 amino acids is the primary constituent of these plaques that hinder the communication between neurons causing cell death, cognitive dysfunction, and behavioral abnormalities [4,5]. Among these Aβ peptides, Aβ1-40 is the most abundant, but Aβ1-42 appears to be essential for initiating Aβ aggregation, and is considered central to the amyloid cascade hypothesis of AD [6]. This hypothesis postulates a central initiating role for Aβ1-42 in the subsequent pathological features of AD, such as neuroinflammation, synapse and neuritic dysfunction, tau hyper-phosphorylation and development of intraneuronal neurofibrillary tangles. Due to their roles in the pathogenesis of AD, Aβ1-42 seems to be a more useful biomarker for AD than Aβ1-40 [6].

Cerebrospinal fluid (CSF) is in direct contact with the extracellular space of the brain and biochemical changes in the brain are thought to be reflected in CSF [7].

Nowadays, there are few works described about devices for Aβ1-42 detection and these works are very recent (from 2010 to now) [8-13.] There is one previously reported (2008), that, so far, is the only one based on screen-printed electrodes [14]. But, for this sensor the Aβ peptides recognition is based on the saccharide-protein interactions, and the analytical signal is the oxidation peak of tyrosine that Aβ peptides have. So, this sensor cannot discriminate between Aβ1-40 and Aβ1-42.

In this work, the first electrochemical immunosensor based on screen-printed electrode for Aβ1-42 detection is described. The biosensor consists of a competitive immunoassay carried out on a screen-printed carbon electrode nanostructured with gold nanoparticles. Concentration of antigen labeled, antibody and secondary labeled antibody are optimized and non-specific binding is also studied. Label used is alkaline phosphatase and a mixture of 3-indoxyl phosphate with silver ions (3-IP/Ag^+) is used as substrate. The analytical signal is based on the anodic stripping of enzymatically generated silver by cyclic voltammetry. The linear range of the immunosensor developed allows the diagnosis of AD because, although the values are not well established, several authors consider 500 pg/mL as an optimum cut-off value to differentiate between patients with dementia and healthy patients [13,15-18].

2. Experimental

2.1. Apparatus and electrodes

SPCE gold nanostructuration is performed with a μStat 8000 potentiostat (DropSens) interfaced to a Pentium 4 2.4 GHz computer system and controlled by DropView 8400 1.0 software.

The voltammetric measurements are carried out using an ECO Chemie μAutolab type II potentiostat/galvanostat interfaced to a Pentium 4 2.4 GHz computer system and controlled by the Autolab GPES software version 4.9. All measurements are performed at room temperature.

Disposable Screen-Printed Carbon Electrodes (SPCEs) are purchased from DropSens. These electrodes incorporate a conventional three-electrode cell configuration, printed on ceramic substrates (3.4 cm × 1.0 cm). Both the working (disk-shaped 4 mm diameter) and counter electrodes are made of carbon inks, whereas the pseudoreference electrode and the electric contacts are made of silver. An insulating layer delimits the electrochemical cell (50 μL) and the electric contacts. The SPCEs are easily connected to the μStat 8000 potentiostat and to the μAutolab potentiostat through the specific DropSens connector in each case.

2.2. Reagents and solution

Tris(hydroxymethyl)aminomethane (Tris), magnesium nitrate, bovine serum albumin fraction V (BSA), β-casein from bovine milk (casein), streptavidin (molecular weight, 66 kDa) and biotin conjugated to alkaline phosphatase (B-AP; dimmer, four units of B per molecule of AP, molecular weight, 160 kDa) are purchased from Sigma. Standard gold (III) tetrachloro complex ($AuCl_4^-$), silver nitrate, hydrochloric acid (37%) and nitric acid (HNO_3) are obtained from Merck. Biosynth supplied the 3-indoxyl phosphate disodium salt.

Aβ1-42 monoclonal antibody recombinant rabbit IgG (clone H31L21) specific to amino acids 707-713 is purchased from Life Technologies. Anti-rabbit IgG (whole molecule) labelled with alkaline phosphatase (anti-IgG-AP) is provided by Sigma. Aβ1-42 and Aβ1-42 labelled with biotin (Biotin-LC-β- Amyloid 1-42) are purchased from Anaspec.

Ultrapure water obtained from a Millipore Direct-QTM 5 purification system from Millipore Ibérica is used throughout the work. All chemicals employed are of analytical reagent grade. Working solutions of streptavidin, Aβ1-42 monoclonal antibody, Aβ1-42 and Aβ1-42 labelled with biotin (biotin-Aβ1-42) are prepared in a 0.1 M Tris-HNO_3 pH 7.2 buffer (buffer 1). Working solutions of secondary alkaline phosphatase labelled antibody are prepared in a

0.1 M Tris-HNO_3 pH 7.2 buffer containing 2 mM $Mg(NO_3)_2$ (buffer 2). A solution containing 1.0 mM 3-IP and 0.4 mM silver nitrate is prepared daily in 0.1 M Tris-HNO_3 pH 9.8 buffer containing 20 mM $Mg(NO_3)_2$ (buffer 3), and stored in opaque tubes at 4^0C. Casein and albumin lyophilized powder are reconstituted in buffer 1.

2.3. Procedures

2.3.1. SPCEs nanostructuration

Gold nanoparticles are generated "in situ" over SPCEs (AuNP-SPCEs) following a method previously reported by Martínez-Paredes *et al*. [19], using µStat 8000 potentiostat. The procedure consists in applying a constant current intensity of -100 µA for 240 s in an acidic solution of 0.1 mM $AuCl_4^-$. Then a potential of +0.1 V for 120 s is applied. Finally, the nanostructured electrodes are rinsed with water and are ready to use. AuNPs generation is performed at room temperature. Using the µStat 8000 potentiostat, gold nanoparticles can be generated over eight different screen-printed carbon electrodes at the same time.

2.3.2. Evaluation of the analytical signal improvement using AuNP-SPCEs

The reaction streptavidin-biotin is used to evaluate the effect of the AuNPs generated over the SPCE. A drop of 10 µL of 0.1 µM streptavidin [20] solution is placed on the nanostructurated surface of the SPCE solution and incubated overnight at 4^0C. The immobilization of the streptavidin on the electrode surface is achieved by physical adsorption. Then, the electrode is washed with buffer 1, and the free surface sites are blocked with 40 µL BSA solution (2%) during 30 min. The electrode is washed again using buffer 2, and a drop of 40 µL B-AP solution (0.1 nM) is dropped on the streptavidin-modified electrode for one hour reaction. After a washing step with buffer 3, the enzymatic reaction is carried out dropping 40 µL of a mixture of 1.0 mM 3-IP/0.4 mM silver nitrate solution on the electrode. The enzymatically silver deposition catalyzed by alkaline phosphatase has been already reported [21]. AP works as the enzymatic label and a mixture of 3-IP with silver ions (Ag^+) as the substrate. AP hydrolyzes 3-IP resulting an indoxyl intermediate. This intermediate reduces the silver ions present in solution resulting in metallic silver (Ag^0) and indigo blue (I) [21]. Thus, the silver enzymatically deposited on the electrode surface can be detected through the redissolution peak when an anodic stripping scan is carried out. After 20 min of enzymatic reaction, an anodic stripping cyclic voltammetric scan is recorded from 0.0 V to +0.4 V at a scan rate of 50 mV/s.

2.3.3. Immunosensor for the detection of Aβ1-42

The following procedure (**Fig. 1**) describes an optimized assay. The working area of SPCE-AuNPs is coated with 10 µL of 0.1 µM streptavidin [20] solution and incubated overnight at 4^0C. After the overnight incubation step, the electrode is washed with buffer 1. Free surface sites of the streptavidin-modified AuNP-SPCE are blocked with 40 µL casein solution (2%) during 30 min. After another washing step with buffer 1, an aliquot of 40 µL of 300 ng/mL biotin-Aβ1-42 solution is dropped on the streptavidin modified electrode for one hour reaction. After a washing step with buffer 1, the sensing part of the immunosensor is completed. Then, 40 µL of a solution of Aβ1-42 and antibody anti-Aβ1-42 (0.5 µg/mL) is dropped for one hour to carry out the competitive reaction. The competition was established via the binding between analyte (Aβ1-42) and the biotin-Aβ1-42 previously immobilized in the electrode surface, for the limited binding sites of the anti-Aβ1-42. Finally, after a washing step with buffer 2, the immunosensor is incubated with 40 µL of an anti-IgG-AP (1:15,000) solution for 60 min and washed with buffer 3. The enzymatic reaction is performed as is explained in **Section 2.3.2**: placing a 40-µL aliquot of the 1.0 mM 3-IP/0.4 mM silver nitrate solution on the sensor, and after 20 min, recording an anodic stripping cyclic voltammetric scan from 0.0 V to +0.4 V at a scan rate of 50 mV/s. Buffers employed have been chosen because of the satisfactory results in immunosensors with similar procedure [22,23].

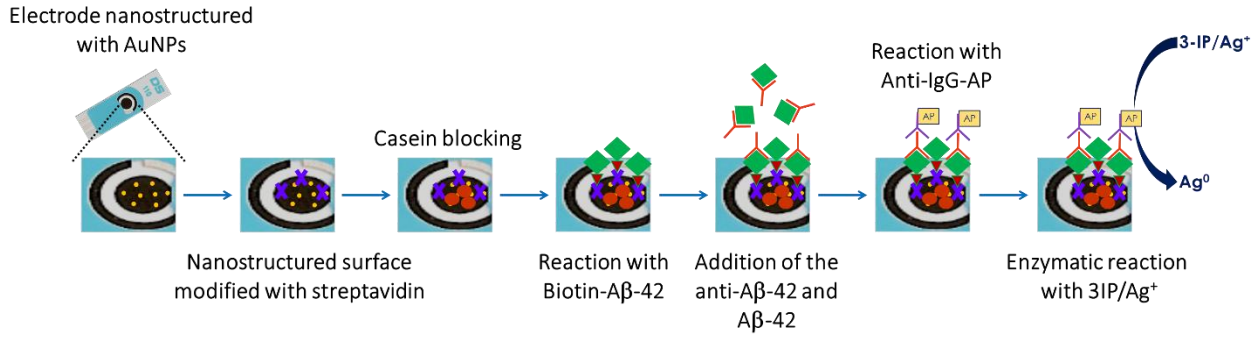

Fig. 1. Schematic representation of the immunosensing strategy for the detection of Aβ1-42.

3. Results and discussion

3.1. Analytical signal improvement using AuNP-SPCEs

The use of this gold nanostructuration is based in works previously reported [24]. It is well know that gold nanostructured surfaces as electrochemical transducers show better

sensitivities than non-nanostructured surfaces [25]. To corroborate this improvement of sensitivity, the assay described in **Section 2.3.2** is carried out using an AuNP-SPCE and a SPCE non-nanostructurated. The non-nanostructurated SPCE is pretreated applying the same procedure than to achieve a AuNP -SPCE but using an acidic solution without $AuCl_4^-$. As **Fig. 2** shows, the capacitive current is slightly higher using a AuNP -SPCE than using a non-nanostructurated one, but the intensity of the peak is much higher using the AuNP-SPCE. So, a AuNP-SPCE is better transducer to develop the immunosensor than a non-nanostructurated SPCE.

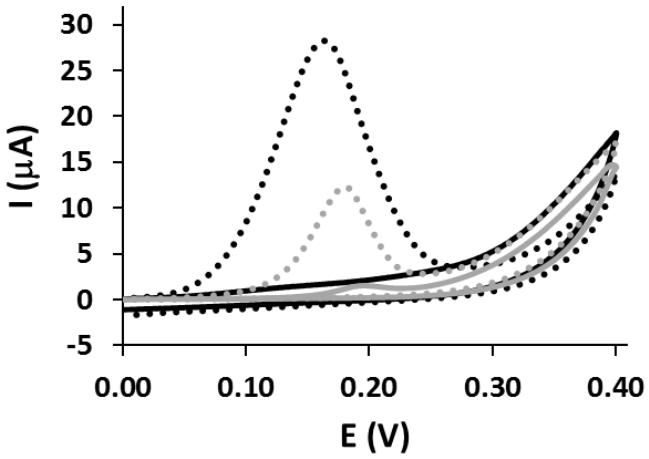

Fig. 2. Cyclic voltammograms for redissolution peak of metallic silver enzymatically deposited on the electrode surface using a AuNP-SPCE (black lines) and a SPCE non-nanostructurated (gray lines). Analytical signal (dashed lines) and background signal (solid lines).

3.2. Optimization of the experimental conditions

The variables involved in the construction of the immunosensor can influence the analytical response, therefore an optimization study was carried out.

Different anti-IgG-AP antibody dilutions were tested: 1:10,000, 1:15,000 and 1:20,000. The dilution chosen for further studies was 1:15,000 because the best compromise between analytical signal and non-specific is achieved (data non shown).

Non-specific binding of anti-IgG-AP over the electrode surface is avoided adding BSA to the solution of this antibody. If BSA is not present in anti-IgG-AP solution, the signal in the absence of biotin-Aβ1-42 is about 14 μA, due to non-specific adsorptions. But, adding 1% BSA concentration to the solution of anti-IgG-AP, these undesirable adsorptions are avoided without an important loss of signal given by the sensor (**Fig. 3**).

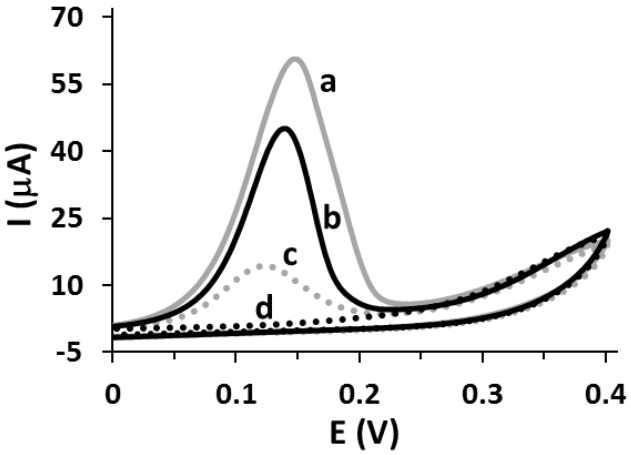

Fig. 3. Cyclic voltammograms given by the immunosensor: in the absence of BSA, with biotin-Aβ1-42 500 ng/mL (a) or without biotin-Aβ1-42 (c). When BSA is added in anti-IgG-AP solution, with biotin-Aβ1-42 500 ng/mL (b) or without biotin-Aβ1-42 (d). Experimental conditions: anti-Aβ1-42 0.3 μg/mL; anti-IgG-AP 1:15,000; 3-IP1.0 mM; Ag^{+}0.4 mM.

The adequate concentration of the biotin-Aβ1-42 is evaluated in order to achieve the best performance of the immunosensor. Although biotin-Aβ1-42 concentration of 500 ng/mL shows the highest analytical signal, a biotin-Aβ1-42 concentration of 300 ng/mL is chosen because the analytical signal achieved is similar and the reproducibility is better (**Fig. 4**). Moreover, higher concentration of biotin-Aβ1-42 than 300 ng/mL saturates the electrode surface and shows worse reproducibility.

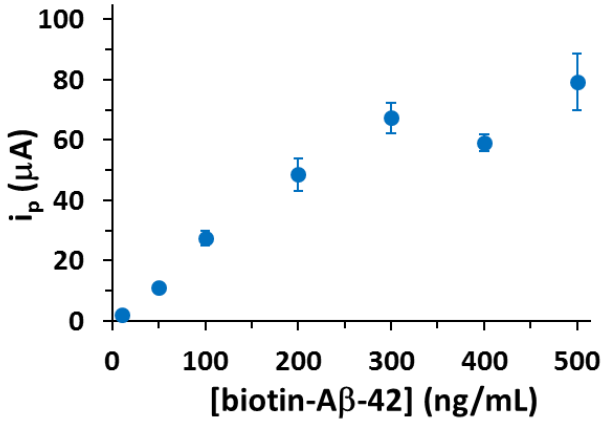

Fig. 4. Peak current intensities obtained for different concentrations of biotin-Aβ1-42. Experimental conditions: casein 2%; anti-Aβ1-42 1 μg/mL; anti-IgG-AP 1:15,000; 3-IP 1.0 mM; Ag^{+} 0.4 mM. Data are given as average *±SD* (n = 3).

The concentration of the antibody anti-Aβ1-42 is a crucial parameter. If it is too high, when the amount Aβ1-42 in the sample is low, the competitive reaction could not be detected, due to there is amount of antibody enough to react with the Aβ1-42 in the sample and with the biotin-Aβ1-42 immobilized on the electrode surface. **Fig. 5** shows the results of the optimization of anti-Aβ1-42 antibody concentration. The highest analytical signal is obtained for a concentration of 1 µg/mL, but in order to assure a lack of amount of antibody, a concentration of 0.5 mg/mL is chosen for further studies.

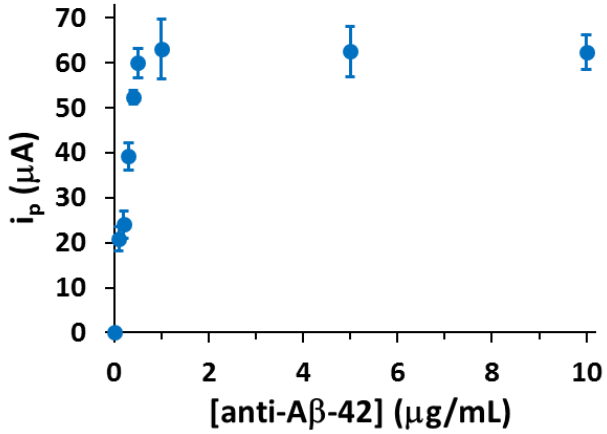

Fig. 5. Peak current intensities obtained for different concentrations of anti-Aβ1-42. Experimental conditions: casein 2%; biotin-Aβ1-42 300 ng/mL; anti-IgG-AP 1:15,000; 3-IP 1.0 mM; Ag^+ 0.4 mM. Data are given as average ± SD (n = 3).

3.3. Analytical characteristics of the immunosensor

After the optimization of these analytical parameters, a calibration plot for Aβ1-42 with the equation $(i_0 - i)/i_0$ (µA) = 18 · Log[Aβ1-42] (ng/mL) + 13, R^2 = 0.991, and a linear range between 0.5 and 500 ng/mL is obtained (**Fig. 6**). The limit of detection (LOD) and the limit of quantification (LOQ) are calculated from the calibration plot using the equations: LOD = 3*sb*/*m* and LOQ = 10*sb*/*m* (wheres *b* is the standard deviation of the intercept and *m* is the slope of the calibration plot). The LOD value thus obtained is 0.1 ng/mL and the LOQ is 0.4 ng/mL.

In order to evaluate the reproducibility of the immunosensors, several sensors are prepared in different days. Each sensor is used for only one measurement (single use). The maximum signal obtained with these sensors is 61 ± 3 µA (n = 6).

This immunosensor shows good analytical characteristics when is compared with others earlier reported [9–12]. The linear range obtained is wider than the achieved by other

methods much more laborious and that required more steps and time of fabrication, for example liquid chromatography tandem mass spectrometry [9] or an immunoassay using carbon fiber microelectrodes [12]. Moreover, so far, there is only one sensor for Aβ peptides (Aβ1-40 and Aβ1-42) detection based on screen-printed electrode and the LOD of this device for both peptides is ≈ 4.5 µg/mL [14].

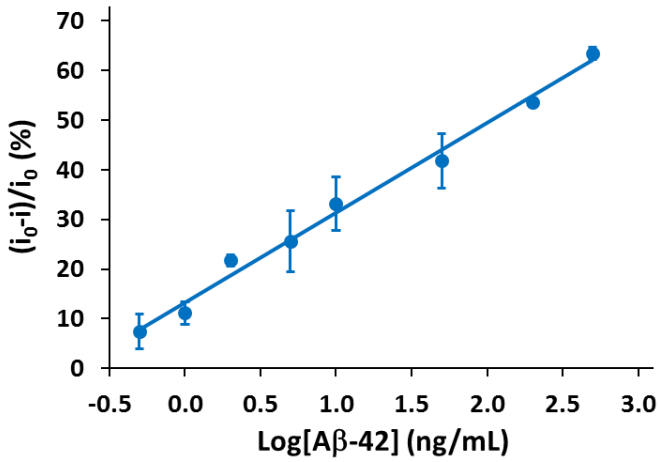

Fig. 5. Calibration plot for the immunosensor in the presence of different concentrations of Aβ1-42: 500, 200, 50, 10, 5, 2, 1 and 0.5 ng/mL. Experimental conditions: casein 2%; biotin-Aβ1-42 300 ng/mL; anti-Aβ1-42 0.5 µg/mL; anti-IgG-AP 1:15,000; 3-IP 1.0 mM; Ag^+ 0.4 mM. Data are given as average ± SD (n = 3).

4. Conclusions

An electrochemical immunosensor based on screen-printed electrodes for Aβ1-42 detection is developed. Several parameters involved in the immunosensing strategy, such as the biotin-Aβ1-42 and the anti-Aβ1-42 antibody concentrations, were optimized leading to an analytical performance without non-specific adsorptions. The sensor developed shows a very low LOD of 0.1 ng/mL and a wide linear range between 0.5 and 500 ng/mL. This linear range allows the diagnosis of AD considering 500 pg/mL as an optimum cut-off value. On the other hand, the fabrication of this immunosensor is simple and it can be a portable and ready-to-use device because of the use of SPCE as transducer.

Acknowledgement

This work has been supported by the Spanish Ministry of Science and Innovation Project (MICINN-12-CTQ2011-24560), and by a Severo Ochoa Predoctoral Grant (BP11-097) attributed to Estefanía Costa Rama by the Government of the Principality of Asturias.

References

[1] M. Prince, M. Prina, M. Guerchet, World Alzheimer Report 2013, Journey of Caring, An Analysis of Long-Term Care for Dementia, Alzheimer's Disease International (ADI), London, 2013.

[2] L.I. Jsselstijn, L.J.M. Dekker, C. Stingl, M.M. van der Weiden, A. Hofman, J.M. Kros, P.J. Koudstaal, P.A.E. Sillevis Smitt, M.A. Ikram, M.M.B. Breteler, T.M. Luider, Serum levels of pregnancy zone protein are elevated inpresymptomatic Alzheimer's disease, J. Proteome Res. 10 (2011) 4902-4910,http://dx.doi.org/10.1021/pr200270z.

[3] F.H. Bouwman, S.N. Schoonenboom, W.M. van der Flier, E.J. van Elk, A. Kok, F. Barkhof, M.A. Blankenstein, P. Scheltens, CSF biomarkers and medial temporal lobe atrophy predict dementia in mild cognitive impairment, Neurobiol. Aging 28 (7) (2007) 1070-1074, http://dx.doi.org/10.1016/j.neurobiolaging.2006.05.006.

[4] J.A. Hardy, G.A. Higgins, Alzheimer's disease: the amyloid cascade hypothesis, Science 256 (1992) 184-185, http://dx.doi.org/10.1126/science.1566067.

[5] M.P. Murphy, H. LeVine, Alzheimer's disease and the amyloid-beta peptide, J. Alzheimer's Dis. 19 (2010) 311-323, http://dx.doi.org/10.3233/JAD-2009-1221.

[6] A.M. Fagan, D.M. Holtzman, Cerebrospinal fluid biomarkers of Alzheimer's disease, Biomark. Med. 4 (1) (2010) 51–63, http://dx.doi.org/10.2217/BMM.09.83.

[7] K. Blennow, H. Hampel, CSF markers for incipient Alzheimer's dis-ease, Lancet Neurol. 2 (10) (2003) 605-613, http://dx.doi.org/10.1016/S1474-4422(03)00530-1.

[8] L. Liu, F. Zhao, F. Ma, L. Zhang, S. Yang, N. Xia, Electrochemical detection of β-amyloid peptides on electrode covered with N-terminus-specific antibody based on electrocatalytic O_2 reduction by Aβ(1-16)-heme-modified gold nanoparticles, Biosens. Bioelectron. 49 (2013) 231-235,http://dx.doi.org/10.1016/j.bios.2013.05.028.

[9] M.E. Lame, E.E. Chambers, M. Blatnik, Quantitation of amyloid beta pep-tides Aβ1-38, Aβ1-40, and Aβ1-42 in human cerebrospinal fluid by ultra-performance liquid chromatography-tandem mass spectrometry, Anal. Biochem. 491 (2011) 133-139, http://dx.doi.org/10.1016/j.ab.2011.08.010.

[10] M. Ammar, C. Smadja, L.G.T. Phuong, M. Azzouz, J. Vigneron, A. Etcheberry, M. Taverna, E. Dufour-Gergam, A new controlled concept of immune-sensing platform for specific

detection of Alzheimer's biomarkers, Biosens. Bioelectron.40 (2013) 329-335, http://dx.doi.org/10.1016/j.bios.2012.07.072.

[11] P. Gagni, L. Sola, M. Cretich, M. Chiari, Development of a high-sensitivity immunoassay for amyloid-beta 1-42 using a silicon microarray plat-form, Biosens. Bioelectron. 47 (2013) 490–495, http://dx.doi.org/10.1016/j.bios.2013.03.077.

[12] S. Prabhulkar, R. Piatyszek, J.R. Cirrito, Z.Z. Wu, C.Z. Li, Microbiosensor for Alzheimer's disease diagnostics: detection of amyloid betabiomarkers, J. Neurochem. 122 (2012) 374-381, http://dx.doi.org/10.1111/j.1471-4159.2012.07709.x.

[13] N. Xia, L. Liu, M.G. Harrington, J. Wang, F. Zhou, Regenerable simultaneous surface plasmon resonance detection of Aβ(1-40) and Aβ(1-42) peptides in cerebrospinal fluids with signal amplification by streptavidin conjugated to an N-terminus-specific antibody, Anal. Chem. 82 (2010) 10151–10157, http://dx.doi.org/10.1021/ac102257m.

[14] M. Chikae, T. Fukuda, K. Kerman, K. Idegami, Y. Miura, E. Tamiya, Amyloid-beta detection with saccharide immobilized gold nanoparticle on carbon electrode, Bioelectrochemistry 74 (1) (2008) 118-123, http://dx.doi.org/10.1016/j.bioelechem.2008.06.005.

[15] T. Tapiola, I. Alafuzoff, S.K. Herukka, L. Parkkinen, P. Hartikainen, H. Soininen, T. Pirttila, Cerebrospinal fluid beta-amyloid 42 and tau proteins as biomarkers of Alzheimer-type pathologic changes in the brain, Arch. Neurol. 66 (3) (2009) 382-389, http://dx.doi.org/10.1001/archneurol.2008.596.

[16] E. Kapaki, G.P. Paraskevas, I. Zalonis, C. Zournas, CSF tau protein and beta-amyloid (1-42) in Alzheimer's disease diagnosis: discrimination from normal ageing and other dementias in the Greek population, Eur. J. Neurol. 10 (2003) 119-128, http://dx.doi.org/10.1046/j.1468-1331.2003.00562.x.

[17] M.I. Kester, L. Boelaarts, F.H. Bouwman, R.L. Vogels, E.R. Groot, E.J. van Elk, M.A. Blankenstein, W.M. van der Flier, P. Scheltens, Diagnostic Impact of CSF Biomarkers in a Local Hospital Memory Clinic, Dement. Geriatr. Cogn. Disord. 29 (2010) 491-497, http://dx.doi.org/10.1159/000313534.

[18] E. Kapaki, I. Liappas, G.P. Paraskevas, I. Theotoka, A. Rabavilas, The diagnostic value of tau protein, β-amyloid (1-42) and their ratio for the discrimination of alcohol-related cognitive disorders from Alzheimer's disease in the early stages, Int. J. Geriatr. Psychiatry 20 (2005) 722-729, http://dx.doi.org/10.1002/gps.1351.

[19] G. Martínez-Paredes, M.B. González-García, A. Costa-García, In situ electrochemical generation of gold nanostructured screen-printed carbon electrodes. Application to the detection of lead under potential deposition, Electrochim. Acta 54 (2009) 4801-4808, http://dx.doi.org/10.1016/j.electacta.2009.03.085.

[20] G. Martínez-Paredes, M.B. González-García, A. Costa-García, Genosensor for detection of four pneumoniae bacteria using gold nanostructured screen-printed carbon

electrodes as transducers, Sens. Actuators B 149 (2010) 329-335, http://dx.doi.org/10.1016/j.snb.2010.06.064.

[21] P. Fanjul-Bolado, D. Hernández-Santos, M.B. González-García, A. Costa-García, Alkaline phosphatase-catalyzed silver deposition for electrochemical detection, Anal. Chem. 79 (2007) 5272-5277, http://dx.doi.org/10.1021/ac070624o.

[22] M.M.P.S. Neves, M.B. González-García, H.P.A. Nouws, A. Costa-García, Anelectrochemical deamidated gliadin antibody immunosensor for celiac dis-ease clinical diagnosis, Analyst 138 (2013) 1956–1958, http://dx.doi.org/10.1039/c3an36728b.

[23] M.M.P.S. Neves, M.B. González-García, H.P.A. Nouws, A. Costa-García, Celiac disease detection using a transglutaminase electrochemical immunosensor fabricated on nanohybrid screen-printed carbon electrodes, Biosens. Bioelectron. 31 (2012) 95-100, http://dx.doi.org/10.1016/j.bios.2011.09.044.

[24] V. Escamilla-Gómez, D. Hernández-Santos, M.B. González-García, J.M.Pingarrón-Carrazón, A. Costa-García, Simultaneous detection of free and total prostate specific antigen on a screen-printed electrochemical dual sensor, Biosens. Bioelectron. 24 (2009) 2678-2683, http://dx.doi.org/10.1016/j.bios.2009.01.043.

[25] G. Martínez-Paredes, M.B. González-García, A. Costa-García, Genosensorfor SARS virus detection based on gold nanostructured screen-printed carbon electrodes, Electroanalysis 21 (2009) 379-385, http://dx.doi.org/10.1002/elan.200804399.

Biographies

Estefanía Costa Rama obtained her B.Sc. degree in Chemistry, focus on Analytical Chemistry, in 2009 (Faculty of Chemistry, University of Oviedo) and the M.Sc. degree in Chemical, Biochemical and Structural Analysis in 2010 (University of Oviedo). At present, she is working toward her Ph.D. degree as a Ph.D. student at the Nanobioanalysis Research Group of the University of Oviedo, supervised by Prof. A. Costa-García. Her research interests include (bio)analytical chemistry and electrochemical (bio)sensors.

María Begoña González-García obtained her B.Sc. degree in Chemistry, focus on Analytical Chemistry, in 1991 (University of Oviedo) and the Ph.D. in Chemistry in 1999 (University of Oviedo). She was associate professor at the University of Oviedo and she was co-worker in the Research Group GRAQ (REQUIMTE). She has a broad experience in electrochemical sensors development. Nowadays, she is a co-worker in the Nanobioanalysis Research Group of the University of Oviedo.

Agustín Costa-García obtained his degree in Chemistry, focus on Analytical Chemistry, in 1974 (University of Oviedo) and the Ph.D. in Chemistry in 1977 (University of Oviedo). Since February 2000 he is Professor in Analytical Chemistry (University of Oviedo). He leads the Nanobioanalysis Research Group of the University of Oviedo and has been supervisor of several research projects developed at the laboratories of the Department of Physical and Analytical Chemistry of the University of Oviedo. Nowadays his research is focused on the development of nanostructured electrodic surfaces and its use as transducers for electrochemical (bio)sensors employing both enzymatic and non-enzymatic labels.

3.2.4. Artículo 6: "Multiplexed electrochemical immunosensor for detection of breast cancer biomarkers"

Resultados sin publicar

Unpublished results

Multiplexed electrochemical immunosensor for detection of breast cancer biomarkers

1. Introduction

According to the World Health Organization (WHO), breast cancer is the second most common cancer in the world, and, by far, the most frequent cancer among women in both developing and developed countries [1]. The high incidence of this cancer in developed countries has been tempered by reductions in mortality, largely attributable to mammographic screening programs and improvements in adjuvant therapy [2]. However, mammography has a limited sensitivity as detection tool and a low positive-predictive value in younger women since they usually are excluded from breast cancer screening programs [3]. Therefore, researchers efforts have been lead to identify critical biochemical changes that seem to be differentially expressed when certain types of cancer are present [3]. Cancer biomarkers are substances that can be detected and measured in tissues, cells or body fluids; their presence and/or concentration level can be related to the presence of cancer [4]. Indeed, these biomarkers may be able to identify the early stages of tumor development, assist in cancer detection, diagnosis and staging, predict and monitor clinical response to a treatment, predict outcomes of the disease, and help in surveillance for disease recurrence [5,6]. Currently, several cancer biomarkers are used in the management of breast cancer. The biomarkers of breast cancer include tissue markers, such as estrogen and progesterone receptors and the human epidermal growth factor receptor 2 (HER2), and circulating markers such as carcinoembryonic antigen and cancer antigen 15-3 (CA15-3) [7-10].

The HER2 gene expresses a transmembrane protein that is overexpressed in approximately 20-30% of breast cancer [10,11]. HER2 overexpression has been related with accelerated growth, recurrence date, progressive metastatic disease and poor rate of disease-free survival [12,13]. HER2 protein has three domains: an extracellular domain (ECD), a short transmembrane region and an intracellular tyrosine kinase domain [14,15]. The extracellular domain fragment of HER2 (HER2 ECD) is released from the surface of tumor cells into the

blood stream. Thus, the concentration of HER2 ECD is measurable in the serum fraction of blood and it is a minimal-invasive and clinically relevant biomarker for breast cancer [15,16]. The serum test avoids the use of tissues (obtained by biopsy) which is required for established methods for assessment of HER2 status (fluorescent *in situ* hybridization (FISH), immunohistochemistry (IHC) and chromogenic *in situ* hybridization (CISH)) [16]. The serum HER2 ECD normal level limit is 15 ng/mL but moderate increase (50 ng/mL) has also been described in the absence of cancer [11,16]. HER2 status should be evaluated since targeted therapies against HER2 are available: for example, the use of Trastuzumab, which is a recombinant humanized monoclonal antibody against HER2 extracellular domain, was approved by the Food and Drug Administration (FDA) in 1998 to treat metastatic breast cancer [14,15]. Thus, a high serum level of HER2 ECD could indicate metastatic cancer or resistance against therapy (e.g. Trastuzumab) [12,15]. Therefore, the major advantage of HER2 ECD determination in serum, besides its diagnostic value, is the possibility of patient follow-up. This is even more important taking into account that the established methods for assessment of HER2 status (IHC, FISH and CISH) are not commonly used for this aim because of the location of the metastases and the cost of biopsies [8].

CA 15-3 is the soluble form of MUC-1, a protein whose normal function is cell protection and lubrication [10,17]. MUC-1 is typically seen to be overexpressed on breast tumor cells; thus, since MUC-1 has been defined as a cancer antigen, its shed form (CA 15-3) is considered as a soluble cancer biomarker that can be detected in serum [10]. CA15-3, in combination with CEA, is the most relevant tumor biomarker in breast cancer [18]. Elevated levels of CA 15-3 are found in the majority of breast cancer patients with distant metastasis [7]; about 60-75% of women with invasive breast cancer (metastasized cancer) present elevated levels of CA 15-3 [17,19]. Although CA 15-3 levels is elevated in only 10% of patients with stage 1 breast cancer and so it has a little value in the early detection, such values provide prognostic information essential for optimum disease management [4,7]. High levels of CA 15-3 may also occur in patients that suffer several different types of advance adenocarcinoma, such as ovarian, pancreatic, gastric or lung cancer [7]. CA 15-3 level of 25-30 U/mL is considered a threshold value [4,17,20,21].

In clinical diagnosis, determination of a single tumor marker often has limited diagnostic value due to most biomarkers are not specific and sometimes they can show elevated level in patients without cancer [20]. HER2 ECD and CA 15-3 are independent indicators for a worse disease free survival and the combination of both is valuable in identifying high-risk breast cancer patients [18]. Several electrochemical immunosensors for HER2 ECD and for CA 15-3

have been described in the bibliography, but only a few of them are based on screen-printed electrodes [8,12,22-27]. Some of the electrochemical immunosensors described for CA 15-3 allow multiplexed analysis in which other biomarkers such as AFP, CEA, CA 125 or CA 19-9 are measured [24-29]. However, a multiplex electrochemical immunosensor for determine simultaneously HER2 ECD and CA 15-3 has not been reported yet.

In this work, we described a dual immunosensor for the simultaneous detection of HER2 ECD and CA 15-3 using dual screen-printed carbon electrodes nanostructured with gold nanoparticles generated *in situ*. Nowadays it is still a challenge to be able to perform multianalyte determination with the same device. When performing multianalyte (e.g. for A and B analytes) determination several approaches are possible [30]: i) measuring the whole signal (positive value either there is only A, only B or both, A and B), ii) using different labels, one for A and another for B iii) using the same label but measuring the signals sequentially, first this due to analyte A and later the sum for A and B, iv) using the same label but using signals spatially resolved and v) using a separation technique. In this case we use the fourth strategy: same label (alkaline phosphatase) and different working electrodes. The immunosensing strategy followed is based on a sandwich-type assay where specific antibodies for these antigens are immobilized by adsorption onto each nanostructured working electrode. The antigen-antibody interaction is recorded using the enzyme alkaline phosphatase as label and a mixture of 3-indoxyl phosphate with silver ions as substrate. The analytical signal is the peak current of the anodic stripping linear-sweep voltammogram of the enzymatically generated silver.

2. Experimental

2.1. Apparatus and electrodes

SPCE gold nanostructuration and voltammetric measurements are performed with a µStat 200 portable bipotentiostat (DropSens) interfaced to a computer system and controlled by NOVA software version 1.9 (Metrohm Autolab). All measurements are performed at room temperature.

Disposable dual screen-printed carbon electrodes (SPCEs) are purchased from DropSens. These electrodes include a four-electrode system configuration printed on the same trip. The format of these dual SPCEs consists of two elliptic working electrodes (6.3 mm^2 each one, semi-major axis of 4 mm and semi-minor axis of 2 mm), a silver pseudo-reference electrode, a carbon counter electrode and electric contacts made of silver. These electrodes

are screen-printed on a ceramic substrate (3.4 x 1.0 x 0.05 cm). An insulating layer delimited the electrochemical cell and the electric contacts. These dual SPCEs are easily connected to the potentiostat by a specific connector supplied by DropSens.

2.2. Reagents and solution

Tris(hydroxymethyl)aminomethane (Tris), magnesium nitrate, 3-indoxyl phosphate disodium salt, silver nitrate, β-casein from bovine milk (casein), bovine serum albumin fraction V (BSA), streptavidin conjugated to alkaline phosphatase (S-AP; streptavidin from *Streptomyces avidinii*) and human serum from human male AB plasma are purchased from Sigma. Standard gold (III) tetrachloro complex ($AuCl_4^-$) are obtained from Merck.

The immunoreagents for HER2 immunoassay are provided by Sino Biological Inc.: Anti-human-HER2 ECD rabbit monoclonal antibody (anti-HER2; capture antibody for HER2 ECD), recombinant human HER2 ECD protein and anti-human-HER2 ECD mouse monoclonal biotinylated antibody (anti-HER2-bio; detection antibody for HER2 ECD). The antibodies for CA 15-3 immunoassay are purchased from Fujirebio Diagnostics: Anti-human-CA15-3 mouse monoclonal antibody (anti-CA15-3; capture antibody for CA15-3) and anti-human-CA15-3 mouse monoclonal biotinylated antibody IgG -this from the CanAg CA 15-3 EIA kit- (anti-CA15-3-bio; detection antibody for CA 15-3). Human CA 15-3 protein is provided by MyBioSource.com.

Ultrapure water obtained from a Millipore Direct-QTM 5 purification system from Millipore Ibérica is used throughout the work. All chemicals employed are of analytical reagent grade. Working solutions of casein, S-AP and immunoreagents are prepared in 0.1 M Tris-HNO_3 pH 7.2 buffer (buffer 1). A solution containing 1.0 mM 3-IP and 0.4 mM silver nitrate is prepared daily in 0.1 M Tris-HNO_3 pH 9.8 buffer containing 20 mM $Mg(NO_3)_2$ (buffer 2), and stored in opaque tubes at 4^0C.

2.3. Procedures

2.3.1. Dual SPCEs nanostructuration

Gold nanoparticles (AuNPs) are generated *in situ* on dual SPCEs (dual AuNP-SPCEs) following a method previously reported by Martínez-Paredes *et al*. [31]. This method consists of applying a constant current intensity of -100 µA for 240 s in an acidic solution of 0.1 mM $AuCl_4^-$ and finally applying a potential of +0.1 V for 120 s. But, since the potentiostat (µStat 200) employed for this research is not able to apply current intensity, therefore, in order to generate gold nanoparticles over the dual SPCEs, a potential of -0.7 V for 240 s in an acidic

solution of 0.1 mM $AuCl_4^-$ is applied. The application of this potential allows the dual SPCEs reaching the desire current intensity of -100 µA. Finally, +0.1 V for 120 s is applied and, after rinsing the nanostructured electrodes with water, they are ready to use. AuNP generation is performed at room temperature.

2.3.2. Immunosensor for the detection of HER2 ECD and CA15-3

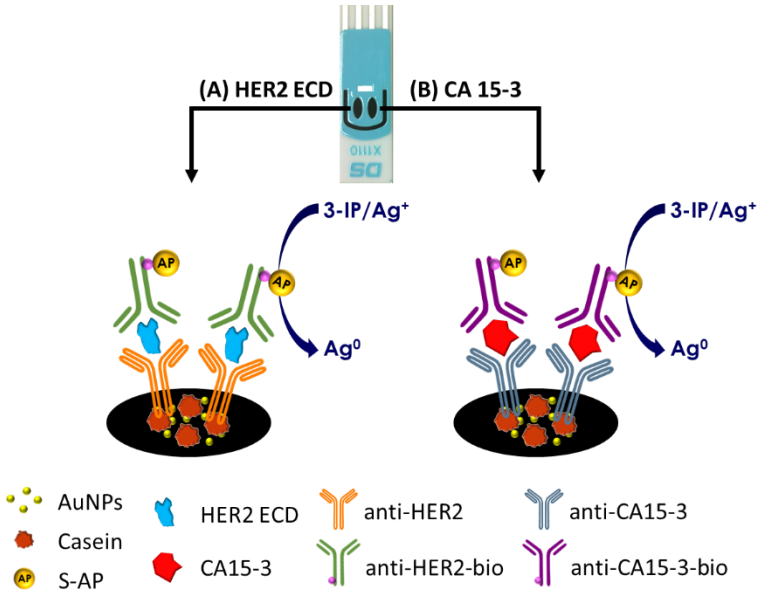

Fig. 1. Schematic representation of the immunoassay for HER2 ECD (A) and CA 15-3 (B) markers in a dual SPCE-AuNP.

The following procedure (**Fig. 1**) describes an optimized assay. Each working electrode of dual AuNP-SPCE is coated with 4 µL of one capture antibody solution (50 $\mu g \cdot mL^{-1}$ anti-HER2 solution and 100 $\mu g \cdot mL^{-1}$ anti-CA15-3 solution) and incubated overnight at 4^0C. After the overnight incubation step, the dual SPCE is washed using buffer 1 (from this point on, all the step are performed covering both working electrodes with the same aliquot). Free surface sites are blocked with 60-µL casein solution (2%) covering working electrodes during 30 min and then another washing step with buffer 1 is carried out. Next, the bi-immunosensor is incubated for 1 hour with a 60-µL aliquot of a mixture (in a 1 : 1 ratio) of a solution containing the antigens (HER2 ECD and CA 15-3) and a solution containing the anti-CA15-3-bio antibody (1 $\mu g \cdot mL^{-1}$) and BSA (1% w/w). Then, a washing step with buffer 1 is carried out, and a 60-µL aliquot of a solution containing anti-HER2-bio (0.5 $\mu g \cdot mL^{-1}$) and BSA (1% w/w) is dropped and leave to react for 30 min. Finally, after a washing step with buffer 1, 60 µL of 0.5 nM S-AP

solution containing 0.1 % BSA is dropped on the electrodes to react for 1 hour. Then, the electrodes are washed with buffer 2 and the enzymatic reaction is performed by dropping a 60-µL aliquot of the 1.0 mM 3-IP/0.4 mM $AgNO_3$ solution. The enzymatical deposition of metallic silver catalyzed by alkaline phosphatase is already reported [32]. After 20 min of reaction, a linear voltammogram between 0 and 0.3 V at 50 $mV \cdot s^{-1}$ is recorded to obtain the electrochemical oxidation current of the enzymatically deposited silver. Since silver is reduced and deposited on the electrode, no cross talk between electrodes is produced.

3. Results and discussion

3.1. Optimization studies

We try to develop the bi-sensor using a procedure previously optimized. The assay conditions for HER2 ECD detection are based in the HER2 ECD immunosensor based on SPCE previously reported by the group of the Prof. Delerue-Matos [8]. The procedure used for the CA15-3 assay is based on preliminary studies developed in this group too.

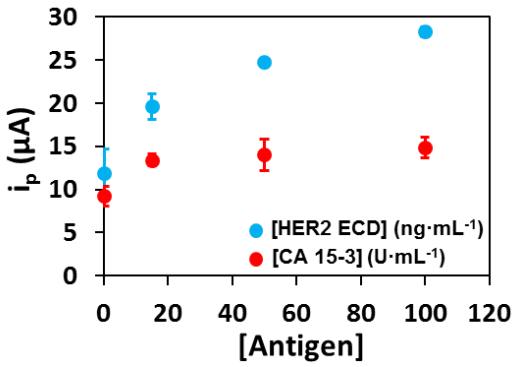

Figure 2. Peak current obtained by linear sweep voltammetry for concentrations of HER2 ECD 0, 15, 50 and 100 $ng \cdot mL^{-1}$ (blue) and CA 15-3 0, 15, 50 and 100 $U \cdot mL^{-1}$ (red). Experimental conditions: anti-HER2 50 $\mu g \cdot mL^{-1}$, anti-CA15-3 100 $\mu g \cdot mL^{-1}$, casein 2%, anti-CA15-3-bio 2 $\mu g \cdot mL^{-1}$ and anti-HER2-bio 1 $\mu g \cdot mL^{-1}$ with BSA 0.5%, S-AP 0.2 nM, 3-IP/$AgNO_3$ 1.0/0.4 mM. Average data ± *SD* are indicated (*n* = 3).

Thus, the procedure we first evaluate is as follows: briefly, after incubating overnight at 4^0C the dual AuNP-SPCE with capture antibodies (4 µL of each one, 50 $\mu g \cdot mL^{-1}$ anti-HER2 and 100 $\mu g \cdot mL^{-1}$ anti-CA15-3 solutions), the electrodes are washed with buffer 1. Then, the free surface sites are blocked with casein during 30 min. Following, a washing step with buffer 1 is carried out, and the dual immunosensor is incubated for 1 hour with 60 µL of a mixture (in a ratio 1 : 1) of a solution containing the antigens and a solution containing the anti-CA15-3-bio

antibody (2 µg·mL^{-1}), the anti-HER2-bio antibody (1 µg·mL^{-1}) and BSA (0.5% w/w). Another washing step with buffer 1 is necessary, and then 60 µL of 0.2 nM S-AP solution is dropped on both electrodes to react for 1 hour. Finally, the electrodes are washed with buffer 2 and the enzymatic reaction is performed. The analytical signal based on the anodic stripping of deposited silver, is recorded as indicates **Section 2.3.2. Fig 2**. shows the results obtained. It can be observed the sensor responds to HER2 ECD concentrations but there is not any effect when the CA 15-3 concentration increases.

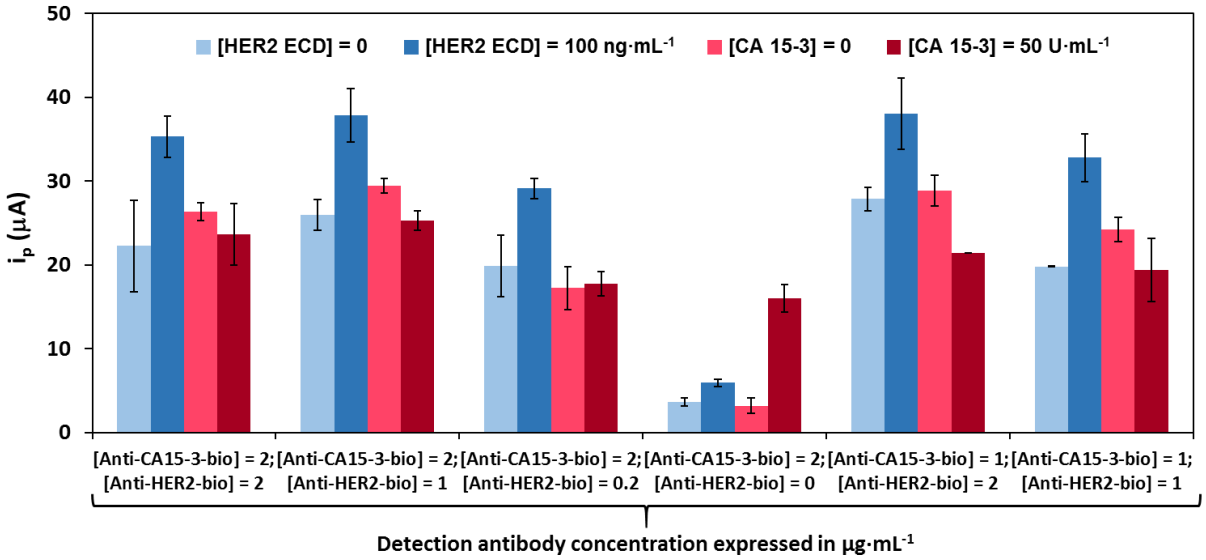

Fig. 3. Effect of the concentration of detection antibodies (expressed in µg·mL^{-1}) in absence of analyte and for analyte concentration [HER2 ECD] = 100 ng·mL^{-1} and [CA 15-3] = 50 U·mL^{-1}. Experimental conditions: anti-HER2 50 µg·mL^{-1}, anti-CA15-3 100 µg·mL^{-1}, casein 2%, BSA 1% in solution of detection antibodies, S-AP 0.2 nM, 3-IP/$AgNO_3$ 1.0/0.4 mM. Average data ± *SD* are indicated (*n* = 3).

Therefore, we presume there are non-specific bindings of detection antibodies that cover up the analytical signal for CA 15-3 detection. Since we can observe analytical signal for HER2 ECD but not for CA 15-3, we suppose the most important non-specific bindings are produced by the anti-HER2-bio. Then, we perform an assay following the same procedure as before but modifying the concentration of this antibody (**Fig. 3**). We decrease the anti-CA15-3-bio concentration too in order to evaluate the effect. The results of this experiment show that the concentration of anti-CA15-3-bio hardly affects the backgrounds and the analytical signals. However, decreasing anti-HER2-bio concentration, the background decreases, indeed when anti-HER2-bio is not present in the assay, and an important analytical signal for CA 15-3

appears (it is the unique case in which analytical signal for CA 15-3 is observed). Therefore, it is possible the anti-HER2-bio binds to anti-CA15-3 (capture antibody for CA 15-3). With the aim of discarding this possibility, the same procedure is performed but in this case, dual AuNP-SPCEs were modified with only one of the capture antibodies (anti-HER2 or anti-CA15-3). Alternatively, to evaluate the background they were not modified with capture antibodies (when dual AuNP-SPCEs are not modified with capture antibody, they are coated with the same volume of buffer 1 (4 µL) and incubated overnight at 4^0C as the modified dual AuNP-SPCE). The results of this experiment are presented in **Fig. 4**. There, it can be observed that the peak current intensities are almost the same when the anti-CA15-3 is present or not. So, anti-HER2-bio does not bind to anti-CA15-3, but the presence of anti-HER2-bio in the assay avoids obtaining an analytical signal for the biomarker CA 15-3.

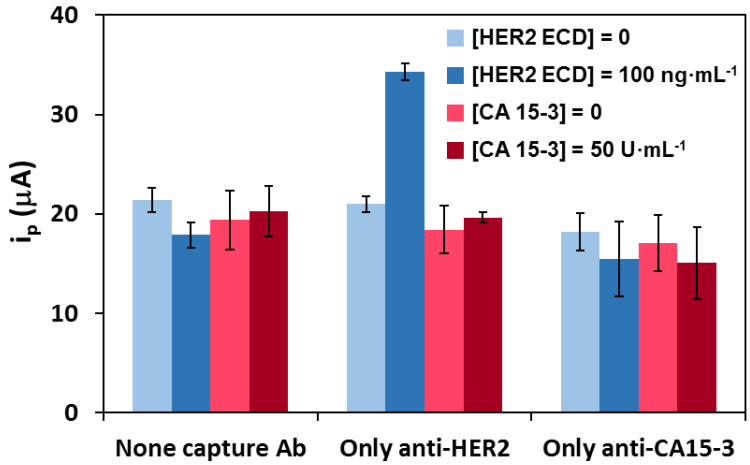

Fig. 4. Peak current given by the dual immunosensor in absence of capture antibodies (no capture Ab) or in presence of only one of them (anti-HER2 50 µg·mL^{-1} or anti-CA15-3 100 µg·mL^{-1}). Analyte concentration tested: [HER2 ECD] 0 and 100 ng·mL^{-1} (blue bars) and [CA 15-3] 0 and 50 U·mL^{-1} (red bars). Experimental conditions: anti-HER2 50 µg·mL^{-1}, anti-CA15-3 100 µg·mL^{-1}, casein 2%, anti-CA15-3-bio 1 µg/ml and anti-HER2-bio 1 µg/ml with BSA 1%, S-AP 0.2 nM, 3-IP/$AgNO_3$ 1.0/0.4 mM. Average data ± *SD* are indicated (*n* = 3).

In order to solve this problem, we propose a new assay procedure. It consists of doing the incubation with anti-HER2-bio in an independent step after the incubation with the analytes and anti-CA15-3 bio. Now, the incubation time of anti-HER2-bio is 30 min with the aim of minimizing non-specific bindings. So, the procedure for the reaction with the detection antibodies is as follow: after blocking the surface with casein, the immunosensor is incubated for 1 hour with a 60-µL aliquot of a mixture (in a ratio 1 : 1) of a solution containing the

antigens (HER2 ECD and CA 15-3) and a solution containing the anti-CA15-3-bio antibody and BSA. Then, after the washing step, a 60-µL aliquot of an anti-HER2-bio solution containing BSA is added and left for react for 30 min. Following this procedure, different concentrations of anti-CA15-3-bio and anti-HER2-bio are tested. The results are summarized in **Fig. 5**.

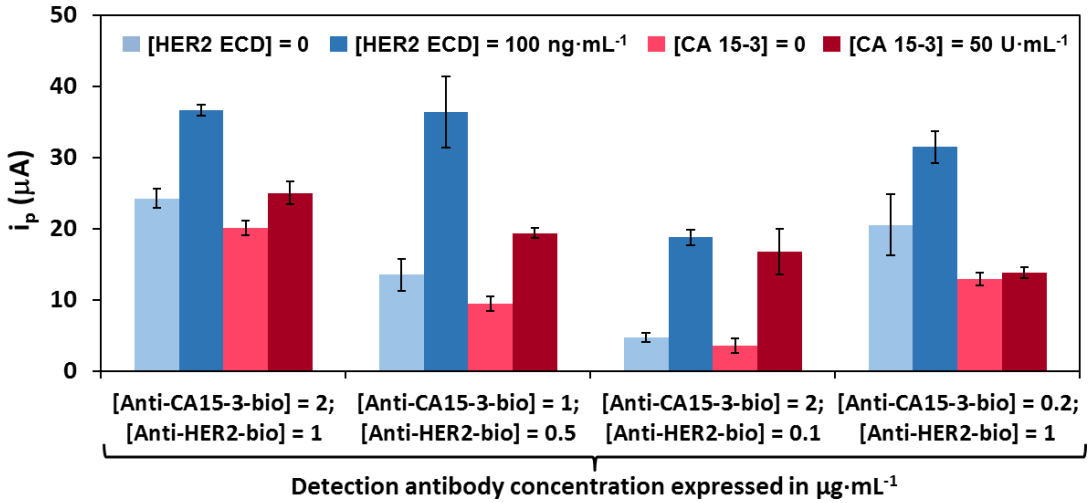

Fig. 5. Effect on the analytical signal of anti-CA15-3-bio and anti-HER2-bio concentrations (expressed in µg·mL^{-1}) in the immunosensor when anti-HER2-bio in an independent step. Analyte concentration tested: [HER2 ECD] 0 and 100 ng·mL^{-1} (blue bars) and [CA 15-3] 0 and 50 U·mL^{-1} (red bars). Experimental conditions: anti-HER2 50 µg·mL^{-1}, anti-CA15-3 100 µg·mL^{-1}, casein 2%, BSA 1% in anti-CA15-3-bio solution, BSA 0.5% in anti-HER2-bio solution (independent step), S-AP 0.2 nM, 3-IP/$AgNO_3$ 1.0/0.4 mM. Average data ± *SD* are indicated (*n* = 3).

As can be seen in **Fig. 5**, the best detection antibody concentrations are 1 and 0.5 µg·mL^{-1} or 2 and 0.1 µg·mL^{-1} (anti-CA15-3-bio and anti-HER2-bio concentration respectively). Using these concentrations, an analytical signal for CA15-3 is observed and the background signals are lower than with the other concentrations tested. Between these two ratios of detection antibody concentrations, we choose the relation 1 and 0.5 µg·mL^{-1} for further studies because it provides analytical signals higher than 2 and 0.1 µg·mL^{-1} (anti-CA15-3-bio and anti-HER2-bio concentration respectively). Since these concentrations of detection antibody show high background, we try to decrease it by increasing the concentration of BSA in anti-HER2-bio and adding BSA in S-AP solution (increasing the concentration of S-AP too). The results of this experiment are summarized in **Fig. 6**. As can be seen in **Fig. 6**, increasing the concentration of S-AP solution to 0.5 nM and adding BSA (1%), the background signals for both antigens decrease considerably. So, finally, the concentrations of both detection

antibodies and S-AP solution chosen were: anti-CA15-3-bio 1 µg·mL^{-1} with BSA 1%, anti-HER2-bio solution 0.5 µg·mL^{-1} with BSA 1% and S-AP 0.5 nM with BSA 0.1%.

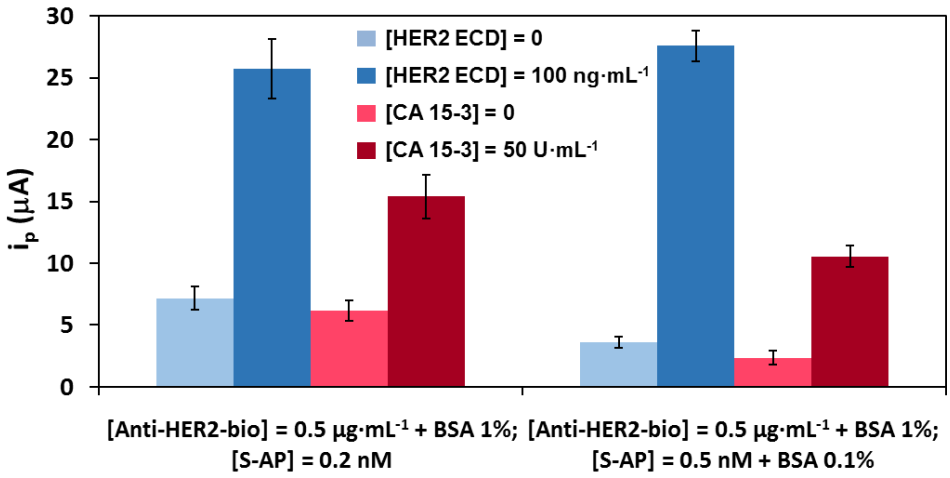

Fig. 6. Effect of concentration of S-AP solution and the use of BSA in S-AP solution on the analytical signal. Analyte concentration tested: [HER2 ECD] 0 and 100 ng·mL^{-1} (blue bars) and [CA 15-3] 0 and 50 U·mL^{-1} (red bars). Experimental conditions: anti-HER2 50 µg·mL^{-1}, anti-CA15-3 100 µg·mL^{-1}, casein 2%, anti-CA15-3-bio 1 µg·mL^{-1} with BSA 1%, anti-HER2-bio solution 0.5 µg·mL^{-1} with BSA 1% (independent step), 3-IP/$AgNO_3$ 1.0/0.4 mM. Average data ± *SD* are indicated (*n* = 3).

Once optimized all these conditions, the effect of capture antibody concentration was evaluated. **Fig. 7** summarizes the results given by the immunosensor using different concentrations of capture antibody concentrations. For the sake of economy and sensitivity, the concentrations for anti-CA15-3 and anti-HER2 were 100 and 50 µg·mL^{-1} respectively.

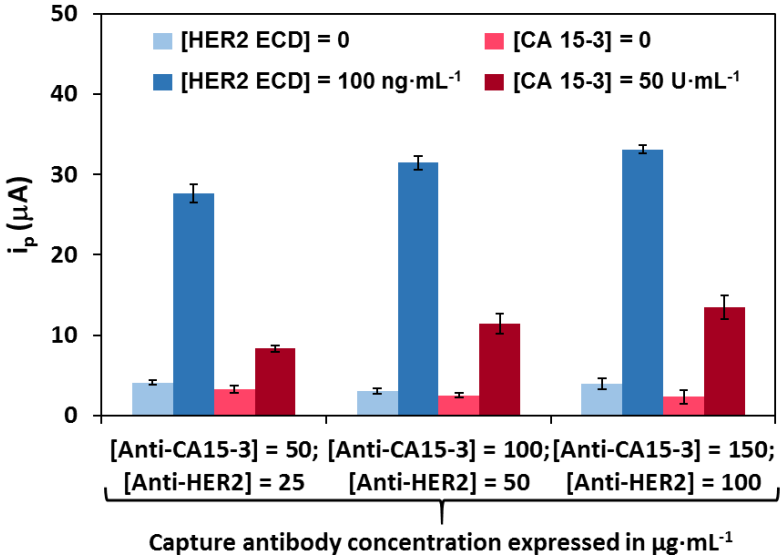

Fig. 7. Effect of concentration of capture antibodies (expressed in µg·mL^{-1}) on the analytical signal. Analyte concentrations tested: [HER2 ECD] 0 and 100 ng·mL^{-1} (blue bars) and [CA 15-3] 0 and 50 U·mL^{-1} (red bars). Experimental conditions: casein 2%, anti-CA15-3-bio 1 µg·mL^{-1} with BSA 1%, anti-HER2-bio solution 0.5 µg·mL^{-1} with BSA 1% (independent step), S-AP 0.2 nM with BSA 0.1%, 3-IP/$AgNO_3$ 1.0/0.4 mM. Average data ± *SD* are indicated (*n* = 3).

3.2. Calibration plot

Under the optimized conditions (indicated in **Section 2.3.2.**), the response of the dual immunosensor in presence of different concentrations of HER2 ECD and CA 15-3 is evaluated (concentrations between 10 and 100 ng·mL^{-1} for HER2 ECD and between 20 and 100 U·mL^{-1} for CA 15-3 are used). A linear relationship between peak current intensity and antigen concentration is found between 10 and 50 ng·mL^{-1} for HER2 ECD and between 20 and 70 U·mL^{-1} for CA 15-3 according to the following equations (**Fig. 8**):

i (µA) = 0.38 [HER2 ECD] (ng·mL^{-1}) + 3.6; R^2 = 0.995, n = 5

i (µA) = 0.16 [CA 15-3] (U·mL^{-1}) + 1.6; R^2 = 0.996, n = 5

The limits of detection (LOD) are calculated from the calibration plot using the equation LOD = 3 s_b/m, where s_b is the standard deviation of the intercept and m is the slope of the calibration plot). In the case of HER2 ECD, LOD is found to be 3.3 ng·mL^{-1} while for CA 15-3, LOD is 5.0 U·mL^{-1}. Considering as cut off for HER2 ECD 15 ng/mL and for CA 15-3 25-30 U/mL, this dual immunosensor could be useful in the diagnostic, treatment and follow-up of breast cancer patients.

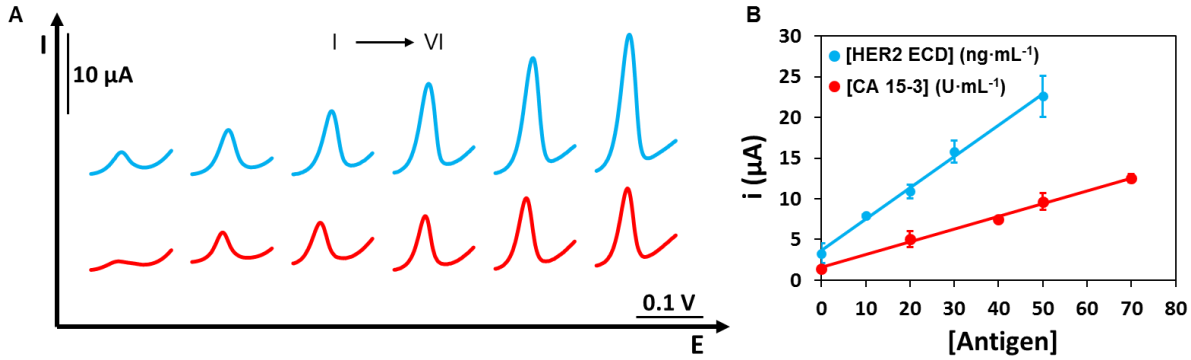

Fig. 8. (A) Linear sweep voltammograms with potential scanned from 0 to +0.3 V obtained in the simultaneous determination of HER2 ECD (blue) and CA 15-3 (red) using the immunosensor developed. [HER2 ECD] (I to VI): 0, 10, 20, 30, 50, 100 ng·mL^{-1}; [CA 15-3] (I to VI): 0, 20, 40, 50, 70, 100 U·mL^{-1}. (B) Calibration curve obtained in the simultaneous determination of HER2 ECD (from 10 to 50 ng·mL^{-1}) and CA 15-3 (from 20 to 70 U·mL^{-1}) using the immunosensor developed. Error bars correspond to the standard deviation of 3 measurements. Experimental conditions: anti-HER2 50 µg·mL^{-1}, anti-CA15-3 100 µg·mL-1, casein 2%, anti-CA15-3-bio 1 µg·mL^{-1} with BSA 1%, anti-HER2-bio solution 0.5 µg·mL^{-1} with BSA 1% (independent step), S-AP 0.2 nM with BSA 0.1%, 3-IP/$AgNO_3$ 1.0/0.4 mM.

4. Conclusions

The current trends in analytical chemistry are focused on developing simple and in situ diagnostics devices. Moreover, it is still an important challenge to be able to determine several analytes with the same device at the same time. Therefore, in this work a disposable dual electrochemical immunosensor for simultaneous detection of two breast cancer biomarkers is developed. Several aspects of the immunoassay are studied in order to achieve an immunosensor able to detect both markers in the range of concentration with clinical importance. But, although finally a bi-inmunosensor with an adequate linear range for both biomarkers is achieved, it should be interesting to test other pairs of antibodies for each marker in order to decrease the non-specific bindings and to improve the sensitivity (overall in the case of CA15-3).

Thus, work is in progress in order to solve these problems. Then, it will be necessary to evaluate the precision and the stability of the immunosensor and to validate its performance in clinical settings.

References

[1] World Health Organization, International Agency for Research on Cancer, GLOBOCAN 2012, ⟨http://globocan.iarc.fr⟩, (accessed 06 April 2016).

[2] N. Patani, Lesley-Ann Martin, M. Dowsett*, Biomarkers for the clinical management of breast cancer: International perspective*, Int. J. Cancer 133 (2013) 1-13, doi: 10.1002/ijc.27997.

[3] A.W.J. Opstal-van Winden, W. Rodenburg, J.L.A. Pennings, C.T.M. van Oostrom, J.H. Beijnen, P.H.M. Peeters, CarlaH. van Gils, A. de Vries, *A bead-based multiplexed immunoassay to evaluate breast cancer biomarkers for early detection in pre-diagnostic serum*, Int. J. Mol. Sci. 13 (2012) 13587-13604, doi: 10.3390/ijms131013587.

[4] B. Bohunicky, S.A. Mousa, *Biosensors: the new wave in cancer diagnosis*, Nanotechnol. Sci. Appl. 4 (2011) 1-10, doi: 10.2147/NSA.S13465.

[5] Biomarkers definitons working group, *Biomarkers and surrogate endpoints: Preferred definitions and conceptual framework*, *Clin. Pharmacol. Ther.* 69 (2001) 89-95, doi: 10.1067/mcp.2001.113989.

[6] Victor V. Levenson, *Biomarkers for early detection of breast cancer: What, when, and where?*, Biochi. Biophys. Acta 1770 (2007) 847-856, doi: 10.1016/j.bbagen.2007.01.017.

[7] M.J. Duffy, D. Evoy, E.W. McDermott, CA 15-3: Uses and limitation as a biomarker for breast cancer, Clin. Chim. Acta 411 (2010) 1869-1874, doi: 10.1016/j.cca.2010.08.039.

[8] R. C. B. Marques, S. Viswanathan, H. P. a Nouws, C. Delerue-Matos, and M. B. González-García, *Electrochemical immunosensor for the analysis of the breast cancer biomarker HER2 ECD,* Talanta 129 (2014) 594-599. doi: 10.1016/j.talanta.2014.06.035.

[9] Joseph A. Ludwig, John N. Weinstein, *Biomarkers in cancer staging, prognosis and treatment selection*, Nat.Rev. Cancer 5 (2005) 845-856, doi: 10.1038/nrc1739.

[10] A. Ravelli, J.M. Reuben, F. Lanza, S. Anfossi, M.R. Cappelletti, L. Zanotti, a. Gobbi, C. Senti, P. Brambilla, M. Milani, D. Spada, P. Pedrazzoli, M. Martino, A. Bottini, D. Generali. *Breast cancer circulating biomarkers: advantages, drawbacks, and new insights*. Tumor Biol. 36 (2015) 6653-6665, doi: 10.1007/s13277-015-3944-7.

[11] M. Yang, X. Yi, J. Wang, F. Zhou, *Electroanalytical and surface plasmon resonance sensors for detection of breast cancer and Alzheimer's disease biomarkers in cells and body fluids*, Analyst 139 (2014) 1814-1825, doi: 10.1039/c3an02065g.

[12] S. Patris, P. de Pauw, M. Vandeput, J. Huet, P. Van Antwerpen, S. Muyldermans, Jean-Michel Kauffmann, *Nanoimmunoassay onto a screen printed electrode for HER2 breast cancer biomarker determination*, Talanta 130 2014 164-170, doi: 10.1016/j.talanta.2014.06.069

[13] I. Diaconu, C. Cristea, V. Hârceagă, G. Marrazza, I. Berindan-Neagoe, R. Săndulescu, *Electrochemical immunosensors in breast and ovarian cancer*, Clin. Chim. Acta 425 (2013) 128-138, doi: 10.1016/j.cca.2013.07.017.

[14] L.J. Tafe, G.J. Tsongalis, *The human epidermal growth factor receptor 2 (HER2)*, Clin. Chem. Lab Med. 50 (2012) 23-30, doi: 10.1515/CCLM.2011.707

[15] L. Lam, N. McAndrew, M. Yee, T. Fu, J.C. Tchou, H. Zhang, *Challenges in the clinical utility of the serum test for HER2 ECD*, Biochim. Biophys. Acta 1826 (2012) 199-208, doi:10.1016/j.bbcan.2012.03.012.

[16] C. Tsé, Anne-Sophie Gauchez, W. Jacot, Pierre-Jean Lamy, *HER2 shedding and serum HER2 extracellular domain: Biology and clinical utility in breast cancer*, Cancer Treat. Rev. 38 (2012) 133-142, doi: 10.1016/j.ctrv.2011.03.008.

[17] A.N. Bhatt, R. Mathur, A. Farooque, A. Verma, B.S. Dwarakanath, *Cancer biomarkers - Current perspectives*, Indian J. Med. Res. 132 (2010) 129-149.

[18] D. Di Gioia , M. Dresse, D. Mayr, D. Nagel, V. Heinemann, P. Stieber, *Serum HER2 in combination with CA 15-3 as a parameter for prognosis in patients with early breast cancer*, Clin. Chim. Acta 440 (2015) 16-22, doi: 10.1016/j.cca.2014.11.001.

[19] Y. Yang, Z. Zhong, H. Liu, T. Zhu, J. Wu, M. Li, D. Wang, Double-layer nanogold and double-strand DNA-modified electrode for electrochemical immunoassay of cancer antigen 15-3, Electroanalysis 20 (2008) 2621-2628, doi: 10.1002/elan.200804373.

[20] Jie Wu, Zhifeng Fu, Feng Yan, Huangxian Ju, *Biomedical and clinical applications of immunoassays and immunosensors for tumor markers*, TrAC - Trends in Analytical Chemistry 26 (2007) 679-688, doi:10.1016/j.trac.2007.05.007.

[21] Chia-Chen Chang, Nan-Fu Chiu, David Shenhsiung Lin, Yu Chu-Su, Yang-Hung Liang, Chii-Wann Lin, *High-Sensitivity Detection of Carbohydrate Antigen 15-3 Using a Gold/Zinc Oxide Thin Film Surface Plasmon Resonance-Based Biosensor*, Anal. Chem. 82 (2010) 1207-1212, doi: 10.1021/ac901797j.

[22] Q. A. M. Al-Khafaji, M. Harris, S. Tombelli, S. Laschi, A. P. F. Turner, M. Mascini, G. Marrazza, *An electrochemical immunoassay for HER2 detection*, Electroanalysis 4 (2012) 735-742, doi: 10.1002/elan.201100501.

[23] Shenguang Ge, Mingwei Sun, Weiyan Liu, Shuai Li, Xiu Wang, Chengchao Chu, Mei Yan, Jinghua Yu, *Disposable electrochemical immunosensor based on peroxidase-like magnetic silica-graphene oxide composites for detection of cancer antigen 15-3*, Sensors Actuators B 192 (2014) 317-326, doi: 10.1016/j.snb.2013.10.127.

[24] Zhentao Cui, Dan Wu, Yong Zhang, Hongmin Ma, He Li, Bin Du, Qin Wei, Huangxian Ju, *Ultrasensitive electrochemical immunosensors for multiplexed determination using mesoporous platinum nanoparticles as nonenzymatic labels*, Anal. Chim. Acta 807 (2014) 44-50, doi: 10.1016/j.aca.2013.11.025.

[25] Shenguang Ge, Feng Yu, Lei Ge, Mei Yan, Jinghua Yu, Dairong Chen, *Disposable electrochemical immunosensor for simultaneous assay of a panel of breast cancer tumor markers*, Analyst 137 (2012) 4727-4733, doi: 10.1039/c2an35967g.

[26] Yafeng Wu, Peng Xue, Kam M.Hui, Yuejun Kang, *A paper-based microfluidic electrochemical immune device integrated with amplification-by-polymerization for the ultrasensitive multiplexed detection of cancer biomarkers*, Biosens. Bioelectron. 52 (2014) 180-187, doi: 10.1016/j.bios.2013.08.039.

[27] Jie Wu, Feng Yan, Xiaoqing Zhang, Yuetian Yan, Jinhai Tang, Huangxian Ju, *Disposable reagentless electrochemical immunosensor array based on a biopolymer/sol-gel membrane for simultaneous measurement of several tumor markers*, Clin. Chem. 54 (2008) 1481-1488, doi: 10.1373/clinchem.2007.102350.

[28] D. Tang, Li Hou, R. Niessner, Mingdi Xu, Zhuangqiang Gao, Dietmar Knopp, *Multiplexed electrochemical immunoassay of biomarkers using metal sulfide quantum dot nanolabels and trifunctionalized magnetic beads*, Biosens. Bioelectron. 46 (2013) 37-43, doi:10.1016/j.bios.2013.02.027.

[29] Michael S. Wilson, Weiyan Ni, *Multiplex Measurement of Seven Tumor Markers Using an Electrochemical Protein Chip*, Anal. Chem. 78 (2006) 6476-6483, doi: 10.1021/ac060843u.

[30] A. Brecht, R. Abuknesha, *Multi-analyte immunoassays application to environmental analysis*, TrAC – Trends in Anal. Chem. 14 (7) (1995) 361-371, doi: 10.1016/0165-9936(95)97065-9.

[31] G. Martínez-Paredes, M.B. González-García, A. Costa-García, In situ electrochemical generation of gold *nanostructured screen-printed carbon electrodes. Application to the detection of lead under potential deposition*, Electrochim. Acta 54 (2009) 4801-4808, doi: 10.1016/j.electacta.2009.03.085.

[32] P. Fanjul-Bolado, D. Hernández-Santos, M.B. González-García, A. Costa-García*, Alkaline phosphatase-catalyzed silver deposition for electrochemical detection*, Anal. Chem. 79 (2007) 5272-5277, doi: 10.1021/ac070624o.

3.3. Capítulo III: Sistemas electroanalíticos utilizando alfileres como electrodos

- Artículo 7: "*Pin-based electrochemical sensor with multiplexing possibilities*"
- Artículo 8: "*Pin-based flow injection electroanalysis*"

3.3.1. Introducción

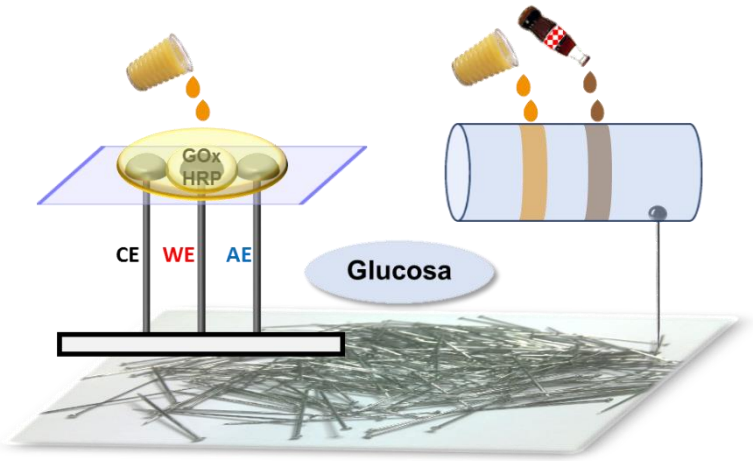

En los capítulos anteriores se han desarrollado metodologías bioelectroanalíticas para el desarrollo de biosensores enzimáticos e inmunosensores para la determinación de pequeñas moléculas de interés (glucosa, fructosa, etanol) y de biomarcadores de enfermedades. En todos los casos se han empleado electrodo serigrafiados de carbono comerciales. En este último capítulo se pretende emplear un transductor distinto que permita disminuir aún más el coste de los dispositivos pero manteniendo las características analíticas. Por ello, en este capítulo se describe el uso de alfileres de acero inoxidable como electrodos para aplicaciones electroanalíticas. Los alfileres que actúan como electrodo de trabajo se modifican con tinta de carbono, mientras que los que actúan como referencia y auxiliar se utilizan sin modificar.

En el primer trabajo se evalúa la modificación de los electrodos de trabajo con la tinta de carbono y la posibilidad de incorporar a esa tinta nanotubos de carbono. Una vez optimizada la modificación, se desarrolla un sensor enzimático para la determinación de glucosa utilizando una metodología muy similar a la empleada para el sensor de glucosa basado en electrodos serigrafiados. Además, también se demuestra la versatilidad de los alfileres como transductores en cuanto a diseño de dispositivos construyendo un dispositivo con cuatro electrodos de trabajo. Este diseño para multidetección se evalúa inmovilizando diferentes concentraciones de un anticuerpo marcado con fosfatasa alcalina sobre cada electrodo de trabajo, y utilizando como sustrato de la enzima la mezcla 3-IP/Ag^{+} como se hizo en el capítulo anterior.

3.3.2. Artículo 7: "Pin-based electrochemical sensor with multiplexing possibilities"

Biosensors and Bioelectronics (en revisión)

En el segundo trabajo, los alfileres son integrados de manera muy sencilla en un sistema de análisis por inyección en flujo, donde constituyen la base de la celda de flujo, obteniéndose unos resultados muy satisfactorios en cuanto a sensibilidad y reproducibilidad para la determinación de glucosa en muestra alimentarias.

Contents lists available at ScienceDirect

Biosensors and Bioelectronics

journal homepage: www.elsevier.com/locate/bios

Pin-based electrochemical sensor with multiplexing possibilities

Estefanía C. Rama, Agustín Costa-García, M. Teresa Fernández-Abedul*

Departamento de Química Física y Analítica, Facultad de Química, Universidad de Oviedo, 33006, Oviedo, Spain

ABSTRACT

This work describes the use of mass-produced stainless-steel pins as low-cost electrodes to develop simple and portable amperometric glucose biosensors. A potentiostatic three-electrode configuration device is designed using two bare pins as reference and counter electrodes, and a carbon-ink coated pin as working electrode. Conventional transparency film without any pretreatment is used to punch the pins and contain the measurement solution. The interface to the potentiostat is very simple since it is based on a commercial female connection. This simple electrochemical system is applied to glucose determination using a bienzymatic sensor phase (glucose oxidase/horseradish peroxidase) with ferrocyanide as electron-transfer mediator, achieving a linear range from 0.05 to 1 mM. It shows analytical characteristics comparable to glucose sensors previously reported using conventional electrodes, and its application for real food samples provides good results. The easy modification of the position of the pins allows designing different configurations with possibility of performing different measurements simultaneously. This is demonstrated through a specific design thatincludes four pin working-electrodes. Antibody labeled with alkaline phosphatase is immobilized on the pin heads and after enzymatic conversion of 3-indoxylphosphate and silver nitrate, metallic silver is determined by anodic stripping voltammetry.

Keywords: pin-based electroanalysis, multiplexed detection, glucose sensor, enzymatic assay, glucose oxidase, alkaline phosphatase.

1. Introduction

Nowadays there is an increasing interest in new strategies for the rapid detection of analytes with clinical, food and environmental importance without the need of sophisticated instrumentation. Since Whitesides' group proposed paper as material for fabricating low-cost microanalytical devices (Martinez *et al*., 2007, 2010) many microfluidic paper-based electroanalytical devices (EμPADs) have been developed to detect a wide variety of analytes (Dungchai *et al*., 2009; Liu *et al*., 2012; Nie *et al*., 2010; Wu *et al*., 2013). Electrochemical detection owns a particular interest for μPADs due to its low cost, portability, ability for miniaturization, low sample consumption and high accuracy at low analyte concentrations (Rungsawang *et al*., 2015). However, the fabrication and integration of electrodes in paper-based platforms in a rapid, efficient and cost-effective way is still a challenge. The most widespread methods are the deposition of carbon or metallic films, using either thick- or thin-film technologies. In most of the cases, stencils are required to deposit the conductive materials on the substrate (Cate *et al*., 2015; Tobjörk and Österbacka, 2011), and their fabrication implies an increase in cost and time. Graphite electrodes can be fabricated withoutstencils using a pen-on-paper approach, by printing on the surface of hydrophobic paper following a template designed using a software (Glavan *et al*., 2014). However, as in the other cases, once the device is finished, the setting of the electrodes in the electrochemical cell cannot be altered.

Besides paper as substrate for low-cost electrode fabrication, commercial transparency film is also a practical option due to its chemical compatibility and disposability (Berg *et al*., 2015; Ruecha *et al.*, 2015). Moreover, since paper is a porous media, the deposition of conductive materials can alter its porosity, wicking and interfacial energy.

In this context, the use of already mass-produced stainless-steel pins makes possible the development of low-cost electroanalytical devices with a versatile disposition of the electrodes. Pins provide a simple solution to the challenge of fabrication and integration of electrodes in miniaturized devices. Their use has only been reported previously in a work made in collaboration with Whitesides group (Glavan *et al*., 2016). We used them in systems fabricated on omniphobic R^F paper or thread to quantify lactate in human plasma. In this case, the enzymatic reaction occurs in solution and the product of the enzymatic reaction is deposited on the paper with the pins, or arrives through the thread at the pin surface. We also demonstrated the fabrication of thread-based arrays for performing multiple measurements, as well as the fabrication of a 96-well plate in paper to perform independent measurements in each well. Stainless-steel pins show several advantages as electrodes since they are: i)

inexpensive, ii) available nearly worldwide, iii) disposable, iv) highly conductive, v) electrochemically stable in neutral or mildly acidic or basic aqueous solutions (Malik *et al*., 1992) and vi) modifiable with conductive ink by simple dip and dry. Moreover, the shape of a pin and its different parts can be used for different purposes; for example, the head can be used as electrode while the sharp tip allow to drill the substrate and to anchor the pins in a support making them easy to handle. Another advantage is that pins offer readily accessible connection points perpendicular to the plane where the solution is added (the shaft of the pins), and therefore, alligator clips, grabber clips or female standard connections are very appropriate. In addition, pins allow the fabrication of devices with modifiable configurations that can be used for multiplexed analysis because of these readily accessible connection points to electrochemical readers.

In the present work, we develop the first amperometric glucose sensor using prefabricated stainless-steel pins as electrodes. The determination of glucose finds important applications in many different areas such as clinical diagnostics, biotechnology and food industry, all of them attracting extensive attention. Indeed, glucose biosensors account for approximately 85% of the world biosensor market, which has been estimated to be around $5 billion (Newman and Turner, 2005; Wang, 2008). In order to fabricate the pin-based device, transparency film was chosen as substrate for the fabrication of the electrochemical device because of its widely availability, lightness, disposability, flexibility and ease to drill it. Moreover, its hydrophobicity makes unnecessary to delimit the electrochemical cell. This work also describes the fabrication of a device with four pin working-electrodes in the same electrochemical cell. As proof-of-concept, different concentrations of an alkaline phosphatase labeled antibody were immobilized on each pin working-electrode. Thus, using 3-indoxyl phosphate and silver nitrate as enzymatic substrates, multidetection possibilities were demonstrated by the oxidation of the silver enzymatically reduced on each working electrode. This is the first time pins are used as both, surface for immobilization of bioreagents and transducers in biosensors for enzymatic sensing.

2. Materials and methods

2.1. Chemicals, materials and apparatus

Glucose oxidase from *Aspergillus niger* (GOx), horseradish peroxidase, Type VI-A (HRP), antimouse IgG conjugated with alkaline phosphatase (antiIgG-AP), glucose assay kit (GAGO20), ferrocene carboxylic acid ($FcCO_2H$), potassium ferrocyanide ($K_4Fe(CN)_6$), silver nitrate ($AgNO_3$), magnesium nitrate ($Mg(NO_3)_2$) and tris(hydroxymethyl)aminomethane (Tris)

were purchased from Sigma-Aldrich. D-(+)-glucose anhydrous was delivered by Merck and 3-indoxyl phosphate disodium salt (3-IP) by Biosynth. N,N-Dimethylformamide (DMF) and isopropyl alcohol were purchased from VWR International. Carbon ink (C10903P14) was provided by Gwent Electronic Materials Ltd and carboxylated multiwalled carbon nanotubes (MWCNTs) from Nanocyl. Ultrapure water obtained from a Millipore Direct-Q^{TM} 5 purification system was used throughout this work. All chemicals were of analytical reagent grade.

Stock solutions of $FeCO_2H$ and glucose, as well as solutions of GOx/HRP/ferrocyanide were prepared daily in 0.1 M phosphate buffer of pH 7.0. The antiIgG-AP was diluted in 0.1 M Tris-HNO_3 pH 7.2 buffer. A solution containing 1.0 mM 3-IP and 0.4 mM $AgNO_3$ was prepared in 0.1 M Tris-HNO_3 pH 9.8 buffer containing 20 mM $Mg(NO_3)_2$ using opaque micro test tubes.

Pins (AIN265925) were supplied by Metalúrgica Folch. Transparency film for photocopier was purchased from Apli Paper S.A.U. The 3-pin Dupont female cable was supplied by Amazon.

Voltammetric and chronoamperometric measurements were performed using an ECO Chemie μAutolab type II potentiostat/galvanostat (Metrohm Autolab B.V.) interfaced to a Pentium 4 2.4 GHz computer system and controlled by the Autolab GPES software version 4.9. The voltammetric measurements performed with the multiplex device were recorded using a μStat 8000 potentiostat (DropSens) interfaced to a Pentium 4 2.4 GHz computer system controlled by DropView 8400 2.0 software

2.2. Fabrication of pin-based devices

Stainless-steel pins with the following dimensions: 26 mm large, 0.59 mm shaft diameter and 1.5 mm head diameter were employed throughout the work. Transparency sheets were cut in rectangles (3 cm x 2 cm approximately) for the fabrication of the electrochemical devices.

For the pin-based device fabrication, the stainless-steel pins were cleaned by sonication in isopropyl alcohol for 20 min. Two of these pins were used without further treatment as reference (RE) and counter electrodes (CE). A stainless-steel pin coated with freshly prepared carbon ink was used as working electrode (WE). Two carbon inks were tested: one was prepared by dispersing carbon ink in DMF (50%, w/w), and the other was prepared adding to this, multiwall carbon nanotubes (in this case the ratio carbon : MWCNTs : DMF was 49.8 : 0.2 : 50, w/w). Both inks were sonicated for 1 hour (37 kHz of frequency and 320 W of power) obtaining homogeneous inks. In order to coat the pins, their head was immersed in the

corresponding ink, and then allowed to dry for 15 min in an oven at 70^0C. This process was repeated 3 times. The effect of the drying time after the last immersion was evaluated.

The design of the one-WE pin-device is shown in **Fig. 1A**. The transparency was drilled with the pins; a pin header without the pins (**Fig. S1**, in Supplementary information) was used as alignment tool for placing the pins at the same distance (1.5 mm approx.) in between. The interface between the pins and the potentiostat was a 3-pin Dupont female cable. This allows the easy, quick and reproducible connection of the pins with the potentiostat for signal recording.

The small size of the pins and the modifiable configuration allow designing multiplex devices. Using the Dupont female cable as interface between pins and potentiostat, a multiplex pin-based device was constructed. This (**Fig. 1B**) consists of four pins acting as working electrodes sharing reference and counter electrodes (bare pins). Two standard pin headers (without including the corresponding pins) were stuck in order to use them as alignment tool for the insertion of the pins. Similarly, two 3-pin Dupont female cables were stuck to obtain six connection points for the six pins (4 WEs, 1 RE and 1 CE).

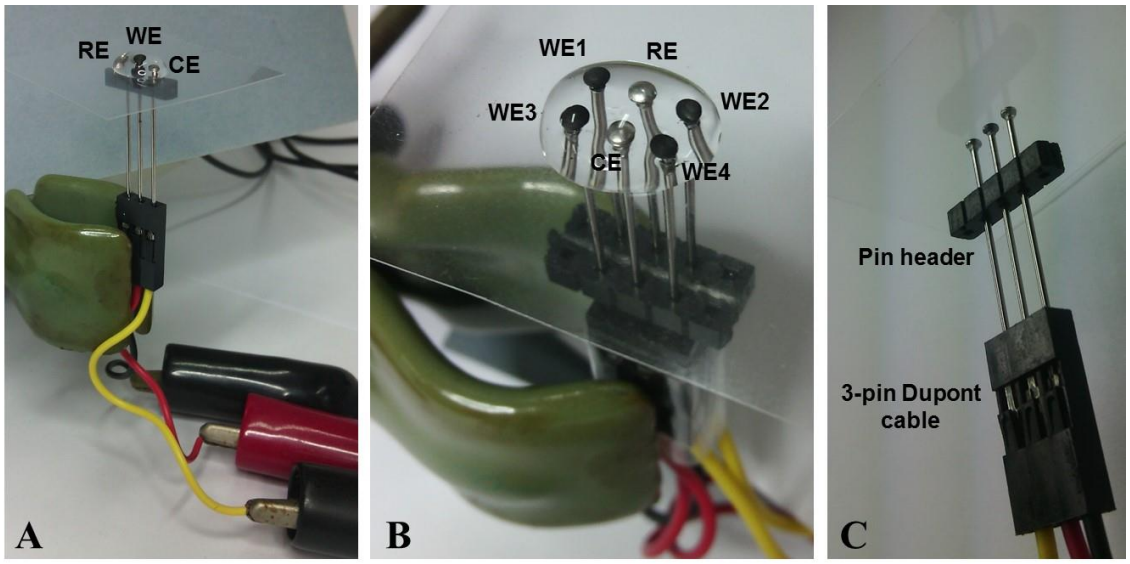

Fig. 1. Photographs of electrochemical cells fabricated using transparency film, stainless-steel pins as reference and counter electrodes (RE and CE) and one (A) or four (B) stainless-steel pins coated with carbon ink as working electrodes (WE). (C) Pin header used as alignment tool and 3-pin Dupont female cable used as interface between the pins and the potentiostat.

2.3. Cyclic voltammograms (CVs) using pin-based electrodes

Using one-WE pin devices, cyclic voltammograms (i-E curves) in solutions of ferrocene monocarboxylic acid or potassium ferrocyanide were recorded by dropping a 70-µL aliquot covering all the three pins. The potential was scanned between 0 and 0.5 V for ferrocene solutions and between -0.2 and 0.7 V for ferrocyanide solutions, at 50 $mV \cdot s^{-1}$ in both cases.

When a four-WE pin-device was used, voltammograms in solutions of ferrocene monocarboxylic acid were performed dropping a 90-µL aliquot of the measuring solution on the transparency film covering the six pins. The potential was scanned between 0.1 and 0.6 V at 50 $mV \cdot s^{-1}$.

For both devices, different pins serving as working, counter and reference electrodes were used for each measurement.

2.4. Procedure for fabrication of and measurement with the enzymatic glucose sensor

The preparation of the glucose sensor phase is based on a previous work reported by our group (Biscay *et al*., 2011). The first step of the procedure for fabricating the single-use glucose sensor is the deposition of 3 µL of a mixture of GOx (3 U/µL), HRP (5 U/µL) and potassium ferrocyanide (20 mM) onto the head of the pins coated with carbon ink (working electrodes). Then, after drying at room temperature (approximately 30-40 min), sensors are ready to use.

To record the analytical signal, a 70-µL aliquot of the glucose solution is deposited on the transparency film covering all the three electrodes. Glucose determination is carried out applying a potential of -0.2 V and the chronoamperogram (i-t curve) is recorded for 50 s. A different pin-based sensor was used for each measurement.

2.5. Procedure for the assay performed in a multiplexed device

Antibody conjugated with the enzyme alkaline phosphatase (IgG-AP), usually employed in the last step of many immunoassays, was immobilized by physical adsorption depositing 3 µL of an IgG-AP solution in 0.1 M Tris-HNO_3 pH 7.2 buffer onto the head of each pin working-electrode, and then leaving until dryness (30-40 min approx.). The enzymatic reaction was performed covering the 6 pins with a 90-µL drop of a 1.0 mM 3-IP / 0.4 mM silver nitrate solution and leaving to react for 20 min. Then, metallic silver generated enzymatically was anodically stripped, recording the linear voltammogram between 0.05 and 0.50 V at 50 $mV \cdot s^{-1}$.

2.6. Real sample analysis

The pin-based sensor designed was tested for use in real food samples: honey and orange juice. In both cases the only sample treatment needed was dilution in phosphate buffer in order to obtain adequate glucose concentration, comprised in between the limits of the linear calibration range. The accuracy of the results given by the enzymatic pin-based sensor was evaluated by analyzing the samples using a commercial glucose enzymatic kit with spectrophotometric detection.

3. Results and discussion

Pins are very promising tools for electroanalysis. One forward step is the demonstration of their use as substrate for bioimmobilization and transducers for sensor fabrication. The characteristics and advantages of pins pave the way to their use for the development not only of enzymatic assays but also of immune, DNA or other affinity-based assays. In this work, the arrangement employed is the basic three-electrode potentiostatic configuration with three stainless-steel pins, one of them coated with carbon ink and acting as working electrode. The pins are drilled on a transparency sheet employing the head of the pin as electrode surface.

3.1. Evaluation of the coating of the pins with carbon ink

In order to obtain an adequate surface area of the working electrodes, stainless-steel pins were coated with carbon ink. Modification with carbon nanotubes is also considered since they have demonstrated to improve the analytical signal (Fanjul-Bolado *et al*., 2007b; Fernández-Abedul and Costa-García, 2008) and have been employed in the first electroanalytical pin-application (Glavan *et al*., 2016). Apart from the composition of the ink, the time of drying is also important. Both were evaluated using a redox probe with well-characterized electrochemical behavior: ferrocene monocarboxylic acid ($FcCO_2H$). Pins were coated with carbon ink and with MWCNTs modified carbon ink. For each one, different times of drying were tested: 15 min, 12, 24 and 48 h. **Fig. 2A** and **2B** show the corresponding cyclic voltammograms recorded in a 0.5 mM $FcCO_2H$ solution in phosphate buffer pH 7.0. Using both inks, the capacitive current decreases considerably when the time of drying increases from 15 min to 12 h. No further improvement is produced as seen in cyclic voltammograms recorded for higher drying times. Therefore, 12 hours was chosen as drying time for the pin coating. When carbon ink and carbon ink modified with MWCNTs were compared (for a 12-hours drying time), the improvement using MWCNTs was very slight. Capacitive current was very similar and the faradaic current changed from 3.7 to 4.1 µA (**Fig. 2C**). Therefore, for the sake

of economy and simplicity, the use of MWCNTs in the ink was discarded. Using carbon ink and a drying time of 12 hours, precision between 5 independent pin devices (with different WE, RE and CE) was studied. The redox probe presented in all these devices a well-defined almost reversible process, with potentials of 269 ± 6 mV (RSD 2.3%) for the anodic and 200 ± 10 mV (RSD 4.9%) for the cathodic process. The difference between potentials is ≈ 69 mV indicating a fast electron transfer. The mean value of anodic and cathodic peak currents was 3.5 ± 0.1 µA (RSD 3.6%) and -3.8 ± 0.1 µA (RSD 3.9%) respectively (CVs shown in Figure 3D). Therefore, the precision and low cost of the pins allow considering them as disposable elements.

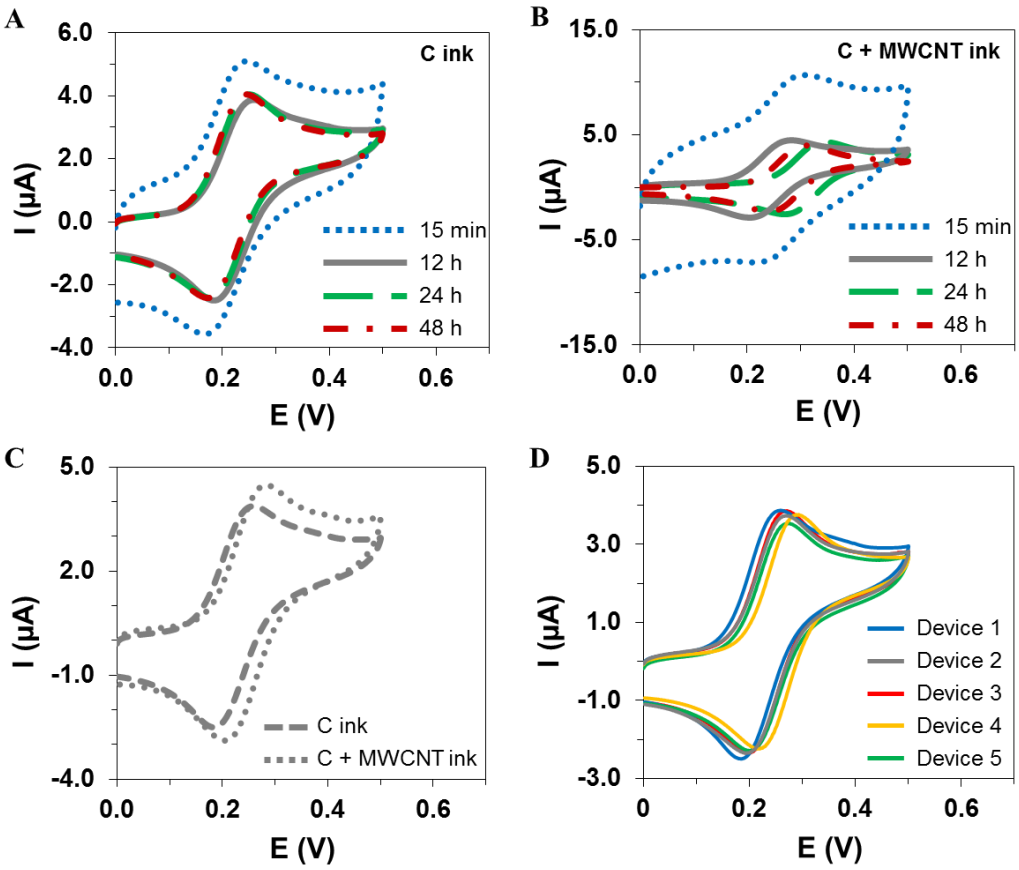

Fig. 2. Comparison of CVs recorded in 0.5 mM $FcCO_2H$ solution in phosphate buffer pH 7.0 at a scan rate of 50 $mV \cdot s^{-1}$: (A, B) using as working electrode a pin coated with (A) carbon ink and (B) carbon ink modified with MWCNTs, and dried for different times: 15 min, 12, 24 and 48 hours; (C) in electrochemical cells using as working electrode a pin coated with carbon ink and a pin coated with carbon ink modified with MWCNTs, both dried for 12 hours; (D) using 5 different devices using as working electrode a pin coated with carbon ink and dried for 12 hours.

3.2. Glucose sensor

The sensor phase of the pin-based glucose sensors consists of enzymes GOx and HRP, and ferrocyanide as mediator. The system ferro/ferricyanide shows a redox process according to the following reaction:

$$[Fe(CN)_6]^{4-} \rightleftharpoons [Fe(CN)_6]^{3-} + 1\ e^-$$

We chose chronoamperometry as detection technique since it is very adequate for portable equipments and allows the determination of glucose concentration by measuring the concentration of the ferricyanide enzymatically generated (**Fig. S2** shows a scheme of the reactions involved). For each mole of glucose, two moles of ferrocyanide are oxidized to ferricyanide (Ruzgas *et al*., 1996; Wang 2008). Applying an appropriate potential, ferricyanide is reduced, and the current measured (at a fixed time) is proportional to its concentration and therefore to this of glucose.

Then, first of all, a cyclic voltammogram was recorded in a 1.0 mM ferrocyanide solution in 0.1 M phosphate buffer of pH 7.0 (**Fig. S3**) with the aim of determining anodic and cathodic peak potentials (*vs*. a stainless-steel quasi-reference electrode) and of setting the most adequate potential for recording the chronoamperograms. A -0.2 V potential was chosen in order to assure the electrochemical reduction of ferricyanide.

Chronoamperograms were recorded for evaluating the response of the bienzymatic sensor in presence of different concentrations of glucose. **Fig. 3B** shows the response of the sensor for concentrations of glucose comprised between 0.05 and 5 mM. When the potential is applied, the capacitive current decreases faster than the faradaic current, and therefore measuring the current at an appropriate time warranties an adequate faradaic/capacitive current ratio. The analytical signal in this case is the current measured at a time of 50 s. A linear relationship between current and glucose concentration was obtained in the range of 0.05 - 1 mM, with a R^2 of 0.9998, according to the equation $|i|$ (µA) = 1.44 [glucose] (mM) + 0.14 (Fig. 3C). The limit of detection (LOD) and the limit of quantification (LOQ) were calculated as $3s_b/m$ and $10s_b/m$ respectively, where m is the slope of the calibration plot, and s_b the standard deviation of the intercept. LOD and LOQ values thus obtained were 0.03 and 0.10 mM respectively. It is interesting to remark that this simple electrochemical biosensor design using pins as electrodes shows an LOD and linear dynamic range similar, or in some cases better, than those obtained with other glucose sensors previously developed, even those employing carbon nanomaterials or nanoparticles on glassy carbon electrodes (Su *et al*., 2014; Ye *et al*., 2015: 0.01 - 0.03 mM and 0.05 - 1.2 mM respectively), using a combination of a paper disk with commercial screen-printed electrodes (Chandra Sekar *et al*., 2014; Kong *et al*., 2014:

LOD of 0.1 mM in both cases), or employing screen-printed electrodes based on paper (Rungsawang *et al*., 2015: LOD of 0.86 mM).

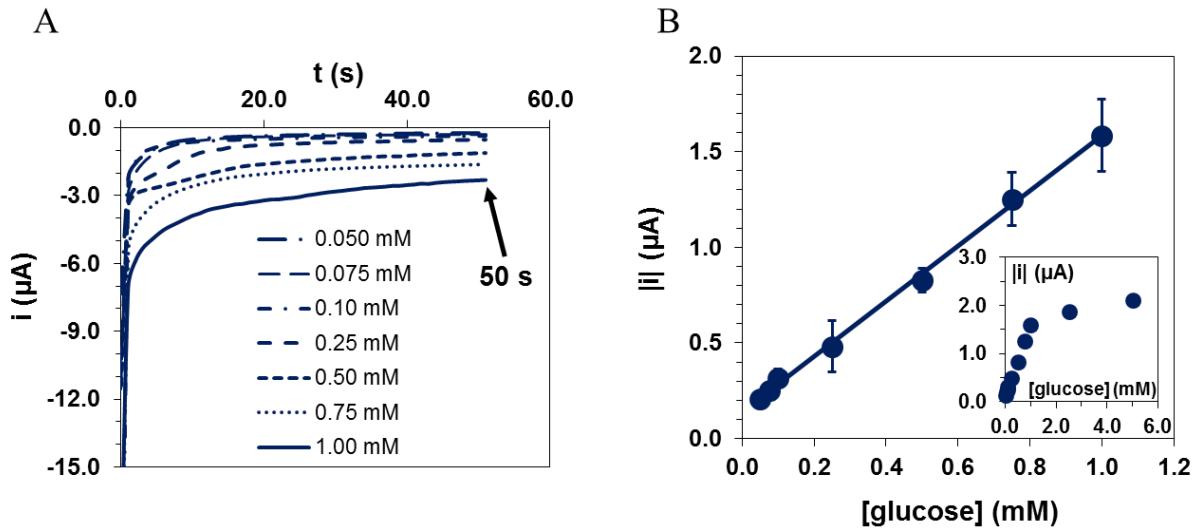

Fig. 3. (A) Chronoamperograms recorded at -0.2 V *vs*. quasi-reference pin electrode for different glucose concentrations using the proposed glucose sensor. (B) Calibration curve and (inset) linear dynamic range obtained by applying -0.2 V (*vs*. stainless-steel quasi-reference electrode) for 50 s. Error bars correspond to the standard deviation of 5 measurements.

In order to evaluate the reproducibility, seven sensors were prepared in different days to carry out seven different measurements in a 0.5 mM glucose solution. The reproducibility estimated in terms of the RSD was 7.8% (the mean value of the current was 0.83 ± 0.06 µA). Precision compares to other electrochemical devices based on paper or transparency (Dungchai *et al*., 2009; Ruecha *et al*., 2015; Rungsawang *et al*., 2015).

Furthermore, the sensor shows Michaelis-Menten kinetic behaviour. The apparent Michaelis-Menten constant (K_M) was calculated using the Lineweaver-Burk linearization obtaining a value of 2.2 ± 0.6 mM (equation: $1/I = 0.590 \cdot 1/C_{glucose} + 0.007$; $R^2 = 0.9990$). This K_M value is comparable, or in some case lower, than those calculated with other enzymatic glucose sensors based on screen-printed (Biscay *et al*., 2011; Kim *et al*., 2014: 1.7 and 1.77 mM respectively) or glassy carbon electrodes (Ye *et al*., 2015; Zou *et al*.,2008: 2.39 and 14.4 mM respectively). Since a low K_M value indicates strong affinity between the enzyme and its substrate, the value obtained with our sensor demonstrates adequate immobilization of enzyme in the active form and high bioaffinity to glucose.

This sensor was applied to glucose determination in two real samples with different matrix and appearance: honey and orange juice. The only pretreatment needed was an adequate dilution in phosphate buffer pH 7.0 in order to obtain a signal in between the linear range. Samples were also analyzed using an enzymatic kit assay with spectrophotometric detection to compare the results, which are summarized in **Table 1**. Comparing the mean values obtained by both methodologies through the Student's *t*-test, we can conclude there are no significant differences between the values labeled at a 0.05 significance level, thus demonstrating the good precision and accuracy of the sensor developed. The total cost of this sensor is less than 0.7 $ (**Table S1**), being enzymes the higher contribution (HRP is the most expensive component of the sensor).

Table 1. Determination of glucose in real samples with the proposed sensor and with the enzymatic kit with spectrophotometric detection. Data are given as average ±*SD* (*n* = 5 for the sensor and *n* = 3 for the enzymatic kit)

Real sample	Glucose sensor	Enzymatic kit
Honey (g/100g)	35 ± 2	36.7 ± 0.3
Orange juice (g/100 mL)	3.7 ± 0.2	3.47 ± 0.04

3.3. Multiplex pin-based device

It is still a challenge to be able to determine several analytes with the same device (multianalyte determination), or alternatively, perform simultaneous measurements. With this aim, using pins as electrodes, we fabricated a multiplex device consisting of four pins acting as working electrodes shown in **Fig. 1B**. In order to evaluate its performance the redox probe $FcCO_2H$ was used. Since the counter electrode should present an area similar to that of the working electrode (commonly is designed to be three times the WE) and now we have four working electrodes, the increase of its area was evaluated. CVs were recorded in 0.5 and 1.0 mM $FcCO_2H$ solutions on two different types of multiplex devices: in one, the counter electrode was a common stainless-steel pin and in the second one, an extra stainless-steel piece was placed surrounding the head of the counter-electrode pin resulting in an area ca. four times bigger. The peak currents were similar in both devices and no other differences were found, indicating there was no limitation of the current due to a small area of the counter electrode. Therefore, it was decided to use only the stainless-steel pin as counter in the multiplex device due to the easier handling. **Fig. 4A** shows the four CVs obtained with this

device. It can be observed that the peak currents and potentials are very similar for the four working electrodes, with a RSD value of 2.5% and 1.7% for anodic and cathodic peak currents respectively. They are very low, even considering that pin coating and device fabrication are hand-made.

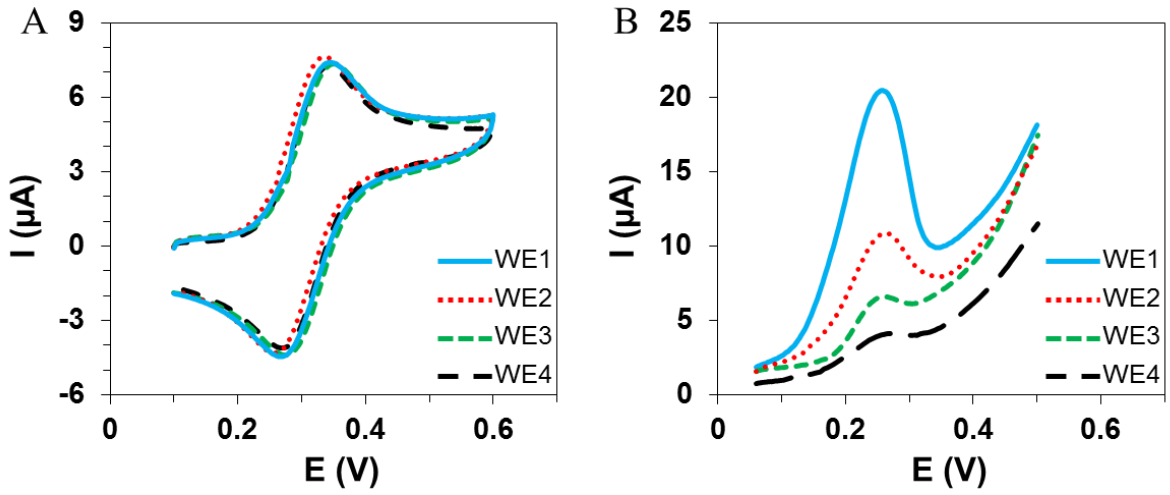

Fig.4. (A) Cyclic voltammograms recorded in 1 mM $FcCO_2H$ solution in phosphate buffer pH 7 at a scan rate of 50 $mV \cdot s^{-1}$ in an electrochemical cell consisting of four pins coated with carbon ink acting as working electrodes. (B) Linear sweep voltammograms from 0.05 V to 0.5 V at a scan rate of 50 $mV \cdot s^{-1}$ for the anodic stripping of metallic silver enzymatically deposited on the electrode surface by adsorption of different concentrations of antiIgG-AP (1:2500 (WE1), 1:5000 (WE2), 1:10000 (WE3) and 1:50000 (WE4)).

Once the precision of the measurements performed in different WEs has been evaluated, the possibility of using this device for multianalyte immunoassays has been tested immobilizing an immunoreagent commonly employed in the last step of many immunoprocedures. As a proof-of-concept the following experiment was carried out: 3 µL of antiIgG-AP solutions of different concentrations (1:2500, 1:5000, 1:10000 and 1:50000 dilutions) in 0.1 M Tris-HNO_3 pH 7.2 buffer were deposited onto the head of four pins coated with carbon ink, leaving there until dryness. Thus, different amounts of AP were adsorbed in each pin. In order to measure the amount of AP, the enzymatic reaction was performed by covering the six pins with a 90-µL drop of the 1 mM 3-IP / 0.4 mM silver nitrate solution, and after 20 min, the analytical signal is recorded (i.e. the peak current obtained recording the anodic stripping linear sweep voltammogram from 0.05 to 0.5 V at a scan rate of 50 $mV \cdot s^{-1}$). Since silver is reduced and deposited on the electrode, no cross talk between electrodes is produced. The enzymatic silver deposition catalyzed by alkaline phosphatase has been already

reported (Fanjul-Bolado *et al*., 2007a) and this procedure was used in several electrochemical immunosensors (Neves *et al*., 2013; Rama *et al*., 2014). **Fig. 4B** shows the linear voltammograms obtained for each working electrode. As it can be seen, peak current increases with the amount of AP adsorbed. This opens the possibility for using this device in multianalyte determination by immobilizing different recognition elements on each working-electrode pin. Moreover, Dupont female cables for more (and less) pins are commercially available, and then their use as well as utilizing transparency as substrate provides an enormous versatility.

4. Conclusions

Mass-produced stainless-steel pins provide the basis for fabricating simple, portable, low-cost and versatile bioelectroanalytical sensors. These devices are based on materials readily available and avoid the use of stencils for electrode fabrication. The use of Dupont female cables allows a quick and reproducible interface between the pins and the potentiostat. The system here developed can be used to fabricate a glucose sensor with satisfactory results when applied to real food sample analysis. The combination of pins and transparency allows a versatile modification of the electrodes position in the electrochemical cell and the possibility of fabricating multiplex electrochemical devices. We demonstrated the fabrication of a device with four working electrodes in the same cell that could be used for multianalyte determination.

Acknowledgement

This work has been supported by the FC-15-GRUPIN14-021 project from the Asturias Regional Government and the CTQ2014-58826-R project from the Spanish Ministry of Economy and Competitiveness (MINECO).

Appendix A. Supplementary information

Supplementary data associated with this article can be found in the online version at http://dx.doi.org.

References

Berg, K.E., Adkins, J.A., Boyle, S.E., Henry, C.S., 2015. Manganese detection using stencil-printed carbon ink electrodes on transparency film. Electroanalysis 27. doi: 10.1002/elan.201500474

Biscay, J., C. Rama, E., González-Garcia, M.B., Pingarrón-Carrazón, J.M., Costa- García, A., 2011. Enzymatic sensor using mediator-screen-printed carbon electrodes. Electroanalysis 23, 209-214. doi: 10.1002/elan.201000471

Cate, D.M., Adkins, J.A., Mettakoonpitak, J., Henry, C.S., 2015. Recent developments in paper-based microfluidic devices. Anal. Chem. 87, 19-41. doi: 10.1021/ac503968p

Chandra Sekar, N., Mousavi Shaegh, S.A., Ng, S.H., Ge, L., Tan, S.N., Chandra, N., Ali, S., Shaegh, M., Huan, S., Ge, L., Ngin, S., 2014. A paper-based amperometric glucose biosensor developed with Prussian Blue-modified screen-printed electrodes. Sensors Actuators B. Chem. 204, 414-420. doi: 10.1016/j.snb.2014.07.103

Dungchai, W., Chailapakul, O., Henry, C.S., 2009. Electrochemical detection for paper-based microfluidics. Anal. Chem. 81, 5821-5826. doi: 10.1021/ac9007573

Fanjul-Bolado, P., Hernández-Santos, D., González-García, M.B., Costa-García, A., 2007a. Alkaline phosphatase-catalyzed silver deposition for electrochemical detection. Anal. Chem. 79, 5272-5277. doi: 10.1021/ac070624o

Fanjul-Bolado, P., Queipo, P., Lamas-Ardisana, P.J., Costa-García, A., 2007b. Manufacture and evaluation of carbon nanotube modified screen-printed electrodes as electrochemical tools. Talanta 74, 427-433. doi: 10.1016/j.talanta.2007.07.035

Fernández-Abedul, M.T., Costa-García, A., 2008. Carbon nanotubes (CNTs)-based electroanalysis. Anal. Bioanal. Chem. 390, 293-298. doi: 10.1007/s00216-007-1686-0

Glavan, A.C., Ainla, A., Hamedi, M.M., Fernández-Abedul, M.T., Whitesides, G.M., 2016. Electroanalytical devices with pins and thread. Lab Chip 16, 112-119. doi: 10.1039/C5LC00867K

Glavan, A.C., Christodouleas, D.C., Mosadegh, B., Yu, H.D., Smith, B.S., Lessing, J., Fernández-Abedul, M.T., Whitesides, G.M., 2014. Folding analytical devices for electrochemical ELISA in hydrophobic R paper. Anal. Chem. 86, 11999-12007. doi: 10.1021/ac5020782

Kim, J.H., Cho, S., Bae, T.S., Lee, Y.S., 2014. Enzyme biosensor based on an N-doped activated carbon fiber electrode prepared by a thermal solid-state reaction. Sensors Actuators, B Chem. 197, 20-27. doi: 10.1016/j.snb.2014.02.054

Kong, F.Y., Gu, S.X., Li, W.W., Chen, T.T., Xu, Q., Wang, W., 2014. A paper disk equipped with graphene/polyaniline/Au nanoparticles/glucose oxidase biocomposite modified screen-printed electrode: Toward whole blood glucose determination. Biosens. Bioelectron. 56, 77-82. doi:10.1016/j.bios.2013.12.067

Liu, H., Xiang, Y., Lu, Y., Crooks, R.M., 2012. Aptamer-based origami paper analytical device for electrochemical detection of adenosine. Angew. Chemie 124, 7031-7034. doi: 10.1002/ange.201202929

Malik, A.U., Mayan Kutty, P.C., Siddiqi, N.A., Andijani, I.N., Ahmed, S., 1992. The influence of pH and chloride concentration on the corrosion behaviour of AISI 316L steel in aqueous solutions. Corros. Sci. 33, 1809-1827. doi: 10.1016/0010- 938X(92)90011-Q

Martinez, A.W., Phillips, S.T., Butte, M.J., Whitesides, G.M., 2007. Patterned paper as a platform for inexpensive, low-volume, portable bioassays. Angew. Chemie 46, 1318-1320. doi: 10.1002/anie.200603817

Martinez, A.W., Phillips, S.T., Whitesides, G.M., Carrilho, E., 2010. Diagnostics for the developing world: microfluidic paper-based analytical devices. Anal. Chem. 82, 3-10. doi: 10.1021/ac9013989

Neves, M.M.P.S., González-García, M.B., Delerue-Matos, C., Costa-García, A., 2013. Multiplexed electrochemical immunosensor for detection of celiac disease serological markers. Sensors Actuators B Chem. 187, 33-39. doi: 10.1016/j.snb.2012.09.019

Newman, J.D., Turner, A.P.F., 2005. Home blood glucose biosensors: A commercial perspective. Biosens. Bioelectron. 20, 2435-2453. doi: 10.1016/j.bios.2004.11.012

Nie, Z., Nijhuis, C.A., Gong, J., Chen, X., Kumachev, A., Martinez, A.W., Narovlyansky, M., Whitesides, G.M., 2010. Electrochemical sensing in paper-based microfluidic devices. Lab Chip 10, 477-483. doi: 10.1039/b917150a

Rama, E.C., González-García, M.B., Costa-garcía, A., 2014. Competitive electrochemical immunosensor for amyloid-beta 1-42 detection based on gold nanostructurated Screen-Printed Carbon Electrodes. Sensors Actuators B Chem. 201, 567-571. doi: 10.1016/j.snb.2014.05.044

Ruecha, N., Rodthongkum, N., Cate, D.M., Volckens, J., Chailapakul, O., Henry, C.S., 2015. Sensitive electrochemical sensor using a graphene–polyaniline nanocomposite for simultaneous detection of Zn(II), Cd(II), and Pb(II). Anal. Chim. Acta 874, 40-48. doi: 10.1016/j.aca.2015.02.064

Rungsawang, T., Punrat, E., Adkins, J., Henry, C., Chailapakul, O., 2015. Development of electrochemical paper-based glucose sensor using cellulose-4-aminophenylboronic acid-modified screen-printed carbon electrode. Electroanalysis 27. doi: 10.1002/elan.201500406

Ruzgas, T., Csöregi, E., Emnéus, J., Gorton, L., Marko-Varga, G., 1996. Peroxidasemodified electrodes: Fundamentals and application. Anal. Chim. Acta 330, 123-138. doi: 10.1016/0003-2670(96)00169-9

Su, S., Sun, H., Xu, F., Yuwen, L., Fan, C., Wang, L., 2014. Direct electrochemistry of glucose oxidase and a biosensor for glucose based on a glass carbon electrode modified with

MoS2 nanosheets decorated with gold nanoparticles. Microchim. Acta 181, 1497-1503. doi: 10.1007/s00604-014-1178-9

Tobjörk, D., Österbacka, R., 2011. Paper Electronics. Adv. Mater. 23, 1935-1961. doi: 10.1002/adma.201004692

Wang, J., 2008. Electrochemical glucose biosensors. Chem. Rev. 108, 814-25. doi: 10.1021/cr068123a

Wang, Y., Li, H., Kong, J., 2014. Facile preparation of mesocellular graphene foam for direct glucose oxidase electrochemistry and sensitive glucose sensing. Sensors Actuators B Chem. 193, 708-714. doi:10.1016/j.snb.2013.11.105

Wu, Y., Xue, P., Kang, Y., Hui, K.M., 2013. Paper-based microfluidic electrochemical immunodevice integrated with nanobioprobes onto graphene film for ultrasensitive multiplexed detection of cancer biomarkers. Anal. Chem. 125, 8661-8668. doi: 10.1021/ac401445a

Ye, Y., Ding, S., Ye, Y., Xu, H., Cao, X., 2015. Enzyme-based sensing of glucose using a glassy carbon electrode modified with a one-pot synthesized nanocomposite consisting of chitosan, reduced graphene oxide and gold nanoparticles. Microchim Acta 182, 1783-1789. doi: 10.1007/s00604-015-1512-x

Zou, Y., Xiang, C., Sun, L.X., Xu, F., 2008. Glucose biosensor based on electrodeposition of platinum nanoparticles onto carbon nanotubes and immobilizing enzyme with chitosan-SiO2 sol-gel. Biosens. Bioelectron. 23, 1010-1016. doi: 10.1016/j.bios.2007.10.009

Supplementary Information

Pin-based electrochemical sensor with multiplexing possibilities

Estefanía C. Rama, Agustín Costa-García, M. Teresa Fernández-Abedul*

Departamento de Química Física y Analítica, Facultad de Química, Universidad de Oviedo,

33006 Oviedo, Spain

**e-mail: mtfernandeza@uniovi.es*

**Tel.: +34 985 10 29 68*

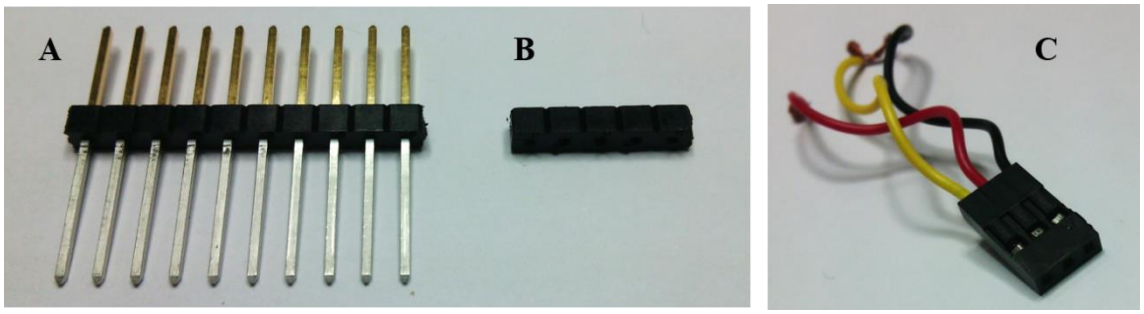

Fig. S1. Photograph of a pin header (A) with pins and (B) after removing the pins. (C) Photograph of a 3-pin Dupont female cable.

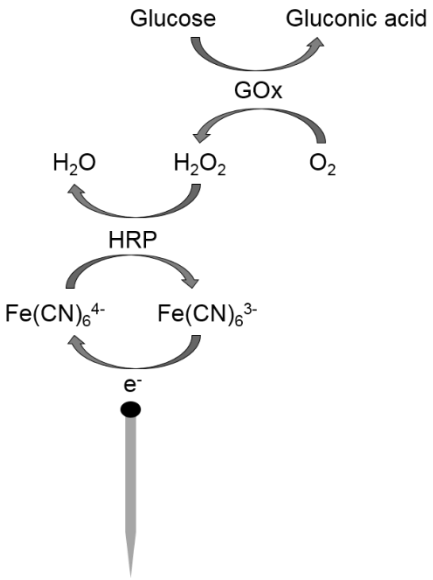

Fig. S2. Enzymatic reactions at the surface of the pin coated with carbon ink (working electrode).

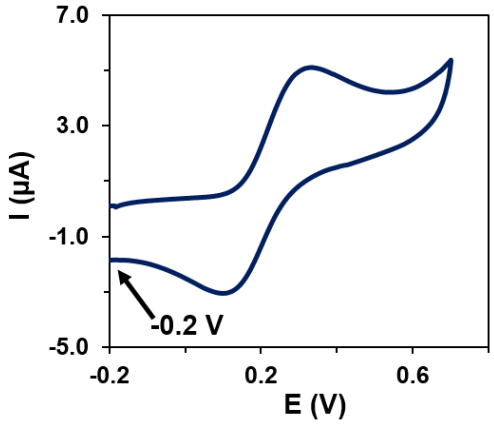

Fig. S3. Cyclic voltammogram recorded in a 1 mM ferrocyanide solution in phosphate buffer pH 7 at a scan rate of 50 $mV \cdot s^{-1}$ in an electrochemical cell fabricated using a pin coated with carbon ink dried for 12 hours as working electrode.

COST ANALYSIS

Table S1 shows a brief analysis of cost for one glucose sensor based on the three-pins device. Excluding labour and capital expenses, the cost of preparing the final system is less than 0.7 $. To note, the higher contribution is due to HRP (77% of the total cost). The prices here considered are for research quantities, but all of the materials and reagents are cheaper if they are purchased in bigger quantities.

Table S1. Cost of fabrication for one glucose sensor based on a three-pins device.

Item	Cost	Cost for sensor
Pins	3.5 $ / 400 pins	< 0.027 $
Carbon ink	32 $ / 50 g	< 0.049 $
DMF	96 $ / L	< 0.006 $
Isopropyl alcohol	100 $ / L	< 0.015 $
Transparency	20 $ / 100 A4 sheet	< 0.002 $
GOx	892.40 $ / g	0.015 $
HRP	311.20 $ / 50 mg	0.54 $
Ferrocyanide	34.10 $ / 5 g	≈ 0.003 $
Total cost for a system with three pins		< 0.7 $

3.3.3. Artículo 8: "Pin-based flow injection electroanalysis"

Analytical Chemistry (en revisión)

analytical chemistry

Article

pubs.acs.org/ac

Pin-based flow injection electroanalysis

Estefanía C. Rama, Agustín Costa-García, M. Teresa Fernández-Abedul*

Departamento de Química Física y Analítica, Facultad de Química, Universidad de Oviedo, 33006, Oviedo, Spain

ABSTRACT

This work describes the use of mass-fabricated stainless-steel pins as new low-cost electrodes for a flow injection analysis (FIA) system with electrochemical detection. The pins serving as electrodes are directly punched in the tubing where solutions flow, being one of the simplest flow cells for FIA. This cell consists of a carbon ink coated pin as working electrode and two bare pins as counter and reference electrodes. The pins are able to perform at least 300 measurements. Moreover, they can be easily replaced showing good repeatability and reproducibility (RSD lower than 6% in all the cases). As a proof-of-concept, the feasibility of the system to determine glucose was evaluated by enzymatic assay using glucose oxidase, horseradish peroxidase and ferrocyanide as electron-transfer mediator. The application of this system to real food samples has shown accurate results.

1. Introduction

Nowadays there is a widespread interest in exploring common, low-cost and disposable materials for the fabrication of sensing devices[1,2]. Particularly, electrochemical techniques result very adequate for developing simple and small-size analytical devices due to its low cost, portability, ability for miniaturization, low sample consumption and high accuracy at low analyte concentrations[3]. On the other hand, the increasing demand of information requires higher number of analysis. Automation, one of the main trends in analytical chemistry, together with simplification and miniaturization[4], plays an important role in this context. From its beginning in 1975 by Ruzicka and Hansen[5,6], flow injection analysis (FIA) has become a mature and important branch of contemporary analytical chemistry, so much that the number of published scientific papers exceeds 20 thousands[7,8]. This analytical technique is widely used in different fields of chemical analysis such as environmental and clinical chemistry or food and agriculture industry. FIA allows for the automation of analysis decreasing human errors and analysis time, and therefore, increasing the accuracy. Moreover, it offers other advantages such as simple and flexible configuration and fast response time[9].

Electrochemical detection, especially amperometry, has been widely coupled to FIA[7,10-13]. Traditionally, a three-electrode potentiostatic flow cell where the working electrode is located on a polymeric block and the reference and counter electrodes are placed downstream is employed. Regeneration of the surface of the working electrode by polishing (e.g. glassy carbon, gold disk) is common and in the case of carbon paste this could be renewed[10]. Nowadays many possibilities of wall-jet[11,12,14-16] or thin-layer[17-18] miniaturized electrochemical cells for electrodes where a whole electrochemical cell (three-electrodes cell) is in the same card are possible. The most widespread methods for fabrication of these electrodes are deposition of carbon or metallic films using either thick-film (e.g. screen-printing[12-15]) or thin film (e.g. sputtering or chemical vapor deposition[16]). But these technologies, in most of the cases, require stencils or masks to deposit the conductive materials on the substrate[1,20], usually ceramic, glass or polymers, increasing the fabrication cost and time. Alternative methods to fabricate low-cost electrodes are printing on the surface of paper using a graphite pen[21] or pencil[22,23]. But, all these methods do not allow modifying the setting of the electrodes in the electrochemical cell once the device is finished. Moreover, the mechanical stability of paper makes it not appropriate for the continuous flow of solution.

Recently, in a work made in collaboration with Whitesides group[24], the use of already mass-produced stainless-steel pins as electrodes have been reported. In this work, we proposed the use of pins as electrodes in paper and thread-based systems to quantify lactate

in human plasma. The use of pins as electrodes makes possible developing devices with a high versatility for the disposition of the electrodes. Moreover, they are inexpensive and disposable, available nearly worldwide, highly conductive, easily storable, electrochemically stable in neutral or mildly acidic or basic aqueous solutions[25] and easily modifiable with conductive inks by simple dip and dry methodologies. We have recently demonstrated the possibility of developing enzymatic biosensors through the determination of glucose by immobilizing glucose oxidase, horseradish peroxidase and ferrocyanide as mediator on the head of a pin coated with carbon ink[26]. Apart from its head as electrode surface, the sharp tip allows drilling the substrate, either flat thin films or flexible polymers, and the stem is useful as connection point to the potentiostat. Moreover, the shape and hardness of pins make them easy to handle and can be stored in small-size boxes.

In the present work, we develop, by the first time, a FIA system with electrochemical detection using mass-fabricated stainless-steel pins as electrodes. The pins are directly inserted in a piece of tubing through solutions flow. Therefore, this system does not require a conventional electrochemical flow cell and the electrodes can be easily replaced. Reference and auxiliary electrodes are located in a tubing piece downstream the working electrode. The accuracy of this system was evaluated and as a proof-of-concept, we tested its feasibility to measure the concentration of glucose, a relevant analyte in clinical and food fields. Glucose was determined by the injection of the product of the enzymatic reaction with enzymes glucose oxidase and horseradish peroxidase, using ferrocyanide as electron-transfer mediator. Ferricyanide enzymatically generated was electrochemically reduced when it passes over the head of the pin inserted in the tubing. Although the low cost of the pins (approx. $3.5 / 400 pins) allows considering them as disposable, the flow over the pinhead cleans the surface obtaining reproducible measurements over time. This allows to use only one pin for many measurements. The accuracy of the results obtained with the FIA system were evaluated by comparison with the results obtained with an enzymatic commercial kit with spectrophometric detection.

2. Experimental section

2.1. Chemicals

Glucose oxidase from *Aspergillus niger* (GOx), horseradish peroxidase, Type VI-A (HRP), ferrocene carboxylic acid (FcCO2H), glucose assay kit (GAGO20) and potassium ferrocyanide (K4Fe(CN)6) were purchased from Sigma-Aldrich. D-(+)-Glucose anhydrous was delivered by Merck. N,N-dimethylformamide (DMF) and isopropyl alcohol were purchased from VWR

International. Graphite ink (C10903P14) was provided by Gwent Electronic Materials Ltd. Ultrapure water obtained from a Millipore Direct-QTM 5 purification system was used throughout this work. All other chemicals were of analytical reagent grade.

Working solutions of $FcCO_2H$ and glucose, as well as solutions of GOx/HRP/ferrocyanide were prepared daily in 0.1 M phosphate buffer, pH 7.0.

2.2. Materials and apparatus

Pins (AIN265925) were purchased for Metalúrgica Folch, S.L. The pins chosen were stainless-steel pins with the following dimensions: 26-mm long, 0.59 mm of shaft diameter and 1.5 mm of head diameter. A 12-cylinder Perimax Spetec peristaltic pump (Spetec GmbH) and a six-port rotatory injection valve (model 1106, Omnifit Ltd.) were used for the flow injection system. Chronoamperometric and voltammetric measurements were performed with a μStat 8000 potentiostat (DropSens) interfaced to a Pentium 4 2.4 GHz computer system controlled by DropView 8400 2.0 software. A homemade saturated calomel electrode (**Figure S-1**) and a pH/mV meter purchased for Crison were used for evaluation of the potential of the quasi-reference electrode (stainless-steel pin). All measurements were carried out at room temperature.

2.3. Pin-based FIA system

The stainless-steel pins were cleaned by sonication in isopropyl alcohol for 20 min. Two of these pins were used as reference and counter electrodes without further treatment. The working electrode was a stainless-steel pin coated with freshly prepared carbon ink. The carbon ink and the procedure used to prepare the working electrode were optimized in a previous work[26]. The carbon ink consisted of a mixture of graphite ink and N,N-dimethylformamide (DMF) with a mass ratio 1:1, prepared using an ultrasonic bath for 1 hour (37 kHz of frequency and 320 W of power) in order to obtain a homogeneous ink. The head of the pins was coated immersing them in the ink and leaving them to dry for 15 min in an oven at 70^0C. This process was repeated 3 times but the drying time after the last immersion was 12 hours instead 15 min in order to assure complete evaporation of the solvent. After that, the pins coated with carbon ink were ready to use as working electrodes.

The flow injection system (**Figure 1A**) consisted of the peristaltic pump for generating a continuous flow of 0.1 M phosphate buffer pH 7.0, and an injection valve equipped with a 100-μL loop. The tube of the pump was of PVC and its diameter was 0.889 mm. The flow rate of the carrier was 1.5 $mL \cdot min^{-1}$ along all the work. The flow cell consisted of three stainless-

steel pins: a carbon-coated pin as working electrode (WE) and two bare pins as reference (RE) and counter (CE) electrodes. The pins were directly inserted in a piece of pump tube of PVC whose diameter was of 1.651 mm. The tube between the injector and the working electrode was also of PVC and its diameter and length was 0.508 mm and 25 cm respectively. The insertion of the pins in the tubing was easily achieved because the thin sharp tip of the pins allows drilling easily the tubing. The shaft of the pins was used to connect them with the potentiostat. Putting the pins upside down favored connecting them to the potentiostat through crocodile clips that also held the tubing system. In order to change WE without disturbing RE and CE pins serving as reference and counter electrodes were inserted in independent tubing. The two pieces of tubing with the pins were interconnected using a T-connector with one of the ends sealed. **Figure 2** shows several carbon-coated pins inserted in tubing ready to use as working electrodes in the FIA system.

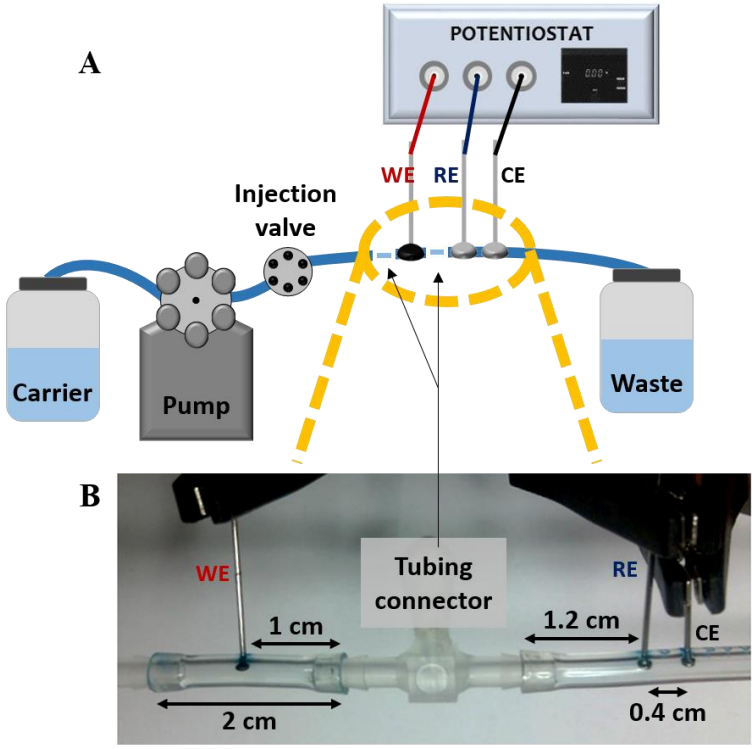

Figure 1. (A) Scheme of the pin-based FIA system. (B) Picture of the pin-based electrochemical flow cell.

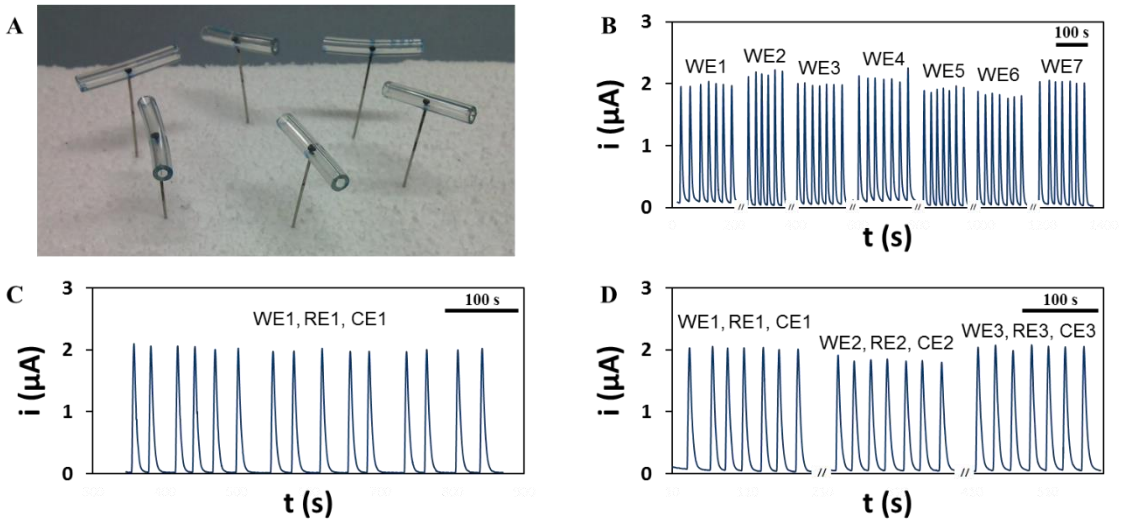

Figure 2. (A) Several pieces of pump tubing with carbon-coated pins inserted ready to use as working electrodes in the FIA system. (B, C, D) Fiagrams performed by injecting a 0.25 mM $FcCO_2H$ solution and applying +0.4 V *vs*. a stainless-steel quasi-reference electrode using: 7 different pins as working electrodes (7 injections for each one) maintaining the same reference and counter electrodes (B), the same pins as working, reference and counter electrodes for 15 injections (C), and 3 different trios of pins serving as working, reference and counter electrodes (7 injections for each group of three) (D).

2.4. Glucose determination

The procedure for measuring the concentration of glucose was as follows. First of all, a mixture of GOx, HRP and ferrocyanide (0.12 U/µL, 0.1 U/µL and 20 mM, respectively) in 0.1 M phosphate buffer pH 7.0 was prepared. Then, this mixture was added to the sample in a volume ratio sample : mixture 95% : 5%, and was left to react for 1 min before injecting into the flow system. Thus, glucose concentration was determined measuring chronoamperometrically the concentration of ferricyanide generated enzymatically (according to the reactions indicated in **Figure S-2**). For each mole of glucose, two moles of ferrocyanide are oxidized to ferricyanide[27,28]. Applying -0.1 V *vs*. stainless-steel quasi-reference electrode, the ferricyanide enzymatically generated was reduced, and the current measured was proportional to the concentration of ferricyanide generated and therefore, to the concentration of glucose in the sample.

Glucose concentration was measured in two real food samples (cola beverage and orange juice). The only sample treatment needed was a dilution in 0.1 M phosphate buffer pH 7.0. In order to test the accuracy of the results obtained, the samples were also analyzed using a commercial glucose kit with spectrophotometric detection.

3. Results and discussion

We have designed a very simple and low-cost electrochemical flow cell based on the use of stainless-steel pins as electrodes. For the sake of simplicity all of them were of stainless steel but in the case of the working electrode, the head (the part of the pin that was inside the flow system) was coated with carbon ink. The tubing employed for inserting the pins was the one used for peristaltic pumps made of PVC that recovers the shape after the puncture avoiding leaking. Two different tubing pieces were employed: one for the working and another for both, the reference and the counter electrodes. The low cost of the pins allows considering them as disposable. However, if they are stable enough and precise measurements are obtained (as in this case), change is not needed and the system can be employed for a long period of time or high number of measurements. In any case, reference and counter electrodes are located in a tubing piece separated from this of the working electrode in order to change them independently.

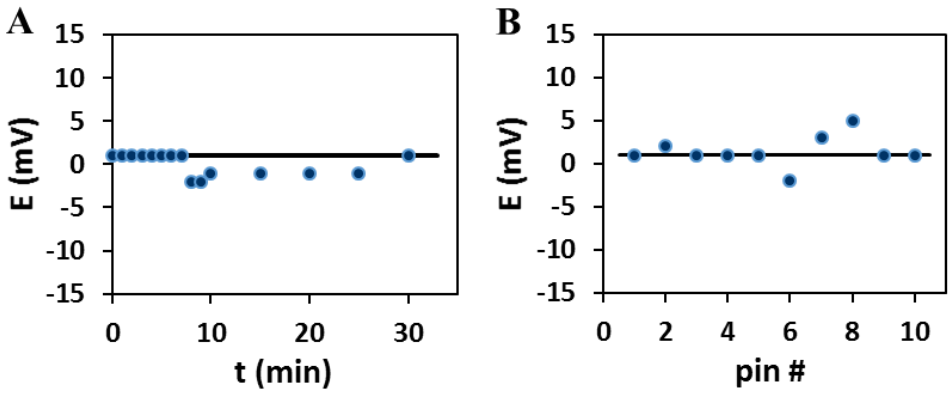

Figure 3. Potential variation between a saturated calomel electrode and (A) one quasi-reference electrode for 30 min, and (B) 10 different quasi-reference electrodes at 5 min.

Since a quasi-reference electrode (stainless-steel pin) is employed, its stability was evaluated measuring the potential between a stainless-steel pin and a saturated calomel electrode. The pin was immersed in one of the arms of a U-shaped glass piece filled with a saturated KCl solution and connected to the potentiometer with a cocrodile clip. As it can be seen in the scheme of **Figure S-1**, the bottom of the other arm is filled with mercury and calomel paste and a platinum-wire electrode was introduced and connected also to the potentiometer. **Figure 3** shows the variations in the potential with time. As it is shown in **Figure 3A**, the initial potential of the reference electrode after immersion in the solution was

1 mV. We can consider that the reference electrode does not need a setup time (period before the potential becomes stable) and that the potential was maintained for 30 min. Over this time, potential does not drift more than 3 mV. Differences between 10 stainless-steel pins is shown in **Figure 3B** and was not higher than 7 mV (most of them showed the same potential, 1 mV). However, it has to be said that 5 more pins showed unstable measurements and were discarded. Therefore, it is important to check the potential of the pin serving as reference electrode before setting the system. Then, although the precision in between different pin-based reference electrodes as well as their low cost ($3.5 / 400 stainless-steel pins) allow considering them as disposable, the stability of the potential and the simplicity of the system make possible to use the same reference in several measurements. In this case all the work (hydrodynamic curve, calibration of $FcCO_2H$ and glucose determination) has been made using the same electrode system (working, reference and counter electrodes) although with the aim of checking the precision, several electrochemical cells were evaluated as commented in the following section.

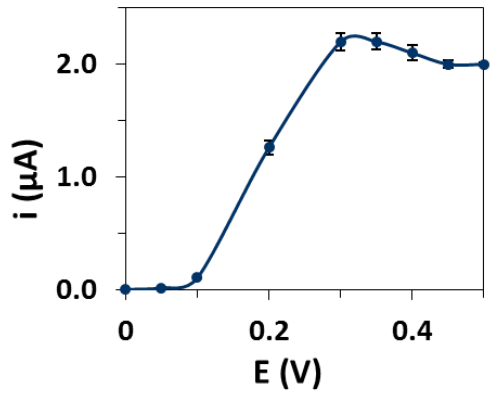

Figure 4. Hydrodynamic curve performed between potentials 0.0 V and +0.5 V *vs*. a stainless-steel quasi-reference electrode injecting a 0.25 mM $FcCO_2H$ solution (1.5 mL·min^{-1} flow rate; each point is the mean of 7 injections).

3.1. Evaluation of the pin-based FIA system

We tested the performance of this pin-based FIA system using ferrocene monocarboxylic acid (FcCO2H) since it is a redox probe with well-characterized electrochemical behavior. First of all, in order to know the behavior under flow conditions, a hydrodynamic curve (i *vs.* E curve) was recorded by injecting a 0.25 mM $FcCO_2H$ solution in a continuous flow (1.5 mL·min^{-1}) of 0.1 M phosphate buffer pH 7.0 and applying potentials

comprised between 0.0 V and +0.5 V *vs*. a stainless-steel quasi-reference electrode (**Figure 4**). Although a lower potential could be applied and this of the quasi-reference electrode has demonstrated to be stable, in order to assure the oxidation of $FcCO_2H$, +0.4 V has been chosen for further studies. The evaluation of noise in the baseline (**Figure S-3**) shows that, although it increases with potential, at +0.4 V it is acceptable (less than 10 nA with a signal of 100 nA for 0.01 mM $FcCO_2H$ solution).

Therefore, applying a potential of +0.4 V as oxidation potential and with the aim of knowing the precision of the system several studies were performed. Firstly, one carbon-coated pin acting as working electrode was tested injecting 15 times a 0.25 mM $FcCO_2H$ solution (**Figure 2C**). An intensity of current in the maximum of 1.99 ± 0.04 µA with an RSD of 1.8 % was obtained. The width of FIA peaks at base line was 27 ± 1 s and, therefore, the sample throughput of the system is 133 h^{-1}. In order to evaluate the precision of the system when different carbon-coated pins were used, several tubing pieces containing pin-based WEs (**Figure 2B**) were tested (without changing the pins serving as reference and counter electrodes).

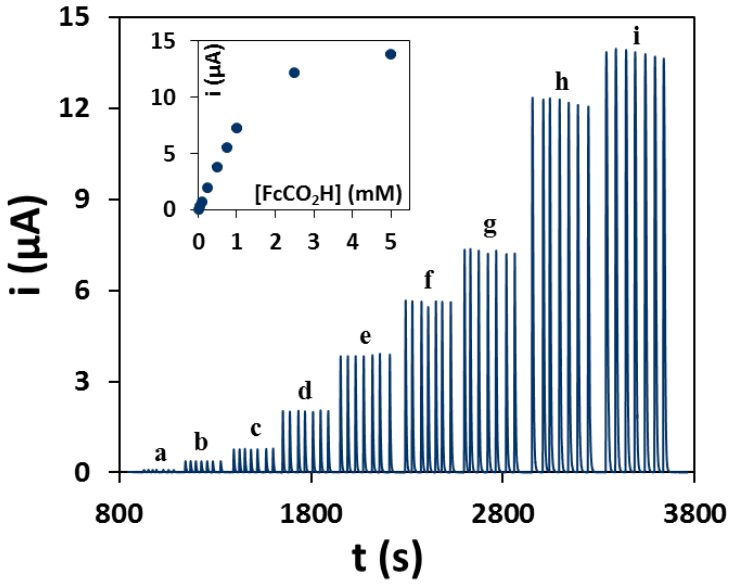

Figure 5. Fiagrams recorded by injecting the following concentrations of $FcCO_2H$ (applying +0.4 V *vs*. stainless-steel quasi-reference electrode; flow rate 1.5 mL·min^{-1}): 0.01 (a), 0.05 (b), 0.10 (c), 0.25 (d), 0.50 (e), 0.75 (f), 1.00 (g), 2.50 (h) and 5.00 (i) mM. Inset: calibration curve in the $FcCO_2H$ concentration range comprised between 0.01 and 5.00 mM (each concentration was injected 7 times).

Injections of a 0.25 mM FcCO2H solution produces a current intensity in the maximum of 1.9 ± 0.1 µA with an RSD of 5.6 % (mean of 7 injections for each one of the 7 carbon-coated pins tested; **Figure 2B**). Moreover, the reproducibility of the system when all the electrodes are changed was also checked. Using a 0.25 mM $FcCO_2H$ solution, the mean of the intensity of current obtained using 3 different trios of pins serving as working, reference and counter electrodes (7 injections in each case) was again 1.9 ± 0.1 µA with a RSD of 5.3 % (**Figure 2C**). These RSD values show the robustness of the system and the high usefulness of pins as electrodes in a flow injection analysis system.

Signals obtained by injecting different concentrations of $FcCO_2H$ were recorded and shown in **Figure 5**. The response of the system to $FcCO_2H$ concentration was linear between 0.01 mM and 1 mM, giving a calibration plot that follows the equation i (µA) = 7.32 [$FcCO_2H$] (mM) + 0.06 with a R^2 = 0.9990.

Apart from the linear relationship, it is worth to note that the stability and robustness of the pins as electrodes were also demonstrated since the same group of pins (working, reference and counter electrodes) was used for more than 300 injections without loss of signal. Moreover, it is important to note that the total cost of this pin-based flow cell (that allows its use as disposable element) was $0.28 (**Table S-1**).

3.2. Glucose determination: calibration and real sample analysis

The feasibility of the pin-based FIA system to measure the concentration of glucose, an analyte that is relevant in several fields such as clinical analysis or food industry, in real samples was evaluated. In this way, a bienzymatic assay employing glucose oxidase (GOx), horseradish peroxidase (HRP) and ferrocyanide as mediator of the electron transfer was performed off-line. The reaction takes place for 1 min and then the mixture is injected. The analytical signal is recorded at -0.1 V (see cyclic voltamogramm in **Figure S-4**). **Figure 6** shows the calibration curve for the measurements of different glucose concentrations with values ranging between 0.025 and 0.500 mM. The sensitivity obtained was 694 nA·mM^{-1} with R^2 = 0.998, showing a good linearity. The limit of detection (LOD) and the limit of quantification (LOQ) calculated according to $3s_b/m$ and $10s_b/m$ criteria respectively, where m is the slope of the linear range and s_b the standard deviation of the intercept, were 0.02 and 0.05 mM respectively. This system achieved lower LOD and LOQ for glucose detection than the pin-based glucose sensor we reported previously[26]. Moreover, when this system is compared with other FIA system for glucose determination, it presents comparable or even better analytical parameters (linear range, LOD and LOQ). For example, Samphao *et al*.[17] obtained a linear

range from 0.2 to 9 mM , a LOD of 0.1 mM and a LOQ of 0.3 mM using screen-printed carbon electrodes modified with manganese oxide, where gold decorated Fe_3O_4 nanoparticles modified with glucose oxidase were immobilized. Zhao *et al*.[29] achieved a linear range comprised between 0.1 to 2.5 mM and a LOD of 0.04 mM using the electrocatalytic oxidation of glucose at a nickel electrode.

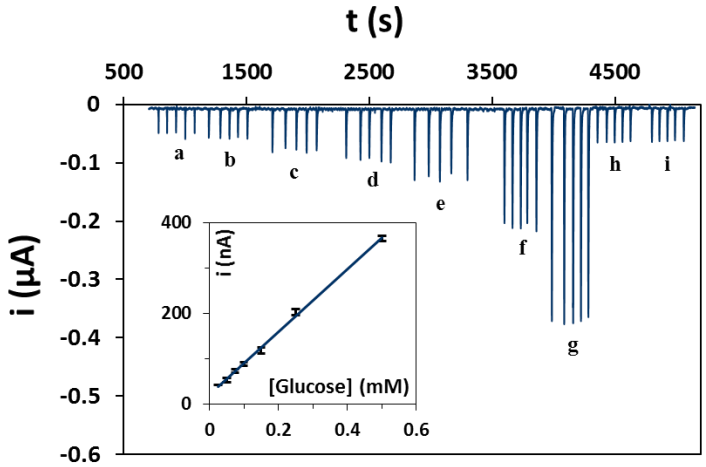

Figure 6. Fiagrams recorded for different concentrations of glucose (0.025 (a), 0.05 (b), 0.075 (c), 0.100 (d), 0.150 (e), 0.250 (f) and 0.500 mM (g)) and for the samples (orange juice (h) and cola beverage (i)) applying a potential of -0.1 V *vs*. a stainless-steel quasi-reference electrode and a 1.5 $mL \cdot min^{-1}$ of flow rate. Inset: calibration plot in the glucose concentration range comprised between 0.025 and 0.500 mM (each point is the mean of 5 measurements).

Two real samples were analyzed using the FIA system developed and the results were compared with the values obtained using a commercial glucose kit with spectrophotometric detection. **Table 1** shows the results given by both methods. The application of the Student's t-test demonstrated that there were no significant differences between the values given by the commercial kit and those obtained with our pin-based FIA system, at a 0.05 significance level. This indicates the good accuracy and precision achieved using the pins as electrodes in a FIA system.

Table 1. Determination of glucose in real samples with the proposed FIA system and with a commercial enzymatic kit with spectrophotometric detection. Data are given as average ±*SD* (*n* = 5 for the FIA system and *n* = 3 for the spectrophotometric kit).

Real sample	FIA system	Commercial kit
Cola beverage (g/100 mL)	3.3 ± 0.3	3.12 ± 0.03
Orange juice (g/100 mL)	3.22 ± 0.07	3.17 ± 0.03

4. Conclusions

Here we have demonstrated that the use of simple stainless-steel pins as electrodes set out a method to assemble and reconfigure devices according to the needs of specific applications. A conventional FIA system was combined with a new electrochemical cell, based on common low-cost stainless-steel pins for generating a highly precise and accurate analytical automatic methodology. The pins, that can be disposable due to its low-cost and easy preparation, also show enough stability for being used in a continuous flow analysis during hundreds of measurements. They can be used as reliable electrodes and offer multiple options for developing electrochemical devices.

Associated content

Supporting information

The Supporting Information is available free of charge on the ACS Publications website.

Scheme of enzymatic reactions and of the saturated calomel electrode; evaluation of the noise; cost analysis and a cyclic voltammogram of ferrocyanide (PDF).

Author information

Acknowledgements

This work has been supported by the FC-15-GRUPIN-021 project from the Asturias Regional Government and the CTQ2014-58826-R project from the Spanish Ministry of Economy and Competitiveness (MINECO).

Notes

The authors declare no competing financial interest.

References

(1) Cate, D. M.; Adkins, J. A.; Mettakoonpitak, J.; Henry, C. S. *Anal. Chem.* 2015, *87* (1), 19–41.

(2) Sanjay, S. T.; Fu, G.; Dou, M.; Xu, F.; Liu, R.; Qi, H.; Li, X. *Analyst* 2015, *140* (21), 7062–7081.

(3) Rungsawang, T.; Punrat, E.; Adkins, J.; Henry, C.; Chailapakul, O. *Electroanalysis* 2015, *27*.

(4) Valcárcel, M. *Principles of Analytical Chemistry: A textbook*, 1st ed.; Springer-Verlag Berlin Heidelberg, 2000.

(5) Ruzicka, J.; Hansen, E. H. *Anal. Chim. Acta* 1975, *78* (1), 145–157.

(6) Ruzicka, J.; Stewart, J. W. B. *Anal. Chim. Acta* 1975, *79*, 79–91.

(7) Trojanowicz, M.; Kolacinska, K. *Analyst* 2016.

(8) Ruzicka, J.; Hansen, E. H. *TrAC Trends Anal. Chem.* 2008, *27* (5), 10–13.

(9) Kulkarni, A. A.; Vaidya, I. S. *J. Crit. Rev.* 2015, *2* (4), 19–24.

(10) Fernández-Abedul, M. T.; Costa-García, A. *Anal. Chim. Acta* 1996, *328* (1), 67–71.

(11) Salazar, P.; Martín, M.; González-Mora, J. L.; González-Elipe, A. R. *Talanta* 2016, *146*, 410–416.

(12) Biscay, J.; González-García, M. B.; Costa-García, A. *Talanta* 2014, *131*, 706–711.

(13) Abad-Villar, E. M.; Fernández-Abedul, M. T.; Costa-García, A. *Anal. Chim. Acta* 2000, *409* (1-2), 149–158

(14) Nakayama, M.; Sato, A.; Nakagawa, K. *Anal. Chim. Acta* 2015, *877*, 64–70.

(15) Dropsens, www.dropsens.com (accessed 22 April 2016).

(16) Micrux Technologies, www.micruxfluidic.com (accessed 22 April 2016).

(17) Samphao, A.; Butmee, P.; Jitcharoen, J.; Svorc, L.; Raber, G.; Kalcher, K. *Talanta* 2015, *142*, 35–42.

(18) Arduini, F.; Neagu, D.; Scognamiglio, V.; Patarino, S.; Moscone, D.; Palleschi, G. *Chemosensors* 2015, *3* (2), 129–145.

(19) José Bengoechea Álvarez, M.; Fernández Bobes, C.; Teresa Fernández Abedul, M.; Costa-García, A. *Anal. Chim. Acta* 2001, *442* (1), 55–62

(20) Tobjörk, D.; Österbacka, R. *Adv. Mater.* 2011, *23* (17), 1935–1961.

(21) Glavan, A. C.; Christodouleas, D. C.; Mosadegh, B.; Yu, H. D.; Smith, B. S.; Lessing, J.; Fernández-Abedul, M. T.; Whitesides, G. M. *Anal. Chem.* 2014, *86*, 11999–12007.

(22) Dossi, N.; Toniolo, R.; Piccin, E.; Susmel, S.; Pizzariello, A. *Electroanalysis* 2013, *25* (11), 2515–2522.

(23) Yang, H.; Kong, Q.; Wang, S.; Xu, J.; Bian, Z.; Zheng, X.; Ma, C.; Ge, S.; Yu, J. *Biosens. Bioelectron.* 2014, *61*, 21–27.

(24) Glavan, A. C.; Ainla, A.; Hamedi, M. M.; Fernández-Abedul, M. T.; Whitesides, G. M. *Lab Chip* 2016, *16*, 112–119.

(25) Malik, A. U.; Mayan Kutty, P. C.; Siddiqi, N. A.; Andijani, I. N.; Ahmed, S. *Corros. Sci.* 1992, *33* (11), 1809–1827.

(26) Rama, E. C.; Costa-García, A.; Fernández-Abedul, M. T. *Biosens. Bioelectron*, submitted.

(27) Bankar, S. B.; Bule, M. V; Singhal, R. S.; Ananthanarayan, L. *Biotechnol. Adv.* 2009, *27* (4), 489–501.

(28) Ruzgas, T.; Csoregi, E.; Emneus, J.; Gorton, L.; Marko-Varga, G. *Anal. Chim. Acta* 1996, *330*, 123–138.

(29) Zhao, C.; Shao, C.; Li, M.; Jiao, K. *Talanta* 2007, *71* (4), 1769–1773.

SUPPORTING INFORMATION

Pin-based flow injection electroanalysis

Estefanía C. Rama, Agustín Costa-García, M.Teresa Fernández-Abedul*

Departmento de Química Física y Analítica, Universidad de Oviedo, Julián Clavería 8, 33006, Oviedo (Spain)

*e-mail: mtfernandeza@uniovi.es

Contents

1. SCHEME OF SATURATED CALOMEL ELECTRODE

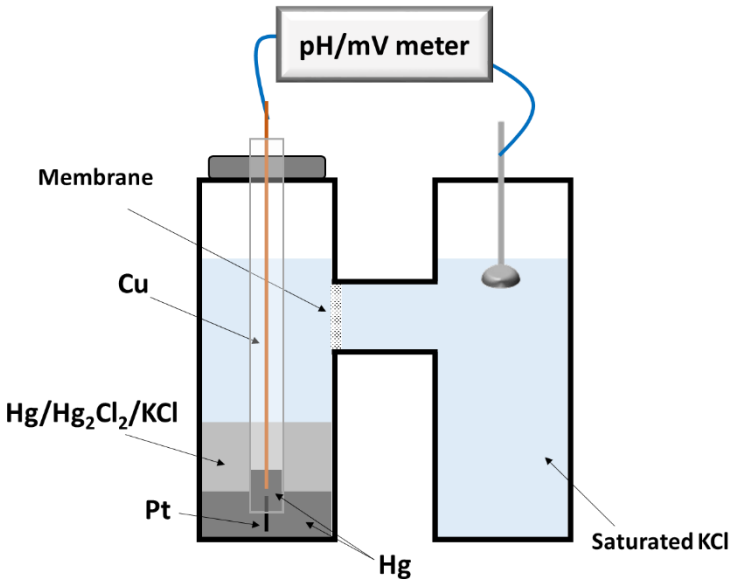

Figure S-1. Scheme of the saturated calomel electrode.

2. SCHEME OF THE ENZYMATIC REACTIONS

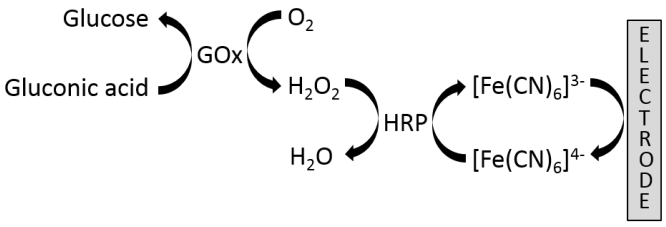

Figure S-2. Scheme of the enzymatic reactions involved in the glucose determination.

3. EVALUATION OF THE NOISE OF THE BASELINE

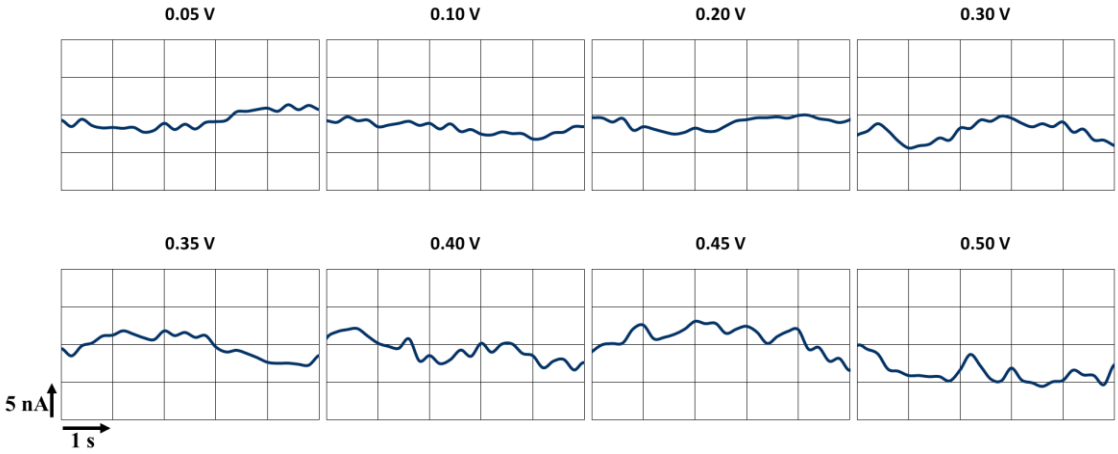

Figure S3. Baseline obtained for different detection potentials *vs*. stainless-steel quasi-reference electrode.

4. COST ANALYSIS

Table S-1 shows a brief analysis of cost for each three-pin system. Excluding labour and capital expenses, and the cost of the conventional instrumentation of a FIA system, the cost of preparing the final system is $0.28. To note, each system is able to perform more than 300 measurements. Moreover, the prices here considered were supplied in research quantities, but all of the materials and reagents are cheaper if they are purchased in bigger quantities.

Table S1. Cost of fabrication for each three-pin analytical system.

Item	Cost	Cost for system
Pins	3.5 $ / 400 pins	< 0.027 $
Carbon ink	32 $ / 50 g	< 0.049 $
DMF	96 $ / L	< 0.006 $
Isopropyl alcohol	100 $ / L	< 0.015 $
Tubing	< 30 $ / 10 m	< 0.18 $
Total cost for system with three pins		< 0.28 $

5. CYCLIC VOLTAMMOGRAM OF FERROCYANIDE

In order to determine anodic and cathodic peak potentials (*vs*. a stainless-steel quasi-reference electrode) for the ferro/ferri system and to set the most adequate potential for recording the chronoamperograms for glucose determination in the FIA system, a cyclic voltammogram was recorded in a 1.0 mM ferrocyanide solution in 0.1 M phosphate buffer of pH 7.0 (**Figure S-4**). This cyclic voltammogram was recorded using an electrochemical cell constructed by drilling the pins in a transparency as is detailed in our previous work of a pin-based biosensor[24]. The cyclic voltammogram (i-E curves) was recorded by dropping a 70-µL aliquot covering all the three pins. The potential was scanned between -0.2 and 0.7 V at 50 $mV \cdot s^{-1}$.

A -0.1 V potential was chosen for recording the analytical signal in the FIA system since this potential is low enough to assure the electrochemical reduction of ferricyanide.

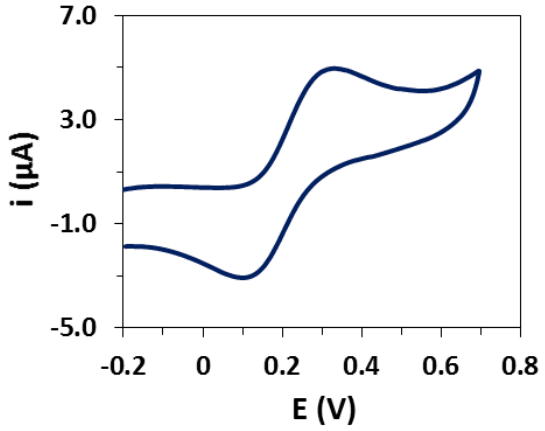

Figure S-4. Cyclic voltammogram recorded in a 1 mM ferrocyanide solution in 0.1 M phosphate buffer pH 7.0 at a scan rate of 50 $mV \cdot s^{-1}$ in an electrochemical cell fabricated using a pin coated with carbon ink as working electrode and two bare pins as counter and reference electrodes.

4. CONCLUSIONES Y PERSPECTIVAS DE FUTURO

4.1. Conclusiones

A lo largo de esta Tesis Doctoral se han desarrollado diferentes biosensores y dispositivos electroanalíticos empleando transductores de carbono. Aunque las conclusiones han sido expuestas en cada uno de los trabajos, de una manera general se pueden resaltar las siguientes ideas:

- ✓ Los electrodos serigrafiados de carbono son útiles para la construcción de biosensores, tanto enzimáticos como inmunosensores, portables y desechables. Además, la enorme variedad de diseños disponible permite construir sensores multianalito para la detección simultánea de varios analitos.
- ✓ La nanoestructuración de estos electrodos serigrafiados de carbono con nanopartículas de oro mediante electrodeposición *in situ* permite mejorar sus características como transductores.
- ✓ La simple adsorción de enzimas sobre electrodos serigrafiados modificados con mediadores redox permite obtener sensores enzimáticos simples, fáciles de usar, portables, desechables y miniaturizados para la detección de pequeñas moléculas de gran interés como la glucosa, la fructosa y el etanol. Estos biosensores presentan buenas características analíticas cuando se aplican para la determinación de estos analitos en muestras reales.
- ✓ Se han desarrollado inmunosensores desechables basados tanto en ensayos competitivos como en ensayos con formato sándwich, para la detección de biomarcadores de enfermedades muy relevantes, como son la enfermedad de Alzheimer y el cáncer de mama.
- ✓ Los alfileres de acero inoxidables modificados con tinta de carbono muestran valiosas ventajas como electrodos y como transductores electroquímicos para biosensores. Además, ofrecen una gran versatilidad en cuanto al diseño de celdas electroquímicas. Esta versatilidad permite construir dispositivos para la detección simultánea de varios analitos, así como también la fácil integración de estos electrodos en sistemas de flujo.

Por otra parte, centrándose en cada uno de los dispositivos desarrollados, en la siguiente tabla (**Tabla 4.1**) se encuentran recogidas sus principales características.

Tabla 4.1. Principales características de los dispositivos electroanalíticos desarrollados a lo largo de esta Tesis Doctoral.

Transductor	Analito	Intervalo lineal	LOD	RSD	Tiempo preparación fase sensora
SPCE con ferrocianuro	Glucosa	0.05 – 1 mM	0.025 mM	2.6 %	≈ 1 h
	Fructosa	0.1 – 1 mM	0.05 mM	1.9 %	≈ 1 h
SPCE con Co-ftalocianina	Etanol	0.05 – 1 mM	0.02 mM	2.1 %	≈ 1 h
AuNPs SPCE	Aβ1-42	0.5 – 500 $ng \cdot mL^{-1}$	0.1 $ng \cdot mL^{-1}$	4.9 %	≈ noche + 1.5 h
AuNPs dual SPCE	HER	10 – 100 $ng \cdot mL^{-1}$	3 $ng \cdot mL^{-1}$	-	≈ noche+ 1.5 h
	CA15-3	20 – 100 $U \cdot mL^{-1}$	5 $U \cdot mL^{-1}$	-	
Sensor alfileres	Glucosa	0.05 – 1 mM	0.03 mM	7.8 %	≈ 30 - 40 min
FIA alfileres	Glucosa	0.025 – 0.5 mM	0.02 mM	-	-

4.2. Conclusions

Along this PhD Memory different biosensors and electroanalytical devices using carbon transducers have been developed. Although the conclusions have been explained in each work, in a general way the following ideas can be outlined:

- ✓ Screen-printed carbon electrodes are useful for the construction of portable and disposable biosensors both enzymatic and immunosensors. Moreover, the enormous variety of designs allows constructing multiplexed sensors for the simultaneous detection of several analytes.
- ✓ Nanostructuration of these screen-printed carbon electrodes with gold nanoparticles by easy *in situ* electrochemical generation allows the improvement of their characteristics as transducer.
- ✓ The simple adsorption of enzymes onto screen-printed electrodes modified with redox mediators allows obtaining simple, easy to use, portable, disposable and miniaturized enzymatic biosensors for small molecules of high interest such as glucose, fructose and ethanol. These biosensors show good analytical characteristics when they are applied for real samples analysis.
- ✓ Disposable immunosensors based on both competitive and sandwich assays for biomarkers of diseases with great importance such as Alzheimer's disease and breast cancer have been developed.
- ✓ Stainless-steel pins modified with carbon ink show valuable advantages as electrodes and as electrochemical transducers for biosensors. Moreover, they offer a huge versatility for the design of electrochemical cells. This versatility allows constructing multiplexed devices, and also the easy integration of these electrodes in flow systems.

On the other hand, focusing in each one of the devices developed, the following table (**Table 4.2**) summarizes their main characteristics:

Table 4.2. Main characteristics of the electroanalytical devices developed along this PhD Thesis.

Transducer	Analyte	Linear range	LOD	RSD	Time sensor phase preparation
Ferrocyanide SPCE	Glucose	0.05 – 1 mM	0.025 mM	2.6 %	≈ 1 h
	Fructose	0.1 – 1 mM	0.05 mM	1.9 %	≈ 1 h
Co-phthalocyanine SPCE	Ethanol	0.05 – 1 mM	0.02 mM	2.1 %	≈ 1 h
AuNPs SPCE	Aβ1-42	0.5 – 500 $ng \cdot mL^{-1}$	0.1 $ng \cdot mL^{-1}$	4.9 %	≈ overnight + 1.5 h
AuNPs dual SPCE	HER	10 – 100 $ng \cdot mL^{-1}$	3 $ng \cdot mL^{-1}$	-	≈ overnight + 1.5 h
	CA15-3	20 – 100 $U \cdot mL^{-1}$	5 $U \cdot mL^{-1}$	-	
Pin-based sensor	Glucose	0.05 – 1 mM	0.03 mM	7.8 %	≈ 30 - 40 min
Pin-based FIA	Glucose	0.025 – 0.5 mM	0.02 mM	-	-

4.3. Perspectivas de futuro

Como se ha podido comprobar, esta Memoria no es un trabajo totalmente cerrado. Por ejemplo, se requieren varios experimentos más para completar alguno de los trabajos (como pasa en el caso del bi-inmunosensor para la determinación de HER2 y CA15-3). Por otro lado, de esta Memoria se pueden extraer varias ideas para futuros trabajos. Algunas de esas ideas pueden ser las siguientes:

A corto plazo:

- Mejorar la sensibilidad para la detección de CA15-3 in el bi-inmunosensor y estudiar la reproducibilidad de este sensor.
- Validar con muestras reales tanto el immunosensor para la Aβ1-42 como el bi-inmunosensor para HER2 y CA15-3.

A largo plazo:

- Desarrollar inmunosensores individuales para otros biomarcadores de la enfermedad de Alzheimer como la proteína tau o la tau fosforilada. Una vez desarrollados estos inmunosensores, se puede construir un sensor multianalito que permita la detección de los tres biomarcadores simultáneamente (Aβ1-42, tau y tau fosforilada).
- Desarrollar nuevas aplicaciones analíticas para los alfileres de acero inoxidables. Por ejemplo, se puede desarrollar un soporte portable con 96 celdas electroquímicas de tres electrodos basados en alfileres para la determinación electroquímica del producto enzimático de un ensayo ELISA en los 96 pocillos directa y simultáneamente. Un paso más será el desarrollar un immunosensor directamente en la cabeza del alfiler.
- De forma más general, avanzar en el desarrollo de metodologías electroanalíticas que permitan reducir el coste, el tiempo y la complejidad de las determinaciones, y también en el desarrollo de análisis multianalito.

4.4. Future prospects

This PhD Memory is not a concluded work as it could be seen. For example, several experiments are required to complete some work (as in the case of the bi-immunosensor for HER2 and CA15-3). But, on the other hand, many ideas for future works can derive from this PhD Memory. Some of these ideas can be the following:

In the short-term:

- To improve the sensitivity for CA15-3 in the bi-immunosensor and to study the reproducibility of this bi-immunosensor.
- Validate with real samples the immunosensors for Aβ1-42 and for HER2 and CA15-3.

In the long-term:

- To develop single immunosensors for other biomarkers of Alzheimer's disease, such as tau protein or tau phosphorylated. Once the single sensors were developed, a multi-analyte sensor could be fabricated in order to be able to determine the three markers simultaneously (Aβ1-42, tau y tau phosphorylated).
- To develop new analytical applications for stainless-steel pins. For example, a portable support with 96 three-electrode pin-based electrochemical cells can be designed for determining the enzymatic product of an ELISA assay in the 96-well plate directly and simultaneously. One step forward will be to construct an immunosensor directly in the coated pin-head.
- In a more general way, to progress in the development of electroanalytical methodologies in order to reduce the cost, the time and the complexity of the determinations, and also in the development of multiplexed analysis.